1978

Heat transfer in in-tube flow of non-Newtonian fluids

Sadanand Dattatray Joshi
Iowa State University

INFORMATION TO USERS

This was produced from a copy of a document sent to us for microfilming. While the most advanced technological means to photograph and reproduce this document have been used, the quality is heavily dependent upon the quality of the material submitted.

The following explanation of techniques is provided to help you understand markings or notations which may appear on this reproduction.

1. The sign or "target" for pages apparently lacking from the document photographed is "Missing Page(s)". If it was possible to obtain the missing page(s) or section, they are spliced into the film along with adjacent pages. This may have necessitated cutting through an image and duplicating adjacent pages to assure you of complete continuity.

2. When an image on the film is obliterated with a round black mark it is an indication that the film inspector noticed either blurred copy because of movement during exposure, or duplicate copy. Unless we meant to delete copyrighted materials that should not have been filmed, you will find a good image of the page in the adjacent frame.

3. When a map, drawing or chart, etc., is part of the material being photographed the photographer has followed a definite method in "sectioning" the material. It is customary to begin filming at the upper left hand corner of a large sheet and to continue from left to right in equal sections with small overlaps. If necessary, sectioning is continued again–beginning below the first row and continuing on until complete.

4. For any illustrations that cannot be reproduced satisfactorily by xerography, photographic prints can be purchased at additional cost and tipped into your xerographic copy. Requests can be made to our Dissertations Customer Services Department.

5. Some pages in any document may have indistinct print. In all cases we have filmed the best available copy.

University
Microfilms
International

300 N. ZEEB ROAD, ANN ARBOR, MI 48106
18 BEDFORD ROW, LONDON WC1R 4EJ, ENGLAND

Heat transfer in in-tube flow of non-Newtonian fluids

by

Sadanand Dattatray Joshi

A Dissertation Submitted to the
Graduate Faculty in Partial Fulfillment of
The Requirements for the Degree of
DOCTOR OF PHILOSOPHY
Major: Mechanical Engineering

Approved:

Signature was redacted for privacy.

In Charge of Major Work

Signature was redacted for privacy.

For the Major Department

Signature was redacted for privacy.

For the Graduate College

Iowa State University
Ames, Iowa

1978

TABLE OF CONTENTS

LIST OF TABLES

LIST OF FIGURES

NOMENCLATURE

a	Defined in Eq. (2.40) ($lb_f\ sec^n/ft^2$)
A	Tube surface area (ft^2)
b	Defined in Eq. (2.40) ($1/°F$)
c_p	Isobaric specific heat (Btu/hr°F)
C_1	Defined in Eq. (4.20)
C_2	Defined in Eq. (4.20)
C_c	Consistency correction (dimensionless)
C_k	Defined in Eq. (4.20)
D	Inside tube diameter (ft)
$D1$	Outside tube diameter (ft)
g	Gravitational acceleration (ft/sec^2)
g_c	Gravitational constant in Newton's law
h	Heat transfer coefficient ($Btu/hrft^2°F$)
J	Conversion constant, 777.66 ($ft\ lb_f/Btu$)
k	Thermal conductivity (Btu/hrft°F)
$k1$	Thermal conductivity of the tube (Btu/hrft°F)
K	Consistency index ($lb_f\ sec^n/ft^2$)
K'	Modified consistency index ($lb_f\ sec^n/ft^2$)
L	Length of the test section (ft)
L_S	Length of the measuring station (ft)
$\dot{m}$	Mass flow rate (lb_m/hr)
$\hat{\dot{m}}$	Dimensionless mass flow, $m\rho_o\bar{u}_o/\mu^2_{a,o}$
n	Flow behavior index (dimensionless)
p	Pressure (lb_f/ft^2)

P	Dimensionless pressure ($pg_c/\rho_o\bar{u}_o^2$)
q"	Heat flux (Btu/hrft^2)
Q	Heat flow rate (Btu/hr)
Q_a	Heat absorbed by fluid (Btu/hr)
Q_s	Heat supplied (Btu/hr)
$\hat{Q}$	Dimensionless heat flux ($g_cJq"/3600\rho_o\bar{u}_o^3$)
r	Radius (ft)
R	Dimensionless radius ($\rho_o u_o r/\mu_o$)
t	Temperature (°F)
T	Dimensionless temperature ($g_cJcp_o t/\bar{u}_o^2$)
u	Axial velocity (ft/sec)
U	Dimensionless axial velocity ($u/\bar{u}_o$)
v	Radial velocity (ft/sec)
V	Dimensionless radial velocity ($v/\bar{u}_o$)
w	Tube wall thickness (ft)
x	Distance from the tube inlet (ft)
y	Distance from the tube wall (ft)
Y	Dimensionless distance from the wall ($\rho_o\bar{u}_o y/\mu_{a,o}$)

Greek Symbols

β	Isobaric coefficient of thermal expansion ($\frac{1}{\rho}\frac{d\rho}{dt}$, °F^{-1})
γ	Consistency parameter ($-\frac{1}{\mu}\frac{d\mu}{dt}$ or $-\frac{1}{K}\frac{dK}{dt}$, °F^{-1})
ρ	Density (lb$_m$/ft^3)
$\hat{\rho}$	Dimensionless density (ρ/ρ_o)
μ	Viscosity (lb$_m$/ft sec)

μ_a	Apparent viscosity, $K(\frac{du}{dy})^{n-1}$
μ_{eff}	Effective viscosity $\frac{\tau_w}{(\frac{\delta\bar{u}}{D})}$ $(lb_f\ sec^n/ft^2)$
$\hat{\mu}$	Dimensionless viscosity (μ_a/μ_o)
τ	Shear stress (lb_f/ft^2)
Δ	$\frac{3n+1}{4n}$ (dimensionless)
Δp	Pressure drop (lb_f/ft^2)
ΔT	$\frac{q''_w\ D}{2k}$ $(°F^{-1})$

Dimensionless Numbers

Br	$4(\frac{\bar{u}}{D})^{n+1}\ \frac{K_o}{Jkt_o}$
f	Fanning friction factor (64/Re)
Gr	Grashof number $\frac{\rho^2 g\beta\Delta t D^3}{\mu_{eff}^2}$
Gz	Local Graetz number $(\frac{\dot{m}c_p}{kx})$
Gz_L	Average Graetz number $(\frac{\dot{m}c_p}{kL})$
Pr	Effective Prandtl number $(\mu_{eff}c_p/k)$
Pr_a	Apparent Prandtl number $(\mu_a c_p/k)$
Ra	Rayleigh number (GrPr)
Re	Effective Reynolds number $(\rho D\bar{u}/\mu_{eff})$
Re_a	Apparent Reynolds number $(\rho D\bar{u}/\mu_a)$

X^+ Dimensionless distance $(\frac{2(x/D)}{RePr})$

Subscripts

am	Arithmetic mean temperature
b	Local bulk temperature
c	Tube centerline
cp	Constant property
e	Tube exit condition
lm	Logarithmic mean temperature
eff	Effective
o	Tube inlet condition
x	At distance x from the inlet
w	Wall temperature
∞	Fully developed condition
$\bar{}$	Bar indicates average quantity

Whenever a subscript is not specified, the properties are evaluated at local fluid bulk temperature.

$$\Delta X_+ = X_{i+1} - X_i$$

$$\Delta X_- = X_i - X_{i-1}$$

$$\Delta Y_+ = Y_{j+1} - Y_j$$

$$\Delta Y_- = Y_j - Y_{j-1}$$

CHAPTER I. INTRODUCTION

According to Newton's rate equation, shear stress is linearly dependent on shear rate. This rate equation is

$$\tau = \mu \left(\frac{du}{dy}\right) \tag{1.1}$$

where μ, a constant of proportionality, is referred to as Newtonian viscosity. For all gases and homogeneous non-polymeric liquids, the above relation holds. There are, however, quite a few industrially important fluids where shear stress and shear rate do not have a linear relationship. These fluids are referred to as non-Newtonian fluids. Industries where non-Newtonian behavior is encountered include those dealing with rubber, plastics, synthetic fibers, petroleum, soaps, detergents, pharmaceuticals, biological fluids, cement, food, paper pulp, paint, chemicals, fermentation processes, oil field operations, ore processing, and printing. Non-Newtonian fluids are commonly divided into three broad categories [1]:

Viscoelastic Fluids: These fluids show a partial elastic recovery upon the removal of deforming shear stress. Such materials possess properties of both fluids and elastic solids. Bitumens, flour dough, napalm, and polymer melts fall in this category.

Time-Dependent Fluids: In these fluids, shear rate is a function of both the magnitude and the duration of shear stress, and possibly of time lapsed between consecutive applications of shear stress. Grease, margarine, shortening, printing inks, and paints fall in this category.

Time-Independent Fluids: In these fluids, shear rate at a given

point is solely dependent upon the instantaneous shear stress at that point. Flow curves (shear stress versus shear rate) for various time-independent fluids are shown in Fig. 1.1.

The discussion will now center on this third category of non-Newtonian fluids. Some time-independent fluids exhibit a yield stress, τ_y. Certain plastic melts, chalk and rock slurries, oil well drilling muds, chocolate mixtures, and tooth paste fall in this category.

Figure 1.1 shows that pseudoplastic and dilatant fluids do not exhibit yield stress. The shear stress and shear rate relationship for these fluids can be described as

$$\tau = K \left(\frac{du}{dy}\right)^n \tag{1.2}$$

where K is the consistency index and n is the flow behavior index. In these fluids, shear stress and shear rate exhibit a log-linear relationship. On a logarithmic plot the flow behavior index, n, is the slope and the consistency index, K, is the intercept on shear stress axis at unit shear rate. The apparent viscosity for these power-law fluids is defined as

$$\mu_a = K \left(\frac{du}{dy}\right)^{n-1} \tag{1.3}$$

from which

$$\tau = \mu_a \left(\frac{du}{dy}\right) \tag{1.4}$$

Fluids having a flow behavior index greater than unity are known as dilatant fluids. In these fluids, there is an increase in apparent

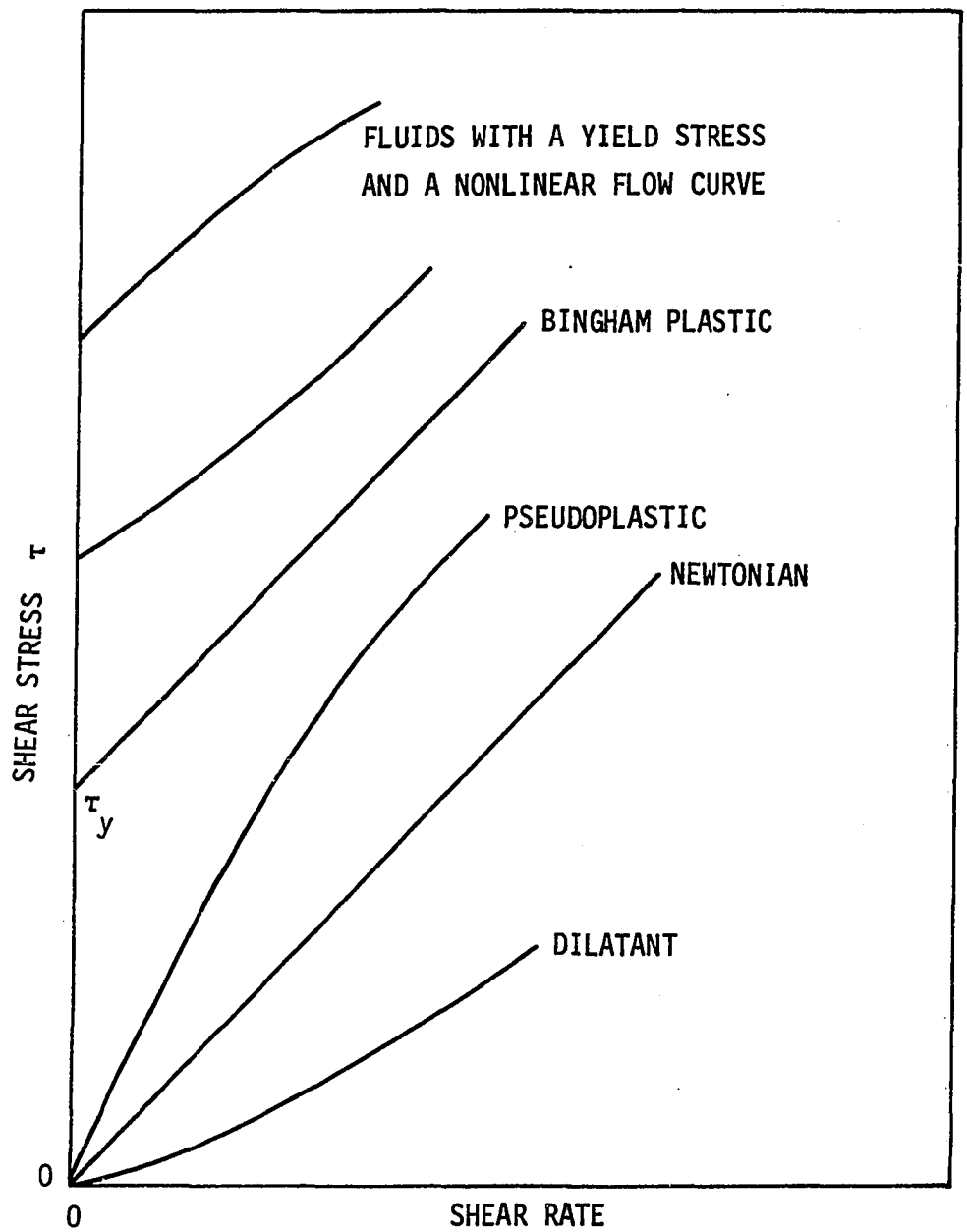

Fig. 1.1 Flow curves of various time-independent fluids (linear axes).

viscosity with increasing shear rate. Aqueous suspensions of titanium dioxide, corn flour solutions, and sugar solutions fall in this category.

Fluids having n less than unity are known as pseudoplastic fluids. In these fluids, the apparent viscosity decreases with increasing shear stress. Polymer solutions or melts, greases, starch suspensions, cellulose acetate, solutions used in rayon manufacturing, mayonnaise, soap and detergent slurries, paper pulp, napalm paint, and dispersion media in certain pharmaceutical industries fall in the category of pseudoplastic fluids.

The majority of the fluids used in the chemical process industry are pseudoplastic. The process industry's application of these fluids is mainly in the laminar flow region because of the inherent highly viscous nature of these fluids. Viscosities of the order of 100 centipoise (about 100 times that of water) are quite common. The laminar in-tube flow of pseudoplastic fluid has two limiting cases: 1) For a flow behavior index of $n = 0$, a uniform velocity profile will be obtained. 2) For a flow behavior index of $n = 1$, the power-law constitutive equation reduces to the Newtonian case, and a parabolic velocity profile is obtained. For all the intermediate values of n, the velocity profile will be somewhere between uniform and parabolic.

The peculiar nature of the velocity profile makes heat transfer to power-law fluids very interesting. An additional complication is that for most of these fluids, K and n are temperature dependent. Usually K is a stronger function of temperature than n. The strong temperature dependence of K causes the velocity profile to undergo substantial

changes and, consequently, alters the heat transfer. The temperature difference from bulk to wall generates a density gradient which may result in a significant superimposed free convection; this further complicates the heat transfer.

In a modern technological world, food and chemical process industries play a major role. Each year, a large number of heat exchangers are designed and manufactured for non-Newtonian fluids, particularly pseudoplastic fluids. Even today, there is a general lack of experimental data and precise methods to predict heat transfer coefficients needed to design these heat exchangers. This was the major motivation to undertake the present study of heat transfer to pseudoplastic fluids.

The majority of the process industry heat exchangers utilize circular tubes. Hence, it was decided to study heat transfer to highly viscous pseudoplastic fluids inside circular tubes. Newtonian fluids ($n = 1$) represent the limiting case of pseudoplastic fluids, and, therefore, for completeness, a study of heat transfer to highly viscous Newtonian fluids is also included. A combined analytical and experimental study is presented here.

In Chapters II, III, and IV, a review of analytical literature, analytical problem formulations, and results are discussed, respectively. In Chapters V, VI, and VII a review of experimental literature, experimental setup, and results are discussed, respectively. Conclusions and recommendations from this study are included in Chapter VIII.

CHAPTER II. REVIEW OF PREVIOUS ANALYTICAL SOLUTIONS

The purpose of this chapter is to review the state-of-the art of analytical solutions for laminar fluid flow heat transfer inside a circular tube. For convenience, the many applicable references are listed in Table 2.1. In this table, UWT refers to a uniform wall temperature and UHF refers to a uniform wall heat flux boundary condition. A Newtonian fluid is a special case of the family of non-Newtonian power law fluids. Conversely, many non-Newtonian heat transfer problems are looked upon as an extension of the corresponding Newtonian problem. This necessitates a clear-cut understanding of analytical solutions for Newtonian fluids.

Constant Property, Newtonian Heat Transfer

Fully developed

The problem of fully developed heat transfer with both UWT and UHF boundary conditions is a simple textbook problem [2,3]. The Nusselt numbers are 3.66 for a UWT and 4.36 for a UHF.

Thermally developing

The interest in laminar flow heat transfer in circular tubes dates back to 1883 when Graetz [4] solved the problem of thermally developing slug flow inside an isothermal tube. A series solution for the temperature profile was obtained. Two years later, Graetz [5] published a solution for a parabolic velocity profile. In honor of his pioneering

Table 2.1. References pertaining to laminar flow in circular tubes

	Newtonian		Non-Newtonian	
	UWT	UHF	UWT	UHF
Constant Properties				
Fully developed	Textbook	Textbook	22	22-24
Thermally developing	4-9,20	8-11,21	25-30	28,30,31
Thermally and hydrodynamically developing	8,12-15,78	8,12-17	25,29	28
Variable μ or K				
Fully developed	32	32-34	--	31
Thermally developing	32,35,36	32,34	39-43	30,31,44,45
Thermally and hydrodynamically developing	36	37	29,46,47	48

work, the problem of developing heat transfer inside an isothermal tube is called the "Graetz problem."

In 1910, Nusselt [6], apparently unaware of Graetz's solution, solved the problem once more in considerable detail and formulated a series solution for the non-dimensional heat transfer coefficient, which was later designated the "Nusselt number." In 1928, Leveque [7] also published a solution to the Graetz problem for high Pr fluids (viscous oils). These fluids have a very thin boundary layer and, hence, Leveque simply assumed linear velocity and temperature profiles. He correlated his predictions for average Nusselt number as

$$Nu_{am} = 1.75\ Gz_L^{1/3} \tag{2.1}$$

Where Gz_L is average Graetz number defined as

$$Gz_L = \frac{\dot{m}c_p}{kL} \tag{2.2}$$

Equation (2.1) is found to be a good approximation (when compared to other solutions) for $Gz > 200$.

In 1954, Kays [8] utilized a finite-difference formulation of the energy equation to solve the Graetz problem, obtaining both local and average Nusselt numbers. Worsøe-Schmidt [9] obtained local Nusselt numbers by using Leveque's technique in the entrance region and an eigenvalue solution further downstream.

At this point, it is appropriate to define various Nusselt numbers used in the heat transfer literature. The local Nusselt number is

$$Nu = \frac{h_x D}{k} \tag{2.3}$$

where $h_x = q''_w/(t_w - t_b)$ and t_w and t_b are local wall and bulk temperatures, respectively. For constant wall temperature heat exchangers, the arithmetic mean or logarithmic mean Nusselt numbers are of greater interest than the local value, since they may be used to determine heat transfer and the fluid outlet bulk temperature.

Consider the energy equation and the rate equations based on various definitions of heat transfer coefficient:

$$Q_w = \dot{m} c_p (t_e - t_o) \tag{2.4}$$

$$q''_w = \frac{Q_w}{A} = h_{am} \left(t_w - \left(\frac{t_o + t_e}{2}\right)\right) \tag{2.5a}$$

$$= h_{lm} \left\{ \frac{t_e - t_o}{\ln \left(\frac{t_w - t_o}{t_w - t_e}\right)} \right\} \tag{2.5b}$$

Kays [2] has also defined the average heat transfer coefficient h_m as

$$h_m = \frac{1}{X^+} \int_o^{X^+} h_{X^+} \, dX^+ \tag{2.6a}$$

where $$X^+ = \frac{2(x/D)}{RePr} = \frac{\pi}{2Gz} \tag{2.6b}$$

This h_m is identical to h_{lm}. If h is known, Eq. (2.4) and either (2.5a) or (2.5b) are utilized to solve for t_e, which then is used to compute Q_w.

A plot of various Nusselt numbers against Graetz numbers is shown in Fig. 2.1. In the thermal entrance length (Gz > 100) the various definitions of Nusselt number give nearly identical values, that is,

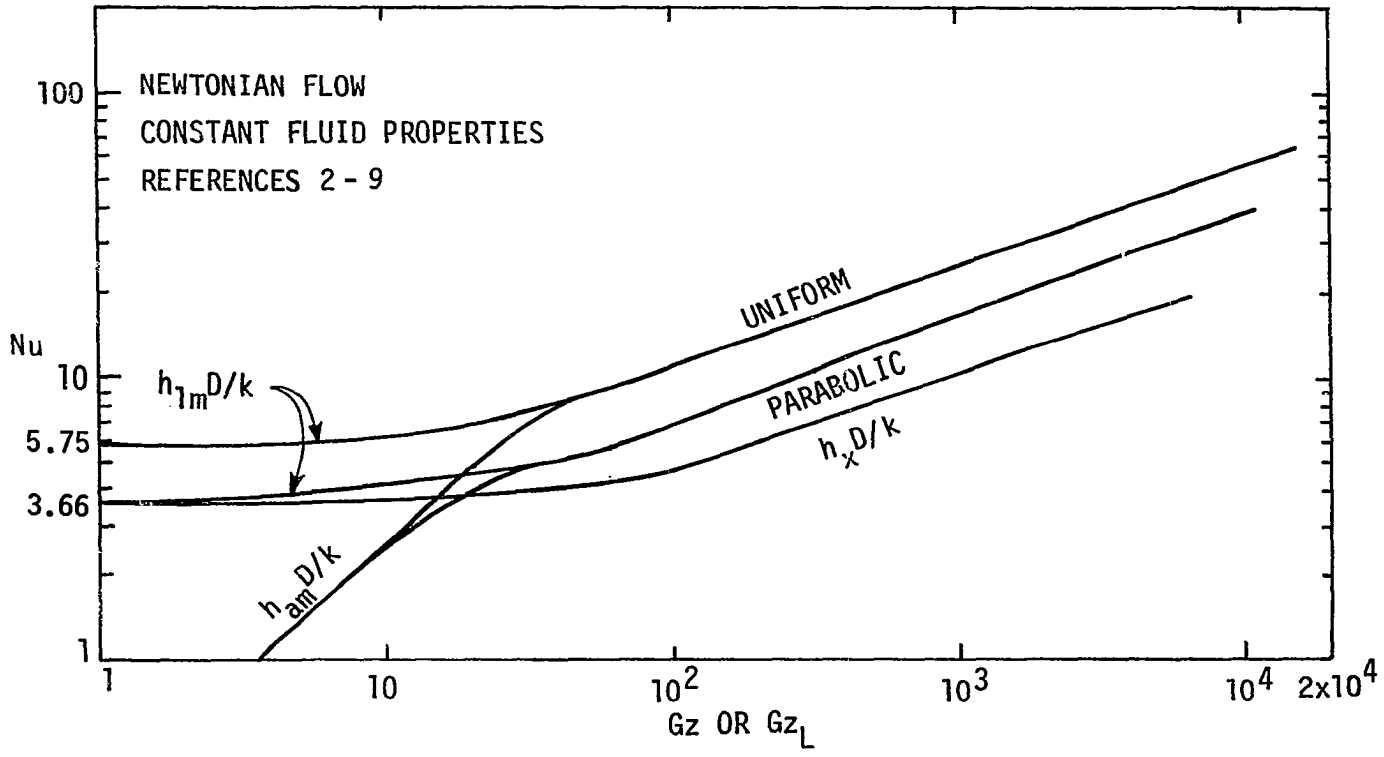

Fig. 2.1 Forced convection heat transfer in a circular tube with uniform wall temperature.

$$Nu_{am} \simeq Nu_{lm} \simeq Nu_{m} \tag{2.7}$$

for both slug and parabolic velocity profiles.

Sellars et al. [10], Siegel et al. [11], and others [8,9,12-17] have developed a solution for the entire thermal length with a UHF boundary condition. In this case, local values are of interest to obtain the wall temperature profile. Sellars et al. have extended the Graetz problem to this boundary condition. The drawback of this method is that one must know a large number of terms in the series solution for UWT before good accuracy can be obtained for UHF. Siegel et al. have presented a direct series solution. Normally, Nusselt numbers for the UHF are plotted against dimensionless axial distance, X^+, which is defined in Eq. (2.6b). A plot of heat transfer predictions for a UHF boundary condition is shown in Fig. 2.2.

Figures 2.1 and 2.2 show that results for slug profile are substantially higher than those for parabolic velocity profile. Mathematically, two extreme cases are represented. For a frictionless fluid, a slug profile solution is valid, while for a real Newtonian fluid a parabolic velocity profile solution is more appropriate. However, developing flow with Newtonian fluids involves a slug velocity profile at the entrance of the tube. The fluid velocity and temperature profiles are developing simultaneously; hence simultaneous solution of the energy and momentum equations is required.

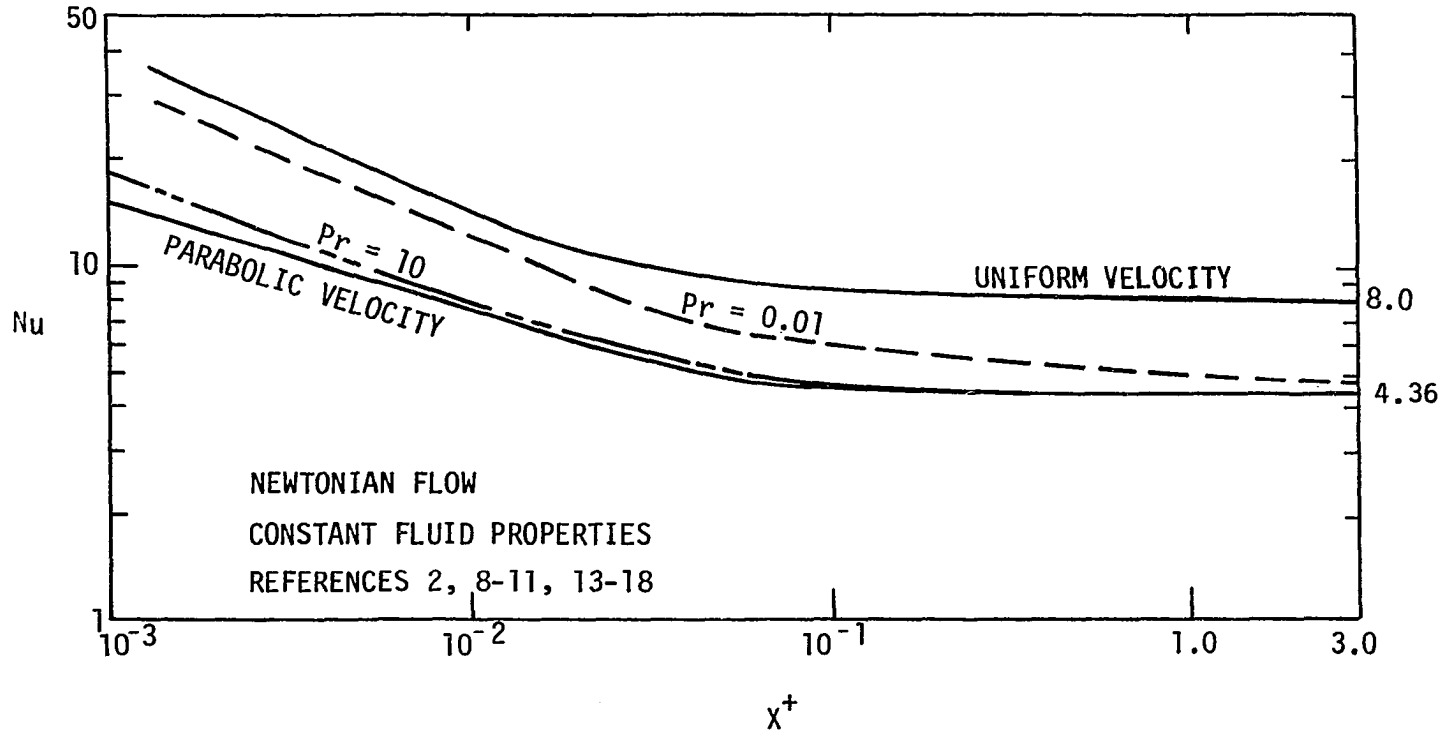

Fig. 2.2 Forced convection heat transfer in a circular tube with uniform wall heat flux.

Thermally and hydrodynamically developing

When velocity and temperature profiles are developing, the heat transfer coefficients are dependent on Pr. For fluids having Pr > 5, the fluid velocity profile develops much faster than the fluid thermal profile and, hence, the parabolic velocity profile solution gives adequately accurate predictions for all engineering calculations.

Tien and Pawelek [18] have studied high Pr fluids with UWT; except for the early part of the entrance region ($X^+ < 10^{-5}$), very little effect of Pr was noticed. However, Kays [8] and others [12-15] have demonstrated a significant effect of Pr on the local Nusselt number values for this boundary condition. A plot of this effect is shown in Fig. 2.3. A similar effect for a UHF is demonstrated by Kays [8] and others [12-18]. A plot of their predictions is shown in Fig. 2.2.

Effects of axial conduction and viscous dissipation

In all of the solutions mentioned in the preceding sections, axial conduction has been neglected, i.e., it has been assumed that conduction in the axial direction is negligible relative to the axial energy transport by the bulk movement of the fluid. The significant non-dimensional parameter in considering the influence of axial conduction is the Peclet Number (Pe = RePr). Singh [19] has suggested, on the basis of analytical studies, that for Pe > 100, axial conduction effects can be neglected. A series solution for thermally developing low Peclet number flow has been obtained by Munakata [20] for UWT and by Hsu [21] for UHF. McMordie and Emery [17] have analytically studied the effect of axial

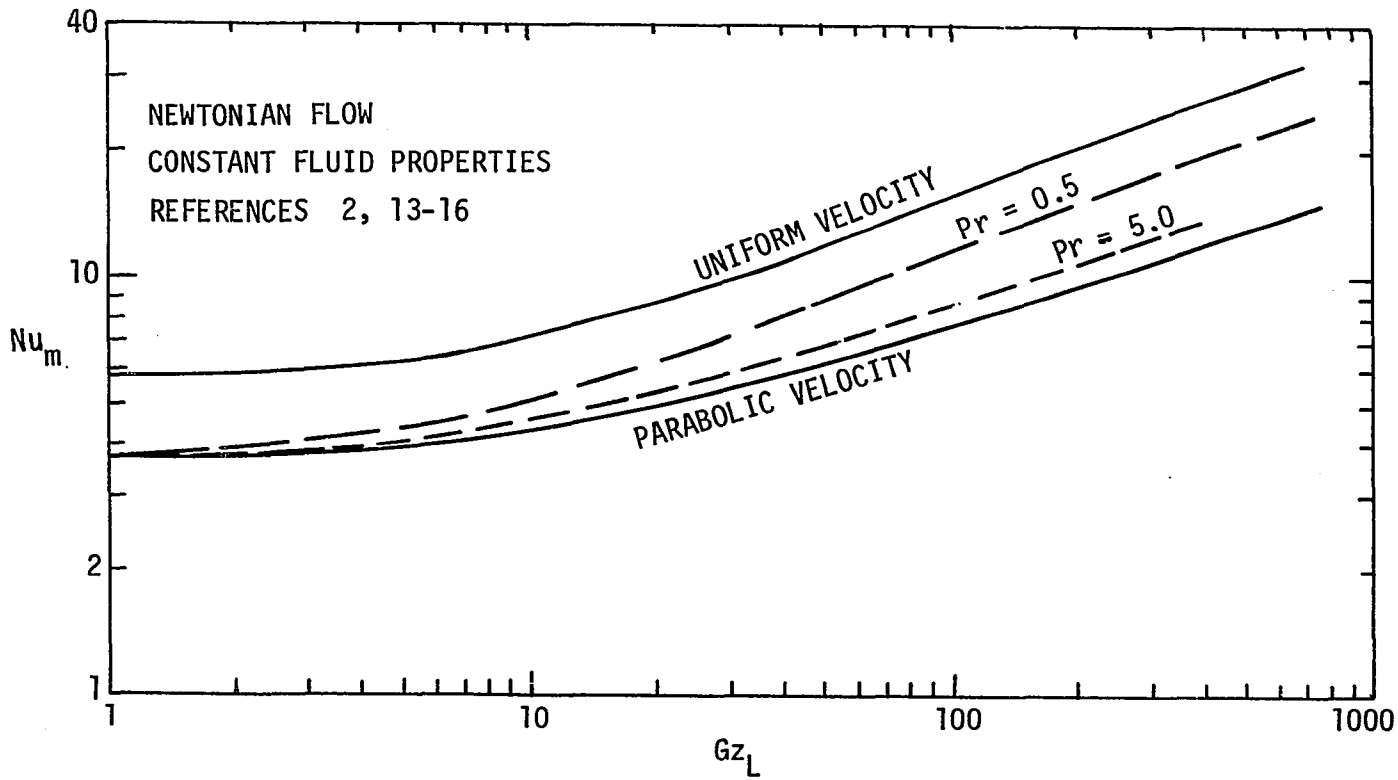

Fig. 2.3 Forced convection heat transfer in a circular tube with developing flows and a uniform wall temperature.

conduction on low Pr fluids (Pr < 0.01, liquid metals) and demonstrated that the thermal entrance region for these fluids is very short (of the order of $\frac{x}{D}$ = 2-3) and, hence, axial conduction can be neglected for virtually all engineering calculations.

Many viscous liquids exhibit a significant amount of viscous dissipation, which causes an increase in fluid temperature near the wall thereby retarding the heat transfer rate at the wall. Normally, the Brinkman number (Br) is used as the measure of viscous dissipation. For most engineering fluids, Br is of the order of 0.01 and, hence, has an insignificant effect on the heat transfer. However, Br of the order of 1 indicates significant viscous dissipation and Br of the order of 10 can even reverse heat transfer at the wall from heating and cooling. Hornbeck [13] has studied this effect and has demonstrated the significant decrease in heat transfer coefficients.

Conclusion

From the preceding discussion it can be concluded that the constant property Newtonian heat transfer solutions are well-established, and there seems to be no need for any further work.

Constant Property, Non-Newtonian Heat Transfer

Fully developed

Beek and Eggink [22] have obtained an exact analytical solution for fully developed heat transfer in in-tube flow of non-Newtonian power-law fluids. For a UWT boundary condition they correlated the asymptotic

Nusselt number as

$$Nu_{\infty} = \frac{n+1}{3n+1} \quad \frac{16\pi}{9} \left\{ \frac{\left(\frac{3n+1}{2n+2}\right)!}{(n/(n+1))!} \right\} \tag{2.8}$$

This expression reduces to 3.66 for n = 1 (Newtonian parabolic flow) and to 5.72 for n = 0 (slug flow).

For a UHF boundary condition, Beek and Eggink [22], Grigull [23], and Kutateladze et al. [24] have obtained exact analytical solutions. Beek and Eggink have correlated their predictions as

$$Nu_{\infty} = 8 \left\{ \frac{15\ n^3 + 23\ n^2 + 9\ n + 1}{31\ n^3 + 43\ n^2 + 12\ n + 1} \right\} \tag{2.9}$$

while Grigull's predictions are correlated as

$$Nu_{\infty} = \frac{-2(N+1)^2}{5 + N - \frac{2}{N+3} - \frac{4 + (N+3)^2}{N+5} - \frac{(N+3)^2}{4}} \tag{2.10}$$

where N = 1/n. Equations (2.9) and (2.10) are identical and both of them reduce to 4.36 for n = 1 and to 8.0 for n = 0.

Thermally developing

The problem of heat transfer to non-Newtonian power law fluid inside an isothermal tube has been always looked upon as an extension of the Graetz problem. Pigford [25] extended Leveque's solution for thermally developing Newtonial flow, Eq. (2.1) to non-Newtonian fluids and has correlated his predictions as

$$Nu = 1.75\ (\Delta\ Gz)^{1/3} \tag{2.11}$$

where $\Delta^{1/3}$ represents a non-Newtonian correction. Physically, Δ represents the ratio of the velocity gradients at the tube wall for non-Newtonial and Newtonian flow, and, hence, is related to the ratio of the respective heat transfer rates at the tube wall. Pigford further demonstrated that for pseudoplastic fluids

$$\Delta = \frac{3n + 1}{4\ n} \tag{2.12}$$

Since Pigford's solution is an extension of Leveque's solution, its validity is restricted to the entrance region.

Lyche and Bird [26], Whiteman and Drake [27], and others [28,29,30] have also solved the problem of thermally developing flow inside a UWT tube. Lyche and Bird have obtained a series solution, while Whiteman and Drake have extended the solution of Sellars et al. [10] to a non-Newtonian case. Most of the investigators have obtained predictions for n = 0.0, 0.5 and 1.0 and their predictions are in fairly good agreement.

The problem of thermally developing flow inside a tube subjected to a UHF boundary condition was solved by McKillop [28], Mizushina et al. [31] and Cochrane [30]. The predictions of these investigators, for n = 0.0 and 0.5 are in good agreement, while predictions for n = 0.25 and 0.75 are obtained only by Cochrane and, hence, no comparison is possible. McKillop's predictions for n = 0.0 and 1.0 are shown in Fig. 2.4. It is distinctly seen that the pseudoplasticity increases the heat transfer coefficients above the Newtonian values. This

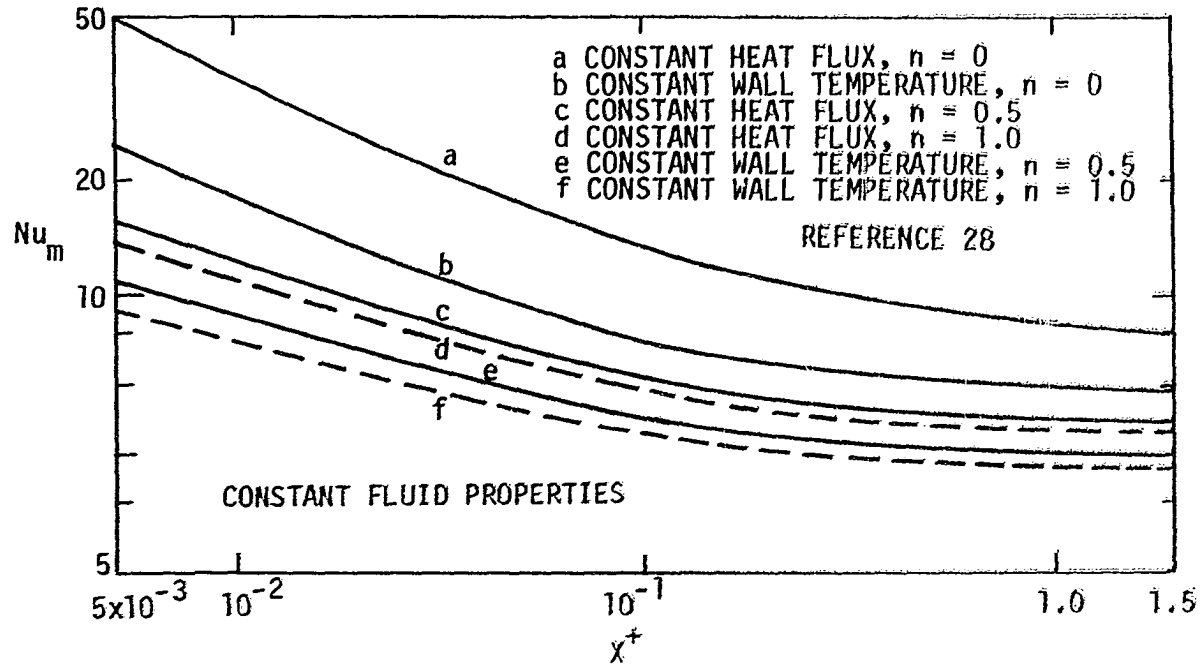

Fig. 2.4 Forced convection heat transfer in a circular tube for the flow of non-Newtonian fluids.

occurs throughout the entire thermal length, with the largest increase occurring at the lower values of n. Mizushina et al. [31] have used Pigford's non-Newtonian correction, $\Delta^{1/3}$, to correlate this increment. However, no analytical basis was given for this correction, and the correction was not verified for any value of n in the thermal entrance region.

Thermally and hydrodynamically developing

The majority of pseudoplastic fluids are highly viscous so that $Pr \gg 5$. Hence, the problem of thermally and hydrodynamically developing flow is only of an academic interest. McKillop [28] demonstrated this effect for n = 0.5 for both UHF and UWT boundary conditions at Pr = 1, 10, and 100. The predicted Nusselt numbers for Pr = 10 and 100 are identical except for the early part of the entrance region ($X^+ < 5x10^{-3}$).

Conclusion

Pr for pseudoplastic fluid is so high that only thermally developing flow is of interest. The traditional non-Newtonian correction, $\Delta^{1/3}$, needs to be verified for various values of n, for both UHF and UWT boundary conditions. In order to do this, heat transfer predictions for various values of n need to be verified and correlated.

Variable-Property Predictions

In all the preceding solutions, it has been assumed that the fluid properties remain constant throughout the flow field. When real heat transfer problems are considered, this assumption is obviously an idealization. The transport properties of most fluids vary with temperature, and, thus, will vary over the flow cross-section of a tube. The temperature-dependent property problem is further complicated by the fact that the properties of different fluids behave differently with temperature. For gases, the specific heat varies only slightly with temperature, but μ and k increase with about the 0.8 power of the absolute temperature. The net result is that Pr does not vary significantly with temperature. Since ρ varies inversely with the first power of the absolute temperature, strong free convection effects may be present.

For most liquids, c_p and k are relatively independent of temperature. But μ, for Newtonian liquids, and K, for pseudoplastic liquids, vary markedly with temperature. This temperature dependence is especially pronounced for viscous oils and pseudoplastic liquids; however, even with water, μ is highly temperature dependent. Pr thus varies with temperature in the same manner as μ or K. The density of liquids varies little with temperature; however, free convection effects arising due to density variation are important for $Ra > 10^4$. Such a high Ra is rarely realized in the flow of highly viscous pseudoplastic and Newtonian liquids; hence, free convection effects for these liquids can be neglected.

Since the temperature dependence of μ and K is of most practical interest, further review of the literature is restricted to the effects of these properties on heat transfer. In the equations cited in the following discussion, all properties are evaluated at liquid bulk temperature, unless stated otherwise.

Variable μ, Newtonian Heat Transfer

Fully developed

Even in long tubes, fluid velocity and temperature profiles do undergo some changes due to μ variation. However, these changes are very small, giving an asymptotic value of Nusselt number.

Yang [32] analytically obtained the solution for both UHF and UWT boundary conditions. The μ-t relation he used is

$$\mu/\mu_w = \left(1 + A \left(\frac{t_w - t}{t_w - t_o}\right)\right)^{-1} \tag{2.13}$$

and his predictions for both boundary conditions were correlated as

$$Nu/Nu_{cp} = (\mu/\mu_w)^{0.11} \tag{2.14}$$

Deissler [33] also solved this problem for a UHF boundary condition for liquids having

$$\mu \propto t^{-1.6} \tag{2.15}$$

The predictions are correlated as

$$Nu/Nu_{cp} = (\mu/\mu_w)^{0.14} \tag{2.16}$$

A similar analysis for the UHF boundary condition has been done by Shannon and Depew [34]. The μ-t relation they used in their calculation is

$$\mu = \mu_o \exp\ (-\gamma(t-t_o)) \tag{2.17}$$

For $\mu/\mu_w < 5$, their predictions are the same as that of Deissler (Eq. (2.16)). However, for $\mu/\mu_w > 10$, Nu/Nu_{cp} is independent of μ/μ_w and shows an asymptotic value of 1.5.

From the preceding discussion, it is evident that there is relatively good agreement on the correction factor for temperature-dependent viscosity. However, some more work is needed to resolve the ambiguities above $\mu/\mu_w > 5$.

Thermally developing

The generalized two-dimensional governing equations with the following assumptions:

1. steady, axisymmetric flow
2. body force absent
3. negligible axial conduction and viscous dissipation
4. μ is temperature-dependent (note that ρ can also be temperature-dependent)

reduce to:

Momentum

$$\rho u \frac{\partial u}{\partial x} + \rho v \frac{\partial u}{\partial y} = - \frac{dp}{dx} - \frac{1\partial}{r\partial r} (\tau r) \tag{2.18}$$

where $\tau = \mu(\partial u/\partial y)$

Energy

$$\rho u c_p \frac{\partial t}{\partial x} + \rho v c_p \frac{\partial t}{\partial r} = \frac{1}{r} \frac{\partial}{\partial r} (r q_r'') \tag{2.19}$$

Continuity

$$\frac{\partial v}{\partial r} + \frac{v}{r} + \frac{\partial u}{\partial x} = 0 \tag{2.20}$$

For thermally developing flow, the fluid velocity profile is fully developed at the onset of heating. This profile does undergo some changes due to μ variation. Often it is assumed that this change in velocity profile is very small and, hence, $\frac{\partial u}{\partial x} = 0$ and $v = 0$. This reduces Eqs. (2.18) to (2.20) to

Momentum

$$\frac{1}{r} \frac{\partial}{\partial r} (r\tau) = - \frac{dp}{dx} \tag{2.21}$$

Energy

$$\rho u c_p \frac{\partial t}{\partial x} = \frac{1}{r} \frac{\partial}{\partial r} (r q_r'')) \tag{2.22}$$

Continuity

$$\frac{\partial u}{\partial x} = 0 \tag{2.23}$$

Equation (2.21) is integrated to obtain the velocity profile which is substituted in Eq. (2.22) to obtain the temperature profile, and, finally, the heat transfer coefficients.

Yang [32] and Shannon and Depew [34] have solved this set of equations (Eqs. (2.21) to (2.23)). Yang obtained the solution for both UWT and UHF boundary conditions. The μ-t relation used by Yang and his

final results are given in Eqs. (2.13) and (2.14), the correction for variable properties is thus the same for developing and developed regions. Shannon and Depew have done a similar analysis for a UHF boundary condition, but their predictions differ from Yang's, particularly in the entrance region. Shannon and Depew correlated their predictions as

$$Nu/Nu_{cp} = (\mu/\mu_w)^m \tag{2.24}$$

where $$m = f(X^+) \tag{2.25}$$

At the entrance of the tube, m is of the order of 0.3 and decreases to 0.14 in the fully developed region. Thus, there is a substantial discrepancy between these two analyses.

Test [35] has done an elaborate analysis for a UWT boundary condition. He argued that the velocity profile does change, due to viscosity change and, hence, $\frac{\partial u}{\partial x} \neq 0$ and $v \neq 0$. Therefore, the inertia terms $\rho u \frac{\partial u}{\partial x}$ and $\rho v \frac{\partial u}{\partial y}$ in the momentum equation and $\rho v c_p \frac{\partial t}{\partial r}$ in the energy equation need to be retained. Test included all these terms and solved Eqs. (2.18) to (2.20) (with an additional viscous dissipation term in Eq. (2.20)) numerically using a logarithmic μ-t relation to approximate the viscosity of SAE60 oil.

Test demonstrated that inclusion of the terms $\partial u/\partial r$ and viscous dissipation $\mu(\frac{\partial u}{\partial y})^2$ does not appreciably alter the results. However, the convection term was found to have some effect. The final predictions for local Nusselt number in the thermal entrance length were correlated as

$$Nu\ (\mu_w/\mu)^{0.05} = 1.4\ (RePr\ \frac{D}{L})^{1/3} \qquad (2.26)$$

Rosenberg and Hellums [36] have also solved Eqs. (2.18) to (2.20) for a UWT boundary condition. An inverse linear μ-t relation was used in their calculation:

$$\frac{1}{\mu} = C_1 + C_2 t \qquad (2.27)$$

Most of the predictions obtained by these authors [36] are restricted to a very small initial portion of the thermal entrance length ($Gz > 10^4$). No correlation was offered and, hence, these predictions of local Nusselt number are only useful to understand the qualitative effects of viscosity variation. Thus, for thermally developing flows, some more work is needed for an entrance region solution for a UHF boundary condition.

Thermally and hydrodynamically developing

In this case, the governing equations are again Eqs. (2.18) to (2.20); however, the fluid will have a slug profile at the entrance of the heated tube. The solutions to these equations are published by Rosenberg and Hellums [36] for a UWT and by Martin and Fargie [37] for a UHF boundary condition.

As mentioned earlier, most fluids having strong temperature-dependent viscosity have Pr >> 5 and, hence, the predictions of thermally developing flow give sufficient accuracy for engineering calculations. No further work seems to be necessary.

Conclusion

There seems to be some more work needed for the UHF boundary condition in the thermal entrance region to clarify the discrepancy in the solutions of Shannon and Depew, and Yang. Some work is also needed in the fully developed region.

Variable K, Non-Newtonian Heat Transfer

In this section the discussion of non-Newtonian heat transfer is restricted to pseudoplastic fluids.

Fully developed

Fully developed heat transfer inside an isothermal tube has not been studied so far. However, Mizushina et al. [31] studied fully developed heat transfer for a tube subjected to a UHF boundary condition. They have demonstrated an asymptotic nature of the consistency correction, and have correlated their prediction as

$$\left(\frac{Nu}{Nu_{cp}}\right)_{\infty} = \Delta^{1/3}\left(\frac{K}{K_w}\right)^{m} \tag{2.28}$$

where $m = 0.14/n^{0.7}$

Mizushina et al. used the following K-t relation in their analysis:

$$K = K_o\left(1 + B\left(\frac{t - t_o}{t_o}\right)\right)^{-n} \tag{2.29}$$

Since this K-t relationship is more complex than that usually encountered,

more work in this area appears to be required.

Thermally developing (UWT)

In this section, solutions for a UWT boundary condition are discussed. The governing Eqs., (2.18) to (2.23), are applicable here also, with the only difference being in the constitutive equation which has been indicated previously as

$$\tau = K\,(du/dy)^n \tag{1.2}$$

In the early days, there were a few experimental studies [1] which resulted in correlations such as

$$Nu_{am} = 1.75(\Delta Gz)^{1/3}\,(K_{am}/K_w)^{0.14} \tag{2.30}$$

In this correlation, as $n \to 0$, $\Delta \to \infty$; thus, this correlation is mathematically inconsistent. The exponent $m = 0.14$ is a mere extension of the Sieder and Tate [38] Newtonian correction, without any analytical basis. Christiansen and Craig [39] realized these shortcomings and presented the first integro-numerical solution for Eqs. (2.21) to (2.23). An arhenius-type constitutive equation was used:

$$\tau = K\,\left(\frac{\partial u}{\partial y}\exp\left(\frac{\Delta H}{RT}\right)\right)^n \tag{2.31}$$

where K, n, and $\Delta H/R$ are constants, T is absolute temperature, and ΔH represents an activation energy per mole of flow. A Sieder-and-Tate type correction to the constant property Nusselt number was devised as

$$\left(\frac{K_{am}}{K_w}\right)^{0.14} = \exp\left(\frac{\Delta H}{R}\left(\frac{1}{T_{am}} - \frac{1}{T_w}\right)\right)^{0.14} \qquad (2.32)$$

Christiansen and Craig have done elaborate calculations to show that their correction gives better predictions than $\Delta^{1/3}\,(K_{am}/K_w)^{0.14}$. Normally, near the tube inlet, constant property and variable consistency Nusselt numbers are expected to be approximately equal. An increment in the Nusselt number due to consistency variation is observed some distance downstream from the tube inlet. In contrast, the Christiansen and Craig solution results in exorbitantly high Nusselt numbers near the tube inlet. Christiansen et al. [40] have extended the Christiansen and Craig solution to the cooling of pseudoplastic fluids.

Forrest and Wilkinson [41] studied the effect of viscous dissipation and internal heat generation. The K-t relation they used is

$$K = K_o\,(1 + B_o(t-t_o))^{-n} \qquad (2.33)$$

A substantial effect of consistency variation was demonstrated. To account for viscous dissipation, the Brinkman number for pseudoplastic fluid is defined as

$$Br = \left(\frac{2\bar{u}}{D}\right)^{n+1} \frac{K_o}{J\,k\,t_o} \qquad (2.34)$$

It was shown that Br of the order of 10 can reverse the heat transfer from heating to cooling. However, for laminar flow with small $\bar{u}$, Br will rarely exceed a value of 0.001, and, hence, viscous dissipation can be neglected for most fluids; but, if the fluid is highly viscous (high K_o), a substantial viscous dissipation can exist.

Kwant et al. [42] have utilized an approximate integral procedure

as well as the Crank-Nicolson numerical scheme to solve Eqs. (2.18) to (2.20). An exponential K-t relation was used in the calculation:

$$K = K_o \exp(-b(t-t_o)) \tag{2.35}$$

Predictions for various n were correlated in terms of the ratio of velocity gradients near the wall at the tube exit as

$$Nu_{lm}/Nu_{cp} = 1 + 0.271 \ln \phi_e + 0.023(\ln\phi_e)^2 \tag{2.36}$$

where $\phi_e = ((\partial u/\partial y)_w/(\partial u/\partial y)_{cp,w})_e$

Popovska and Wilkinson [43] have also developed a numerical solution. The K-t relation they used in their analysis is

$$K(t) = \exp(A + Bt + Ct^2 + \cdots) \tag{2.37}$$

They have concluded that Eq. (2.30) gives good predictions in the entrance region for all engineering calculations.

From the preceding discussion it is seen that there are numerous publications in this area, and sound analytical bases exist to predict heat transfer coefficients for the UWT boundary condition.

Thermally developing (UHF)

There are comparatively few studies in this area. Mizushina et al. [31] have also studied thermally developing flows. The K-t relation they used is given in Eq. (2.29). Their predictions for entrance region are correlated as

$$Nu = 1.41\ \Delta^{1/3}\ Gz^{1/3}\ (K/K_w)^{0.10/n^{0.7}} \qquad (2.38)$$

A fully developed correlation, Eq. (2.28) suggested by Mizushina et al. has been already discussed. Thus, Mizushina et al. have suggested two asymptotic equations to correlate predictions.

Cochrane [30] has utilized the Crank-Nicolson scheme to solve Eqs. (2.18) to (2.20). The viscous dissipation was also included in the energy equation, the effect of which was demonstrated to be insignificant. The τ-t relation he used is given in Eq. (2.31). For n = 1.0, 0.75, and 0.5 predictions are obtained for $\Delta H/RT$ = 5 and 10. Thus, the predictions were not extensive enough to allow the development of a generalized correlation. Cochrane's predictions for n = 0.5 are plotted in Fig. 2.5. A peculiar maximum Nusselt number is seen in his solution. No explanation is given for this phenomenon.

Equation (2.31) has its inherent weakness. For most fluids it is very difficult to know ΔH, the activation energy, unless the correct chemical composition of the fluid is known. This equation can be looked upon as

$$\tau = K(t)\ (\partial u/\partial y)^n \qquad (2.39)$$

where $K(t) = K \exp (n\ \Delta H/RT)$

This is an exponential form of K(t), and if n is constant, this equation is useful; however, for most pseudoplastic fluids, n is generally a function of the temperature, and it is difficult to use Eq. (2.39). These limitations of the constitutive equation notwithstanding, Cochrane

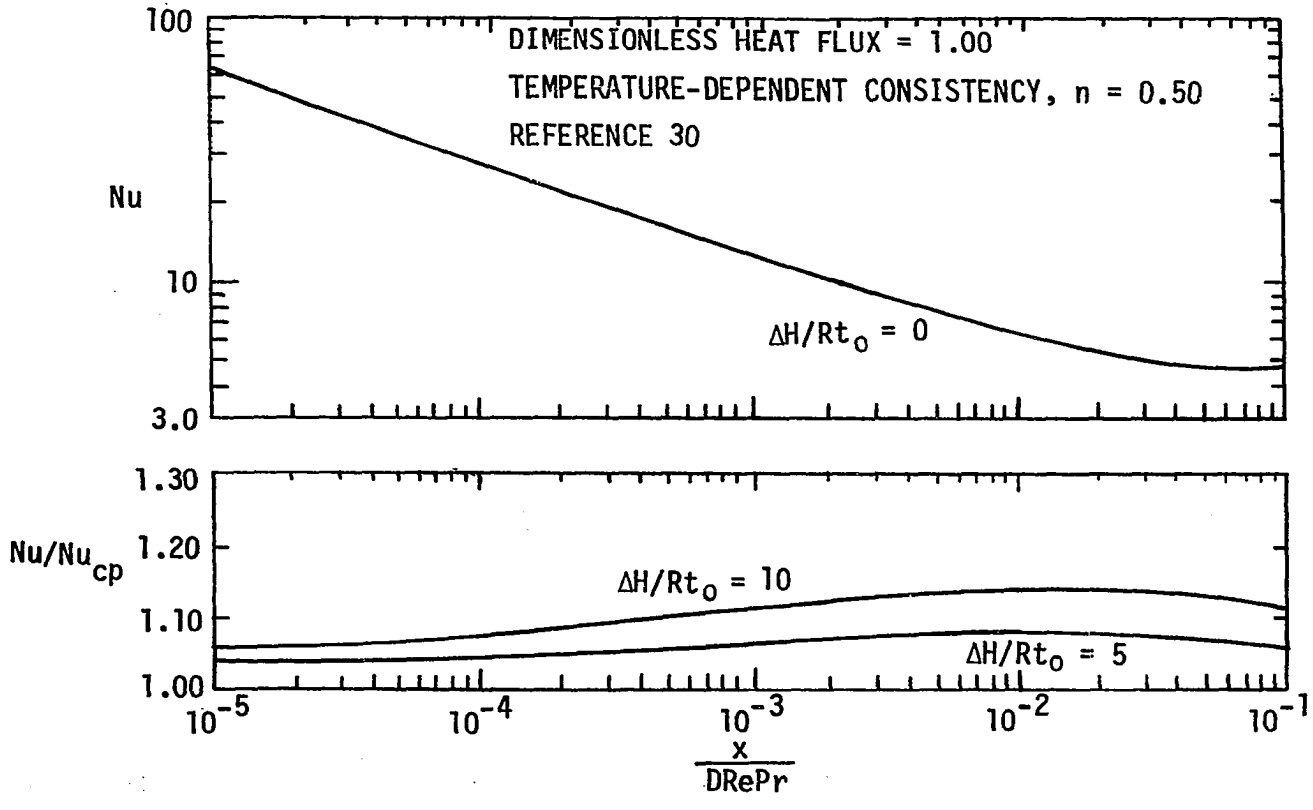

Fig. 2.5 Local Nusselt number for pipe flow with uniform heat flux and temperature-dependent consistency, (n = 0.50).

has provided an excellent foundation for future work.

Forrest and Wilkinson [44] have also developed an integro-numerical solution to study, in particular, the effect of viscous dissipation and internal heat generation. For a single value of wall heat flux, and for n = 0.5, predictions were obtained for various values of viscous dissipation and internal heat generation. A substantial effect of viscous dissipation was found at Br = 10.0. The K-t relation they used is given in Eq. (2.33). Mahalingam et al. [45] also published an integro-numerical solution to the energy equation. The K-t relation they used is given by

$$K = a \exp(-bt) \tag{2.40}$$

The solution was used to compute tube wall temperatures, which were compared with the authors' experimental results. A variation of the order of 15 to 20 percent was noticed. The predictions are not given in terms of n and, hence, are difficult to compare with other available solutions.

From the preceding discussion, it is seen that with variable K, only two predictions are available for n = 0.5 and 0.75. More predictions with variable K to cover a wider range of heat fluxes are needed for such intermediate values of n. There is also a need to establish a generalized correlation to correlate the predictions.

Thermally and hydrodynamically developing

In this case, Eqs. (2.18) to (2.20) need to be solved simultaneously. Korayem [29] and others [46,47] developed a solution for a UWT boundary condition while Bader et al. [48] developed a solution for a UHF boundary condition. Most of the pseudoplastic fluids are highly viscous and have $Pr >> 5$, thus, thermally developing solutions give adequately accurate predictions. Thus, there seems to be no need for further work in this area.

Conclusion

From the preceding discussion it is seen that a sound analytical basis is available to predict heat transfer coefficients for a UWT. However, for a UHF, for the entire thermal length, more predictions are needed over a wider range of heat fluxes, i.e., a wider range of K/K_w. To facilitate the work of a design engineer, a generalized correlation needs to be established.

Scope for Further Work and Problem Definition

The preceding review of literature indicates the need for further work in the following areas:

1) For Newtonian fluids, more predictions are needed to clarify the discrepancy between Yang's [32] and Shannon and DePew's [34] predictions in the entrance region for a UHF boundary condition. For completeness, predictions are also needed in the fully developed region.

2) For pseudoplastic fluids, a sound analytical basis exists to predict heat transfer coefficients for the UWT boundary condition. However, for a UHF boundary condition, more predictions are needed with variable K for both developing and thermally developing regions. This is particularly true for intermediate values of n, e.g., n = 0.75, 0.5. The predictions are also needed over a wider range of heat flux (wider range of K/K_w). There is also a need for a generalized correlation over a wide range of n and heat fluxes.

In addition to these areas, the following comments can be made about some of the deficiencies in presently available analytical solutions:

1) Various investigators use different forms of K-t or μ-t, and this makes it difficult to compare their predictions. The inadequacy of Cochrane's [30] τ-t relation, Eq. (2.31), has been already shown (Eq. 2.39). The literature [45] shows that most of the viscous pseudoplastic fluids exhibit the K-t relation given in Eq. (2.40). This exponential relationship is independent of n; hence, even if n is a function of temperature over a certain range, Eq. (2.40) can be used. Thus, a pseudoplastic analysis needs to be done for this K-t form.

2) All of the preceding solutions have used implicit numerical schemes. Very recently Pletcher [49] has developed a direct, simple, explicit numerical scheme using a stable Dufort-Frankel [50] method. This non-iterative method is economical of computer time, and has been used effectively to solve heat transfer problems by Pletcher and Nelson [51,52] and by Hong and Bergles [53, 54, 55]. It is desirable

to develop such a scheme to predict heat transfer in pseudoplastic fluids.

3) Most of the correlations for fully developed Newtonian or pseudoplastic fluids are of the form as shown in Eq. (2.16) or Eq. (2.28). For UHF this involves iteration for an unknown wall temperature t_w and μ_w. A direct, non-iterative equation would be welcomed by the designer.

From this discussion, a specification of the analysis to be performed is obtained as follows:

To devise an explicit numerical scheme to solve the problem of heat transfer in steady laminar flow of a pseudoplastic fluid inside a circular tube and, for completeness, the Newtonian case is also to be considered. The fluid consistency index, K, and density, ρ, are to be considered temperature-dependent; however, the free convection effects can be assumed to be negligible. All other fluid properties, such as k, c_p, and n, are independent of temperature. The inertia and viscous dissipation terms are to be retained in the momentum and energy equation, respectively. The K-t relation applicable to most industrial fluids

$$K = a \exp(-bt) \tag{2.40}$$

where a and b are constants, is to be used. The predictions are to be obtained for n = 1.0, 0.75, 0.50, and 0.25 for thermally developing flow inside a tube subjected to a UHF boundary condition, and presented in the form

$$Nu = f(Nu_{cp}, X^+, n) \tag{2.41}$$

CHAPTER III. NUMERICAL ANALYSIS

Introduction

After reviewing the literature, as summarized in the previous chapter, it was decided to develop an explicit numerical scheme to solve the problem of thermally developing heat transfer to the in-tube flow of pseudoplastic fluids with temperature-dependent properties. In this chapter, this scheme is described in detail. The coupled momentum and energy equations are solved explicitly. The method and the computer code developed can handle constant wall heat flux and constant wall temperature boundary conditions.

Problem Formulation

Statement of the problem

The problem considered here is a steady laminar flow of a pseudoplastic fluid inside a circular tube. The tube is subjected to a uniform wall heat flux boundary condition. At the inlet of the heated tube ($x = 0$), the fluid velocity profile is fully developed and the temperature profile is uniform. The fluid thermophysical properties can either be dependent or independent of temperature; however, buoyancy (free convection) effects are assumed to be negligible. The problem involves determining the temperature profile development and the variation in heat transfer coefficient along the axis.

In the present analysis, K and ρ are assumed to be temperature-dependent, while k, c_p, and n are assumed to be constant. However, as mentioned in the previous chapter, for viscous pseudoplastic

and Newtonian fluids, the K or μ variation is of primary importance, and the free convection effects arising due to ρ variation are insignificant. Hence, the buoyant term in the momentum equation is neglected. As free convection is neglected, the governing equations in the present problem are two-dimensional and axisymmetric. The results are thus independent of the geometric orientation of the tube.

The influence of pseudoplasticity on the fully developed velocity profile is shown in Fig. 3.1. The Newtonian fluid (n = 1.0) has a parabolic velocity profile. As n decreases, the fluid velocity profile becomes flatter and flatter, generating sharp velocity gradients near the wall and, finally, for n = 0, a slug profile is observed. A similar behavior is observed for the temperature profile. Considering the physics of the problem, boundary layer approximations are used here which state that the second derivatives in the stream-wise direction, $\partial^2/\partial x^2$, are negligible compared to those in the radial direction, $\partial^2/\partial r^2$, and the entire momentum equation for the radial direction can be dropped.

In the present problem, the fluid velocity is fully developed at the onset of heating; hence, at the inlet, v = 0. However, due to property variations the fluid velocity profile will undergo changes. Most of the previous analyses have assumed that these changes are negligible ($\partial u/\partial x = 0$, $v = 0$). For the fluids having strong temperature-dependent K or μ, $\partial u/\partial x$ may be significant and $v \neq 0$. It was thus decided to retain all inertia terms in the momentum equation, and retain the convective terms in the energy equation.

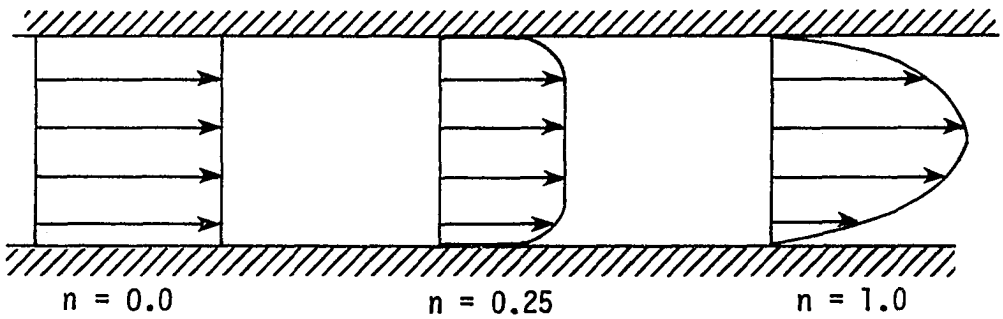

Fig. 3.1 Laminar velocity profiles for pseudoplastic fluids.

For the viscous pseudoplastic fluids, the viscous dissipation term may be significant [41,44]. However, Cochrane [30] and others [31,45] have found that the term has little effect on the results. Due to lack of clearcut guidelines, this term is retained in the present analysis.

Governing equations

In formulating the equations, the following assumptions are made:

1) Steady, axisymmetric flow

2) Axial conduction is neglected

3) Free convection effects are negligible

4) Usual boundary layer approximations are valid

5) Fluid properties K and ρ are temperature-dependent, while k, c_p, and n are temperature-independent.

With these assumptions, the general governing equations in cylindrical coordinates reduce to

momentum

$$\rho u \frac{\partial u}{\partial x} + \rho v \frac{\partial u}{\partial y} = - \frac{dp}{dx} + \frac{1}{r} \frac{\partial}{\partial y} (r\tau) \tag{3.1}$$

energy

$$\rho u c_p \frac{\partial t}{\partial x} + \rho v c_p \frac{\partial t}{\partial y} = \frac{\partial}{\partial y} (rk \frac{\partial t}{\partial r}) + \mu_a (\frac{\partial u}{\partial y})^2 \tag{3.2}$$

continuity

$$\frac{\partial}{\partial x}(\rho ur) + \frac{\partial}{\partial y}(\rho vr) = 0 \tag{3.3}$$

In these equations $\tau = K(\partial u/\partial y)^n$ with $(n \leq 1)$

and $\mu_a = K(\partial u/\partial y)^{n-1}$

The global continuity equation is also applicable:

$$\int_A \rho u dA = \text{constant} \tag{3.4}$$

Far away from the tube inlet, fully developed velocity and temperature profiles exist. In this region $v = 0$, $\frac{\partial u}{\partial x} = 0$, and $\frac{\partial t}{\partial x} = \frac{dt}{dx}$. The governing equations are then

momentum

$$-\frac{dp}{dx} + \frac{1}{r}\frac{\partial}{\partial y}(r\tau) = 0 \tag{3.5}$$

energy

$$\rho u c_p \frac{dt}{dx} = \frac{\partial}{\partial y}\left(rk\frac{\partial t}{\partial y}\right) + \mu_a \left(\frac{\partial u}{\partial y}\right)^2 \tag{3.6}$$

continuity

$$\frac{\partial u}{\partial x} = 0 \tag{3.7}$$

The boundary conditions for this problem are

For the velocity profile:

$$u(x,o) = 0,\ v(x,o) = 0,\ (\partial u/\partial y)_c = 0$$

For the temperature profile:

$$(k \frac{\partial t}{\partial y})_w = q''_w \quad \text{and} \quad (\frac{\partial t}{\partial y})_c = 0$$

The initial conditions are

$$u(o,y) = u(y)$$

$$t(o,y) = t_o$$

$$p(o) = p_o$$

Thus, there are four equations, (3.1) to (3.4), and four unknowns, u, v, t, and p, and there are sufficient boundary and initial conditions. Therefore, this problem is mathematically well posed.

Non-dimensionalized governing equations

The governing equations were non-dimensionalized. The list of standard non-dimensional parameters is given in the list of symbols. The resulting non-dimensional equations are

momentum

$$\hat{\rho}U \frac{\partial U}{\partial X} + \hat{\rho}V \frac{\partial U}{\partial Y} = - \frac{dP}{dX} + \frac{1}{R} \frac{\partial}{\partial Y} (R\hat{\mu}_a \frac{\partial U}{\partial Y}) \qquad (3.8a)$$

where

$$\hat{\mu}_a = \frac{\mu_a}{(\mu_a)_{w,o}} = \frac{K(\partial U/\partial Y)^{n-1}}{(K(\partial U/\partial Y)^{n-1})_{w,o}} \qquad (3.8b)$$

energy

$$\hat{\rho}\hat{U}\hat{C}_p \frac{\partial T}{\partial X} + \hat{\rho}\hat{V}\hat{C}_p \frac{\partial T}{\partial Y} = \frac{1}{R}\frac{\partial}{\partial Y}\left(R\hat{k}\frac{\partial T}{\partial Y}\right) + \hat{\mu}_a \left(\frac{\partial U}{\partial Y}\right)^2 \tag{3.9}$$

continuity

$$\frac{\partial}{\partial X}(\hat{\rho}UR) + \frac{\partial}{\partial Y}(\hat{\rho}VR) = 0 \tag{3.10}$$

global continuity

$$\hat{\dot{m}} = \int_{\hat{A}} \hat{\rho}U d\hat{A} = \text{constant} \tag{3.11}$$

The non-dimensional boundary and initial conditions are

$$U(X,0) = 0 \quad , \quad V(X,0) = 0$$

$$\left(\frac{\partial U}{\partial X}\right)_c = 0 \quad , \quad \left(\hat{k}\frac{\partial T}{\partial Y}\right)_w = \hat{Q}_w$$

$$\left(\frac{\partial T}{\partial Y}\right)_c = 0 \quad , \quad U(0,Y) = U(Y)$$

$$T(0,Y) = T(Y) \quad , \quad P(0) = P_o$$

Finite-Difference Formulation

Dufort-Frankel method

Figure 3.2 shows the finite difference grid used in the present analysis. An ordinary second-order explicit, central difference at point (i,j) is

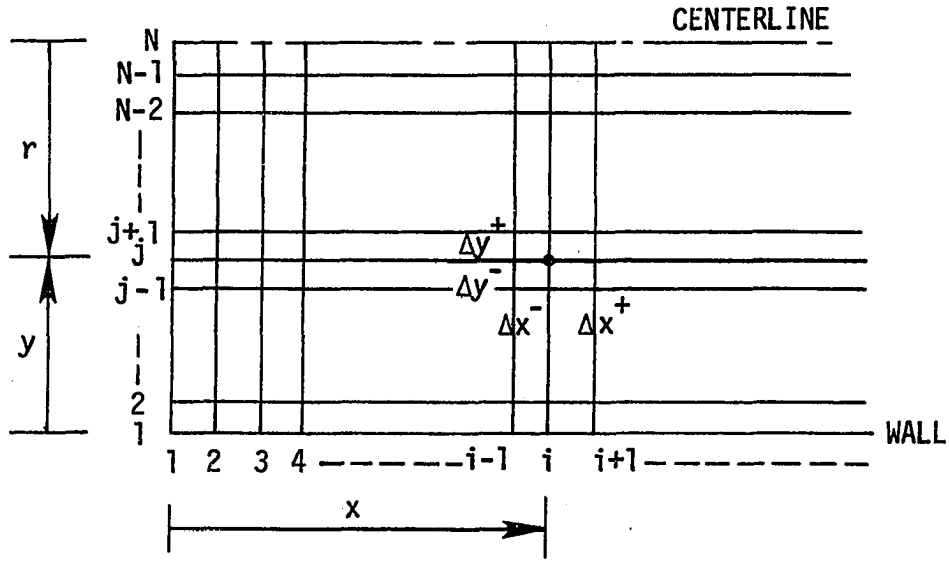

Fig. 3.2 The finite-difference grid.

$$\left(\frac{\partial^2 U}{\partial Y^2}\right) = \frac{U_{i,j+1} + U_{i,j-1} - 2U_{i,j}}{\Delta Y^2} + O(\Delta Y)^2 \qquad (3.12)$$

This formulation is found to be unstable. In the Dufort-Frankel method, the term $U_{i,j}$ is replaced by averaging $\frac{U_{i+1,j} + U_{i-1,j}}{2}$. This averaging is a special feature of the Dufort-Frankel method [50], which considerably enhances the stability of this explicit scheme. With this averaging Eq. (3.12) is modified to

$$\left(\frac{\partial^2 U}{\partial Y^2}\right)_{i,j} = \frac{U_{i,j+1} + U_{i,j-1} - U_{i+1,j} - U_{i-1,j}}{\Delta Y^2} + O\left(\Delta Y^2, \frac{\Delta X^2}{\Delta Y^2}\right) \qquad (3.13)$$

This equation is rewritten as

$$U_{i+1,j} = U_{i,j+1} + U_{i,j-1} - U_{i-1,j} - \left(\frac{\partial^2 U}{\partial Y^2}\right)_{i,j} \Delta Y^2 + O\left(\Delta Y^2, \frac{\Delta X^2}{\Delta Y^2}\right) \qquad (3.14)$$

It is seen that in this finite-difference formulation (Eq. (3.14)), $U_{i+1,j}$ can be solved explicitly in terms of known variables at the previous two streamwise steps, namely i and i-1.

Apparent viscosity formulation

The apparent viscosity for pseudoplastic fluids is

$$\mu_a = K \left(\frac{\partial u}{\partial y}\right)^{n-1} \qquad (1.3)$$

The finite-difference formulation for Eq. (3.8a) is

$$(\hat{\mu}_a)_{i,j} = K_{i,j} \left(\frac{U_{i,j+1} - U_{i,j-1}}{\Delta Y_+ + \Delta Y_-} \right)^{n-1} \Big/ (\mu_{a,o})_w \qquad (3.15)$$

It is seen from Eqs. (1.3) and (3.15) that as $(\partial U/\partial Y)_{i,j} \to 0$ $\hat{\mu}_{a,i,j} \to \infty$. Thus, at the tube centerline and in the region very close to it, $\hat{\mu}_{a,i,j}$ will be of an unrealistically high magnitude. To overcome

this singularity, the viscosity is computed from the wall, along the radius, up to the edge of the boundary layer, i.e., up to a point where

$$\left| \frac{U_{i,j}}{U_c} \right| < 0.995 \qquad (3.16)$$

All the points laying in between the edge of the boundary layer and the tube centerline, are assigned the same $\hat{\mu}_{a,i,j}$ value, as that on the edge of the boundary layer. Later, it will be seen from the results of the numerical analysis that this approximation does not affect the accuracy of the final predictions.

Finite-difference equations

The Dufort-Frankel finite-difference formulations and also the standard ordinary explicit formulations of non-dimensional momentum, energy and continuity equations are given in Appendix A.

Consistency, Stability, and Convergence of the Numerical Solution

Lax's equivalence theorem [56] states that for a well-posed initial value problem and its finite-difference approximation, consistency and stability are necessary and sufficient conditions for convergence. This criterion is valid for linear partial difference equations. However, even in the case of non-linear partial differential equations, this criterion was found to hold fairly well, even though, Lax's theorem has

never been proven for non-linear partial differential equations.

Consistency

Consistency deals with the degree to which the finite-difference equations approximate the partial differential equation. The difference between the two is called truncation error. A finite-difference representation of a partial differential equation is said to be consistent if the truncation error vanishes as the mesh is refined, i.e., Lim. mesh $\rightarrow$ 0, T.E. $\rightarrow$ 0.

Consistency is generally studied by expanding the dependent variables in a Taylor series and then estimating the truncation error. Generally, the smaller the truncation error, the faster is the convergence of the numerical scheme [56]. In the standard explicit scheme

$$\left(\frac{\partial U}{\partial Y}\right)_{i,j} = \frac{U_{i,j+1} - U_{i,j}}{\Delta Y} - \left(\frac{\partial^2 U}{\partial Y^2}\right)\frac{\Delta Y}{2} + \cdots$$
$$= \frac{U_{i,j+1} - U_{i,j}}{\Delta Y} + O(\Delta Y) \qquad (3.17)$$

where $O(\Delta Y)$ represents truncation error of the order ΔY. In the Dufort-Frankel scheme,

$$\left(\frac{\partial U}{\partial Y}\right)_{i,j} = \frac{U_{i,j+1} - U_{i,j-1}}{2\Delta Y} - \frac{\Delta Y^2}{3!}\left(\frac{\partial^3 U}{\partial Y^3}\right) + \cdots$$
$$= \frac{U_{i,j+1} - U_{i,j-1}}{2\Delta Y} + O(\Delta Y)^2 \qquad (3.18)$$

where $O(\Delta Y)^2$ represents truncation error of the order ΔY^2, which is

smaller than that noted for the standard ordinary explicit scheme. The finite-difference approximation of the second derivative by Dufort-Frankel scheme is

$$\left(\frac{\partial^2 U}{\partial Y^2}\right)_{i,j} \doteq \frac{U_{i,j+1} - U_{i+1,j} - U_{i-1,j} + U_{i,j-1}}{\Delta Y^2} + O(\Delta Y^2) + O\left(\frac{\partial^2 U}{\partial X^2}\right)\left(\frac{\Delta X^2}{\Delta Y^2}\right) \tag{3.19}$$

The truncation error here is

$$O\left(\frac{\Delta X^2}{\Delta Y^2}\right) + O(\Delta Y^2)$$

Thus, this formulation is mathematically consistent only if ΔX goes to zero faster than ΔY. This requirement, will severely restrict the step size in the streamwise direction. Fortunately, the entire term consists of $(\partial^2 U/\partial X^2)(\Delta X/\Delta Y)^2$ and for boundary layer flows, $\partial^2 U/\partial X^2$ is negligibly small as compared to other terms in the momentum equation. Therefore, even for $(\Delta X/\Delta Y) \simeq 1$, Eq. (3.19) satisfies the consistency requirement. The complete consistency analyses of momentum and energy equations are given in Appendix B (Eqs. (A.1) and (A.2)).

Stability

The essence of stability in obtaining the solution is that the sequence of numerical procedures must be such that errors from any source (round-off, truncation error, etc.) are not permitted to be amplified and swamp the solution, i.e., errors from any source must be damped as the calculations proceed from step to step. Mathematically,

this is expressed as: the error at the nth level should not grow when the computation is completed for the solution at the n+1 level.

O'Brien et al. [57] have used Von Neumann's criterion to compute stability of linear partial differential equations. This method has been found to give fairly good results even for the non-linear partial differential equations. In this method, local error is assumed to be of the form

$$\delta_{i,j} = e^{\alpha X} e^{\beta Y} \tag{3.20}$$

If D represents the exact solution of the partial differential equation and D+δ' represents the solution of its finite-difference approximation, then D+δ' must also satisfy the partial differential equation. The coefficients of the derivative terms are assumed locally constant or error free. This is a simplification and gives rise to a "local" stability criterion, but if the requirement is checked at each grid point, then it is reasoned that an instability could not originate. The condition for the error not to grow is $\left|\frac{\delta_{i+1,j}}{\delta_{i,j}}\right| < 1$, which can be reduced to

$$e^{\alpha \Delta X} < 1 \tag{3.21}$$

For the ordinary explicit method, a maximum allowable step size (ΔY) is found to be

$$(\Delta X)_{\max,j-1,N} \left\{ \frac{V_{i,j}}{U_{ij}\,\Delta Y_-} + \frac{(R_j+R_{j+1})(\hat{\mu}_{a,i,j}+\hat{\mu}_{a,i,j+1})}{2\hat{\rho}_{i,j}\,R_j\,U_{i,j}\,\Delta Y_+\,(\Delta Y_+ + \Delta Y_-)} + \right.$$

$$\left.\frac{(R_j+R_{j-1})(\hat{\mu}_{a,i,j}+\hat{\mu}_{a,i,j-1})}{2\hat{\rho}_{i,j}U_{i,j}R_j\Delta Y_-(\Delta Y_+ + \Delta Y_-)}\right\} \leq 1 \qquad (3.22)$$

Even though certain assumptions were made to simplify this stability analysis, the actual proof that the equations remain stable can be seen from the solutions obtained.

The Dufort-Frankel finite difference approximations do not have severe stability constraints [52,55,58]. In the present solution, the apparent viscosity μ_a is a function of local velocity gradient $(\partial U/\partial Y)_{i,j}$. This has some ramifications on the stability of the finite-difference scheme. In fact, some difficulty was encountered when computing with variable properties for n = 0.25.

Madni [58] has used similar finite-difference Dufort-Frankel approximations, and has found similar limitations on step sizes in turbulent, buoyent jet flows. In these turbulent flows, the local effective viscosity and thermal conductivity are dependent on the local velocity gradient $\partial U/\partial Y$. From the stability analysis, Madni has developed a stability criterion for uniform axial and radial grid spacing as

$$\Delta X_+ \leq \min_{j=2,N}\left\{\frac{U_{i,j}\,\Delta Y}{V_{i,j}+\dfrac{\hat{\mu}_{a,i,j-1}-\hat{\mu}_{a,i,j+1}}{2\Delta Y}}\right\} \qquad (3.23)$$

This criterion was found to give results which were too conservative and, hence, it was not used in the present numerical scheme, where no instability was noticed except for the case of n = 0.25. The instability in this case was eliminated by taking smaller axial step sizes, near

the tube inlet of the order of $(1/6)^{th}$ of the tube radius. This step size was much larger than that obtained from the criterion suggested by Madni.

In the present analysis, for n = 0.5, excellent results were obtained by taking axial step sizes equal to almost half of the tube radius at the tube entrance; further downstream the step sizes were increased to be equal to the tube radius. Somewhat smaller axial steps, of the order of one quarter of the tube radius at the tube entrance were employed for the variable property computation.

Method of Solution

Grid spacing in the radial direction

One of the major decisions to be made was the selection of the number of grid points along the radial direction in the tube. A simple procedure was followed to estimate an appropriate number of grid points. A straight-line fit was used to estimate the velocity gradient at the wall

$$\left(\frac{\partial U}{\partial Y}\right)_w = \frac{U_{i,2} - U_{i,1}}{\Delta Y_w} \tag{3.24}$$

A third-degree polynomial fit was also used to calculate the velocity gradient at the wall. The four points near the wall were used to do this as follows:

$$\left(\frac{\partial U}{\partial Y}\right)_w = (PSA)\ U_{i,1} + (PSB)\ U_{i,2} + (PSC)\ U_{i,3} + (PSD)\ U_{i,4} \tag{3.25}$$

where

$$PSB = \frac{1 + DYM + DYM^2}{\Delta Y_w \; DYM^2}$$

$$PSC = -\frac{1 + DYM + DYM^2}{\Delta Y_w \; (1+DYM) \; DYM^3}$$

$$PSD = \frac{1}{\Delta Y_w \; (1+DYM+DYM^2) \; DYM^3}$$

$$PSA = -(PSB + PSC + PSD)$$

and $$DYM = \Delta Y_j / \Delta Y_{j-1} \qquad (3.26)$$

It was found that for n = 1 to 0.5, the uniform grid spacing (DYM = 1) in the radial direction gave excellent results. (This was verified by using DYM = 1.05 and 1.10; no significant difference in the final predictions was noticed). However, for n = 0.25, a nonuniform grid spacing (DYM = 1.05) was found to give sufficient accuracy. In all the numerical computations, the radial grid spacing was refined until the velocity gradients at the wall, calculated by linear fit and polynomial fit, agreed to within 0.5 percent.

Numerical procedure

In the Dufort-Frankel finite-difference equation, the unknown variable at the i+1,j level is written in terms of known variables at the previous two streamwise (axial) steps, namely i and i-1. In a similar fashion, the equations of momentum, energy and continuity are

written explicitly and solved for the unknown values at streamwise step i+1 in terms of the previous streamwise steps (see Appendix A). Once all variables at streamwise step i+1 are known, they can be utilized to evaluate unknowns at streamwise step i+2. Thus, a "marching procedure" along the streamwise direction is followed. A flow chart of the numerical marching scheme used here is given in Fig. 3.3.

It should be noted here that the Dufort-Frankel method is a three-level method which utilizes information at the i and i-1 levels to calculate the variable at the i+1 level. At the inlet of the tube (x=0) information is known only at one station, i=1, and, hence, this three-level method cannot be used. In order to overcome this difficulty, for the first few initial steps (usually about the first 10 steps, near the tube inlet) a standard ordinary explicit method which requires information only from the previous step is used. The initial stability requirement for the ordinary explicit method allows larger initial steps, ΔX, in the axial direction; however, as the calculations progress along the axial direction, the stability requirement for the ordinary explicit scheme demands smaller and smaller axial steps. Therefore, an ordinary explicit scheme is used only for the first few steps and then the Dufort-Frankel method takes over. In general, it is desirable to use the largest possible ΔX, as this means fewer steps to cover the flow field and, hence, less computer time.

Once the Dufort-Frankel finite-difference equations take over, the step size for these equations is chosen as a constant multiple of the boundary layer thickness. This axial step size is increased progressively

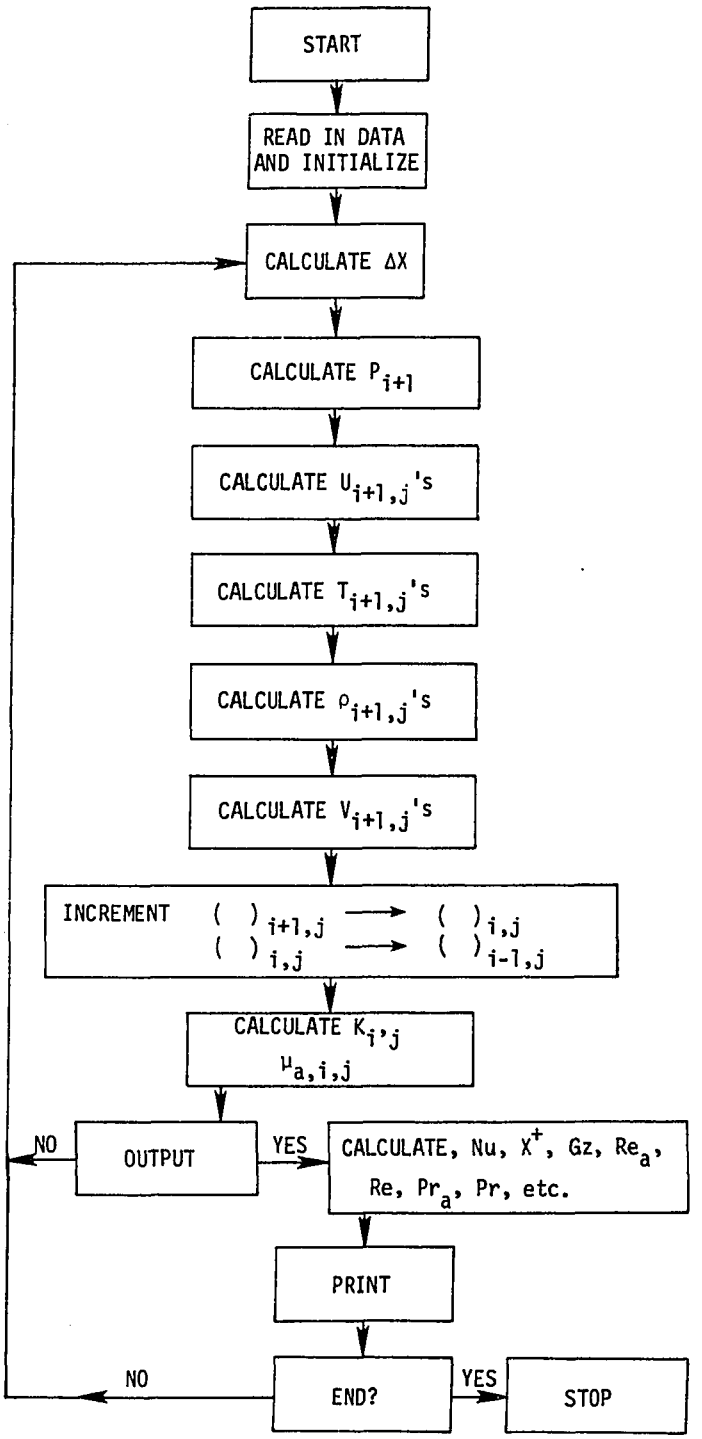

Fig. 3.3 A flow chart of the computer program.

as the calculation marches forward in the axial direction. The axial step size is increased until it is equal to the radius of the circular tube. This point is reached normally near the fully developed region ($V \simeq 0$, $\frac{\partial U}{\partial X} \simeq 0$).

To start with, the pressure at location i+1, P_{i+1} is computed from the integral form of the global continuity equation. Details of this calculation are shown in Appendix C. Now, the $U_{i+1,j}$ at all j's are computed from the momentum equation, (A.1) or (A.4), as all variables at previous streamwise levels are known. After this, the finite difference form of the energy equation, (A.2) or (A.5), is solved to obtain the temperature $T_{i+1,j}$ at all j's. The fluid density is then computed at all j's, and substituted in the continuity equation, (A.3) or (A.6), to compute $V_{i+1,j}$ at all j's. This completes one set of calculations.

After this, all i+1 variables are assigned the value of these variables at the i location. The previous i location becomes the i-1 location. At this new i location, $K_{i,j}$ and $\mu_{a,i,j}$ are calculated. All variables are again known at i and i-1 locations, and another forward step is marched in an axial direction by repeating the same procedure.

It should be noted here that each variable is calculated explicitly at each location. No iterations or simultaneous solutions are necessary; this saves considerable computer time.

Calculations of viscosities and flow parameters

The viscosity of pseudoplastic fluids is defined in two ways. First, the apparent viscosity is

$$\mu_a = K \left(\frac{\partial u}{\partial y}\right)^{n-1} \tag{1.3}$$

This viscosity is used in the numerical computational procedure. The other viscosity is called the effective viscosity. This is defined as the viscosity that would have existed at the wall if the fluid would have been Newtonian.

For Newtonian fluids $$\tau = \left[\mu \left(\frac{\partial u}{\partial y}\right)\right]_{Newt} \tag{3.27}$$

and, hence,

$$\mu_{eff} = \frac{\tau_w}{\left(\frac{\partial u}{\partial y}\right)_{Newt,w}} = \frac{K\left(\frac{\partial u}{\partial y}\right)^n_w}{(8\ \bar{u}/D)} \tag{3.28}$$

This viscosity definition has been used by Skelland [1] and others [59,60].

From the definitions of effective and apparent viscosities, Reynolds numbers were computed as

$$Re = \frac{\rho D \bar{u}}{\mu_{eff}} \quad \text{and} \quad Re_a = \frac{\rho D \bar{u}}{\mu_a} \tag{3.29}$$

Similarly Pr and Pr_a were computed. The effective Reynolds number Re gives the following well-known relation for the fully developed friction factor for laminar flow of Newtonian fluids

$$f = \frac{16}{Re} \tag{3.30}$$

Based on these parameters, a non-dimensional length X^+ is calculated as

$$X^+ = 2(x/D)/RePr \tag{3.31}$$

and the Graetz number is

$$Gz = \pi/2X^{+} \tag{3.32}$$

Calculation of heat transfer results

The major aim of the analysis was to predict heat transfer coefficients and Nusselt numbers along the tube length. However, before computing these parameters the following procedure was followed to ensure the accuracy of the numerical computation

1) At each axial location the heat balance of the heat supplied along the tube wall, Q_s, and the heat absorbed by fluid, Q_a, were assessed:

$$Q_s = \int_o^x dQ_s = q''_w \pi D \int_o^x dx \tag{3.33}$$

$$Q_a = \dot{m} c_p (t_x - t_o) \tag{3.34}$$

In no instance, did the difference between the two exceed 0.3 percent. In most of the calculations, this difference never exceeded 0.1 percent.

2) At each axial location, the wall temperature gradient $(\partial t/\partial r)_w$ was computed by linear and polynomial fit as shown for $(\partial u/\partial r)_w$ in Eqs. (3.24) and (3.25), and then wall heat flux was computed as

$$[q''_w]_{\text{prediction}} = -(k\frac{\partial t}{\partial r})_w \tag{3.35}$$

For a UHF boundary condition, the wall heat flux q''_w was known, and, therefore, in all numerical computations, it could be verified that the

difference between the q''_w and $[q''_w]_{prediction}$ did not exceed 0.20 percent. In most of the calculations, this difference never exceeded 0.01 percent.

At station x, at which the output was desired, knowing velocity and temperature profiles, the bulk temperature was computed as

$$t_b = \frac{\int_o^{r_w} tur\ dr}{\int_o^{r_w} ur\ dr} \tag{3.36}$$

The local heat transfer coefficient is defined as

$$q''_w = h_x\ (t_w - t_b) \tag{3.37}$$

and, therefore,

$$h_x = \frac{q''_w}{(t_w - t_b)} \tag{3.38}$$

The local Nusselt number based on tube diameter, D, is

$$Nu = \frac{h_x D}{k} \tag{3.39}$$

Substituting Eq. (3.38) into Eq. (3.39) yields

$$Nu = \frac{q''_w D}{k(t_w - t_b)} \tag{3.40}$$

Computer code

A computer code which was developed to solve this problem is given in Appendix D. This code was developed from the computer code, developed by Nelson [51] for the Newtonian heat transfer. A considerable

modification of this code was done to utilize it for non-Newtonian flow and heat transfer. Some of the features of this code are as follows:

1) Two most commonly encountered boundary conditions in heat transfer studies, namely, a constant wall heat flux and a constant wall temperature can be used.

2) The fluid density, specific heat, thermal conductivity, coefficient of thermal expansion, flow behavior index, and the consistency index, are incorporated as temperature-dependent function sub-programs. This facilitates use of the main program for either constant fluid property conditions or variable fluid property conditions, where any specified fluid property-temperature relationship can be used. The free convection effects are neglected in the governing equations as they are estimated to be small.

3) The program can handle thermally developing or thermally and hydrodynamically developing flows.

4) Provision is made in the program to handle either an isothermal or a nonisothermal temperature profile at the entrance of the heated tube.

5) Provision is made in the program so that at the axial position, at which the program stops, all the variables at that station are recorded on a disc. Then, when it is desired to proceed further downstream, the results of the last axial station from the previous calculation can be read from the disc, and computation from that axial station onwards can be started.

6) With very little modification, the present numerical scheme can be modified to compute heat transfer calculations for flow of pseudoplastic fluid over a flat plate.

CHAPTER IV. NUMERICAL RESULTS AND DISCUSSION

In this chapter, the predictions obtained from the numerical scheme developed in Chapter III are discussed. These predictions are for the flow of pseudoplastic fluid inside a circular tube subjected to a uniform wall heat flux boundary condition. At the onset of heating, the fluid velocity profile is fully developed and isothermal.

Constant Property Predictions

Heat transfer

The assumption of constant thermophysical properties is highly restrictive, particularly with regard to K. For most pseudoplastic fluids, with every 25-30°F change in temperature, K undergoes a change of about 50 to 100 percent. However, constant property predictions provide the basis for the comparison of the variable property predictions. In the computer code developed, all the fluid properties were incorporated as subroutines. For this analysis, constant values were assigned to these subroutines.

In this analysis, the predictions for the local Nusselt numbers were obtained for the entire thermal length, for n = 1.0, 0.75, 0.5 and 0.25. For the fully developed case, the temperature difference $(t_w - t_b)$ is constant and, hence, a constant asymptotic value of Nusselt number is obtained.

Table 4.1 shows that the fully developed predictions of the present analysis are in excellent agreement with the analytical

Table 4.1. Comparison of non-Newtonian Nusselt numbers for the fully developed region

n	Nu_∞		
	Present	Ref. 22-23	Eq. (4.1)
1.0	4.36	4.36	4.36
0.75	4.50	4.50	4.48
0.50	4.75	4.75	4.70
0.25	5.31	5.31	5.25
0.10	6.25	6.25	6.46

predictions of Beek and Eggink[22] and Grigull [23] which are correlated by Eqs. (2.9) and (2.10) respectively. These two correlations give identical results and account for the increase in Nusselt number due to pseudoplasticity. However, these correlations are highly complex and, therefore, Pigford [25] and Mizushina et al. [31] have suggested a simple correlation

$$Nu_\infty = 4.36\ \Delta^{1/3} \tag{4.1}$$

where

$$\Delta = \frac{3n+1}{4n} \tag{4.2}$$

The non-Newtonian correction, $\Delta^{1/3}$ is simple and gives accurate results within 1.1 percent, in the range of n = 1.0 to 0.25, and within 3.0 percent at n = 0.1 (see Table 4.1). It is important to note that as $n \to 0$, $\Delta \to \infty$ and, hence, this correction is mathematically inconsistent. However, since most engineering fluids have n > 0.25, Eqs. (4.1) and

(4.2) can be used for all engineering calculations. The excellent agreement of the present predictions with these equations and previous predictions demonstrates the success of the present explicit finite-difference scheme.

Figures 4.1 to 4.4 are plots of local Nusselt numbers against dimensionless distance, X^+, for the entire thermal length, for n = 1.0, 0.75, 0.5 and 0.25 respectively. In these plots the present local Nusselt number predictions are compared with available predictions [8,9,11,16,30,31,44]. The excellent agreement with these predictions further confirms the accuracy of the present explicit finite-difference scheme.

For the case of n = 1.0 (Fig. 4.1), the present predictions and those of other investigators [9,11,17] are lower than the predictions of Kays [8]. This may be due to the large grid spacing used by Kays in his computation.

Figure 4.5 is a composite plot of local Nusselt numbers against X^+ for various values of n. It is distinctly seen that the effect of pseudoplasticity is to increase heat transfer coefficients above the Newtonian values. This increase is quite substantial at lower values of n. To account for this effect, Mizushina et al. [31] have suggested that the fully developed correction $\Delta^{1/3}$ could be used. However, they never established the validity of this correction in the thermal entrance region.

The non-Newtonian correction, $\Delta^{1/3}$, was applied to all of the present data as indicated in Fig. 4.6. It is seen that throughout the

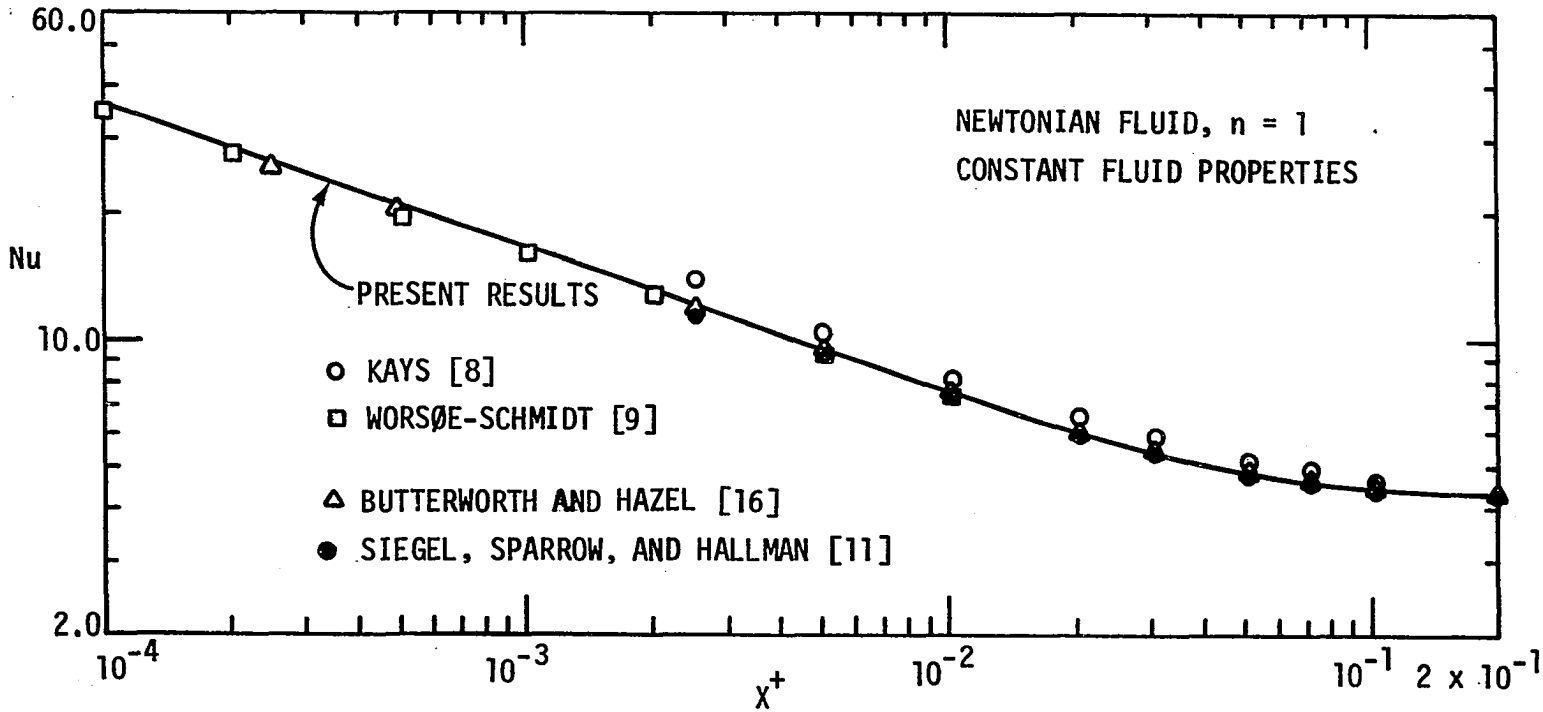

Fig. 4.1 Comparison of present numerical solution with available predictions (n = 1).

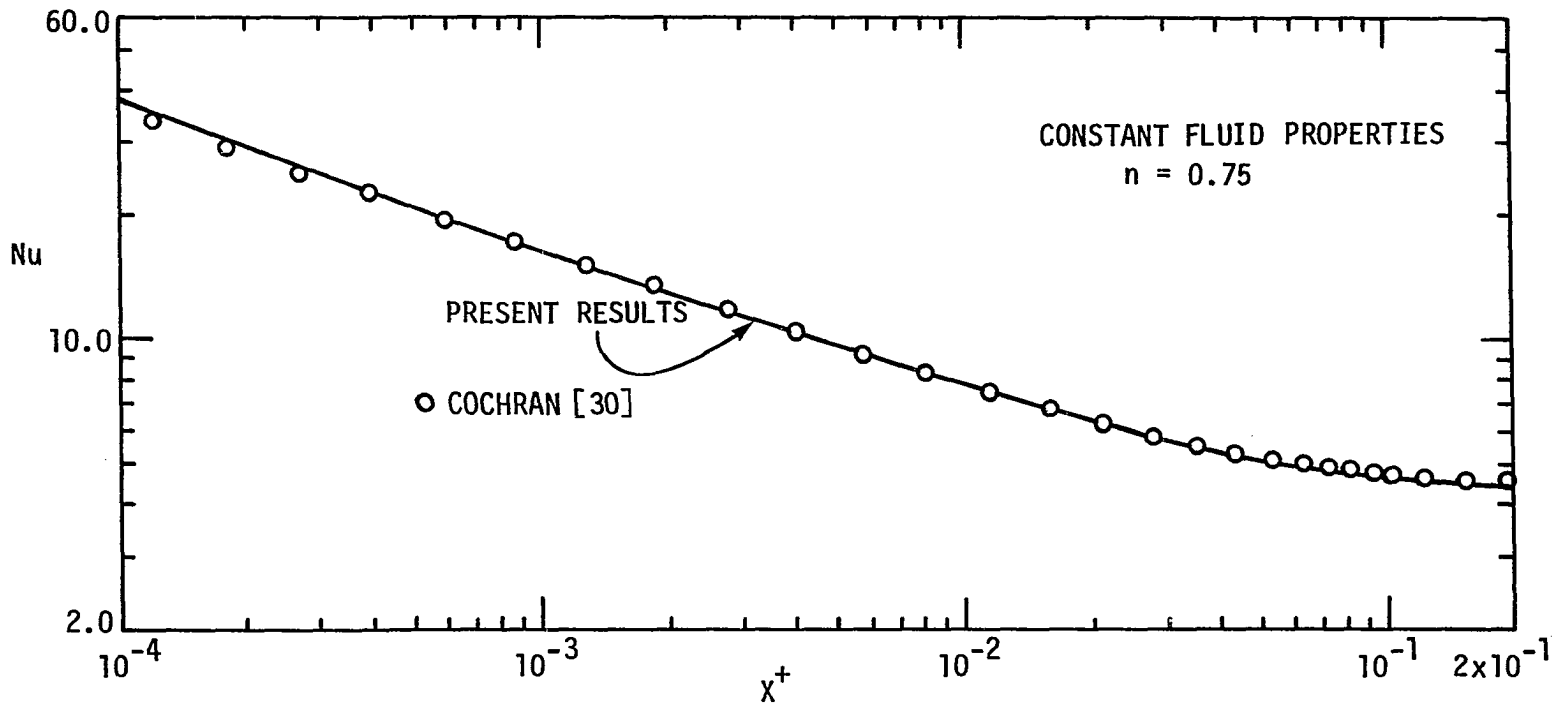

Fig. 4.2 Comparison of present numerical solution with available prediction (n = 0.75).

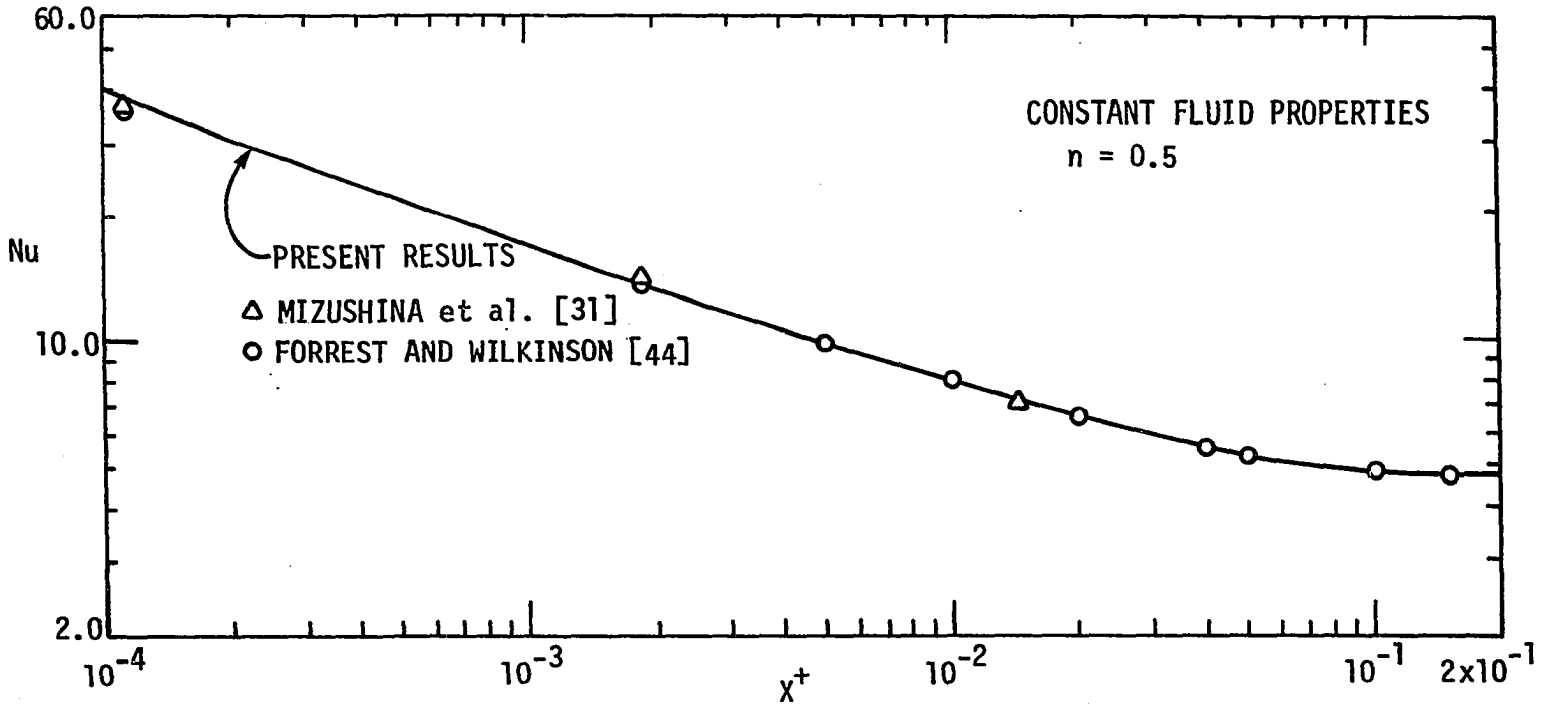

Fig. 4.3 Comparison of present numerical solution with available predictions (n = 0.5).

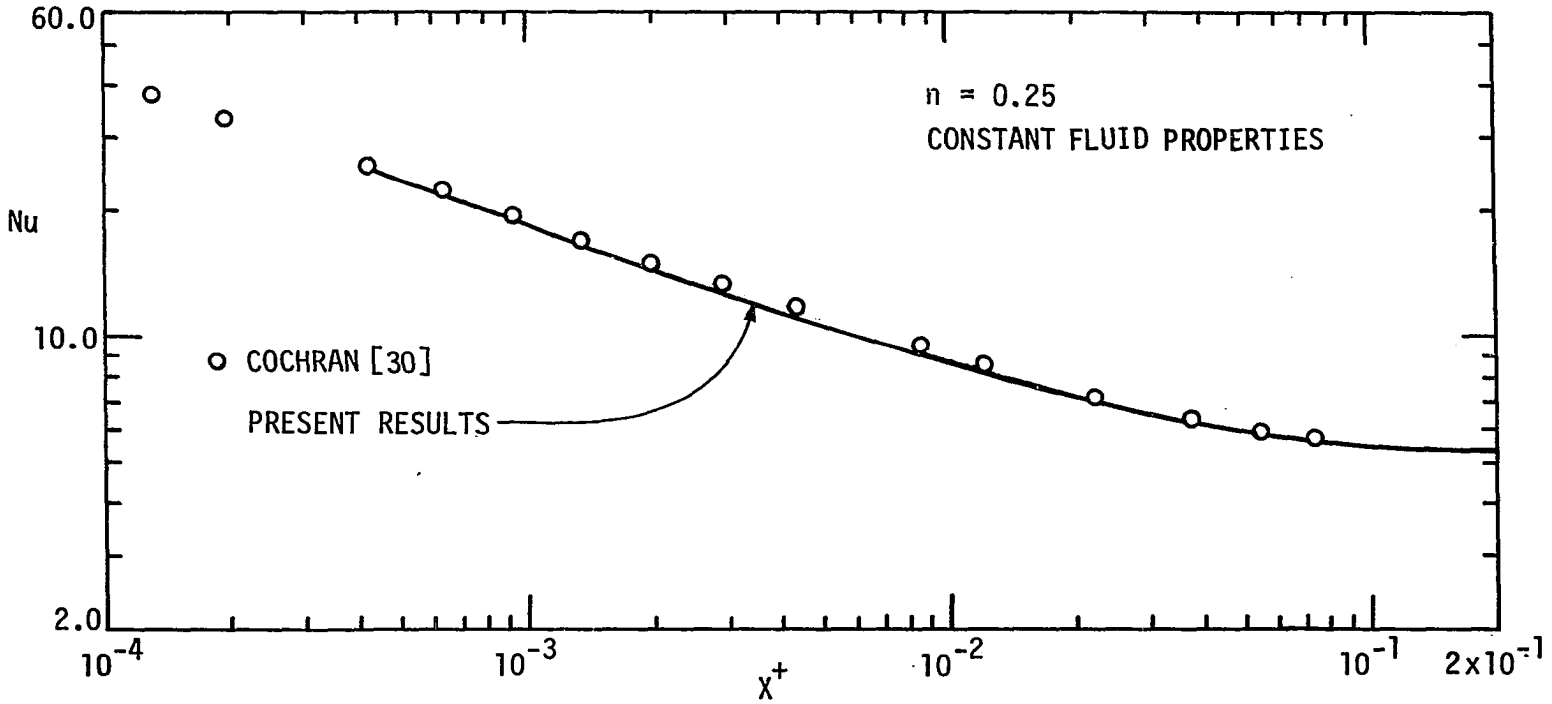

Figure 4.4 Comparison of present numerical solution with available predictions (n = 0.25).

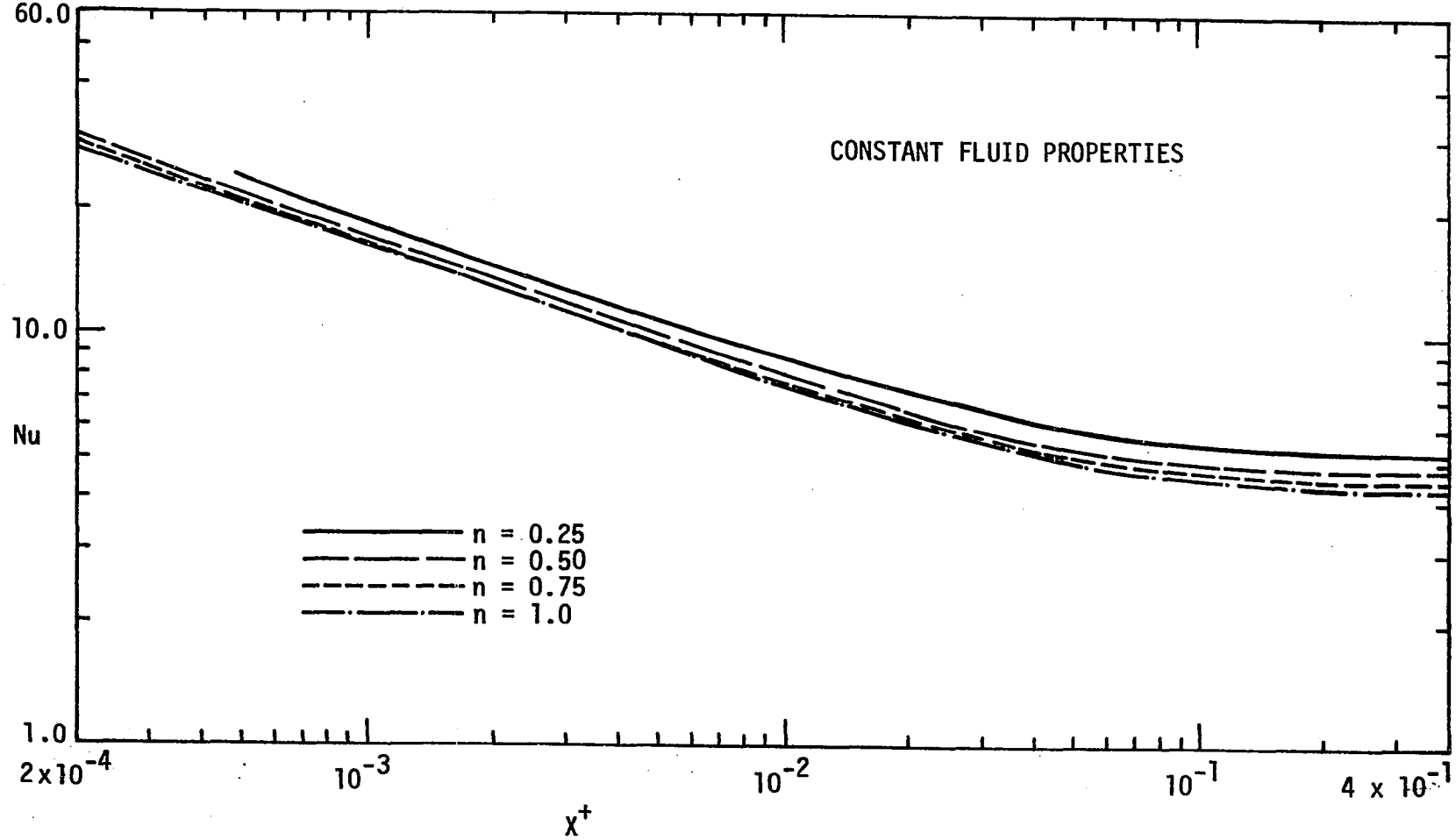

Fig. 4.5 Results of the present numerical analysis for laminar in-tube flow of power law fluids.

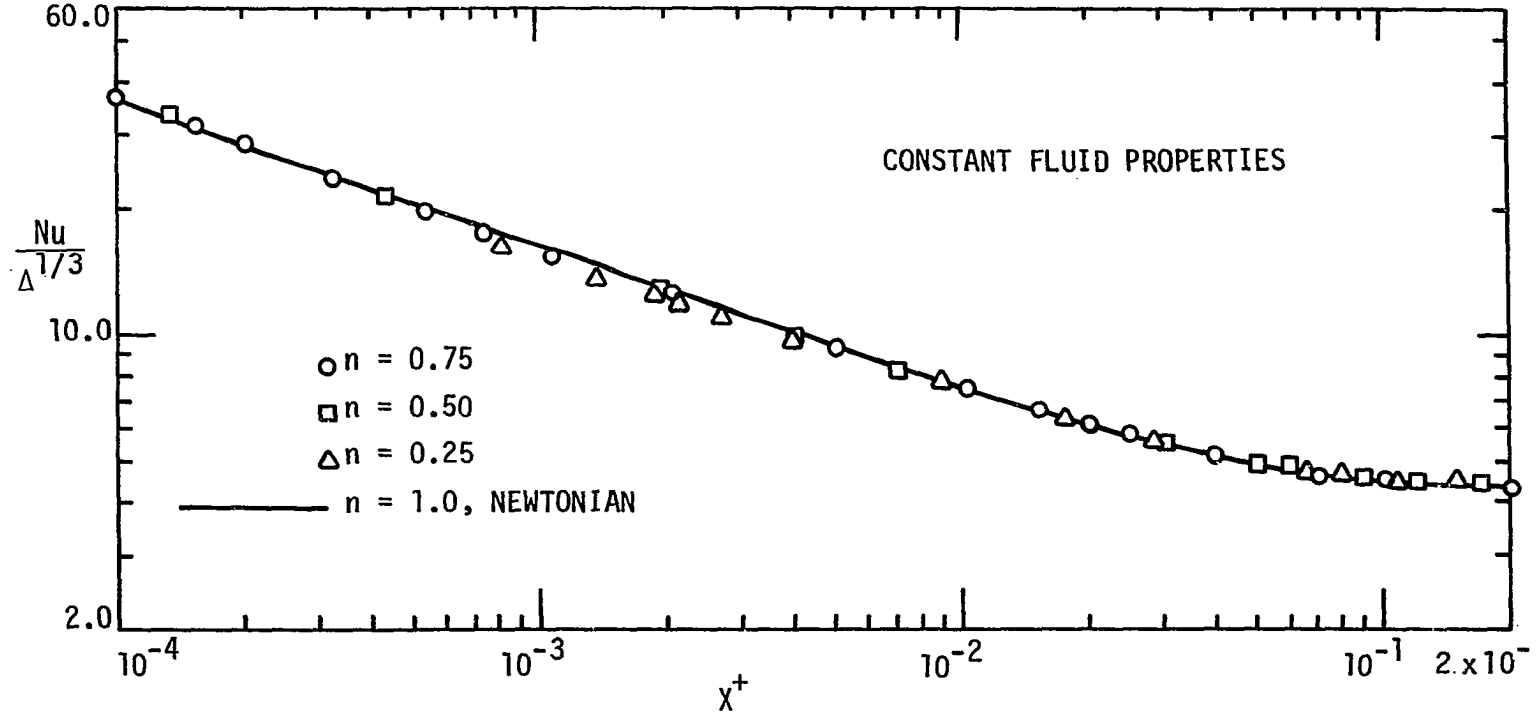

Fig. 4.6 Comparison of corrected Nusselt numbers for non-Newtonian flow predictions with Newtonian flow predictions.

entire thermal length this correction gives excellent results for $n = 0.75$ and 0.50. However, for $n = 0.25$, this correction somewhat over corrects (2-3 percent) in the early part of the entrance region ($X^+ < 2 \times 10^{-3}$). In light of the fact that the non-Newtonian correction employed is "approximate", the corrected Nusselt numbers are in excellent agreement with the Newtonian predictions. This confirms the validity of the non-Newtonian correction, $\Delta^{1/3}$, to account for an increment in heat transfer due to pseudoplasticity throughout the entire thermal length. The tabulated predictions are given in Appendix E.

Pressure drop

For the hydrodynamically developed, in-tube flow of pseudoplastic fluids, it can be shown that [1]

$$\frac{dp}{dx} = -\frac{4K}{D}\left(\frac{3n+1}{4n}\right)^n \left(\frac{8\bar{u}}{D}\right)^n \tag{4.3}$$

For constant property flow, Eq. (4.3) will give a constant pressure gradient dp/dx. A comparison of the predictions from Eq. (4.3) and from the present numerical scheme is given in Table 4.2.

Table 4.2. Comparison of pressure gradients

n →	1.0	0.75	0.5	0.25
dp/dx, numerical	-0.046	-35.40	-11.92	-3.09
dp/dx, Eq. (4.3)	-0.046	-35.38	-11.92	-3.07

There is a $\pm$ 1 to 2 percent variation in the pressure gradient at various axial grid cross-sections along the tube length. This slight variation is simply due to finite-difference approximations, which are inherent in the numerical calculations. The constant average values of dp/dx are given in Table 4.2.

Most of the numerical studies calculate dp/dx while, most of the experimental studies evaluate f, the friction factor. In Chapter III, it was shown that for pseudoplastic fluids,

$$f = 16/Re \tag{3.30}$$

Where Re is based on the μ_{eff}, defined in Eq. (3.28). A comparison of the Fanning friction factor obtained from Eq. (3.30) and the predictions from the numerical computation is given in Table 4.3.

Table 4.3. Comparison of Fanning friction factors

n →	1.0	0.75	0.50	0.25
Re →	284.2	8.3	24.6	13.6
f, numerical	0.056	1.931	0.650	1.185
f, Eq. (3.30)	0.056	1.928	0.650	1.182

It is seen that the f values are in excellent agreement with the theoretical results, in accordance with the results given in Table 4.2.

Conclusion

The present heat transfer predictions are in excellent agreement with the available predictions. The pressure drop and friction factor predictions are also in excellent agreement with the theoretical predictions. This confirms the success of the present explicit numerical scheme.

The non-Newtonian heat transfer correction, $\Delta^{1/3}$, is also confirmed for the entire thermal length.

Variable Property Predictions

Introduction

In this section, heat transfer predictions for pseudoplastic fluids with variable properties are given. The constitutive equation for a pseudoplastic fluid is

$$\tau = K\left(\frac{\partial u}{\partial y}\right)^n \quad \text{with} \quad (n \leq 1) \tag{1.2}$$

For Newtonian fluids, n = 1, and K represents the viscosity, μ. Most of the power-law fluids are highly viscous in nature and exhibit a strong temperature dependence for K, while n is normally a weak function of temperature.

As mentioned earlier in Chapter III, in the present analysis the following assumptions are made:

1) K and ρ are temperature-dependent, but the free convection effects are negligible.

2) k, c_p, and n are temperature-independent. The assumption of

constant k, c_p, and n is not highly restrictive, since for many liquids these properties are very weak functions of temperature.

3) The fluid has a fully developed, isothermal velocity profile at the onset of heating.

The K-t relation used is

$$K = a \exp(-bt) \tag{2.40}$$

where a and b are constants. This log-linear relationship is found to be valid for most pseudoplastic fluids [45]. Many Newtonian fluids also exhibit this kind of temperature dependence of viscosity.

The ρ-t relation used here is

$$\rho = A1 + A2\eta + A3\eta^2 + A4\eta^3 \tag{4.4}$$

where A1 to A4 are constants and $\eta = (t-50.0)/50$.

This relation holds for most aqueous solutions. It is important to note that the free convection effects were neglected, as the density variation is quite negligible as compared to the K variation. However, density variation was accounted for in the convective and inertia terms in the governing equations.

The objective of this analysis was to evaluate the effect of variable K on the heat transfer coefficient for flow of a pseudoplastic fluid inside a tube. For the uniform wall heat flux boundary condition, predictions are to be obtained for various n values, for the entire thermal length.

A parameter to account for variable consistency

Shannon and Depew [34] and Hong and Bergles [54,55] have done analyses for fully developed heat transfer with Newtonian fluids. These investigators have used "arhenius-relations" for μ-t as

$$\mu = \mu_o \exp(-\gamma(t-t_o)) \tag{2.17}$$

where

$$\gamma = -\frac{1}{\mu}\frac{d\mu}{dt} = \text{constant} \tag{4.5}$$

Hong and Bergles have defined a non-dimensional viscosity parameter as $\gamma\Delta T$. This parameter is similar to $\beta\Delta T$ in the Grashof number which accounts for density variation. For the constant wall heat flux condition, ΔT is replaced by

$$\Delta T = \frac{q''_w D}{2k} \tag{4.6}$$

and, hence, from Eqs. (4.5) and (4.6)

$$\gamma\Delta T = \left(-\frac{1}{\mu}\frac{d\mu}{dt}\right)\left(\frac{q''_w D}{2k}\right) \tag{4.7}$$

It is important to note that until now this parameter was used only for fully developed Newtonian heat transfer. In the present analysis this concept is extended to pseudoplastic fluids, where in Eqs. (4.5) and (4.7) μ is replaced by K.

Since $K = a \exp(-bt)$

$$\gamma = \frac{-1}{K}\left(\frac{dK}{dt}\right) = b = \text{constant} \tag{4.8}$$

and

$$\gamma\Delta T = \left(-\frac{1}{K}\frac{dK}{dt}\right)\left(\frac{q''_w D}{2k}\right) \tag{4.9}$$

This parameter can be varied by either varying wall heat flux or by selecting a fluid with different γ.

Numerical variables

In the present analysis, variable property predictions were obtained for n = 0.75 and n = 0.50 for the entire thermal length. For a given pseudoplastic fluid, different values of $\gamma\Delta T$ were obtained by varying the wall heat flux, q''_w. The predictions were obtained for four different values of $\gamma\Delta T$ which were sufficient for correlation.

The limiting case of a pseudoplastic fluid is a Newtonian fluid (n = 1.0) and, therefore, for completeness, variable property predictions were also obtained for the Newtonian case. For this case, properties of highly viscous transformer oil are used. The transformer oil has a strong temperature-dependent viscosity, which for the most part can be described by an exponential function (Eq. 2.40). For this Newtonian case, predictions were obtained for the entire thermal length for two different values of $\gamma\Delta T$ (two heat fluxes).

The analytical procedure followed here was identical with the one followed for constant property analysis, with the only difference being that the appropriate K-t and ρ-t relations were incorporated in the fluid property subroutines.

For the Newtonian case alone, with the variable μ assumption, an additional analysis was made for the fully developed region. Simpson's

rule for numerical integration was used to solve the differential equations occurring in this analysis. The predictions were obtained for six different values of $\gamma\Delta T$, two of which were the same as used in the Dufort-Frankel marching scheme. This duplication was done to varify the fully developed Newtonian prediction for both schemes. The details of this Newtonian fully developed analysis are given in Appendix F.

Nusselt number results

The variable property local Nusselt number predictions, for the entire thermal length and for various $\gamma\Delta T$ values are tabulated in Appendix G. Figures 4.7 and 4.9 are the plots of local Nusselt numbers against dimensionless distances, X^+, for n = 1.0, 0.75, and 0.5 respectively. In these plots, continuous smooth curves were drawn through the predicted data points; however, for clarity, the data points are not shown.

The Newtonian predictions, for the entire thermal length, for $\gamma\Delta T$ = 2.35 and 3.77 and also the predictions from the special fully developed analysis are shown in Fig. 4.7. The fully developed predictions by both schemes for $\gamma\Delta T$ = 2.35 and 3.77 are identical (see Appendix F and G).

Figures 4.7 to 4.9 distinctly show that there is a substantial increase in heat transfer coefficient when heating, due to temperature-dependent properties. For the given wall heat flux (given $\gamma\Delta T$) the increment in heat transfer is much more pronounced at n = 0.5 than

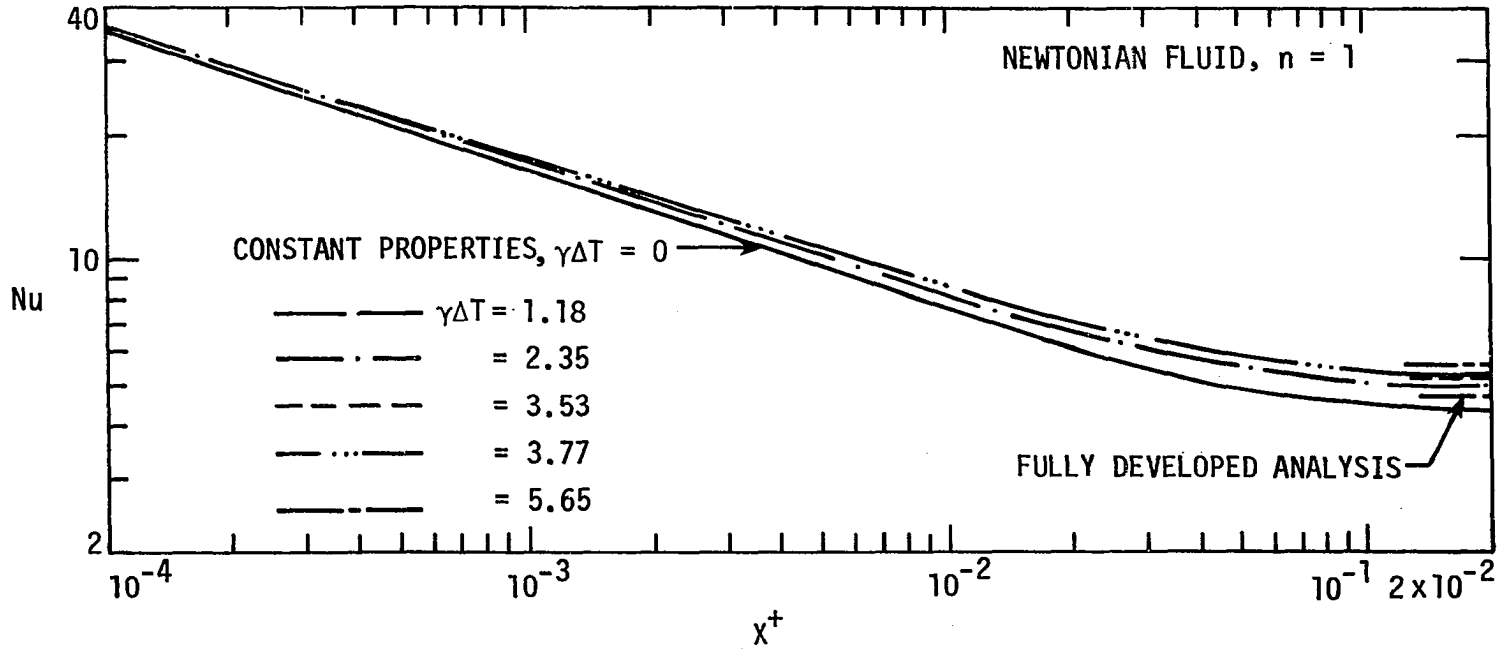

Fig. 4.7 Dependence of Nusselt number on dimensionless distance and viscosity parameter (n = 1).

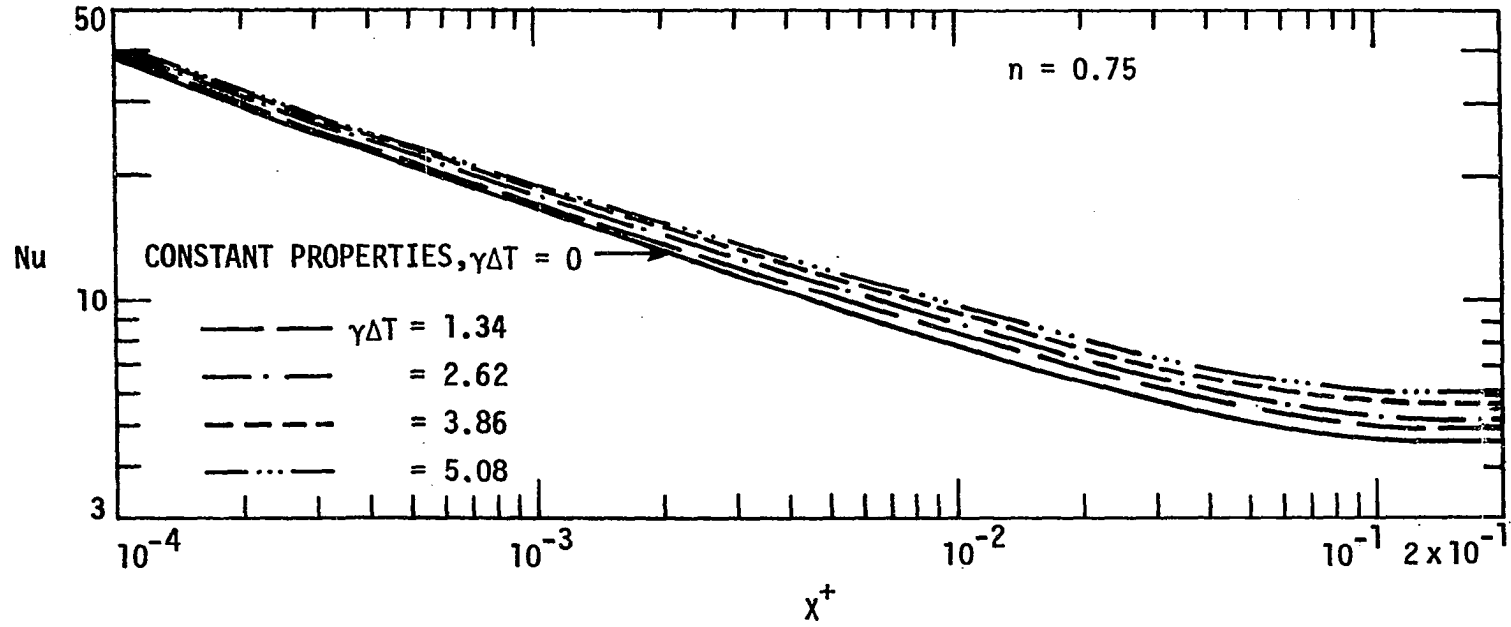

Fig. 4.8 Dependence of Nusselt number on dimensionless distance and consistency parameter (n = 0.75).

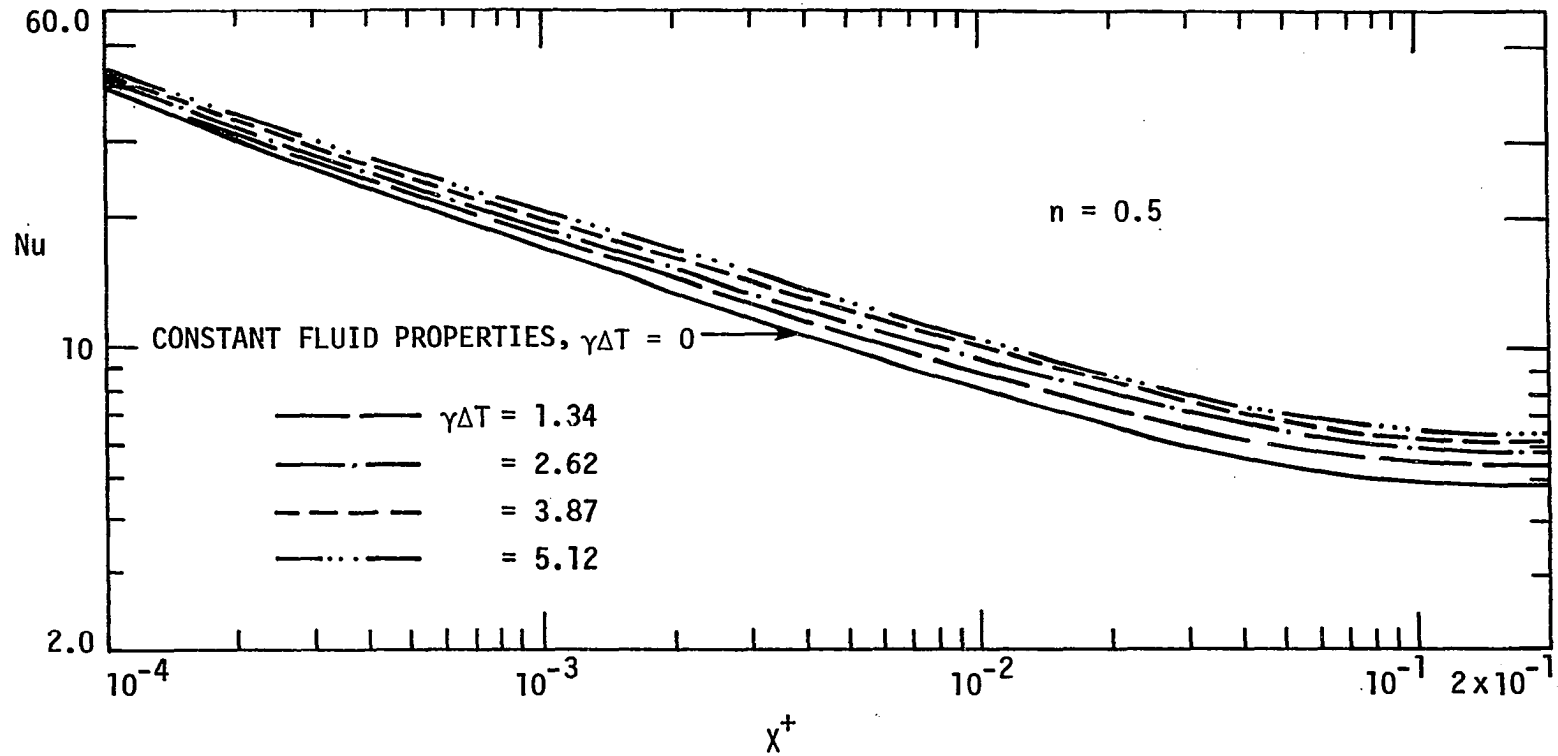

Fig. 4.9 Dependence of Nusselt number on dimensionless distance and consistency parameter (n = 0.5).

that at n = 1.0. As expected, the effect of variable properties is greater in the fully developed region than in the thermal entrance region.

This increase in heat transfer coefficient is mainly due to the variation in temperature-dependent K for pseudoplastic fluids and temperature-dependent μ for Newtonian fluids. In order to correlate this effect, for each n at constant $\gamma\Delta T$ and at several axial locations, a ratio of variable property and corresponding constant property Nusselt numbers, $(Nu/Nu_{cp})_{X^+}$ was calculated and plotted against the corresponding ratio $(K/K_w)_{X^+}$. At the tube entrance, $(K/K_w) = 1.0$. As the fluid progresses downstream inside the tube, progressively higher values of (K/K_w) are observed. Thus, for a given wall heat flux, lower values of (K/K_w) exist in the thermal entrance region, and comparatively higher values of (K/K_w) exist in the fully developed region.

For n = 1, a logarithmic plot of $(Nu/Nu_{cp})_{X^+}$ against $(\mu/\mu_w)_{X^+}$ is shown in Fig. 4.10; for clarity, the data points are not shown. Similar plots of Nusselt number ratio for n = 0.75 and n = 0.5 (with abscissa $(K/K_w)_{X^+}$) are shown in Figs. 4.11 and 4.12, respectively. All of these plots have similar characteristics. These logarithmic plots show that

1) For the Newtonian fluid in the entire thermal development region (entrance as well as fully developed), a log-linear relationship is observed. The slope of this straight line is 0.14 and therefore

$$\left(\frac{Nu}{Nu_{cp}}\right) = (\mu/\mu_w)^m \qquad (4.10)$$

where m = 0.14. These results are similar to those obtained by

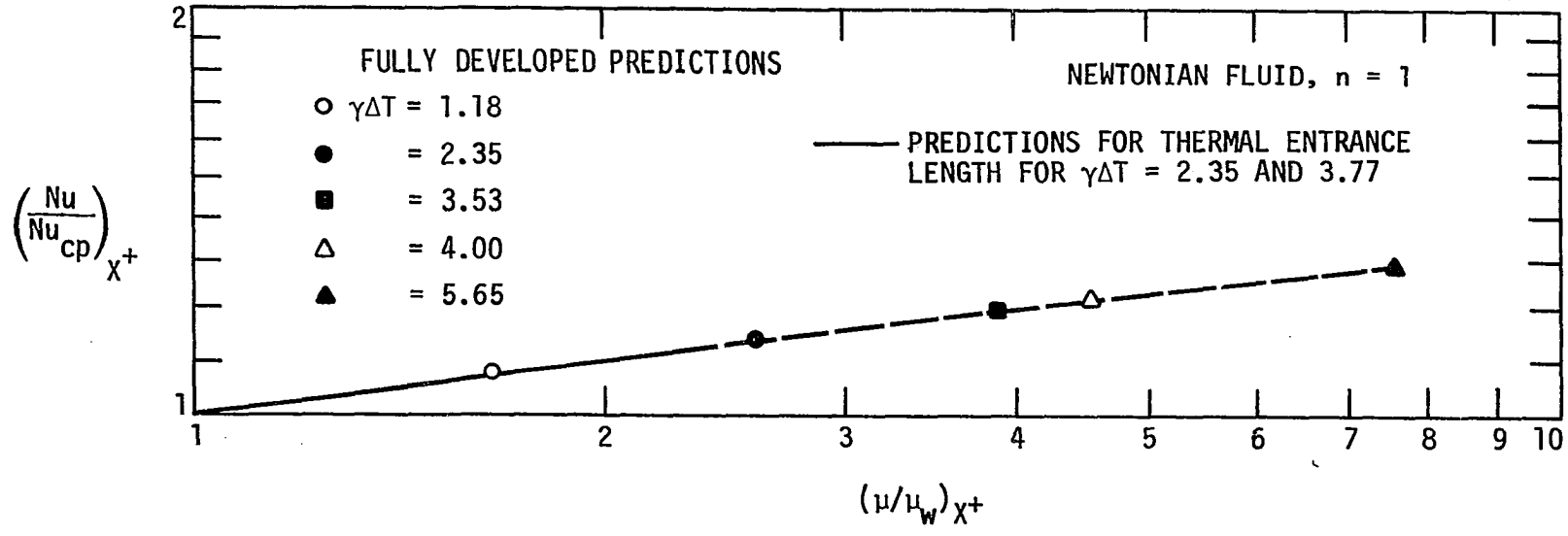

Fig. 4.10 Dependence of Nusselt number ratio on viscosity ratio (n = 1).

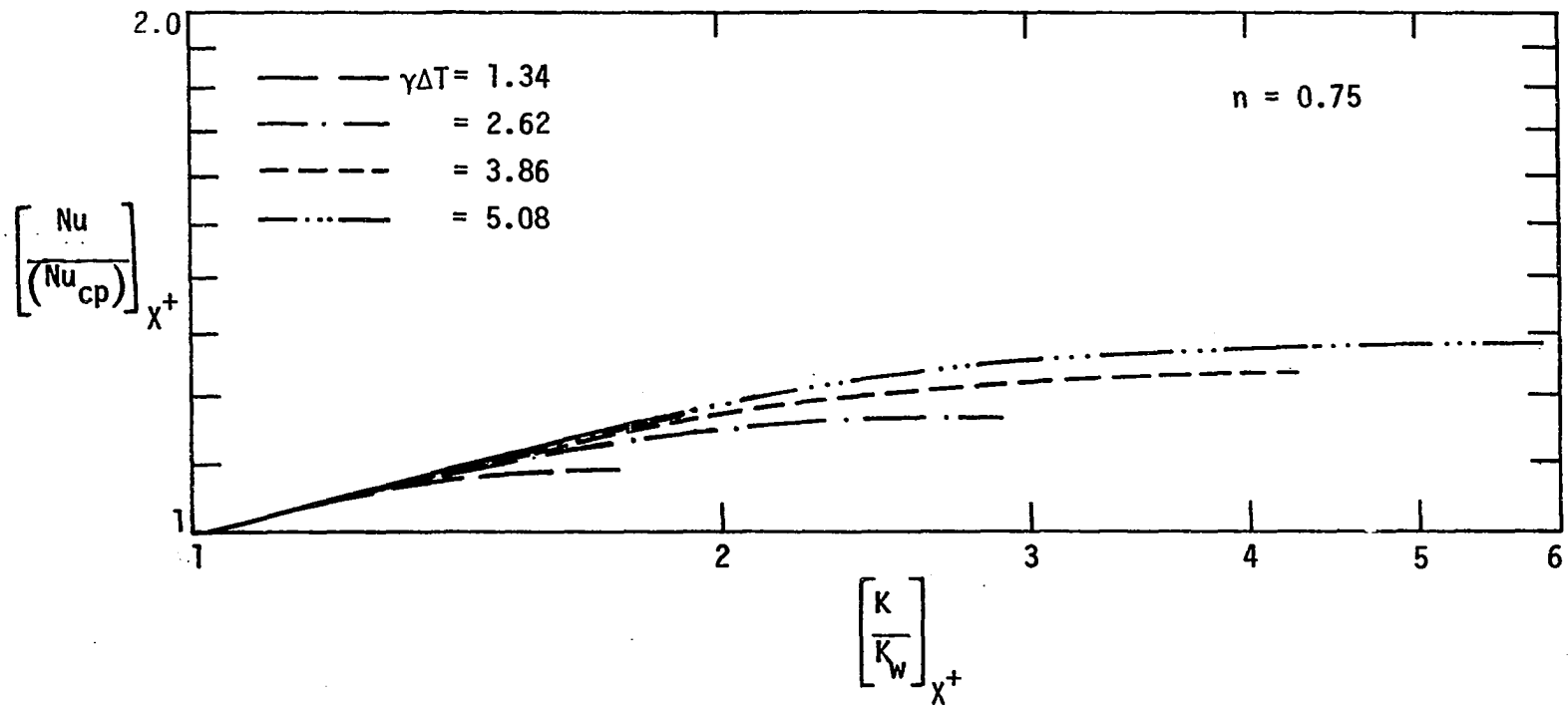

Fig. 4.11 Dependence of Nusselt number ratio on ratio of consistency indices (n = 0.75).

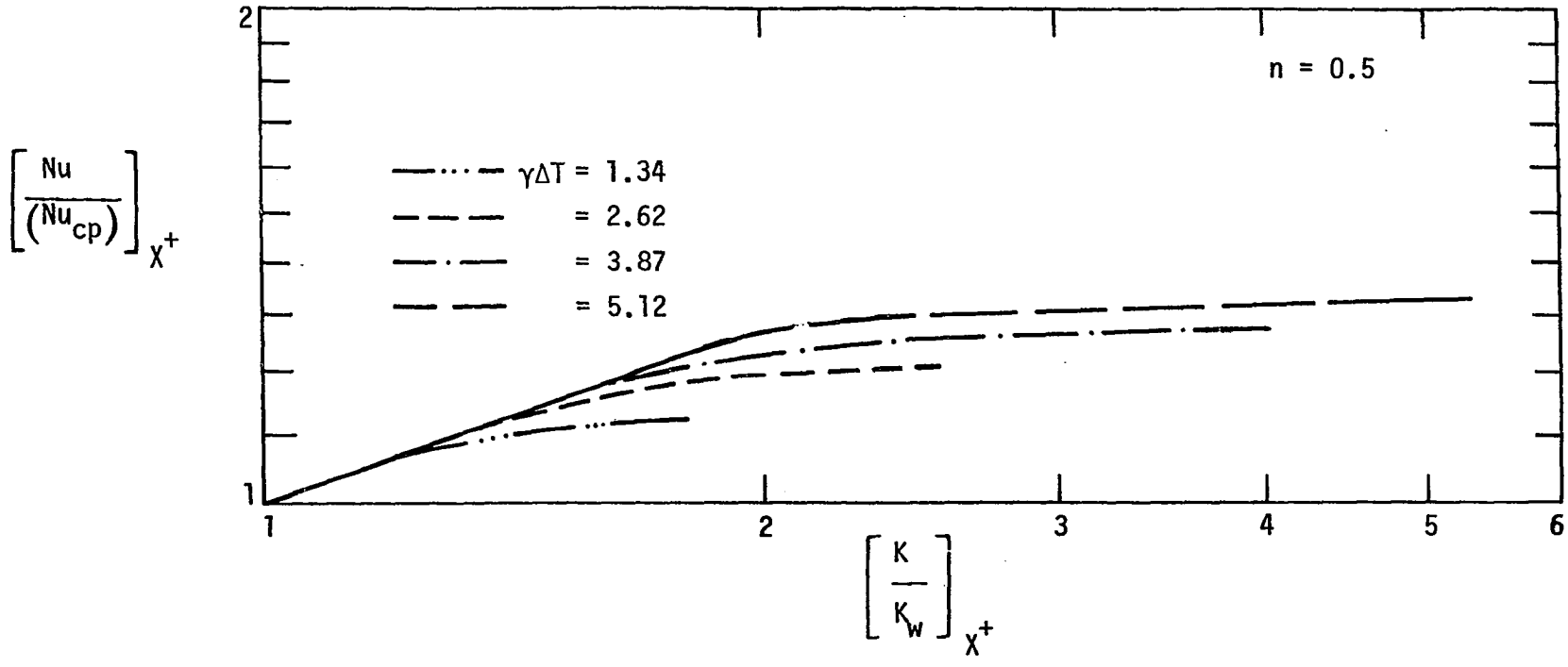

Fig. 4.12 Dependence of Nusselt number ratio on ratio of consistency indices (n = 0.5).

Yang [32] (see results and discussion in Appendix F for further details).

2) For n = 0.75 and 0.5, a log-linear relationship is observed near the tube inlet (thermal entrance region). The slopes of these straight lines are dependent on n. For n = 0.75 and 0.5, the m values are 0.25 and 0.36, respectively.

3) For a given heat flux, at higher values of K/K_w, i.e., in the fully developed region, an asymptotic value of the ordinate is observed for n = 0.75 and 0.5. The value of this asymptotic ordinate is independent of $(K/K_w)_{X^+}$ but is dependent on $\gamma\Delta T$.

4) For n = 0.75 and 0.5 and for a given $\gamma\Delta T$, the value of the asymptote is a function of n.

5) For the given two $\gamma\Delta T$ values, the difference between asymptotic values of $(Nu/Nu_{cp})_\infty$ is larger at n = 0.5 than at n = 0.75, while for n = 1.0, there are no asymptotes.

Thus it is seen from Figs. 4.10 to 4.12 that in the entrance region, the Nusselt number ratio is a function of n and K/K_w while in the fully developed region the ratio is a function of n and $\gamma\Delta T$. This can be mathematically summarized as

$$\left(\frac{Nu}{Nu_{cp}}\right)_{X^+} = f(n,\ \gamma\Delta T,\ (K/K_w)_{X^+}) \qquad (4.11)$$

The functional relationship is quite complex, and it is difficult to obtain a simple correlation. Therefore, an approximate correlation is developed which is sufficiently accurate for design purposes.

The variable property predictions are tabulated in Appendix G.

Development of a variable consistency correction

The consistency correction is devised in two steps: 1) thermal entrance correction and 2) fully developed correction.

In the thermal entrance region, for a given n, a log-linear relationship is observed between $(Nu/Nu_{cp})_{X^+}$ and $(K/K_w)_{X^+}$. The slope, m, of these straight lines was found from Figs. 4.10 to 4.12. This is tabulated in Table 4.4.

Table 4.4. Predictions of m in the thermal entrance length

n	m
1.0	0.14
0.75	0.25
0.50	0.36

A linear regression analysis for these three points gives

$$m = 0.58 - 0.44n \tag{4.12}$$

with a correlation coefficient of 0.999. Thus, for the thermal entrance region, the local Nusselt number can be written in terms of the corresponding constant property Nusselt number as

$$(Nu)_{X^+} = (\bar{Nu}_{cp})_{X^+} \quad (K/K_w)^m_{X^+} \tag{4.13}$$

As noted earlier, for the fully developed region, the predictions were obtained for four different values of $\gamma\Delta T$ at each of two values of

n, 0.75 and 0.5. For n = 1, the predictions were obtained for two different values of $\gamma\Delta T$. However, for the Newtonian case alone an independent fully developed analysis was done, in which predictions were obtained for six different values of $\gamma\Delta T$. Two of these predictions have $\gamma\Delta T$ identical to those used in the Dufort-Frankel numerical scheme. These fully developed predictions are tabulated in Table 4.5

A plot of $(Nu/Nu_{cp})_\infty$ against $\gamma\Delta T$ for n = 1.0, 0.75, and 0.5 is shown in Fig. 4.13. Each of these three curves is correlated by second-order polynomial.

For n = 1.0

$$\left(\frac{Nu}{Nu_{cp}}\right)_\infty = 1.0 + 0.069\gamma\Delta T - 0.0033(\gamma\Delta T)^2 \qquad (4.14)$$

For n = 0.75

$$\left(\frac{Nu}{Nu_{cp}}\right)_\infty = 1.0 + 0.0847\gamma\Delta T - 0.0051(\gamma\Delta T)^2 \qquad (4.15)$$

For n = 0.50

$$\left(\frac{Nu}{Nu_{cp}}\right)_\infty = 1.0 + 0.0961\gamma\Delta T - 0.0067\ (\gamma\Delta T)^2 \qquad (4.16)$$

The generalized form of Eqs. (4.14) to (4.16) is

$$\left(\frac{Nu}{Nu_{cp}}\right)_\infty = 1.0 + C_1(n)\gamma\Delta T - C_2(n)(\gamma\Delta T)^2 \qquad (4.17)$$

The coefficients C_1 and C_2 are functions of n. A linear regression analysis was used to correlate C_1 and C_2

Table 4.5. Fully developed heat transfer predictions

n	$\gamma\Delta T$	$(Nu/Nu_{cp})_\infty$
1.0	0.0	1.00
	1.18	1.08
	2.35	1.14
	3.53	1.20
	3.77	1.21
	4.00	1.23
	5.65	1.28
0.75	0.0	1.00
	1.34	1.11
	2.62	1.18
	3.86	1.25
	5.08	1.30
0.50	0.0	1.00
	1.34	1.12
	2.62	1.21
	3.87	1.27
	5.12	1.32

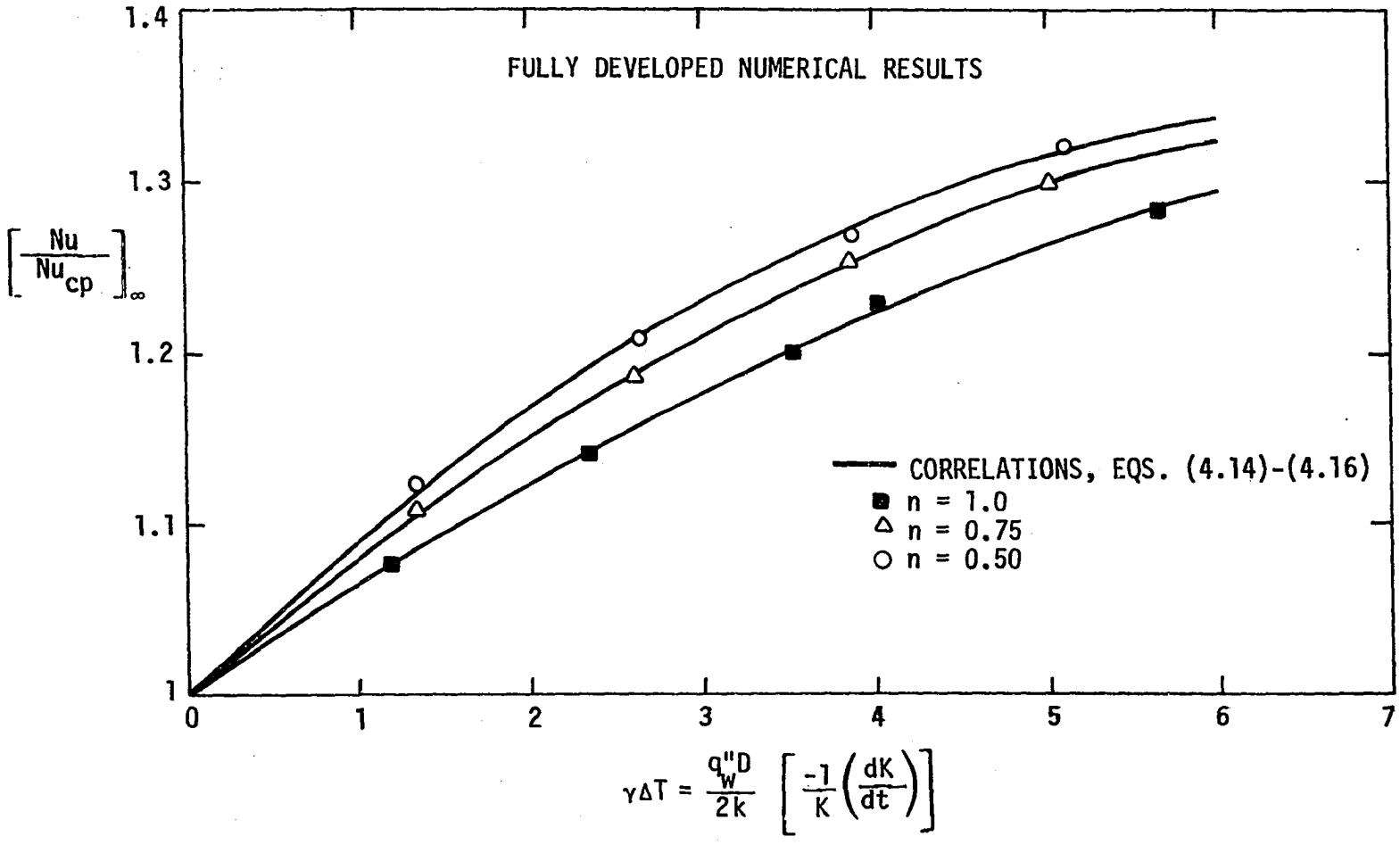

Fig. 4.13 Dependence of Nusselt ratio on $\gamma\Delta T$.

$$C_1(n) = 0.12392 - 0.05420n \tag{4.18}$$

and

$$C_2(n) = 0.010133 - 0.0068n \tag{4.19}$$

With this Eq. (4.17) is rewritten as

$$\left(\frac{Nu}{Nu_{cp}}\right)_\infty = 1 + C_k \tag{4.20}$$

where

$$C_k = C_1(n)\gamma\Delta T - C_2(n)(\gamma\Delta T)^2$$

Equation (4.20) is a generalized correlation for the fully developed region. For a given fluid, n and b are known, and for a given heat flux, $\gamma\Delta T$ is estimated; then, using Eq. (4.20, $(Nu/Nu_{cp})_\infty$ can be estimated explicitly. All the available predictions for fully developed flows of Newtonian and pseudoplastic fluids [31-34] are of the form given in Eq. (4.10). For the constant wall heat flux boundary condition, t_w and μ_w are unknown quantities, and iterations are essential to evaluate Nu. The present proposed correlation (Eq. (4.20)) does not involve any iterations, and, therefore, it is highly useful for design purposes. A plot of $(Nu/Nu_{cp})_\infty$ is shown in Fig. 4.14. This plot demonstrates the validity of the proposed fully developed correlation.

The value of $\gamma\Delta T$ used in the present numerical scheme ($\gamma\Delta T \leq 8$) is sufficiently high to cover most of the pseudoplastic fluids and heat duties encountered in practice. However, some sort of extension was needed to cover extreme values of $\gamma\Delta T$. It is to be emphasized here

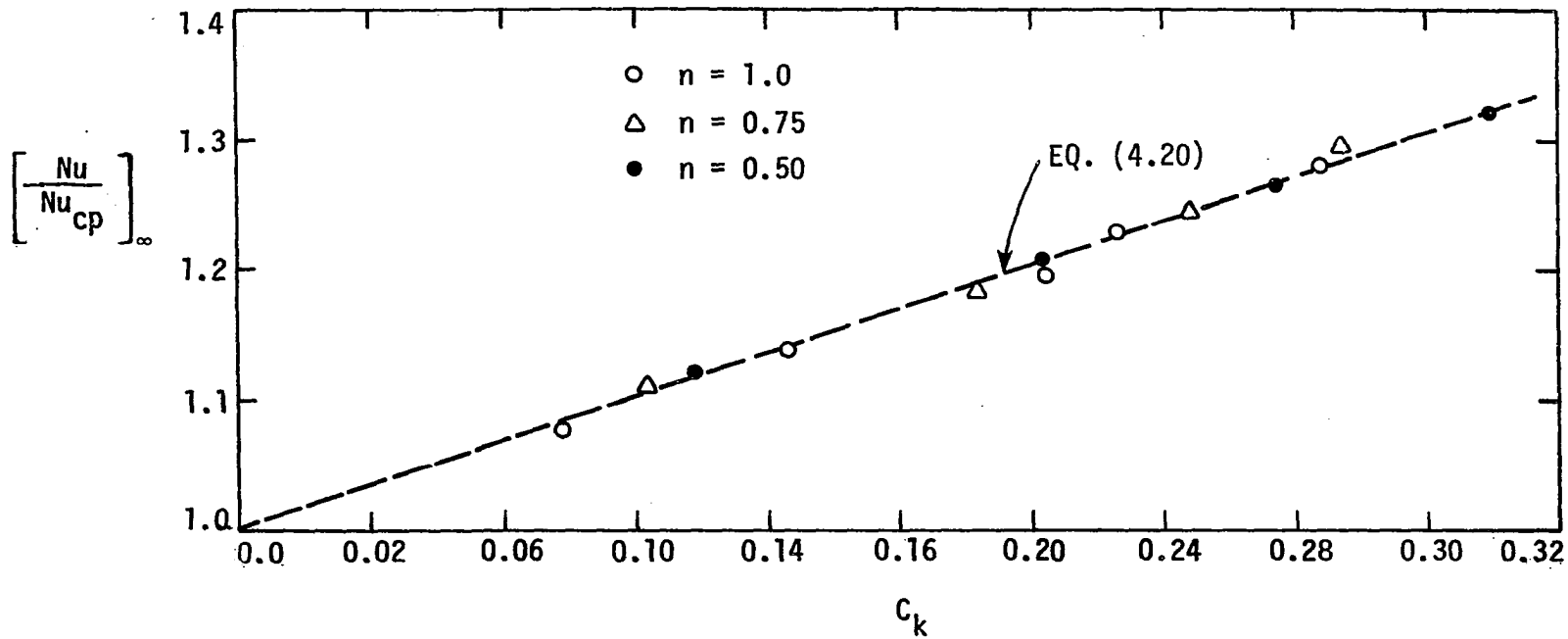

Fig. 4.14 Dependence of Nusselt ratio on consistency correction factor C_k.

that the extension is needed only for the fully developed region, while the results for the thermal entrance region are well established by the present analysis, independent of $\gamma\Delta T$.

For the fully developed case, for a given n, the physics of the present problem seems to indicate that with an increase in $\gamma\Delta T$ there should be an increase in $(Nu/Nu_{cp})_\infty$. However, in the present correlation, Eq. (4.20), the maximum value of $(Nu/Nu_{cp})_\infty$ occurs at

$$(\gamma\Delta T)_{max} = \frac{C_1(n)}{C_2(n)} \tag{4.21}$$

Thus, for $\gamma\Delta T > (\gamma\Delta T)_{max}$, Eq. (4.20) will give incorrect predictions. In order to overcome this difficulty, attempts were made to correlate $\gamma\Delta T$ and $(Nu/Nu_{cp})_\infty$ in such a fashion that all the coefficients in the correlation should have positive values. Attempts were made to fit either various polynomials or exponential forms, but all these attempts gave much poorer correlations of the present numerical predictions. Some attempts were made to extend the present correlation to higher values of $\gamma\Delta T$, but these attempts are too speculative, and since no experimental or numerical data are available for higher $\gamma\Delta T$ values, it was not possible to devise an extended correlation. The data of Bassett and Welty [61] have $\gamma\Delta T$ of the order of 20, but these data are restricted to the entrance region and can be reduced by the present analysis. More data are needed for such high $\gamma\Delta T$ values in the fully developed region to devise a meaningful correlation.

Design procedure

The effect of two corrections, namely the thermal entrance correction and the fully developed correction, is schematically shown in Fig. 4.16. As seen from this figure, in the proposed correlation, the thermal entrance region and the fully developed region are well correlated, but the transition region from the thermal entrance to fully developed section is slightly underpredicted. There have been two experimental studies [45,61] in this area. It will be shown later that the present proposed correction gives excellent results when applied to these experimental data sets, thus implying an insignificant effect of the overcorrection.

The problem still unresolved is how to estimate point "crit" in Fig. 4.16, i.e., determination of a point up to which the thermal entrance correction is applied and after which a fully developed correction is applied. A simple procedure to determine $((K/K_w)_{X^+})_{crit}$ is as follows:

For a given fluid, b and n are known and a wall heat flux q''_w is also known. Using Eq. (4.20), $(Nu/Nu_{cp})_\infty$ is estimated; also using Eq. (4.12), the thermal entrance correction exponent m is estimated. Thus as shown in Fig. 4.15, the intersection of fully developed correction and entrance region correction is a transition point "crit" at which the $(K/K_w)_{X^+}$ value is $((K/K_w)_{X^+})_{crit}$.

Thus,

$$\left(\frac{Nu}{Nu_{cp}}\right)_{X^+} = (C_c)^m \qquad (4.22)$$

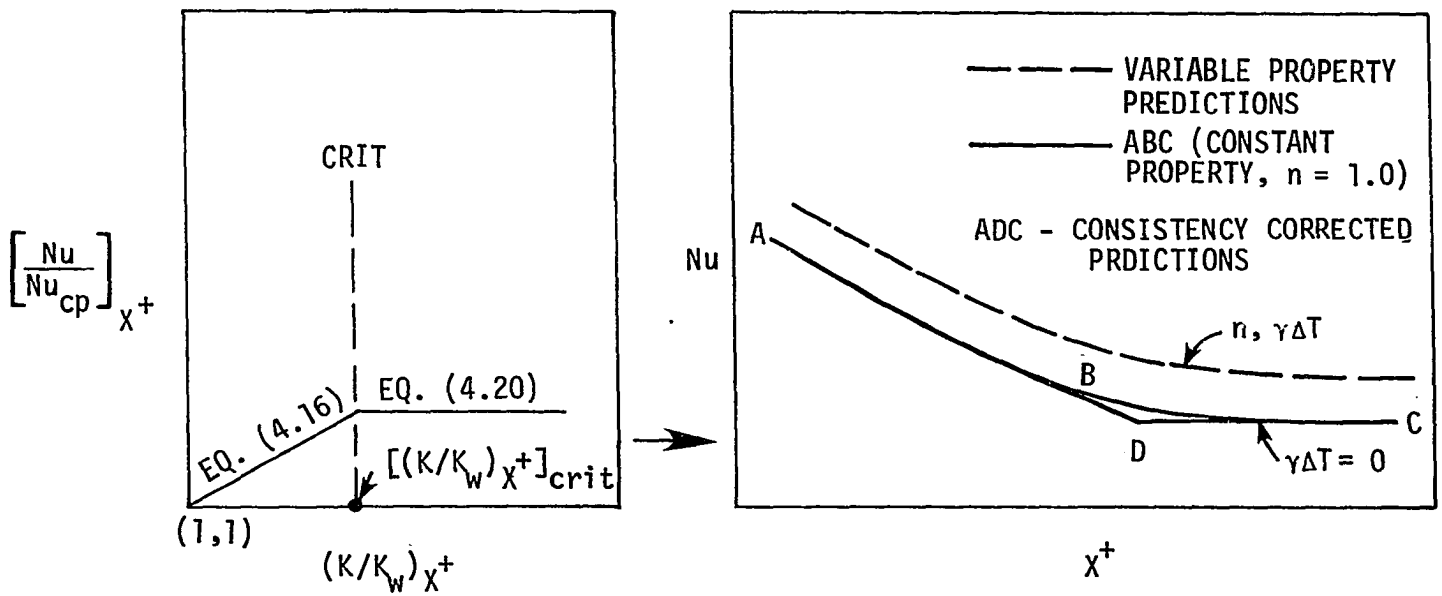

Fig. 4.15 Schematic diagram of the consistency correction.

where

$$C_c = (K/K_w)_{X^+} \quad \text{for} \quad (K/K_w)_{X^+} \leq ((K/K_w)_{X^+})_{crit}$$

and

$$C_c = ((K/K_w)_{X^+})_{crit} \quad \text{for} \quad (K/K_w)_{X^+} > ((K/K_w)_{X^+})_{crit}$$

In conclusion, pseudoplastic fluids having temperature-dependent fluid properties exhibit substantially higher heat transfer coefficients than Newtonian fluids. This increase is due to

1) Pseudoplasticity, which can be accounted for by applying the non-Newtonian correction, $\Delta^{1/3}$
2) Variable consistency effects, which can be accounted for by applying the $(C_c)^m$ correction.

Summary and Conclusions

An explicit stable numerical scheme has been developed to solve the problem of heat transfer in in-tube flow of pseudoplastic fluids. The explicit scheme does not involve iterations and, hence, is normally economical. The Newtonian results (Eq. 4.10)) have established m = 0.14 which is independent of X^+ and ratio of μ/μ_w as indicated by Shannon and Depew [34]. Thus the present results are similar to those obtained by Yang [32].

From the constant property analysis, a non-Newtonian correction $\Delta^{1/3}$ is established to account for the increase in heat transfer coefficients due to pseudoplasticity above the Newtonian values.

A substantial increase in heat transfer occurs due to temperature-dependent K. This increase was found to be a function of n and X^+. To account for this increase, a two-step correction $(C_c)^m$, one for the entrance region and one for the fully developed region is devised.

An unique explicit correlation, which avoids iteration is devised to calculate Nusselt numbers in the fully developed region (Eq. (4.20)).

CHAPTER V. REVIEW OF EXPERIMENTAL STUDIES

Introduction

The purpose of this chapter is to review the state-of-the-art of experimental studies for laminar heat transfer inside a circular tube. For convenience, the general scheme of the review of literature is given in Table 5.1. In this table UWT refers to a uniform wall temperature and UHF refers to a uniform wall heat flux boundary condition.

Table 5.1. Experimental studies of laminar flow heat transfer in circular tubes

	UWT	UHF
Newtonian	[62-71]	[34,72-84]
Non-Newtonian	[39,43,85-90]	[31,45,48,61]

A Newtonian fluid is a special case of the family of non-Newtonian power-law fluids. Conversely, many non-Newtonian heat transfer problems are looked upon as an extension of the corresponding Newtonian problem. This necessitates a clear cut understanding of heat transfer in Newtonian fluids.

In any experimental study, all fluid properties are temperature-dependent. Normally, density variations (free convection) and K- or μ-variations play a dominant role in altering the heat transfer rates at the wall. In a horizontal tube, forced convection and superimposed free

convection are perpendicular to each other, while in the vertical tube free and forced convection act along the same vertical axis. Thus, the physics of the problem in horizontal and vertical tubes is different and, hence, the geometric orientation of the tube is considered in the following discussion. However, for highly viscous fluids, the effect of K- or μ- variation is dominant, while the effect of ρ-variation is insignificant; hence, the results of these studies are independent of the tube orientation. Therefore, even though the literature review concentrates on the horizontal tube, the vertical tube literature with K- or μ- variation alone is also considered.

Newtonian Heat Transfer

UWT boundary condition

Isothermal wall tubes with only fully developed heat transfer are not of practical interest, since impractically long tubes are required to reach this point. However, if some local (or, more realistically, sectional local) data are available, the fully developed region might be displayed. In heat exchanger design, heat transfer in the entrance length is of interest and most UWT studies report average heat transfer coefficients.

Since the earliest studies it was felt that the Graetz solution for forced laminar flow of fluid through a tube did not adequately account for the variable property effects encountered in actual flow conditions. In 1929, Keevil and McAdams [62] acknowledged this fact. In 1931, Kirkbride and McCabe [63] clearly demonstrated the effect of free convection for in-tube flow of water and various light oils;

however, no quantitative estimation of this effect was given. In 1932, Drew [64] reported experiments with glycerol as a working fluid and demonstrated considerable increases in heat transfer coefficient with increases in temperature difference.

The pioneering work to correlate the effects of viscosity and density variation was reported by Colburn [65]. He conducted experiments with water and various oils as working fluids and proposed the following correlation:

$$Nu_{am} = 1.65(Gz_{am}\ \phi)^{1/3} \tag{5.1}$$

where $$\phi = \frac{\mu_{am}}{\mu_{ft}}\ (1.0 + 0.015Gr_{ft}^{1/3})^3$$

and $$t_{ft} = t_{am} + \frac{1}{2}\ (t_w - t_{am})$$

There is an apparent difficulty with ϕ having a multiplier of Gz, since the effect of free convection does not diminish as Gz becomes large, but remains a constant multiplier. Therefore, at high Gz values, Eq. (5.1) overestimates Nu_{am}.

In 1936, Sieder and Tate [38] published their famous results for the flow of viscous oils inside a tube. The authors obtained many data for the flow of viscous oils through a vertical tube. Data for flow of viscous oils through horizontal tube were also gathered from the previous investigations [62-65]. It was argued that, for viscous fluids, the density variation and, hence, free convection effects

are negligible. Thus, the observed increase in heat transfer (heating) or decrease in heat transfer (cooling) is solely due to viscosity variations. This increment was accounted for as

$$Nu_{am}/Nu_{cp} = (\mu_{am}/\mu_w)^{0.14} \tag{5.2}$$

This viscosity correction exponent 0.14 was subsequently widely accepted in the heat transfer literature.

Kern and Othmer [66] applied the Sieder-and-Tate-type viscosity corrections to Colburn's correlation and correlated their data and some previous data as

$$Nu_{am}\left(\frac{\mu_w}{\mu_{am}}\right)^{-0.14} = 2.25M\left(\frac{1.0+0.01Gr_{ft}^{1/3}}{\log Re}\right) \tag{5.3}$$

$$\text{where} \qquad M = 1.86\left(RePr\frac{D}{L}\right)^{1/3}$$

Their correlation, being an extension of Colburn's equation, has the same weaknesses as that of Colburn's correlation.

After 1943, all the experimental studies in this area [3,67-70], with one exception [71], have adopted the following general form of correlation

$$Nu_{am}\left(\frac{\mu_w}{\mu_{am}}\right)^{0.14} = C(Gz + DRa^e)^{1/3} \tag{5.4}$$

where C, D, and e are constants. In this correlation, the Seider-and-Tate viscosity correction is employed, Gz accounts for forced convection,

and Ra accounts for free convection. The additive form insures that at high Gz, the Ra term will be of less importance while at low Gz, the Ra term will become dominant. Thus, Nusselt number is altered by μ- and ρ-variation, and corrections for these variations are applied independently. The detailed list of various experimental studies (Table 5.1) and their correlations is given in Table 5.2. In this table

$$Y = Nu_{am} \, (\mu_w/\mu_{am})^{0.14} \tag{5.5}$$

McAdams [3] examined the data of Eubank and Proctor [67] and modified their correlation in such a fashion that the correlation reduces to normal forced convection in the absence of free convection ($Ra_{am} = 0$) and to normal natural convection in the absence of forced convection ($Gz_{am} = 0$). Nevertheless, with D/L in the expression, this can never be the case, since the transfer of heat by natural convection to fluids in horizontal pipes is independent of length, L. Oliver [68] realized this problem with McAdam's correlation and, hence, suggested a correlation, Eq. (5.9), which will go to normal natural convection in the absence of forced convection. However, he conceded that for the tubes having length to diameter ratio less than 70, L/D needs to be retained along with Ra to fit experimental data. Depew and August [70] have used the correction factor F_3 to avoid the anomaly caused by the use of the arithmetic mean temperature difference. Without the use of the correction factor, the calculated values of Nu_{am} are greater than the asymptote $Nu_{am} = 2Gz/\pi$ for low Gz (Fig. 2.1).

Each of these correlations is devised from the experimental data

Table 5.2. Experimental studies in horizontal laminar tube flow subjected to UWT boundary condition

Investigator	Ref	Working fluid	Correlation	
Eubank and Proctor	[67]	various oils	$Y = 1.75\ [Gz_{am}+12.6(\frac{Ra_{am}\ D}{L})^{0.4}]^{1/3}$	(5.6)
McAdams	[3]	various oils and viscous fluids	$Y = 1.75\ [Gz_{am}+0.04(\frac{Ra_{am}\ D}{L})^{0.75}]^{1/3}$	(5.7)
Oliver	[68]	water, ethyl alcohol, mixture of glycerol-water (80-20)	$Y = 1.75\ [Gz_{am}+0.0083(Ra_{am})^{0.75}]^{1/3}$	(5.8)
Brown and Thomas	[69]	water	$Y = 1.75\ [Gz_{am}+0.0012(Gz_{am}Gr_{am}^{1/3})^{4/3}]^{1/3}$	(5.9)
Depew and August	[70]	water, ethylene glycol, mixture of the glycol and water	$Y = 1.75F_3\ [Gz_{am}+0.12(Gz_{am}Gr_{am}^{1/3}Pr_{am}^{0.36})^{0.88}]$	(5.10)
Jackson et al.	[71]	air	$Nu_{am} = 2.67\ [Gz_{am}+(0.0087)^2\ (Ra_w)^{1.5}]^{1/6}$	(5.11)

for certain fluids and, hence, the choice of the correlation to be used should be based on the working fluid. The correlation of Depew and August, Eq. (5.10), fits all the data [67,68,69,70,71] with ± 40 percent and, hence, this correlation is probably the best for any general design purpose.

UHF boundary condition

Quite a few experimental studies are reported for fully developed heat transfer with the UHF boundary condition. In the fully developed region, free convection may play a dominant role in determining the heat transfer rates at the wall. This effect is clearly shown in the upper portion of Fig. 5.1.

McComas and Eckert [72] and others [73-75] reported studies with air, while studies with water are reported by Ede [76] and others [77-81]. Siegwarth et al. [82] and Shannon and Depew [34] conducted studies with ethylene glycol as the working fluid. Bergles and Simonds [81] studied two boundary conditions, namely axially and circumferentially uniform heat flux (zero wall conductivity, ZC) and axially uniform average heat flux but circumferentially uniform temperature at each axial location (infinite wall conductivity, IC).

In these experimental studies, a substantial disagreement among various investigations for a given fluid as well as among results for each of these three fluids is noticed (Fig. 5.1). To resolve this, Morcos and Bergles [83,84] have obtained extensive experimental data for two fluids (water, ethylene glycol) and for two tubes (metal tube -

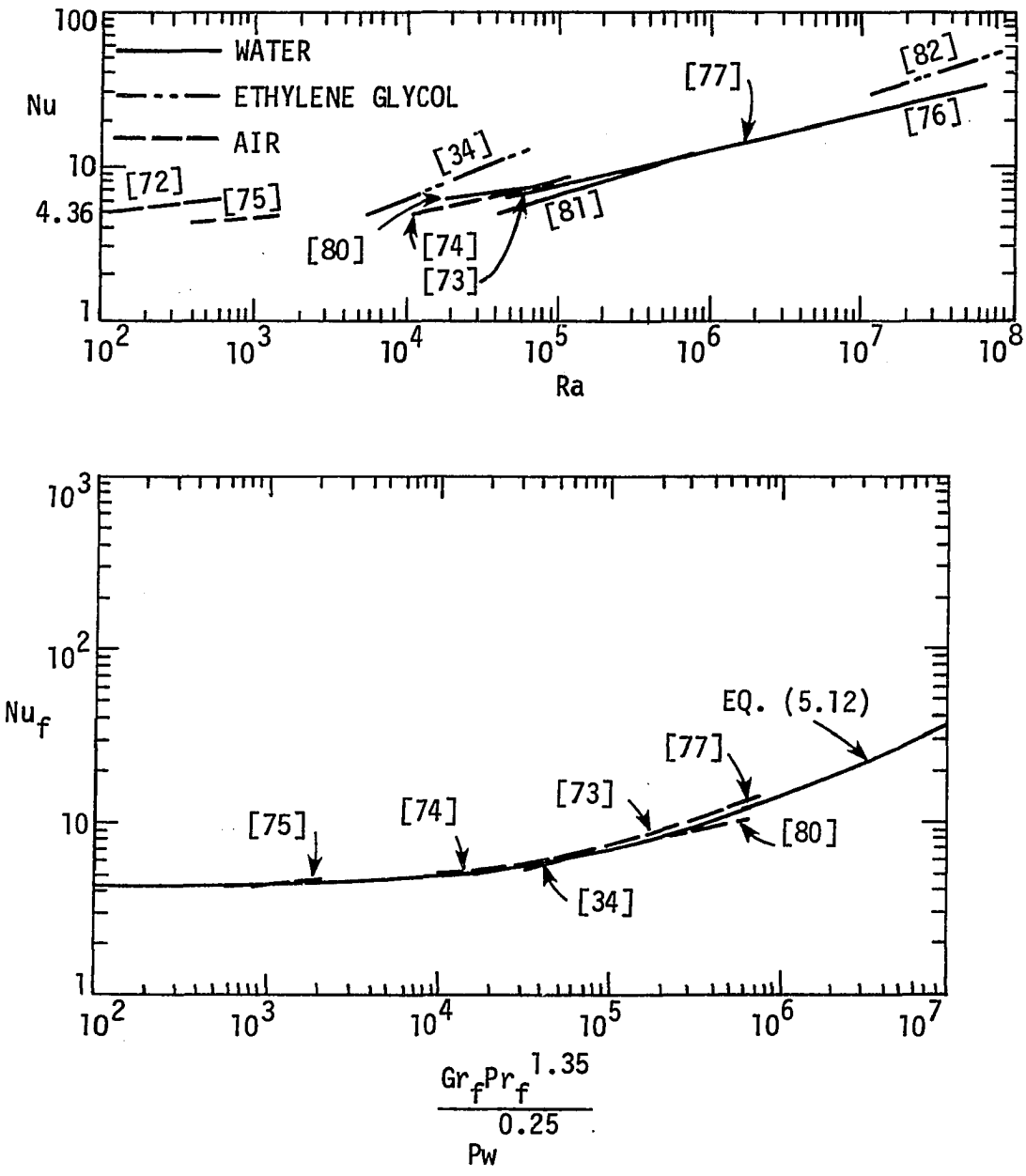

Fig. 5.1 Comparison of fully developed, heat transfer data for a UHF boundary condition.

IC and glass tube - ZC) and have correlated their data as

$$Nu_f = \left[(4.36)^2 + \left(0.055 \left(\frac{Gr_f Pr_f^{1.35}}{P_w^{0.25}}\right)^{0.40}\right)^2\right]^{1/2} \qquad (5.12)$$

where $P_w = hD^2/(kl\ w)$, kl is tube wall conductivity, and w is tube wall thickness. The dimensionless tube wall parameter P_w accounts for circumferential conduction. It is important to note that Eq. (5.12) is based on the film temperature which is an alternative way to account for temperature-dependent properties. A comparison of this correlation with data from other studies [33,73-77,80] is shown in Fig. 5.1. It is seen that Eq. (5.12) correlates data for various fluids and for various tubes very well.

The discussion so far has been restricted to the fully developed case. For the thermal entrance length, data are available for air [74], for water [77-80], and for ethylene glycol [34]. The only correlation available for the entrance length is given by Petukhov and Polyakov [77] as

$$Nu = Nu_{cp}\ [1 + (\frac{Ra}{B})^4]^{0.045} \qquad (5.13)$$

where $B = 10^4/X^+$ for $X^+ \leq 3.4 \times 10^{-3}$

and $B = 1.8 \times 10^4 + 55(\frac{X^+}{2})^{-1.7}$ for $X^+ > 3.4 \times 10^{-3}$

This correlation correlates most of the data very well; however, it is important to note that the free convection reduces the entrance length

and if free convection is strong ($Ra > 5 \times 10^5$), the entrance length is very short and can be neglected for engineering calculations.

From the preceding discussion it is seen that there is enough data and correlations are well established for this case; therefore, no further work seems to be necessary.

Conclusions

The preceding discussion of Newtonian heat transfer inside a horizontal tube shows that there are abundant data and well established correlations which are adequate for important fluids, such as air, water, and ethylene glycol. No further work seems to be necessary with either the UWT or UHF boundary condition. More viscous fluids, where free convection is not important, have been extensively tested with UWT, but more data appear to be required for UHF conditions.

Non-Newtonian Heat Transfer

Excellent reviews of the literature for heat transfer to various non-Newtonian fluids have been published by Skelland [1], Metzner [60], and others [85,86]. The following review of literature is restricted to pseudoplastic fluids.

In most of the experiments the dimensionless numbers are based on the μ_{eff}, which is defined as

$$\mu_{eff} = \frac{\tau_w}{\left(\frac{du}{dy}\right)_{Newt,w}} = \frac{K'\left(\frac{8\bar{u}}{D}\right)^n}{\left(\frac{8\bar{u}}{D}\right)} \tag{3.28}$$

where $k' = K \left(\frac{3n+1}{4n}\right)^n$

During experiments, the average velocity, $\bar{u}$ can be calculated from the fluid mass flow rate, while τ_w is obtained from the pressure drop. A flow curve is then constructed, and K', n, and, hence, K are obtained. The details of this procedure are given in Appendix I.

UWT boundary condition

Metzner et al. [87] conducted experiments with various carbopol and methocel (carboxymethylcellulose, CMC) solutions and correlated their data for Gz > 100 as

$$Nu_{am} = 1.75 \left(\frac{K_{am}}{K_w}\right)^{0.14} (\Delta Gz_L)^{1/3} \qquad (2.30)$$

This equation is a straightforward extension the Newtonian constant property solution, with a non-Newtonian correction $\Delta^{1/3}$ and a Seider-and-Tate-type non-Newtonian consistency correction.

Charm [88] and Charm and Merrill [89] used applesauce, banana puree, etc. as the working fluids, and the correlation they suggested was

$$Nu_{am} = 2(Gz_L)^{1/3} \left(\frac{K_{am}}{2K_w} \left(\frac{3+1/n}{3-1/n}\right) \right)^{0.14} \qquad (5.17)$$

Gluck [90] obtained extensive data with various carbopol solutions. Metzner and Gluck [91] incorporated the effect of free convection and correlated the data of Gluck and others [88,89]. They have extended the

Eubank and Proctor [67] correlation, Eq. (5.6), for Newtonian fluids to the non-Newtonian case as follows:

$$Nu_{am} = 1.75\Delta^{1/3} \left(\frac{K_{am}}{K_w}\right)^{0.14} \left[Gz_L + 12.6 \left(PrGr\frac{D}{L}\right)_w^{0.4}\right]^{1/3} \tag{5.18}$$

Prandtl and Grashof numbers contain μ_{eff} evaluated at wall temperature and wall shear rate. The authors argued that near the wall, μ_{eff} will be lowest and the resistance to convective motion is least and, hence, it is appropriate to use wall values.

Oliver and Jenson [92] obtained extensive data with various methocel and polyox solutions. Their data were poorly correlated by Eq. (5.18); hence, they modified the Newtonian Eq. (5.9) to correlate their data as

$$Nu = 1.75 \left(\frac{K_{am}}{K_w}\right)^{0.14} (Gz_L + 0.0083(GrPr)_w^{0.75})^{1/3} \tag{5.19}$$

It is important to note that Eq. (5.19) does not have the non-Newtonian correction $\Delta^{1/3}$. Christiansen et al. [40] also have reported some experimental data which showed fairly good agreement for large Gz values with their analytical solution, which was already discussed in Chapter II. However for $Gz < 250$, large scatter was noticed, which was attributed to natural convection effects which were neglected in their analysis. Christiansen et al. [40] also have reported some data for cooling of pseudoplastic fluids.

From the preceding discussion, it is seen that there are abundant

data with this boundary condition. There is an apparent discrepency between the various correlations Eqs. (2.30) and (5.19). In Eqs. (5.18) and (5.19) the effect of free convection is included while in Eqs. (2.30) and (5.17), free convection effects are not included. However, for viscous fluids, in Eq. (5.19) the term $0.0083\ (GrPr)_w^{0.75}$ will be very small as compared to the Gz_L, and the final results of Eqs. (5.19) and (2.30) will be different by a factor of $\Delta^{1/3}$.

UHF boundary condition

Mizushina et al. [31] have conducted an experimental study with methocel solutions. The data were obtained for $X^+ = 5\times10^{-3}$ to 0.15 and compared with their analytical solution (see Chapter II), their two-step correlation is

$$Nu = 4.36\Delta^{1/3}(K/K_w)^{0.1/n^{0.7}} \quad \text{for } X^+ \geq 0.05 \qquad (2.28)$$

and,

$$Nu = 1.41\ (\Delta Gz)^{1/3}\ (K/K_w)^{0.1/n^7} \quad \text{for} \quad X^+ < 0.05 \qquad (2.38)$$

A large scatter (± 50-60 percent) was found between these correlations and the data.

Bassett and Welty [61] have obtained data with methocel and polyox solutions. The rheological model they used was

$$\frac{\partial u}{\partial y} = E_1\tau + E_2\tau^2 + E_3\tau^3 \qquad (5.20)$$

where E_1, E_2 and E_3 are constants. It is important to note that in the

strict sense this is not a pseudoplastic model. The data, obtained for Gz = 200 to 30,000, were correlated by

$$Nu = 1.85\ Gz^{(1/3)} - (0.03/\Delta) \tag{5.21}$$

Mahalingam et al. [45] have obtained data with various methocel solutions with n varying from 0.34 to 0.75. The data reported (23 points) are in the range of $X^+ = 3.9\times10^{-4}$ to 2.2×10^{-3}. The authors correlated their data by

$$Nu = 1.46\ \left(\frac{K}{K_w}\right)^{0.14} \Delta_w^{1/3}[Gz + 0.0083(GrPr)_w^{0.75}]^{1/3} \tag{5.22}$$

This correlation is similar to Eq. (5.19) suggested by Oliver and Jensen [92] for a UWT boundary condition.

Bader et al. [48] have reported a study involving uniform velocity at the onset of heating. Their data are in good agreement with their analytical solution which varies little from the parabolic velocity solution. No correlation was given. As mentioned earlier, it is important to note that most pseudoplastic fluids have Pr >> 5 and, hence, the problem of simultaneous development of velocity and temperature profile is of little interest.

From the preceding discussion it is seen that the correlations of Mizushina et al. are not adequate. Mahalingam et al. have devised a correlation, but their data are few (only 23 points for $X^+ = 3.9\times10^{-4}$ to 2.2×10^{-3}). Bassett and Welty have not used a pseudoplastic constitutive equation; but their data for 5.4 percent methocel exhibit a pseudoplastic

behavior on a K against $(\partial u/\partial y)$ plot. Mahalingam et al. have used a free convection correction in their correlation while Mizushina et al. and Bassett and Welty have not included free convection in their correlation. This is an apparent discrepancy. The data of Bassett and Welty as well as that of Mahalingam et al. are restricted to the entrance region. The data for the fully developed region are almost non-existent.

Conclusion

There are sufficient data and well established correlations for a UWT boundary condition. However, for a UHF boundary condition, more data are needed for the entire thermal length.

Scope for Further Work

The preceding review of literature indicates the need for further work for pseudoplastic fluids with a UHF boundary condition in the following areas:

1) More experimental data are required in the thermal entrance region as well as in the fully developed region.

2) There is a need to establish a generalized correlation for various n values.

3) The data of various investigators [45,61] need to be compared.

CHAPTER VI. EXPERIMENTAL SETUP AND PROCEDURE

Introduction

The object of the present experimental investigation was to obtain new experimental data for the flow of pseudoplastic fluids inside a circular tube subjected to a constant wall heat flux boundary condition. The fluid velocity is fully developed at the onset of heating.

The experimental data are to be obtained for the entire thermal length. Two fluids and two tubes of different length are utilized to cover a wide range of conditions. These data are to be compared with the solution developed in Chapters III and IV as well as experimental results of other investigators noted in Chapter V.

In this chapter, the details of the experimental facility and test procedure are described.

Experimental Setup

Test loop

The test facility utilized here was constructed in the ISU Heat Transfer Laboratory by Morcos and Bergles [83] and later used by Hong [54]. This facility was designed to allow flexibility in testing different tubes; hence, both test sections utilized in the present study were installed in the apparatus simultaneously. By operating a few shut off valves, one test section can be brought into operation at a time. However, several modifications and improvisations were made in the test facility for the flow of viscous pseudoplastic fluids.

A schematic diagram of the test loop is shown in Fig. 6.1 and

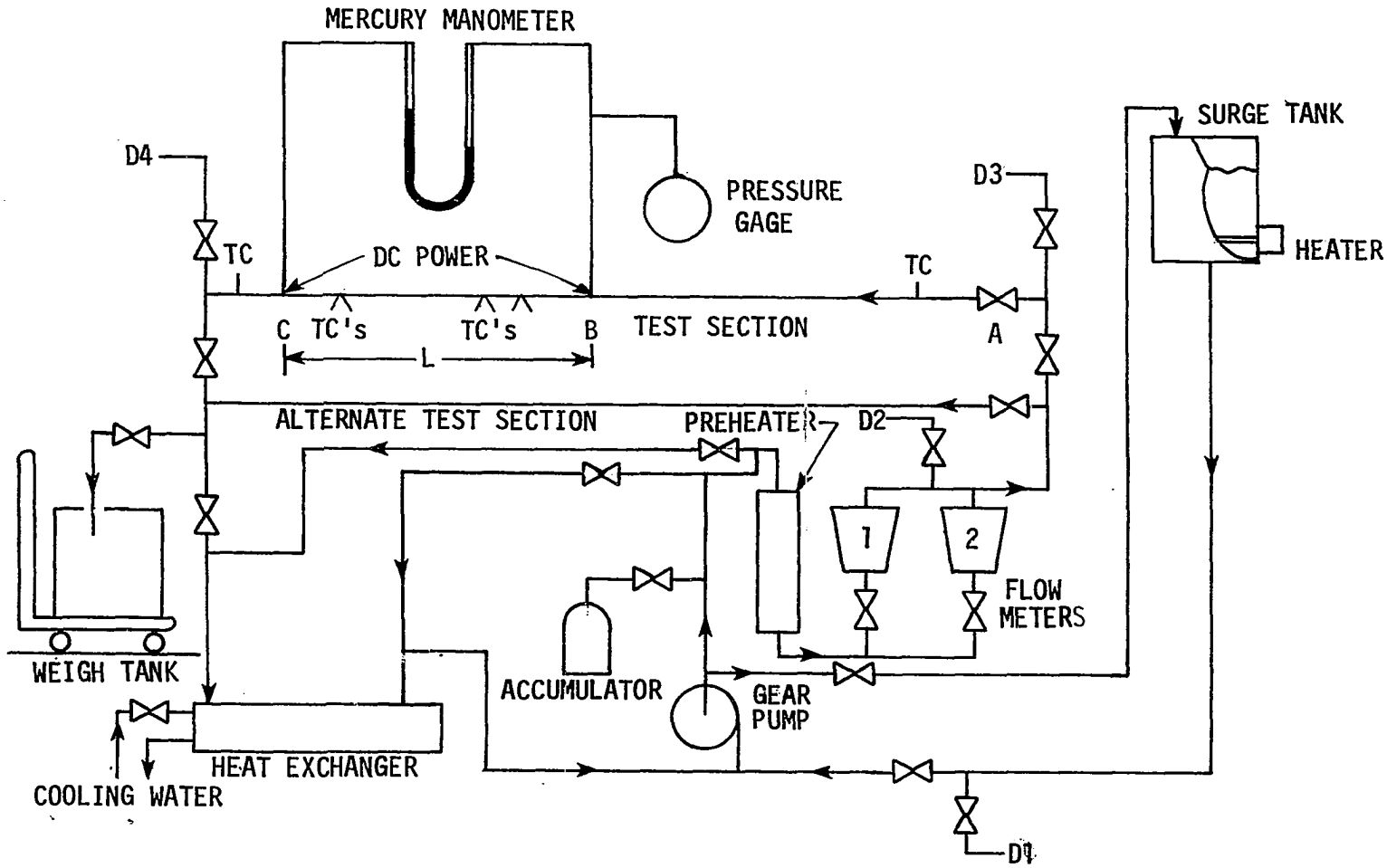

Fig. 6.1 Schematic diagram of test loop.

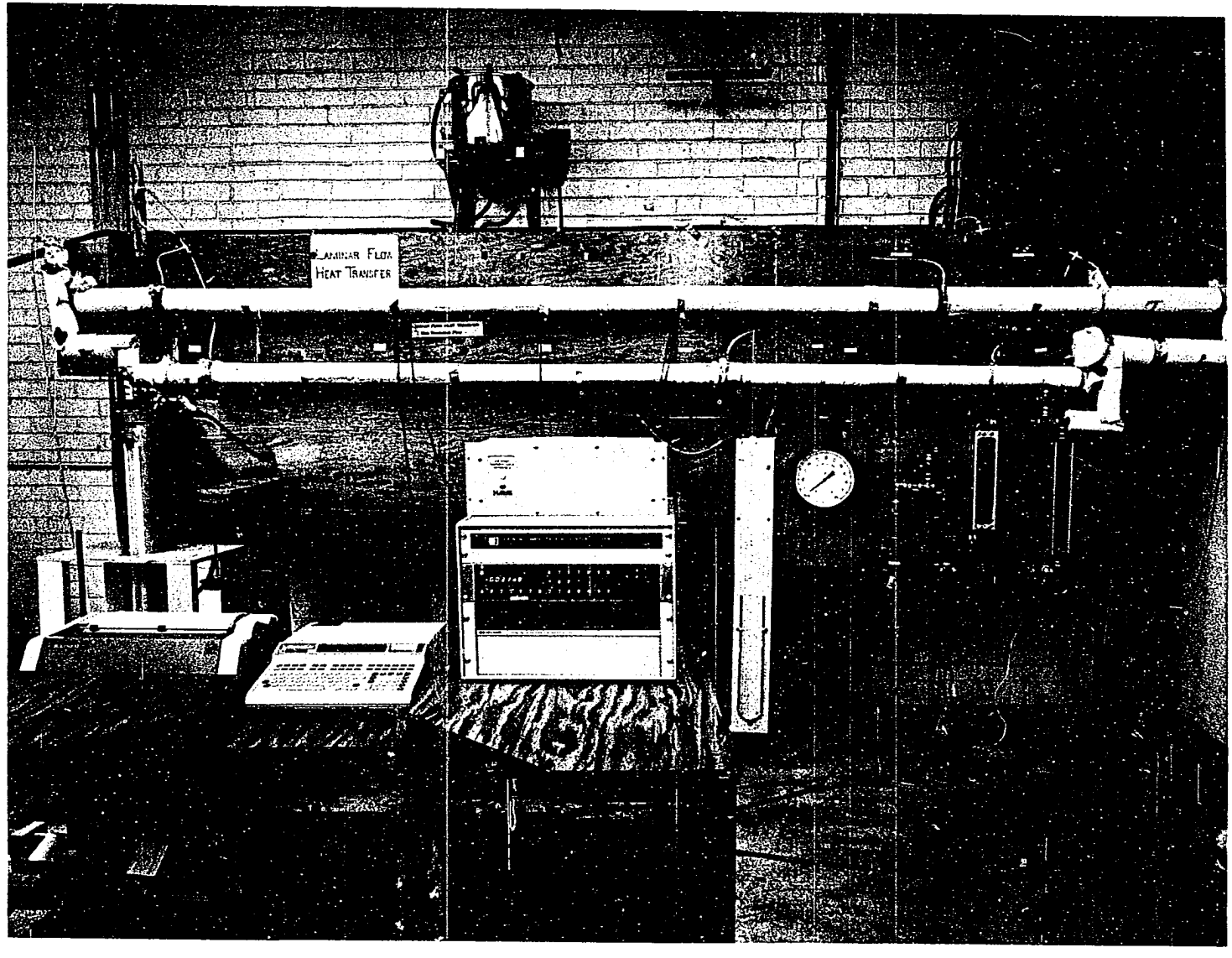

Fig. 6.2 Photograph of experimental apparatus.

a photograph is presented in Fig. 6.2. The loop is a closed loop, low pressure system with all piping made of copper tube and brass fittings. Several drains are provided in the test loop to facilitate introduction of the test fluid.

The working fluid was stored in a five gallon stainless steel tank, which was equipped with an electric heater. The fluid was circulated with a gear pump (Oberdorfer #3000R, Gelber pump, 600 rpm, pulley driven, with 1/2 hp, 1725 rpm, Dayton capacitor ac motor). This positive displacement pump was found to be essential to pump highly viscous non-Newtonian fluids. A one-gallon accumulator, charged with nitrogen, was installed at the pump outlet to dampen pressure fluctuations. After passing the accumulator, some flow was bypassed for flow control, while the rest of the fluid entered the test section line. In the test section line, fluid passed through a preheater, flowmeters, and through the test section; it then merged with the bypass-line fluid, and then passed through the heat exchanger, where it was cooled and then returned to the pump.

Two flowmeters were provided in the test section line. The first flowmeter used was Brooks rotometer (Model 1307, Size 7) with Monel float which could measure up to 0.39 GPM of water, while the other flowmeter (Model 1110, Size 8) had a stainless steel float (8-Rv-114) which could measure up to 1.45 GPM of water. For the pseudoplastic fluids, apparent viscosity is a function of du/dy (Eq. (1.3)) and also, K is highly sensitive to temperature. In addition, most pseudoplastic fluids undergo degradation with time; hence, it was not possible to obtain a

consistent, stable flowmeter calibration. Therefore at the outlet of the test section, a weigh tank was incorporated to measure the flow rate, while the flowmeter was simply used as a flow indicator. At the end of each run, the fluid from the weigh tank was pumped back to the top stainless steel tank.

Test section

Two thin-walled, 304 stainless steel, circular tubes were used as test sections. The wall thickness of the tube was a compromise between minimum thickness required for maximum electrical resistance and sufficient mechanical strength. The details of these test sections are given in Table 6.1, Fig. 6.3. and Fig. 6.4. Each of these tubes had an inlet calming section, AB, to allow the velocity profile to be fully developed at the entrance of the heated test section, BC.

Table 6.1. Test section details

	Test Section I	Test Section II
Inner diameter (in.)	0.401	0.506
Outer diameter (in.)	0.441	0.562
Total length (ft)	11.00	12.25
Heated length (ft)	5.98	8.98
Calming length (ft)	3.5	2.5
Number of axial temperature measuring stations on the heated test section	4	8

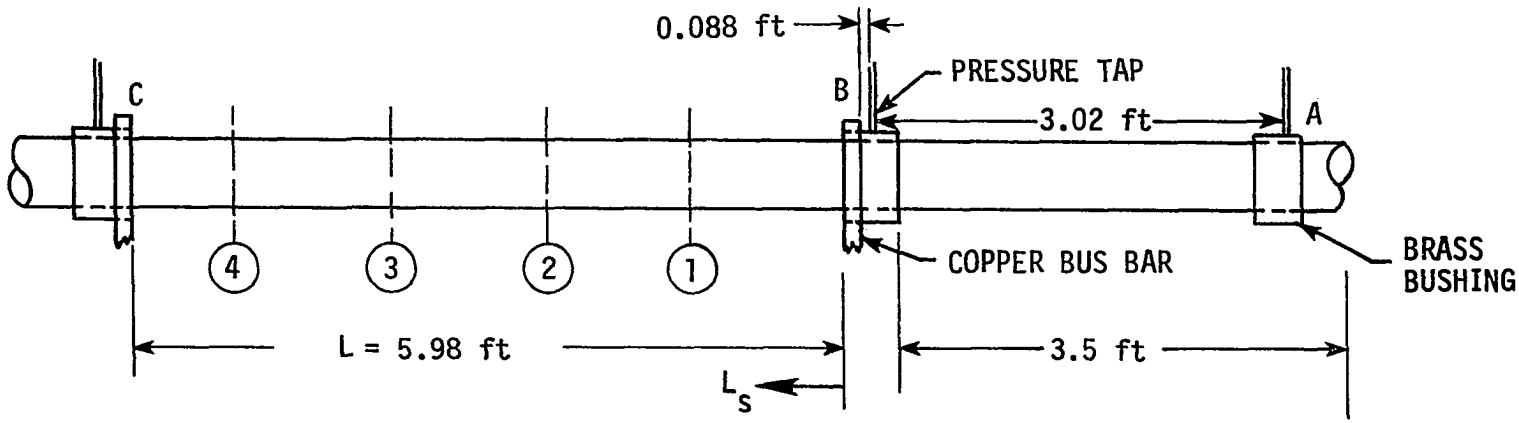

THERMOCOUPLE ATTACHMENT

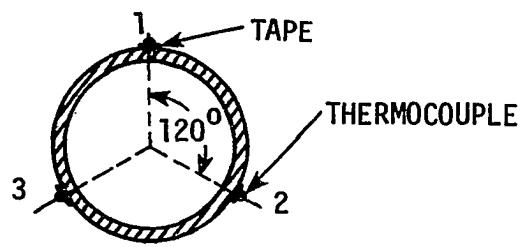

MEASURING STATION NO.	L_s ft	x/D	L_s/L
1	0.92	27.60	0.154
2	1.94	57.67	0.324
3	3.68	110.04	0.616
4	5.03	150.41	0.842

Fig. 6.3 Schematic diagram of Test Section I.

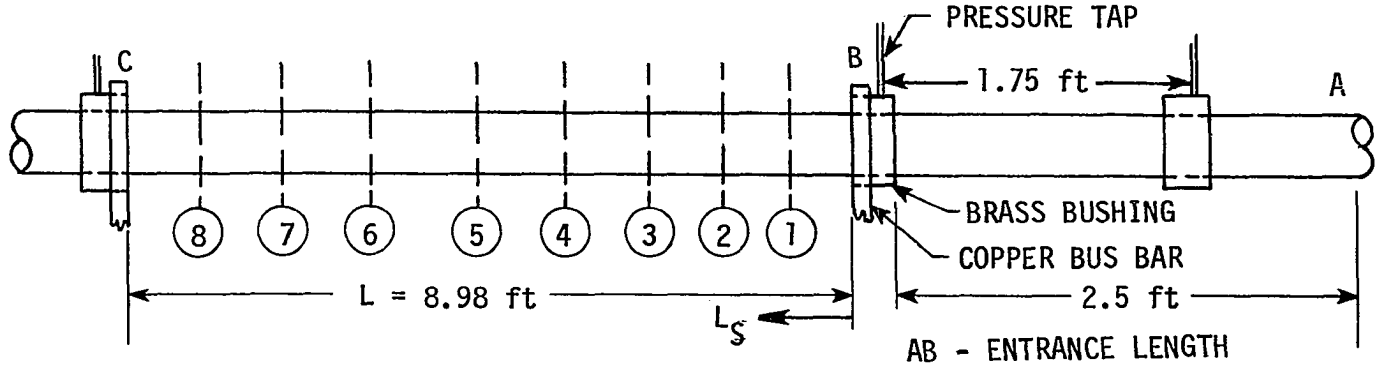

THERMOCOUPLE ATTACHMENT

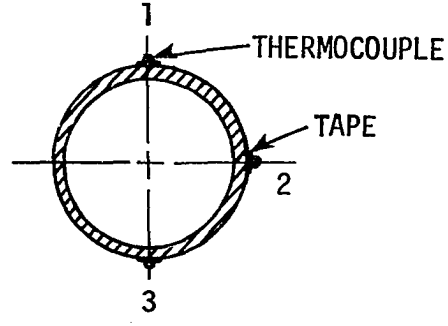

MEASURING STATION NO.	L_s ft	x/D	L_s/L
1	0.41	9.63	0.045
2	0.99	23.57	0.111
3	2.47	58.49	0.275
4	3.97	94.03	0.441
5	5.48	129.81	0.610
6	6.98	165.35	0.776
7	7.81	185.09	0.869
8	8.64	204.77	0.961

Fig. 6.4 Schematic diagram of Test Section II.

Several copper-constantan thermocouples (Leeds Northrup duplex-30 gage wire, glass wrap - glass braid, Model #G-T-30) were installed on the outside wall, along the length of the heated test section. These thermocouples were electrically insulated from the test section with vinyl plastic electrical tape (Scotch Brand No. 33+, 0.007 in. thick).

At each axial location, three thermocouples were mounted as shown in Figs. 6.3 and 6.4. This arrangement was considered adequate to distinguish circumferential temperature gradients caused by free convection.

The test section was heated by a dc current passed directly through the tube wall. The electric power supply was a 25 kw dc, 125 v, 200 amp compound-wound generator driven by an induction motor. Power cables were connected through a copper bus bar to two brass bushings soldered on each end of the heated section. A dummy load was used in series with the test section in order to boost the resistance and provide better control.

On each brass bushing, an arrangement was devised to measure the fluid pressure. On the test section, three 1/32 in. holes, 120° apart were drilled near the inlet. On the inside diameter of the brass bushing, a circumferential slot was made, 0.25 in. wide and 0.0825 in. deep. The three holes on the tube were matched exactly with this slot. One single stem came out of this slot, so that an average inlet fluid pressure could be measured. Such an arrangement was also made at the inlet and the outlet of the heated length.

To minimize the heat loss, the complete test section was heavily insulated with 1/4 in. thick Armaflex and 1 in. thick fiberglass insulation. Large portions of the piping before and after the test section were also heavily insulated. The ends of the test sections were electrically (as well as thermally to some extent) insulated from the rest of the loop by means of short pieces of Buna N pressure hose.

Measurements and controls

The fluid flow rate through the test section was adjusted by controlling ball valves in the bypass lines. The flow rate was precisely controlled by a needle valve placed upstream of the test section. The flowmeters were used as the flow indicators, while the actual flow rate was measured with a weigh tank at the end of each run.

The fluid inlet pressure was measured by a simple pressure gauge, while the pressure drop across the heated length was measured by an U-tube mercury manometer with a resolution of 0.025 in.

The desired power input was supplied to the test section by adjusting a dummy load in series with the test section. However, precise control was obtained by monitoring the shunt field rheostat of the compound-wound dc generator. The power input to the test section was determined by measuring the current and the total voltage drop across the test section. The voltage drop was measured by a digital voltmeter (DigiTec Model 294, dc) with an accuracy of ± 1.0 percent and 0.005 v resolution. The current was measured by means of a calibrated Esterline Angus Shunt (240 amp/100 mv) connected in series with the test section.

The voltage across the shunt resistance was monitored with a digital millivoltmeter (Hewlett-Packard 3490A, multimeter) with a resolution of 0.001 mv.

The tube wall temperatures were measured by the copper-constantan thermocouples attached on the outside wall of the tube. The inlet temperature of the fluid was measured by a thermocouple probe installed directly in the fluid stream at the inlet of the entrance length. A few thermocouples were also mounted on the outside wall of the entrance section. All of these thermocouples normally used to read within $\pm 0.05°F$, and, thus, provided an accurate estimation of the fluid inlet temperature. A few inches from the outlet of the heated test section, a Kinecs Mixer, 6 in. long, was introduced inside a tube to ensure a thorough mixing of the outlet fluid. Immediately after the mixer, another thermocouple probe was directly installed in the fluid stream to measure the fluid outlet temperature.

The thermocouple millivoltage signals were measured by Hewlett-Packard data acquisition system [93] in the ISU Heat Transfer Laboratory. This data acquisition system contains

1) Hewlett-Packard Model 9825A Calculator
2) Hewlett-Packard Model 98210A advanced ROM (Read Only Memory)
3) Hewlett-Packard 98213A general/extended input-output ROM
4) Hewlett-Packard Model 98034A interface
5) Hewlett-Packard Model 9871A printer
6) Hewlett-Packard Model 3050B System consisting of
   Model 3455A digital voltmeter
   Model 3495A scanner (40 channels)

7) Kaye Instruments Model K170-36C ice-point reference

A functional diagram of the Data Acquisition System is shown in Fig. 6.5 and photographs are shown in Figs. 6.6 and 6.7.

This system facilitates the data acquisition efficiently and accurately. It takes only several seconds to read all thermocouples and check the energy balance.

Experimental Procedure

Test fluids

Two pseudoplastic fluids, 1.0 percent and 0.9 percent by weight aqueous solution of HEMC (XD - 7630.02 - cellulose ether powder, the Dow Chemical Company) were used as the working fluids. These two fluids have substantially different viscosities, and for a given temperature, these two fluids exhibit substantially different K and n values. These water solutions were chosen because they definitely form pseudoplastic fluids which are fairly stable, no health or fire hazard is associated with them, and they are relatively easy to obtain and prepare in large quantities. These fluids are quite viscous (about 100 cp), but they could be handled by the gear pump in the test loop. The details of the solution preparation are given in Appendix H.

These fluids have strong temperature-dependent consistency index K. A temperature change of the order of 30°F, causes K to change almost 100 percent. On the other hand, the flow behavior index is a weak function of temperature. In these solutions, n varied over the approximate range of 0.55 to 0.80. The experimental determination of

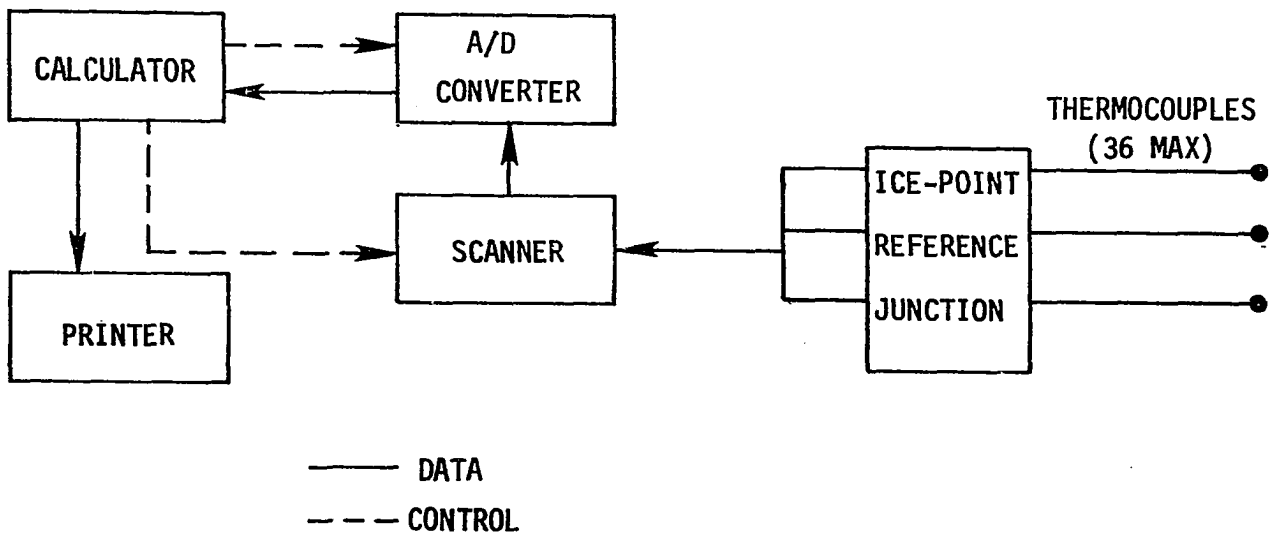

Fig. 6.5. Functional diagram of the Data Acquisition System.

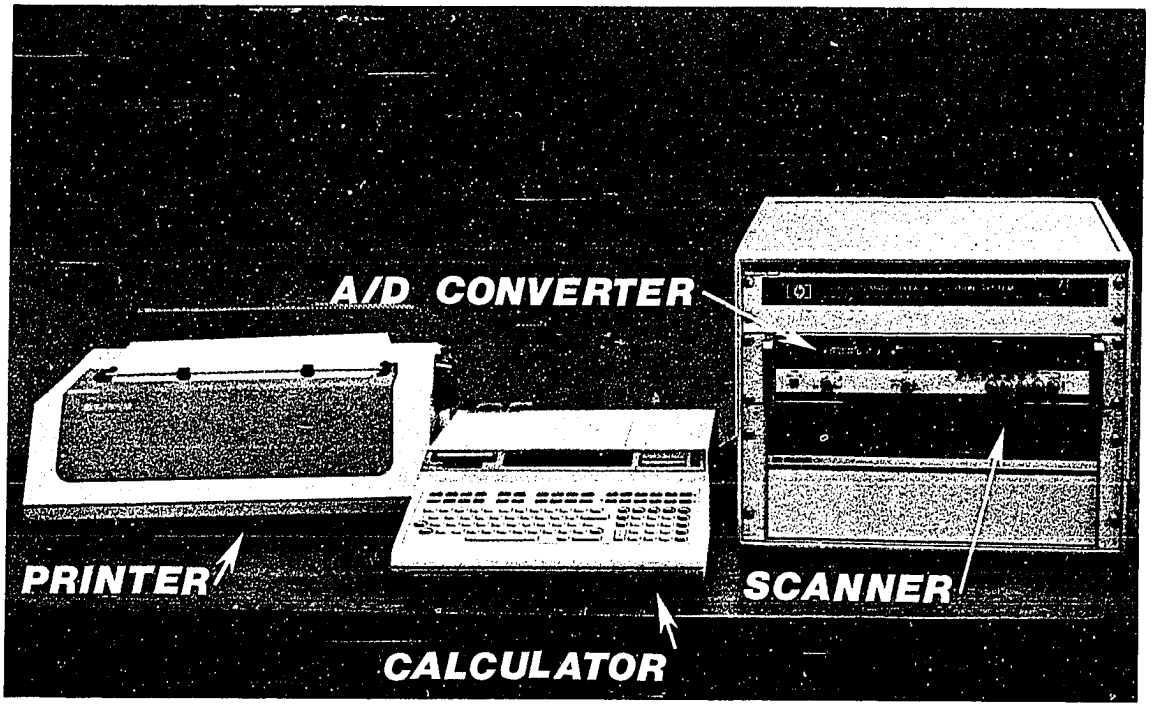

Fig. 6.6 Printer, calculator, and A/D converter/scanner.

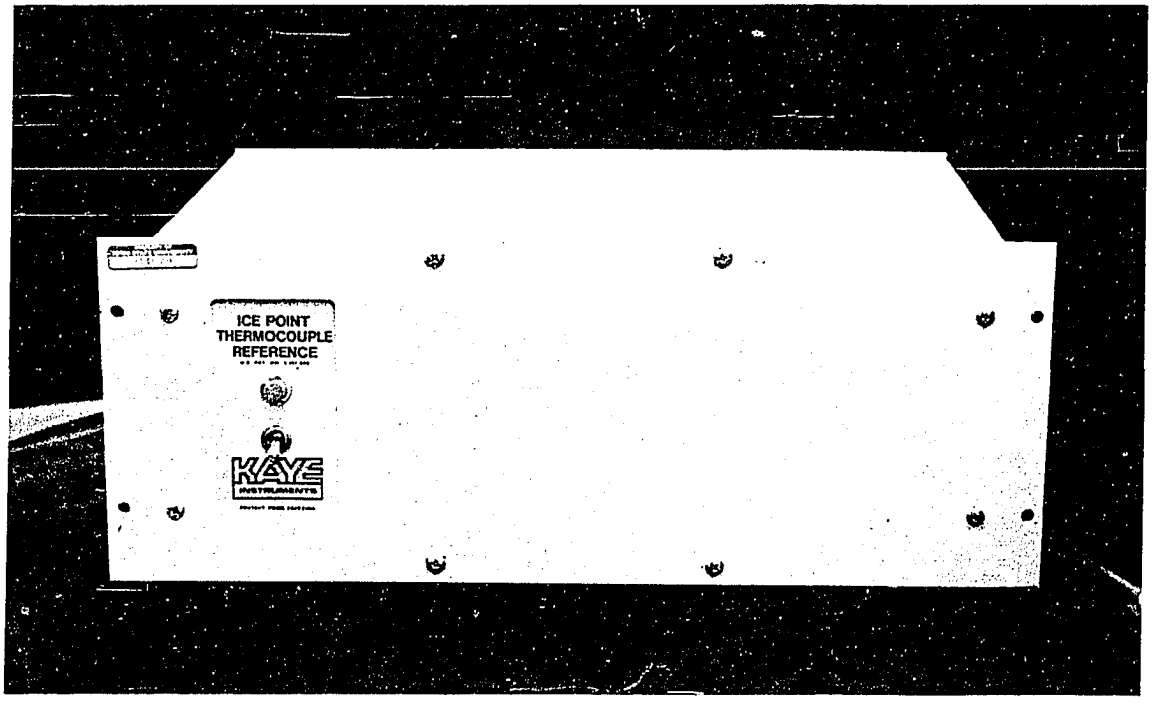

Fig. 6.7 Ice-point reference.

K and n for these fluids is given in Appendix I.

Since these solutions are very weak solutions, all fluid properties, other than K and n, were assumed to be the same as the water solvent [39, 94,95,96]. The details of these properties are given in Appendix J.

These fluids were found to exhibit aging, and, therefore, K and n varied with time. To account for this aging, rheological tests were done before and after heat transfer runs to evaluate K and n. The averaging procedure developed to account for this variation is also described in detail in Appendix I.

Filling the test loop

A critical part of the experiments was to fill the test loop with the working fluid so that no air was entrained in the system. Since the working fluids were highly viscous, entrained air bubbles were frequently present in the fluid. On these entrained air bubbles, the viscous force was so high and the buoyant force was so small that normally it took about 3-4 hours for an air bubble to rise two feet inside a fluid column. Entrained air causes erroneous flow rate measurements, augmented heat transfer, foaming and other undesirable behavior.

In order to avoid this problem and ensure an air bubble free solution inside the test loop, four drains, D_1, D_2, D_3 and D_4 (Fig. 6.1) were incorporated in the test loop. To begin with, all valves and drains were closed. The top tank was filled with the working fluid and liquid was allowed to stay there for a day or two. After this, only drain D_1 was opened and the fluid was drained by gravity into bottles.

During each draining, the top tank was almost emptied and the fluid was collected in bottles which were emptied back in the top tank. This draining was done about 3-4 times and took about a day. Later, in a similar fashion, the fluid was drained through drains D_2, D_3 and D_4. Care was also taken to wait for at least 3-4 hours between the consecutive draining operations so that the fluid in the top tank did not have any entrained bubbles.

These draining operations were done about 20 times and took about a week. In this way it was ensured that no air bubbles were present in the system. This was checked by looking through the glass flow-meters and observing the fluid coming out of the drain as it passed to a bottle for collection through a transparent tygon tubes. Finally, drains D_3 and D_4 were closed, and the complete test loop was filled with the working fluid. It is important to note that all the draining of the fluid was done by gravity flow; the gear pump was not started to avoid foaming of the solution.

Operating procedure

The test loop was first filled by the working fluid as described in the previous section. An adequate liquid level was always maintained in the top tank so that the complete loop remained flooded, thereby ensuring that no air was introduced into the system.

In each heat transfer test sequence, the gear pump was started to circulate the liquid through the loop. The desired flow rate was established by adjusting several bypass line valves and the needle valve

upstream of the test section. The dc generator unit was started, and the desired power was established by adjusting dummy loads and the shunt field rheostat of the generator. The cooling water was circulated through the heat exchanger. The temperature at the inlet of the test section was adjusted by controlling the heat exchanger cooling water rate and the power input in the preheater. Intermittent adjustment of the shunt field rheostat of the generator was required to compensate for oscillation of the voltage.

Usually it took about one hour to reach steady-state flow and thermal conditions. Once steady-state conditions were reached, fluid flow rate, current, voltage drop and pressure drop were recorded. The wall temperatures and fluid inlet and outlet temperatures were recorded by the Data Acquisition System. The recorded data were further reduced by this system.

At the end of each test run, the fluid running through the test section was directly collected in the weigh tank, and the average fluid flow rate was estimated. When this fluid was pumped back to the top tank, there was often sufficient agitation inside the tank to entrain air bubbles. Several hours were allowed to pass between two consecutive runs so that the agitated tank fluid could settle and the entrained air bubbles could escape.

The experimental variables in these experiments were as follows:

0.9 percent HEMC solution: Flow rate: 36-310 lb_m/hr

Heat flux: 1100-5450 $Btu/hrft^2$

Pr: 560-1344

Re: 3.5-61

n values (70°-130°F): 0.55-0.76

1.0 percent HEMC solution: Flow rate: 41-287 lb_m/hr

Heat flux: 700-1800 $Bru/hrft^2$

Pr: 940-1980

Re: 2-26

n values (70°-130°F): 0.6-0.85

Data Reduction

In the heat transfer experiments, the total heat supplied through the tube wall should be equal to the enthalpy rise of the fluid. However, due to the uncertainties in the estimation of heat loss through the insulation and measurement of outlet fluid temperature at the tube exit, the exact heat balance is rarely achieved. A Kinecs Mixer was installed at the outlet of the test section to cause thorough mixing of the fluid and improve the accuracy of the outlet temperature measurement. Generally, the error was less than 5 percent. However, at very low flow rates, the error was as high as 15 percent. Since the outlet temperature is subject to the greatest uncertainty, the heat input was taken from the electrical power input, as corrected for the heat loss through the insulation. The radial heat loss to the surroundings through the insulation was estimated to be 1.5 percent of the total power input. The details of this calculation are outlined elsewhere [53,54,83].

The local bulk temperatures at the wall temperature measuring sections were computed from the inlet temperature, flow rate, and actual power input. A linear variation in bulk temperature from the inlet to the exit of the heated length was assumed. The wall temperatures were measured on the outside surface of the tube. A one-dimensional, steady-state heat conduction equation with uniform internal heat generation was solved to compute inside wall temperature. This temperature drop from the outside to inside was always less than 1°F. The circumferential average inside wall temperature was computed from the three inner wall temperature readings by Simpson's rule. The difference in these readings rarely exceeded 1.5°F, indicating circumferentially uniform wall temperature and strongly suggesting the absence of free convection.

The local heat transfer coefficient was calculated by employing the measured heat flux based on the inside tube surface area, the average inner wall temperature, and the calculated local bulk fluid temperature at the measuring station

$$\bar{h} = q''_w/(t_w - t_b) \tag{6.1}$$

The Nusselt number was then calculated as follows

$$Nu = \bar{h}D/k \tag{6.2}$$

The Reynolds number Re and Prandtl number Pr were computed based on μ_{eff} and properties evaluated at local fluid bulk temperature. Local x^+ was computed as

$$X^+ = \frac{2(x/D)}{RePr} \tag{2.6b}$$

The fluid velocity profile was fully developed at the onset of heating, and, therefore, a linear variation in the pressure from the inlet to the exit of the tube was assumed. However, due to heating, fluid velocity does undergo changes and, hence, some variation in dp/dx may occur. This variation was assumed to be negligible, and, therefore, the friction factor was calculated as

$$f = 2g_c \frac{D}{\rho \bar{u}^2} \frac{\Delta p}{L} \tag{6.3}$$

The pressure drop Δp was measured by a U-tube mercury manometer with resolution of 0.05 in. The fluid bulk temperature at the midpoint of the heated section was utilized to evaluate all physical properties in Eq. (6.3).

A sample calculation for the data reduction is given in Appendix K, and a computer program utilized for data reduction is given in Appendix L.

CHAPTER VII. EXPERIMENTAL RESULTS AND DISCUSSION

In the heat transfer experiments, 72 data points were obtained for each 0.9 percent and 1.0 percent HEMC solution. The data reduction was discussed in Chapter VI and the tabulation of the experimental data is given in Appendix M. In the following discussion, all the fluid properties were evaluated at the fluid bulk temperature, unless mentioned otherwise.

Experimental Results

Figure 7.1 shows a plot of local Nusselt number against dimensionless distance X^+. Although there is data scatter, the trends are very discernible. Generally, the local Nusselt numbers for 1.0 percent HEMC solution are somewhat lower than those for the 0.9 percent HEMC solution. Most of the data exhibit substantially higher Nusselt numbers than the constant property Newtonian predictions. In the numerical solution to this problem (Chapter IV), it was demonstrated that this increase is due to

1) Non-Newtonian effects. This was accounted for by employing the correction $\Delta^{1/3}$. Generally, this correction is not large. For example, for n = 0.5, $\Delta^{1/3} = 1.08$.

2) Consistency index variation effects. Most of the pseudo-plastic fluids exhibit a strong temperature dependence of K. This was also true for the 0.9 percent and 1.0 percent HEMC solutions. For example, for the 0.9 percent HEMC solution,

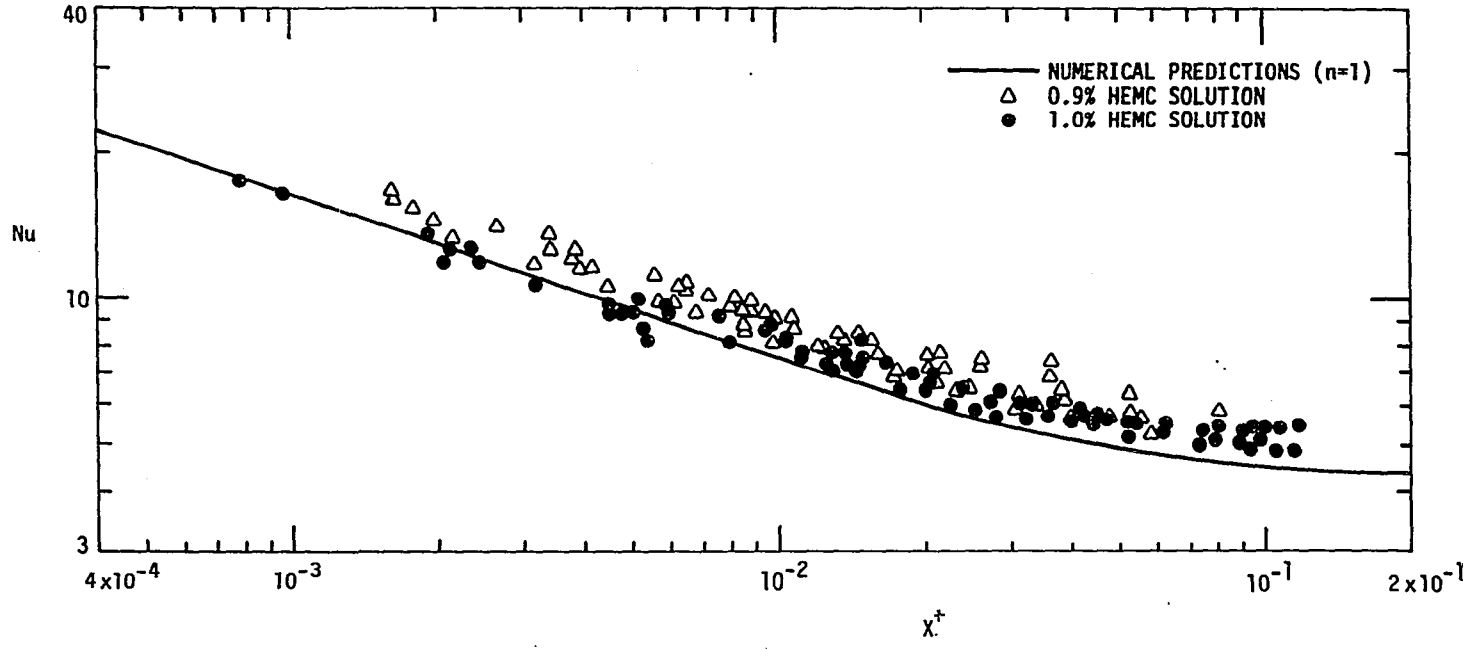

Fig. 7.1 Plot of experimental heat transfer data.

At 65°F, $K = 2.08\ lb_f \frac{sec^n}{ft^2}$, $n = 0.57$

At 130°F, $K = 0.23\ lb_f \frac{sec^n}{ft^2}$, $n = 0.76$

Thus, with a two-fold change in temperature the K value decreases by a factor of 9, while n increases by a factor of 1.3. With heating, K_w is normally much smaller than K_b, resulting in a reduced flow resistance near the wall. This increases the fluid velocity and, consequently, the heat transfer coefficients at the wall. The consistency index correction $(C_c)^m$ was designed to account for the K-variation from bulk to wall conditions. In Chapter IV, it was shown that

$$(C_c)^m = f(n,\ K/K_w,\ X^+,\ \gamma\Delta T) \qquad (4.11)$$

Figure 7.2 is a plot of $Nu/(\Delta_w)^{1/3}$ against X^+. It is noted that in the analysis, n was assumed to be constant. Since the working fluids in these experiments exhibited a temperature dependence of n, the n value at wall was used to calculate the non-Newtonian correction. Even though this correction is small, it was felt to be appropriate, as the wall condition controls the heat transfer [89,90]. It is seen that the non-Newtonian correction marginally reduces scatter in the data, however, the ordinate still has substantially higher values than the constant property Newtonian predictions. This further demonstrates the small magnitude of the non-Newtonian correction.

Figure 7.3 is a plot of $Nu/(\Delta_w)^{1/3}(C_c)^m$ against X^+. It is seen that by applying the consistency index correction, the scatter in the data is much reduced, and data for both fluids show a continuous trend.

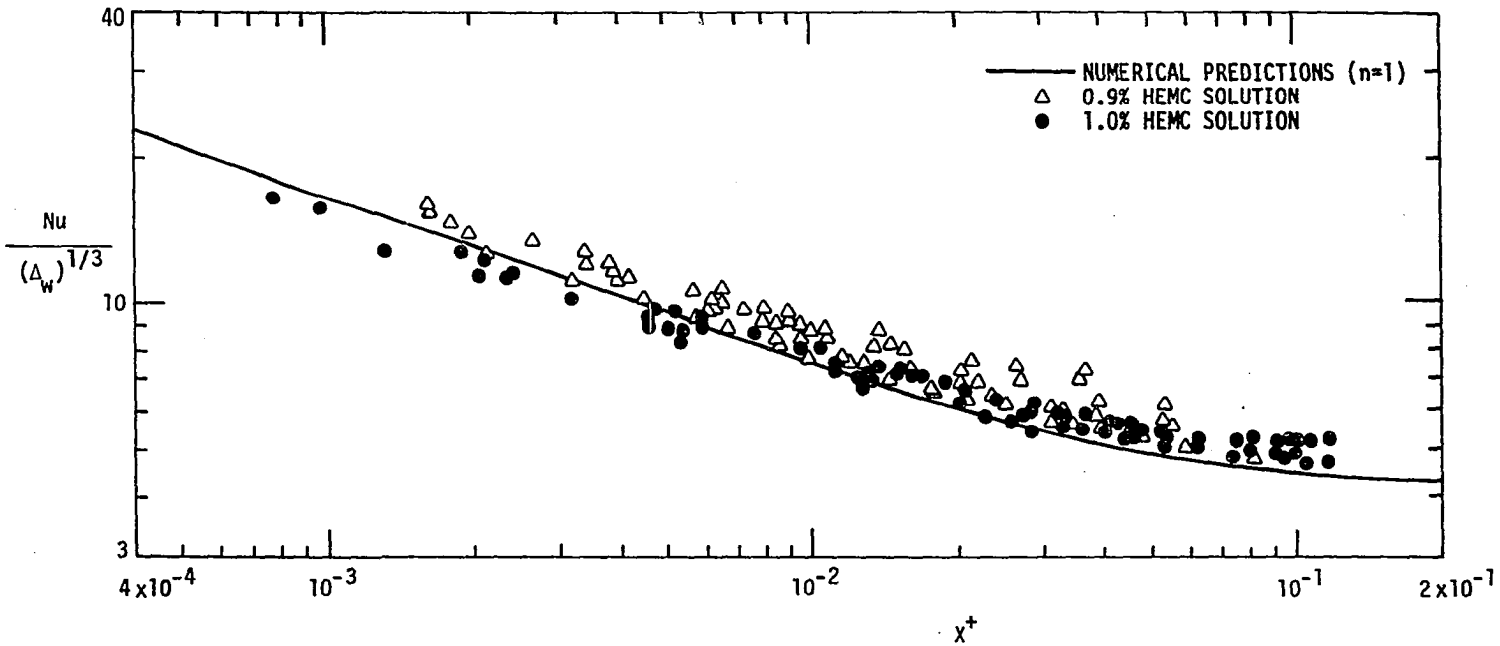

Fig. 7.2 Plot of experimental heat transfer data with non-Newtonian correction.

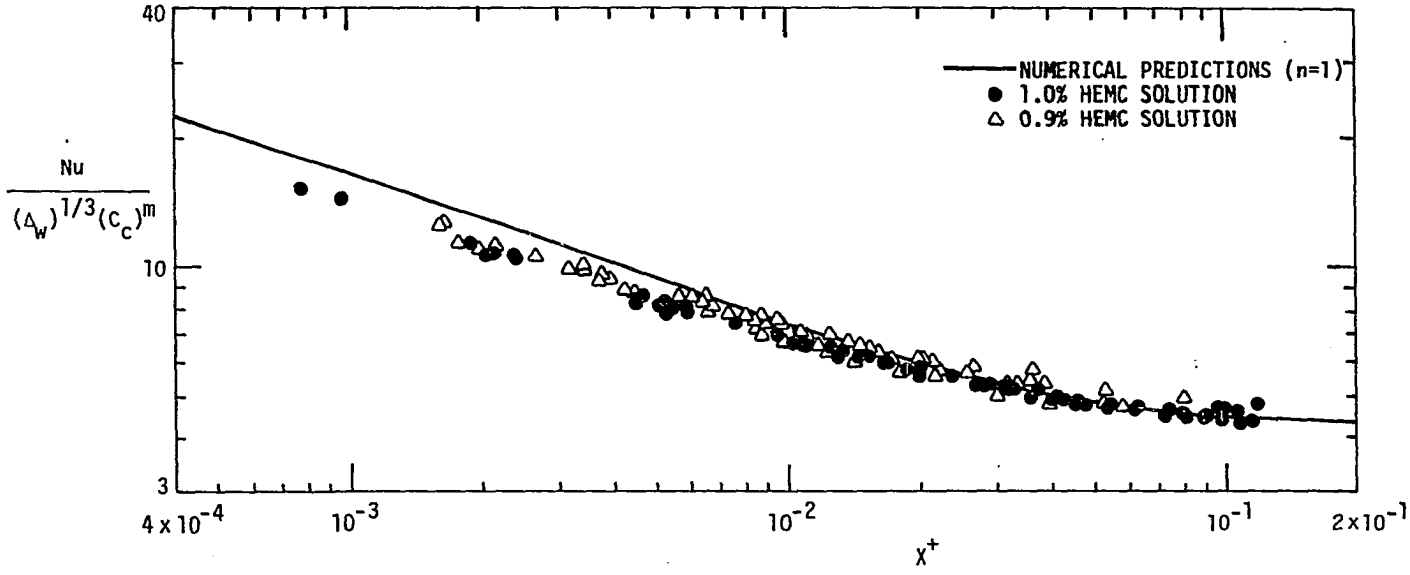

Fig. 7.3 Plot of experimental heat transfer data with non-Newtonian correction and temperature-dependent consistency correction.

For $X^+ > 10^{-2}$, the corrected non-Newtonian experimental data are in excellent agreement with constant property Newtonian predictions. However, for $X^+ < 10^{-2}$, the consistency correction overcorrects the data so that they lie below the constant property Newtonian predictions. The lower the value of X^+, the larger the deviation is from the numerical predictions. The maximum discrepancy occurs at $X^+ \simeq 10^{-3}$ where the data are about 15.0 percent lower than the numerical predictions. These lower values may be due to

1) An excessive consistency correction
2) A systemmatic error in the experimental data
3) In the numerical analysis it was assumed that

$$K = a \exp(-bt) \tag{2.40}$$

and, hence $\gamma = b = \text{constant}$

However, the present working fluids exhibit a more complex K-t relationship (see Appendix I) as

$$K = a \exp(-bt-ct^2) \tag{7.1}$$

and, hence $\gamma = b + 2ct$

Thus, γ is a function of temperature; the result is an overcorrection of the experimental data. In order to overcome this difficulty, a first-order exponential curve, Eq. (2.40), was fit for each 10°F interval (see Appendix J). This approximation may have caused some error, particularly in the entrance length, by overestimating values of $\gamma\Delta T$ and (K/K_w).

The data for length $X^+ < 10^{-2}$, correspond to measuring stations

very close (several inches) to the inlet of the heated test section. The heating was accomplished by passing current directly through the tube. The resistance heating of electrical end connections (which was kept to a minimum by choosing brass bushings and copper bus bars) might have caused axial conduction near the tube inlet, resulting in higher wall temperatures and, hence, lower Nusselt numbers.

Normally, for the heat exchanger design, the length of interest is $X^+ > 10^{-2}$, where numerical predictions and experimental data are in excellent agreement. There is some discrepancy for the length $X^+ > 10^{-2}$. However, present predictions and data are in sufficiently good agreement and, hence, the predictions are accurate enough for all design purposes.

Figure 7.4 is plot of $Nu/((\Delta_w)^{1/3}(C_c)^m)$ against X_w^+. Here the maximum deviation of the data from the numerical predictions is less than 8.0 percent. The fluid conditions near the wall control the heat transfer rates, and this is particularly significant for pseudoplastic fluids which exhibit flat velocity and temperature profiles; thus, by evaluation X^+ at wall conditions, a better agreement is obtained between the experimental data and numerical predictions. However, the results are obtained for a constant wall heat flux boundary condition, where wall temperature is an unknown and, hence, it is more convenient for design purposes to base as many parameters as possible on a known fluid bulk temperature.

In these experiments, the average friction factors over the heated length were also measured. The results of these measurements are

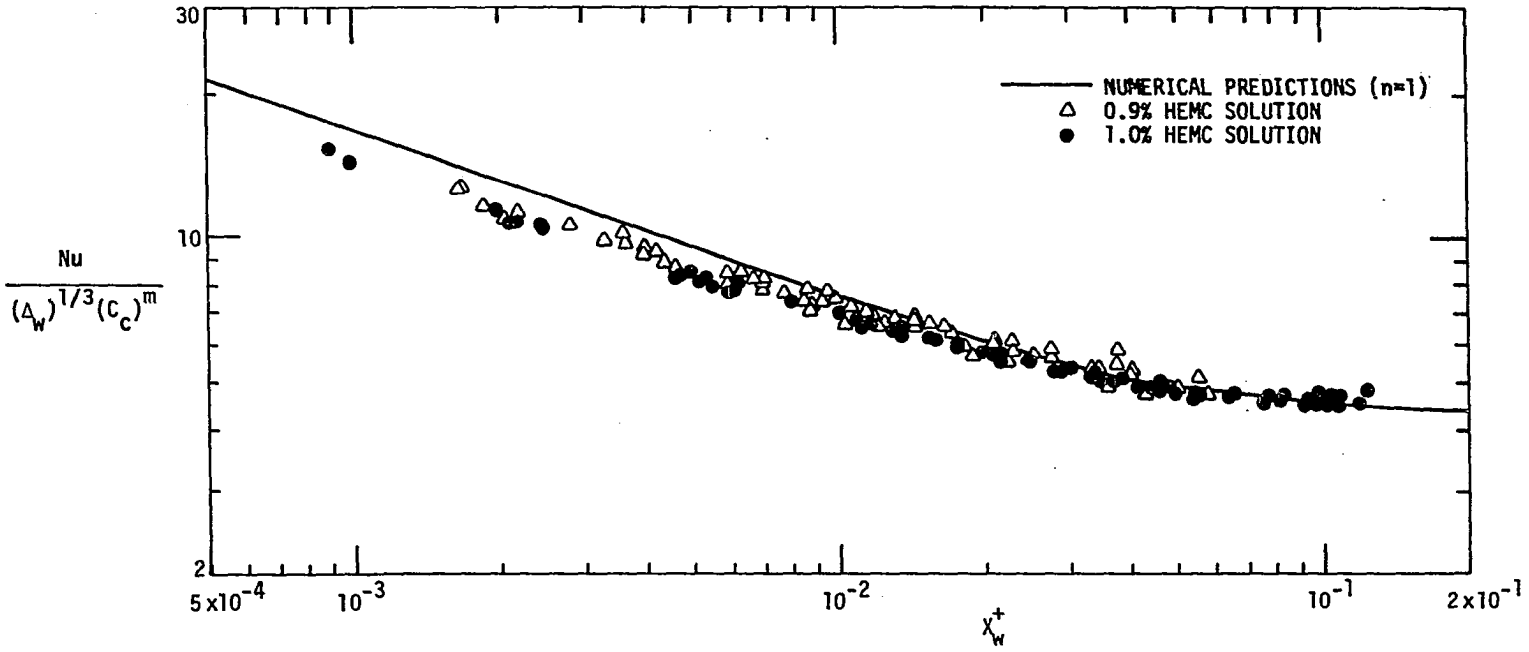

Fig. 7.4 Plot of experimental heat transfer data with non-Newtonian correction and temperature-dependent consistency correction, with X^+ evaluated at wall temperature.

tabulated in Appendix M. In the following section, a statistical analysis of the data is given.

Statistical Analysis of the Data

The conclusions drawn from any experimental data are not valid unless the validity of the data is verified and their significance is established [97]. The statistical analysis of the data was done here to establish the "goodness" of the experimental data.

Employing the analysis of propogation of errors [98], it can be shown that the error in the estimation of X^+ is less than 0.5 percent, while the error in the estimation of Nusselt number is of the order of 3.0 percent. Since the error in X^+ is much smaller than that in Nu, for simplicity, it was assumed that all the error was present only in the ordinate while the abscissa was error free.

Churchill and Usagi [99] have developed a scheme to correlate in-tube heat transfer data. In Fig. 7.3, two distinct asymptotes are seen; one near the tube inlet ($X^+ < 2x10^{-2}$) and the other far away from the tube entrance in the fully developed region. The value of fully developed Newtonian, constant property Nusselt number is 4.36 [1,3]. A linear regression analysis of all the entrance region data ($X^+ < 2x10^{-2}$, 86 data points) at 90 percent confidence level gives

$$\frac{Nu}{(\Delta_w)^{1/3}(C_c)^m} = 1.79(X^+)^{-0.294} \qquad (7.2)$$

This asymptote and 4.36 were combined as

$$Y = \frac{Nu}{(\Delta_w)^{1/3}(C_c)^m} = \left((1.79(X^+)^{-0.294})^{xn} + 4.36^{xn} \right)^{1/xn} \tag{7.3}$$

which reduces to

$$Y = 4.36\ [(0.411(X^+)^{-0.294})^{xn} + 1.0]^{1/xn} \tag{7.4}$$

With this correlation format, at lower values of X^+, Eq. (7.2) is dominant, while at higher values of X^+, the asymptotic term 4.36 is dominant. Various values of xn were tested, and for each xn, the standard deviation was computed as

$$\sigma_{yx} = \sqrt{\frac{(\hat{Y}-Y)^2}{(ND-2)}} \tag{7.5}$$

where $\hat{Y}$ is the value computed from the correlation, and ND represents the number of data points (144).

The value of xn = 6.0 was found to be most suitable, giving $\sigma_{yx} = 0.07$, thus exhibiting excellent agreement with data. With xn = 6.0, Eq. (7.4) reduces to

$$Y = \frac{Nu}{(\Delta_w)^{1/3}(C_c)^m} = 4.36\ [(0.411(X^+)^{-0.294})^6 + 1.0]^{1/6} \tag{7.6}$$

The major difficulty here was to establish confidence limits on this non-linear correlation. In order to accomplish this, Eq. (7.6) was rewritten as

$$\log_{10}Y = \log_{10}A + \frac{1}{B}\log_{10}(X) \tag{7.7}$$

where $X = (0.411\ (X^{+})^{-0.294})^{6} + 1$

A log-linear plot of Y against X is shown in Fig. 7.5. A linear regression analysis was done on this straight line at various confidence levels to obtain upper and lower limits for the line as a whole and by the point-by-point method [100]. With this analysis, even at a 99 percent confidence level, extremely narrow band widths were obtained for the correlation because of the large number of experimental data points. Virtually coincident upper and lower limits of the correlation bands and correlation coefficient of 0.99 indicates the goodness of the experimental correlation.

Even though the goodness of correlation is demonstrated, the scatter in the data need to be accounted for. A future point technique [100] was adapted to obtain band widths for data points. At each point

$$Y_{up} \text{ and } Y_{low} = Y \pm t(10,142)\ \sigma_{yx} \sqrt{1 + \frac{1}{ND} + \frac{(x-\bar{x})^2}{\Sigma(x-\bar{x})^2}} \qquad (7.8)$$

where $\bar{x}$ represents the centroid of the data set and t represents the "t" distribution value at 90 percent confidence level and 142 degrees of freedom. Figure 7.5 shows that these bands encompass data very well, indicating the success of the statistical analysis. These confidence bands from Fig. 7.5 are transformed to coordinates of interest in Fig. 7.6. Here also the data bands encompass data very well, indicating the success of coordinated transformation and confirming the success of the statistical analysis. Thus, it can be concluded that the experimental data are well correlated by Eq. (7.6).

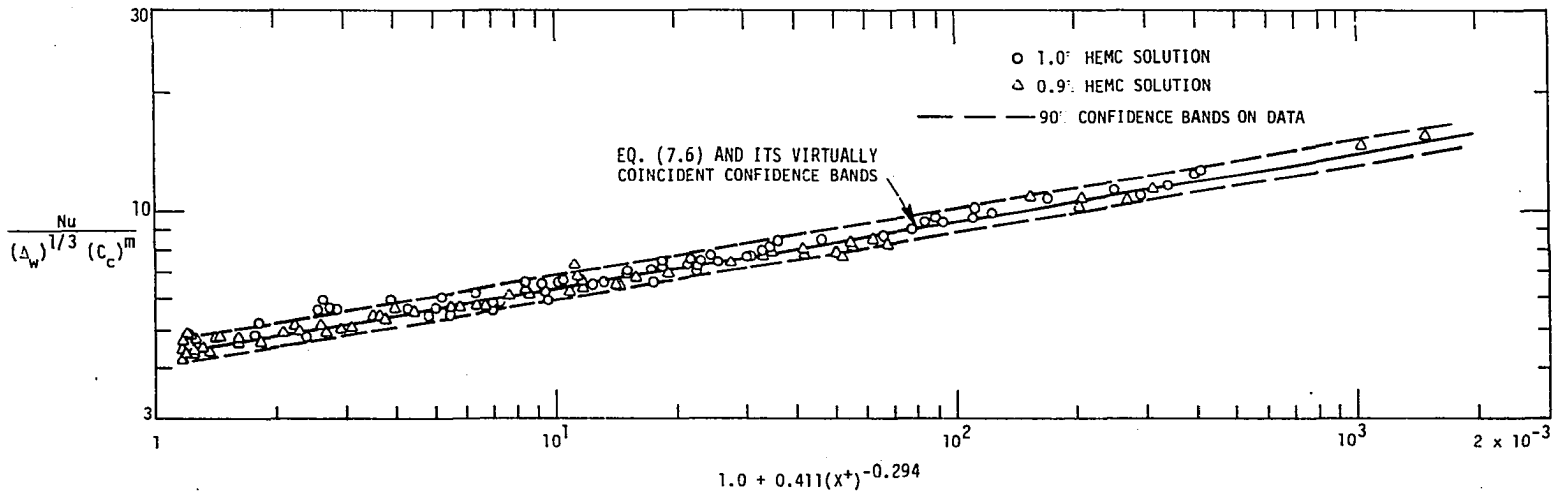

Fig. 7.5 Confidence limits on the data and correlation.

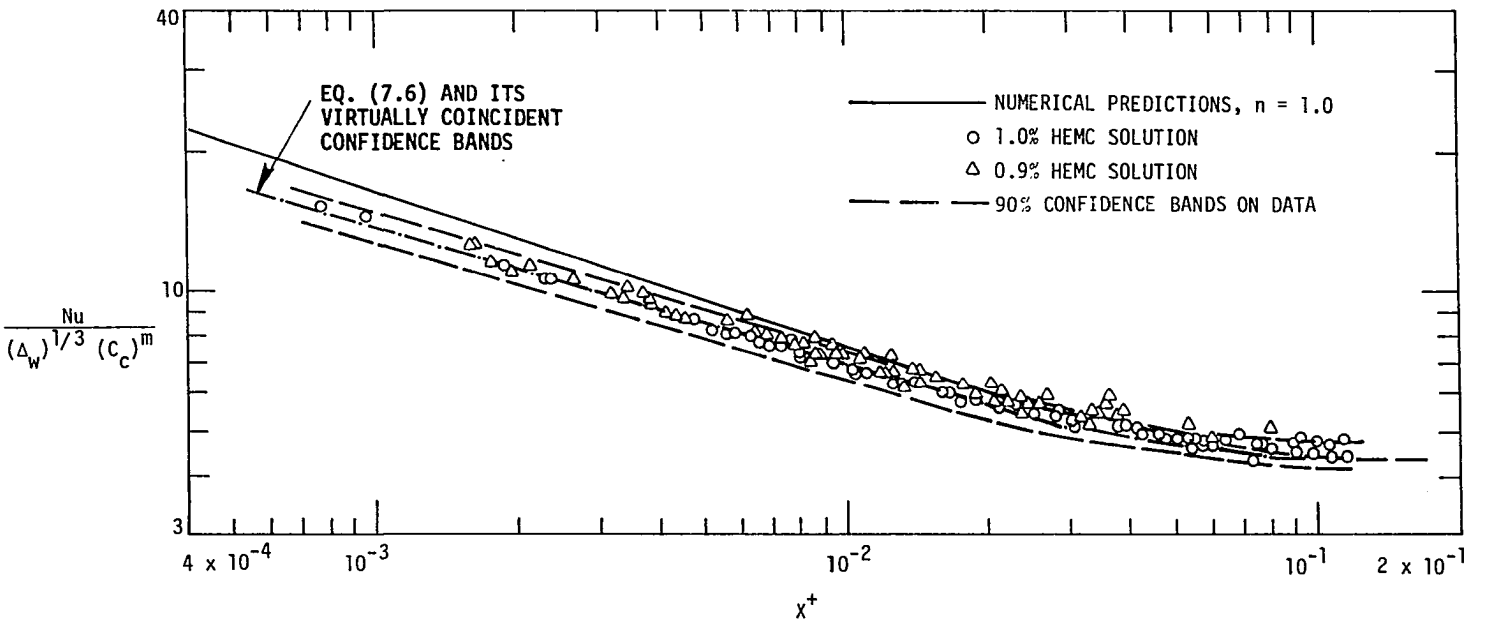

Fig. 7.6 Confidence limits on the data and correlation.

In Fig. 7.6, the constant property Newtonian predictions are also shown. These predictions are correlated by Churchill and Ozoe [101] as

$$Nu = 4.36\ ((0.376(X^+)^{-0.33})^6 + 1.0)^{1/6} \tag{7.9}$$

The comparison of Eqs. (7.6) and (7.9) show some deviation for $X^+ < 10^{-2}$. For design purposes, reasonable accuracy is obtained by using either Eq. (7.6) or Eq. (7.9).

Comparison with Previous Data

As mentioned earlier, two experimental studies are reported in this area: Mahalingam et al. [45] and Bassett and Welty [61]. The data of Mahalingam et al. were obtained with a methocel solution exhibiting the following K-t relation:

$$K = a \exp(-bt) \tag{2.40}$$

while n was demonstrated to be independent of temperature.

Bassett and Welty obtained data for various methocel solutions. The constitutive equation they fit to their viscometeric data was

$$\left(\frac{du}{dy}\right) = E_1\tau + E_2\tau^2 + E_3\tau^3 \tag{5.20}$$

where E_1, E_2, and E_3 are constants. This is not a pseudoplastic model. However, their flow curve (τ against $\frac{du}{dy}$ plot) for 5.4 percent methocel solution is almost log-linear. Thus, for purposes of comparing their

data with those of this study, it was possible to assume pseudoplasticity and utilize the relation given in Eq. (7.1) and n was found to be temperature-dependent. Unfortunately, as mentioned earlier, this K-t relation was still inconsistent with the numerical model and, hence, for each 10°F interval, a separate Eq. (2.40) was fitted. After this, the data of Mahalingam et al. and Bassett and Welty were reduced as outlined in Chapter VI, and are plotted in Fig. 7.7 and Fig. 7.8.

In Fig. 7.7, the ordinates are much higher than the constant property Newtonian predictions, indicating inadequacy of the non-Newtonian correction alone to correlate the data. To this ordinate, the consistency correction $(C_c)^m$ was applied and the results are shown in Fig. 7.8. In this plot, for comparison, the upper and lower scatter bands of the present data are also plotted. For the sake of clarity, the actual data points from the present experiemnts are not shown. This plot is used in all the subsequent discussion, unless mentioned otherwise.

The data of Mahaligam et al. were for $\gamma\Delta T < 10.0$. Their data lie above the present data and are in excellent agreement with the numerical predictions. Mahalingam et al. have correlated their data as

$$\frac{Nu}{(\Delta_w)^{1/3}} \left(\frac{K_w}{K}\right)^{0.14} = 1.46(Gz + 0.0083\ (GrPr)_m^{0.75})^{1/3} \qquad (5.22)$$

In the present analysis only the K(t) correction is used, and it corrects the experimental data very well, thus suggesting strongly that free convection is not a factor.

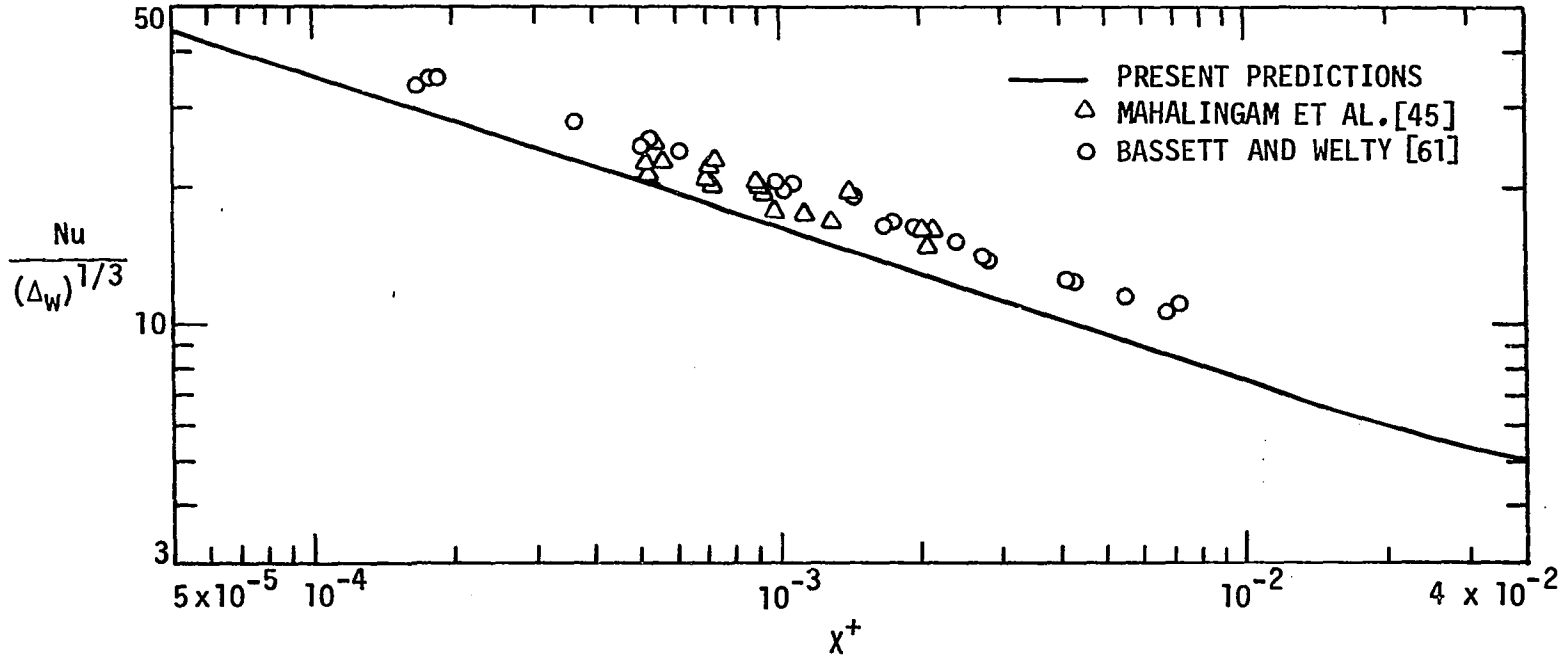

Fig. 7.7 Comparison of numerical predictions and experimental results.

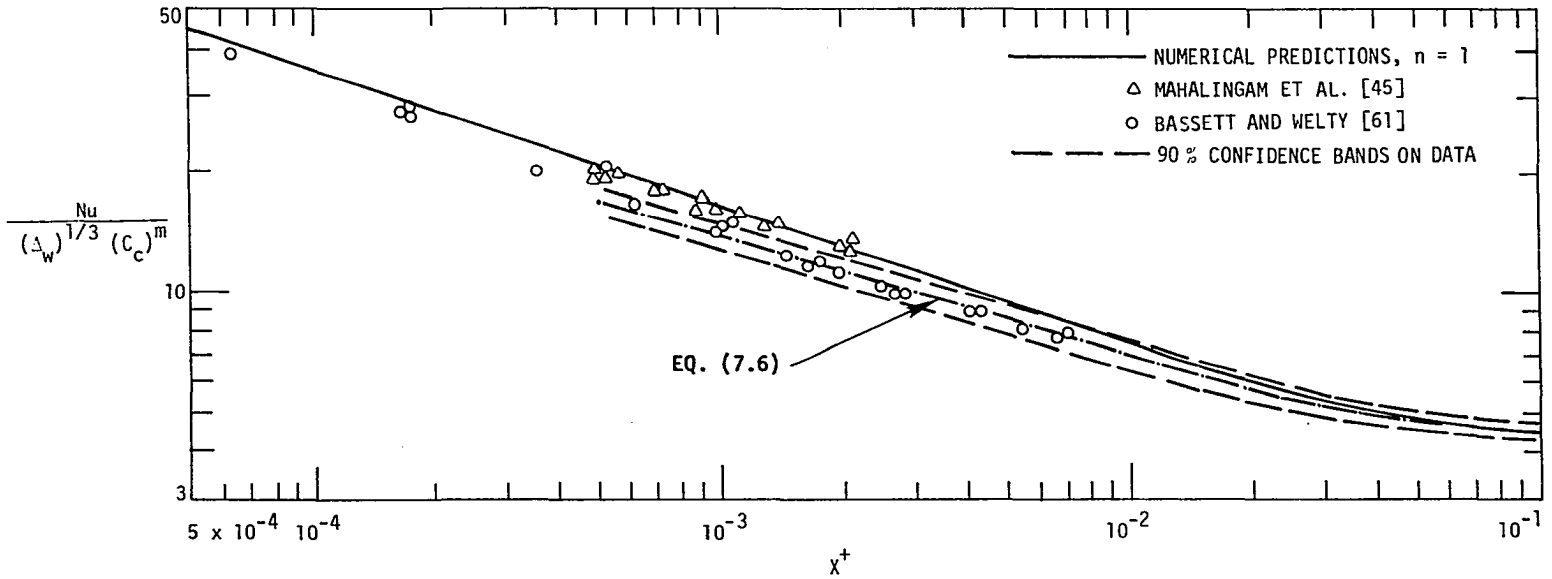

Fig. 7.8 Comparison of present experimental data and numerical predictions with available experimental data.

The data of Bassett and Welty are for $\gamma\Delta T$ of the order of 20.0, which is beyond the range of the present fully developed analysis. Fortunately, these data are for the thermal entrance region and, hence, can be compared to present predictions. Bassett and Welty have correlated these data within $\pm$ 10 percent as

$$Nu = 1.85 \left(\frac{\pi}{2X^+}\right)^{\frac{1}{3}} - \frac{0.03}{\Delta} \tag{5.21}$$

Their data for $X^+ > 3x10^{-4}$ are in excellent agreement with the present data and is well correlated by Eq. (7.6) showing less than $\pm$ 3 percent deviation. Thus, Eq. (7.6) is better correlation for these data than Eq. (5.21).

It is important to emphasize here that the working fluids of Mahalagam et al. have the same K-t dependence, Eq. (2.40), and n is independent of temperature as assumed in the numerical calculations. This seems to be a factor in the excellent agreement of the data with the numerical predictions.

The working fluids in the present experiment and those used by Bassett and Welty exhibit a K-t dependence of the second order as described in Eq. (7.1). Therefore, γ is a function of temperature, instead of being constant. In addition, n is also a function of temperature. Thus, these two variables are different than that assumed in the numerical calculation. In particular, the temperature-dependent γ tends to overestimate the consistency correction, $(C_c)^m$ and, hence, overcorrects the data points. Therefore, the corrected

non-Newtonian data points lie below the constant property Newtonian predictions. The effect of temperature-dependent γ is particularly significant in the early part of the entrance region. In spite of these discrepancies in the numerical assumptions and experimental characteristics, the data are in excellent agreement for $X^+ > 10^{-2}$, while for $X^+ < 10^{-2}$ the deviation is not very large. Therefore, over the entire thermal length, the results of the numerical predictions give sufficient accuracy for design purposes. Therefore, constant property Newtonian predictions, with non-Newtonian correction and consistency correction are recommended for design purposes.

Conclusions

Heat transfer in laminar in-tube flow of non-Newtonian pseudo-plastic fluid was studied. An extensive experimental data were obtained (144 points) for two HEMC solutions in two different tubes for the entire thermal length. In this case, the heat transfer coefficients are substantially higher than the constant property Newtonian predictions. This increase above the Newtonian results is accounted for by applying the following corrections:

1) Non-Newtonian correction, $\Delta_w^{1/3}$. This correction is generally small.

2) Variable consistency index correction $(C_c)^m$. This correction is quite significant.

With these two corrections, non-Newtonian experimental data are in excellent agreement with the constant property Newtonian predictions

for $X^+ > 10^{-2}$. For $X^+ < 10^{-2}$, the data lie below the numerical predictions. At $X^+ = 10^{-3}$, the discrepancy is of the order of 15.0 percent. A Statistical analysis at 90 percent confidence was done to demonstrate the goodness of the data and the data were correlated by Eq. (7.6).

The data of Mahalingam et al. [45] are in excellent agreement with the numerical predictions, while data of Bassett and Welty [61] are in excellent agreement with the present data. This is because the analytical assumption and working fluid characteristics for K-t and n-t dependence are precisely the same for the data of Mahalingam et al. There is some discrepancy in these characteristics of working fluids for the data of Bassett and Welty. In spite of this, their data are in fairly good agreement with the predictions. Thus, for the entire thermal length, the present experimental data and other data [45,61] are in sufficiently good agreement with the numerical predictions and, hence, constant property Newtonian predictions with non-Newtonian and consistency corrections are recommended for design purposes.

CHAPTER VIII. CONCLUSIONS AND RECOMMENDATIONS

This study deals with the heat transfer in laminar in-tube flow of non-Newtonian (pseudoplastic) fluids. The tube wall was subjected to the uniform wall heat flux boundary condition. This is a numerical and experimental study; the theoretical and experimental results are compared. Previous analyses and test results are also compared with the results of this study. The following conclusions can be drawn:

1) A stable, explicit, numerical scheme was developed, using the Dufort-Frankel finite-difference technique to solve this problem. The usual boundary layer assumptions were made. A constant property analysis was done for n = 1.0, 0.75, 0.5, and 0.25. This analysis indicated that there is an increase in the heat transfer coefficient due to pseudoplasticity, which can be accounted for by employing a non-Newtonian correction, $\Delta^{1/3}$. It is important to point out that this correction is valid up to n = 0.1, but most engineering fluids have n > 0.25, thus, this correction can be used for most engineering calculations.

2) For the variable property analysis, it was assumed that

$$K = a \exp(-bt) \tag{2.40}$$

and a dimensionless parameter $\gamma\Delta T$, Eq. (4.9), was defined for a UHF condition. The predictions were obtained for various values of $\gamma\Delta T$ and for n = 1.0, 0.75, and 0.5. It was demonstrated that

$$\frac{Nu}{Nu_{cp}} = f(n, X^+, K_b/K_w, \gamma\Delta T) \tag{4.11}$$

A two-step method was employed to correlate these predictions:

For the entrance region

$$m = 0.58 - 0.44n \tag{4.12}$$

and for the fully developed region

$$\frac{Nu}{Nu_{cp}} = 1 + C_k \tag{4.20}$$

A generalized consistency correction, $(C_c)^m$, was developed, Eq. (4.22), to account for the increment in the Nusselt number due to consistency index variation. Thus, two corrections, namely, $\Delta^{1/3}$ and $(C_c)^m$, were employed to account for the increase in the non-Newtonian Nusselt number above the constant property Newtonian prediction.

3) For the Newtonian case alone, with variable μ, an additional analysis was made for the fully developed region. The predictions of this analysis are in excellent agreement with other predictions obtained using the Dufort-Frankel marching scheme.

4) For the fully developed case, predictions for various n values and for various $\gamma\Delta T$ values are correlated to obtain a non-iterative explicit solution as given in Eq. (4.20). This solution has significant advantages over previous iterative solution (Eq. (4.10)), and is highly useful for design purposes.

5) The heat transfer experiments were conducted for 0.9 percent and 1.0 percent HEMC solutions. Nusselt numbers for these solutions, for the entire thermal length, are substantially higher than those for the constant property Newtonian Nusselt numbers. To these non-Newtonian Nusselt numbers, the non-Newtonian correction, $(\Delta_w)^{1/3}$, and the temperature-

dependent consistency index correction, $(C_c)^m$, was applied and plotted in Fig. 7.6. It is seen that these corrected Nusselt numbers are in excellent agreement with constant property Newtonian predictions for $X^+ > 10^{-2}$, while for $X^+ < 10^{-2}$ the experimental data lie somewhat lower than the numerical predictions. In general, the experimental data are in sufficiently good agreement with numerical predictions. Therefore, constant property Newtonian predictions with non-Newtonian and consistency index corrections are recommended for design purposes.

6) The data of Mahalingam et al. [45] are in excellent agreement with the numerical predictions. The assumptions of the numerical analysis correspond to the characteristics of the methocel solution used by Mahalingam et al., namely the K-t relation as given in Eq. (2.40) and n independent of temperature. The present consistency index correction alone corrects the numerical predictions quite well, strongly suggesting the absence of free convection effects.

7) The data of Bassett and Welty [61] are in excelleng agreement with the present data. Most of their data are for $X^+ < 10^{-2}$. The maximum discrepancy between their data and the present numerical solution seems to occur at $X^+ = 10^{-3}$ and it is of the order of 15 percent.

8) The present data and data of Bassett and Welty lie below numerical predictions for $X^+ < 10^{-2}$. The present working fluids and the 5.4 percent methocel solution used by Bassett and Welty exhibit a weak temperature dependence of n and K-t relation as given in Eq. (7.1). This proposed correction factors thus tend to overcorrect data in the early part of the entrance region. However, this deviation is not

substantial and, therefore, numerical predictions are sufficiently accurate for the design purposes.

9) Finally, it can be concluded that there is good agreement between numerical predictions and various experimental data. A generalized correlation method is developed from the numerical predictions to correlate Nusselt numbers for various n values and a wider range of heat fluxes.

Although this study has shown a good agreement between the experimental data and numerical solution which can be used for design purposes, further work can be pursued in the following areas

1) A similar explicit numerical analysis is required for a UWT boundary condition and needs to be compared with available predictions and experimental data.

2) In this study, results are obtained for the in-tube heating of pseudoplastic fluids. Many industrial applications involve the cooling of pseudoplastic fluids. These heating results are also probably applicable to the case of cooling. However, experimental data need to be obtained for this cooling case and compared with the numerical predictions.

3) A second-order K-t relation needs to be incorporated in the numerical scheme such as

$$K = a \exp(-bt - ct^2) \qquad (7.1)$$

4) Bingham plastic represents a major class of non-Newtonian fluids. A similar analytical and experimental study is required for these fluids.

5) Laminar flow is inherently associated with low magnitudes of heat transfer coefficients. Recently, there have been many studies dealing with augmentation of heat transfer in Newtonian in-tube flow [102,103]. A substantial improvement in the heat transfer performance is demonstrated by employing various static mixers. A similar augmentation study for non-Newtonian fluids is required.

BIBLIOGRAPHY

1. Skelland, A. H. P. Non-Newtonian Flow and Heat Transfer. New York: John Wiley and Sons, Inc., 1967.

2. Kays, W. M. Convective Heat and Mass Transfer. New York: McGraw-Hill Book Company, 1966.

3. McAdams, W. H. Heat Transmission. 3rd edition. New York: McGraw-Hill Book Company, 1954.

4. Graetz, L. "Über die Wärmeleitungsfähigkeit Von Flussigkiten." Annalen der Physik 23 (1883): 79-94.

5. Graetz, L. "Über die Wärmeleitungsfähigkeit Von Flussigkiten." Annalen der Physik 25 (1885): 337-357.

6. Nusselt, W. "Die Abhängigkeit der Wärmeübergangszahl von der Rohrlange." Zietschrift des Vereines Deutscher Ingenieure 54 (1910): 1154.

7. Leveque, A. "Les Lois de la Transmission de Chaleur par Convection." Annales des Mines Paris-Mem. Ser. 12, 13 (1928): 283-290.

8. Kays, W. M. "Numerical Solutions for Laminar Flow Heat Transfer in Circular Tubes." Transactions of ASME 77 (1955): 1254-1274.

9. Worsøe-Schmidt, P. M. "Heat Transfer in the Thermal Entrance Region of Circular Tubes and Annular Passage with Fully Developed Laminar Flow." International Journal of Heat and Mass Transfer 1(1967): 541-551.

10. Sellars, J. R.; Tribus, M. and Kline, J. S. "Heat Transfer to Laminar Flow in Round Tube Flat Conduit - the Graetz Problem Extended." Transactions of ASME 78 (1956): 441-448.

11. Siegel, R., Sparrow, E. M. and Hallman, T. M. "Steady Laminar Heat Transfer in a Circular Tube with Prescribed Wall Heat Flux." Applied Scientific Research A7 (1958): 385-392.

12. Ulrichson, D. L. and Schmitz, R. A. "Laminar-Flow Heat Transfer in the Entrance Region of a Circular Tube." International Journal of Heat and Mass Transfer 8 (1968): 253-258.

13. Hornbeck, R. W. "An All-Numerical Method for Heat Transfer in the Inlet of a Tube." ASME Paper No. 65-WA/HT-36 (1965).

14. Roy, D. N. "Development of Laminar Flow in Circular and Coaxial Tubes with and without Heat Transfer." Ph.D. Thesis, University of Calcutta, Bengal Engineering College, Weat Bengal, India, 1966.

15. Manohar, R. "Analysis of Laminar-Flow Heat Transfer in Entrance Region of Circular Tubes." International Journal of Heat and Mass Transfer 12 (1969): 15-22.

16. Butterworth, D. and Hazel, T. D. "Forced Convective Laminar Flow Heat Transfer in the Entrance Region of a Tube." AERE-R6057 Harwell 1969.

17. McMordie, R. K. and Emery, A. F. "A Numerical Solution for Laminar Flow Heat Transfer in Circular Tubes with Axial Conduction and Developing Thermal and Velocity Fields." Journal of Heat Transfer 89 (1967): 11-16.

18. Tien, C. and Pawelek, R. A. "Laminar Flow Heat Transfer in the Entrance Region of Circular Tubes." Applied Scientific Research A13 (1964): 317-331.

19. Singh, R. N. "Heat Transfer by Laminar Flow in a Cylindrical Tube." Applied Scientific Research A7 (1958): 325-340.

20. Munakata, T. "The Calculation of Laminar Heat Transfer in a Tube." International Chemical Engineering 15, No. 1 (1975): 193-196.

21. Hsu, C. J. "An Exact Analysis of Low Peclet Number Thermal Entry Region Heat Transfer in Transversely Non-Uniform Velocity Fields." AIChE Journal 17, No. 3 (1971): 732-740.

22. Beek, W. J. and Eggink, R. "Warmteoverdracht Naar een Laminaire Stroming Van een Neit-Newtonse Vloeistof in enn Ronde Buise." De Ingenuir, Chemische Techniek 7 (1962): 81-89.

23. Grigull, U. V. "Wärmeübergang an Nicht-Newtonsche Flussigkeiten bei Laminar Rohrströmung." Chemie-Ingenieur-Technik 8/9 (1956)): 553-556.

24. Kutateladze, S. S.; Khabakhpasheva, Ye. M.; Popov, V. I.; Gruzdeva, I. M. and Perepelitsa, B. V. "Hydraulic Resistance and Heat Transfer in Stabilized Flow of Non-Newtonian Fluids." Heat Transfer, Soviet Research 2, No. 6 (1970): 114-123

25. Pigford, R. L. "Nonisothermal Flow and Heat Transfer Inside Vertical Tubes." Chemical Engineering Progress Symposium 51, No. 17 (1955): 79-92.

26. Lyche, B. C. and Bird, R. B. "The Graetz-Nusselt Problem for a Power Law Non-Newtonian Fluid." Chemical Engineering Science 6, (1956): 35-41.

27. Whiteman, I. R. and Drake, W. G. "Heat Transfer to Flow in a Round Tube with Arbitrary Velocity Distribution." Transactions of ASME 80, (1958): 728-732.

28. McKillop, A. A. "Heat Transfer Laminar Flow of Non-Newtonian Fluids in Entrance Region of a Tube." International Journal of Heat and Mass Transfer 7 (1964): 853-862.

29. Korayem, A. Y. "Non-Isothermal Laminar Flow of Non-Newtonian Fluids in the Entrance Region of Pipe." Ph.D. Thesis, University of California, Davis, 1965.

30. Cochrane, G. F. "A Numerical Solution for Heat Transfer to Non-Newtonian Fluids with Temperature Dependent Viscosity for Arbitrary Conditions of Heat Flux and Surface Temperature." Ph.D. Thesis, Oregon State University, 1969.

31. Mizushina, T.; Ito, R.; Kuriwake, Y. and Yahikazawa, K. "Boundary Layer Heat Transfer in a Circular Tube to Newtonian and Non-Newtonian Fluids." Kagaku Kogaku 31 (1967): 250-255.

32. Yang, K. T. "Laminar Forced Convection of Liquids in Tubes with Variable Viscosity." Journal of Heat Transfer 84 (1962): 353-362.

33. Deissler, R. G. "Analytical Investigation of Fully Developed Laminar Flow in Tubes with Heat Transfer with Fluid Properties Variable along the Radius." NACA TN 2410, 1951.

34. Shannon, R. L. and Depew, C. A. "Forced Laminar Flow Convection in a Horizontal Tube with Variable Viscosity and Free Convection Effects." Journal of Heat Transfer 91 (1969): 251-258.

35. Test, F. L. "Laminar Flow Heat Transfer and Fluid Flow for Liquids with Temperature Dependent Viscosity." Journal of Heat Transfer 90 (1968): 385-392.

36. Rosenberg, D. E. and Hellums, J. D. "Flow Development and Heat Transfer in Variable Viscosity Fluids." Industrial and Engineering Chemistry Fundamentals 4 (1965): 417-422.

37. Martin, B. W. and Fargie, D. "Effect of Temperature-Dependent Viscosity on Laminar Forced Convection in the Entrance Region of a Circular Pipe." The Proceedings of the Institution of Mechanical Engineers 186, No. 24 (1972): 307-316.

38. Sieder, E. N. and Tate, G. E. "Heat Transfer and Pressure Drops of Liquid in Tubes." Industrial and Engineering Chemistry 28 (1936): 1429-1435.

39. Christiansen, E. B. and Craig, S. E., Jr. "Heat Transfer to Pseudoplastic Fluids in Laminar Flow." AIChE Journal 8, 1402 (1962): 154-160.

40. Christiansen, E. B.; Jensen, G. E. and Tao, F. S. "Laminar Flow Heat Transfer." AIChE Journal 12, No. 6 (1966): 1196-1202.

41. Forrest, G. and Wilkinson, W. L. "Laminar Heat Transfer to Power Law Fluids in Tubes with Constant Wall Temperature." Transactions of the Institution of Chemical Engineers 51 (1973): 331-338.

42. Kwant, P. B.; Zwaneveld, A. and Dijkstra, F. C. "Non-Isothermal Laminar Pipe Flow-I Theoretical." Chemical Engineering Science 28 (1973): 1303-1316.

43. Popovska, F. and Wilkinson, W. L. "Laminar Heat Transfer to Newtonian and Non-Newtonian Fluids in Tubes." Chemical Engineering Science 32 (1977): 1155-1164.

44. Forrest, G. and Wilkinson, W. L. "Laminar Heat Transfer to Power Law Fluids in Tubes with Constant Wall Heat Flux." Transactions of the Institution of Chemical Engineers 52 (1974): 10-16.

45. Mahalingam, R.; Tilton, L. O. and Coulson, J. M. "Heat Transfer in Laminar Flow of Non-Newtonian Fluids." Chemical Engineering Science 30 (1975): 921-929.

46. Bader, H. J. "Heat Transfer in Non-Newtonian Fluids with Temperature Dependent Viscosity." M.S. Thesis, University of California, Davis, 1965.

47. McKillop, A. A.; Harper, J. C.; Bader, H. J. and Korayem, A. Y. "Variable Viscosity Entrance-Region Flow of Non-Newtonian Liquids." International Journal of Heat and Mass Transfer 13 (1970): 901-909.

48. Bader, H. J.; McKillop, A. A. and Harper, J. C. "An Experimental and Analytical Study of Entrance Flow of Non-Newtonian Fluids." Heat Transfer Conference, Vol. IV, Paper No. Rh 1, Paris-Versailles, 1970.

49. Pletcher, R. H. "On Finite-Difference Solution for the Constant-Property Turbulent Boundary Layer." AIAA Journal 7, No. 2 (1969): 305-311.

50. Dufort, E. C. and Frankel, S. P. "Stability Conditions in the Numerical Treatment of Parabolic Differential Equations." Mathematical Tables Aids Computation 7 (1953): 135-153.

51. Nelson, R. M. "An Explicit Finite Difference Analysis for Developing Turbulent Internal Flows with Heat Transfer and Property Variation." M.S. Thesis, Iowa State University, Ames, May, 1972.

52. Pletcher, R. H. and Nelson, R. M. "Heat Transfer to Laminar and Turbulent Flow in Tubes with Variable Fluid Properties." Proceedings of the Fifth International Heat Transfer Conference, Tokyo, Japan II, Paper No. FC 4.5 (1974): 146-150.

53. Hong, S. W. "Laminar Flow Heat Transfer in Ordinary and Augmented Tubes." Ph.D. Thesis, Iowa State University, Ames, Iowa, 1974.

54. Hong, S. W. and Bergles, A. E. "Analysis of Combined Forced and Free Laminar Convection in Horizontal Tubes." Heat Transfer Laboratory Report, HTL-4, ISU-ERI-Ames-741555, Iowa State University, 1974.

55. Hong, S. W. and Bergles, A. E. "Analysis of Combined Forced and Free Convection in the Entrance Region of Horizontal Tubes." Recent Advances in Engineering Science. Proc. Annual Meeting of the Society of Engineering Science, Inc., Bethlehem, Pa. 14 (Nov. 1977): 453-469.

56. Richtmyer, R. D. and Morton, K. W. Difference Methods for Initial-Value Problems, 2nd edition, New York: Wiley, 1967.

57. O'Brien, G. G.; Hyman, M. A. and Kaplan, S. "A Study of the Numerical Solution of Partial Differential Equations." Journal of Mathematics and Physics 29 (1951): 223-241.

58. Madni, I. K. "A Finite-Difference Analysis of Turbulent, Axisymmetric, Buoyant Jets and Plumes." Ph.D. Thesis, Iowa State University, Ames, 1975.

59. Metzner, A. B. and Reed, J. C. "Flow of Non-Newtonian Fluids - Correlation of the Laminar, Transition, and Turbulent-Flow Regions." AIChE Journal 4 (1955): 434.

60. Metzner, A. B. "Heat Transfer in Non-Newtonian Fluids." Advances in Heat Transfer, pp. 357-397. Vol. 2. Edited by J. P. Hartnett and T. F. Irvine, Jr. New York: Academic Press, 1965.

61. Bassett, C. E. and Welty, J. R. "Non-Newtonian Heat Transfer in the Thermal Entrance Region of Uniformly Heated Horizontal Pipes." AIChE Journal 21, No. 4 (1975): 699-706.

62. Keevil, C. S. and McAdams, W. H. "How Heat Transmission Affects Fluid Friction in Pipes." Chemical and Metallurgical Engineering 36 (1929): 464.

63. Kirkbride, C. G. and McCabe, W. L. "Heat Transfer to Liquids in Viscous Flow." Industrial and Engineering Chemistry 23 (1931): 625-631.

64. Drew, T. B. "Heat Transfer in Stream Line Flow - II - Experiments with Glycerol." Industrial and Engineering Chemistry 24 (1932): 152-157.

65. Colburn, A. P. "Forced Convection Heat Transfer Data." Transactions of AIChE 29 (1933): 174-210.

66. Kern, D. Q. and Othmer, D. F. "Effect of Free Convection on Viscous Heat Transfer in Horizontal Tubes." Transactions of AIChE 39 (1943): 517-555.

67. Eubank, O. C. and Proctor, W. S. "Effect of Natural Convection on Heat Transfer with Laminar Flows in Tubes." S. M. Thesis in Chemical Engineering, M.I.T., 1951.

68. Oliver, D. R. "The Effect of Natural Convection on Viscous Flow Heat Transfer in Horizontal Tubes." Chemical Engineering Science 17 (1962): 335-350.

69. Brown, A. R. and Thomas, M. A. "Combined Free and Forced Convection Heat Transfer for Laminar Flow in Horizontal Tubes." Journal of Mechanical Engineering Science 7, No. 4 (1965): 440-448.

70. Depew, C. A. and August, S. E. "Heat Transfer Due to Combined Free and Forced Convection in a Horizontal and Isothermal Tube." Journal of Heat Transfer 97 (1971): 380-384.

71. Jackson, T. W.; Spurlock, J. M. and Purdy, K. R. "Combined Free and Forced Convection in a Constant Temperature Horizontal Tube." Journal of the American Institute of Chemical Engineers 7 (1961): 38-45.

72. McComas, S. T. and Eckert, E. R. G. "Combined Free and Forced Convection in a Horizontal Circular Tube." Journal of Heat Transfer 88 (1966): 147-153.

73. Mori, Y.; Futagami, K.; Tokuda, S. and Nakamura, M. "Forced Convective Heat Transfer in Uniformly Heated Horizontal Tubes, 1st Report-Experimental Study on the Effect of Buoyancy." International Journal of Heat and Mass Transfer 12 (1969): 1535-1552.

62. Keevil, C. S. and McAdams, W. H. "How Heat Transmission Affects Fluid Friction in Pipes." Chemical and Metallurgical Engineering 36 (1929): 464.

63. Kirkbride, C. G. and McCabe, W. L. "Heat Transfer to Liquids in Viscous Flow." Industrial and Engineering Chemistry 23 (1931): 625-631.

64. Drew, T. B. "Heat Transfer in Stream Line Flow - II - Experiments with Glycerol." Industrial and Engineering Chemistry 24 (1932): 152-157.

65. Colburn, A. P. "Forced Convection Heat Transfer Data." Transactions of AIChE 29 (1933): 174-210.

66. Kern, D. Q. and Othmer, D. F. "Effect of Free Convection on Viscous Heat Transfer in Horizontal Tubes." Transactions of AIChE 39 (1943): 517-555.

67. Eubank, O. C. and Proctor, W. S. "Effect of Natural Convection on Heat Transfer with Laminar Flows in Tubes." S. M. Thesis in Chemical Engineering, M.I.T., 1951.

68. Oliver, D. R. "The Effect of Natural Convection on Viscous Flow Heat Transfer in Horizontal Tubes." Chemical Engineering Science 17 (1962): 335-350.

69. Brown, A. R. and Thomas, M. A. "Combined Free and Forced Convection Heat Transfer for Laminar Flow in Horizontal Tubes." Journal of Mechanical Engineering Science 7, No. 4 (1965): 440-448.

70. Depew, C. A. and August, S. E. "Heat Transfer Due to Combined Free and Forced Convection in a Horizontal and Isothermal Tube." Journal of Heat Transfer 97 (1971): 380-384.

71. Jackson, T. W.; Spurlock, J. M. and Purdy, K. R. "Combined Free and Forced Convection in a Constant Temperature Horizontal Tube." Journal of the American Institute of Chemical Engineers 7 (1961): 38-45.

72. McComas, S. T. and Eckert, E. R. G. "Combined Free and Forced Convection in a Horizontal Circular Tube." Journal of Heat Transfer 88 (1966): 147-153.

73. Mori, Y.; Futagami, K.; Tokuda, S. and Nakamura, M. "Forced Convective Heat Transfer in Uniformly Heated Horizontal Tubes, 1st Report-Experimental Study on the Effect of Buoyancy." International Journal of Heat and Mass Transfer 12 (1969): 1535-1552.

74. Hussain, N. A. and McComas, S. T. "Experimental Investigation of Combined Convection in a Horizontal Circular Tube with Uniform Heat Flux." Heat Transfer Conference, Vol. IV, Paper No. NC 3.4, Paris-Versailles, 1970.

75. Lichtarowicz, A. "Combined Free and Forced Convection Effects in Fully Developed Laminar Flow in Horizontal Tubes." Heat and Mass Transfer by Combined Forced and Free Convection, Paper No. C114/71. London, Institution of Mechanical Engineers, 1972.

76. Ede, A. J. "The Heat Transfer Coefficient for Flow in a Pipe." International Journal of Heat and Mass Transfer 4 (1961): 105-110.

77. Petukhov, B. S. and Polyakov, A. F. "Experimental Investigation of Viscogravitational Fluid Flow in a Horizontal Tube." High Temperature 5 (1967): 75-81.

78. Petukhov, B.S. and Polyakov, A. F. "Effect of Free Convection on Heat Transfer during Forced Flow in Horizontal Pipe." High Temperature 5 (1967): 348-351.

79. Petukhov, B. S.; Polyakov, A. F. and Strigin, B. K. "Heat Transfer in Tubes with Viscous-Gravity Flow." Heat Transfer-Soviet Research 1 (1969): 24-31.

80. Shannon, R. L. and Depew, C. A. "Combined Free and Forced Laminar Convection in a Horizontal Tube with Uniform Heat Flux." Journal of Heat Transfer 90 (1968): 353-357.

81. Bergles, A. E. and Simonds, R. R. "Combined Forced and Free Convection for Laminar Flow in Horizontal Tubes with Uniform Heat Flux." International Journal of Heat and Mass Transfer 14 (1971): 1989-2000.

82. Siegwarth, D. P.; Miskell, R. D.; Redal, T. C. and Hanratty, T. J. "Effect of Secondary Flow on the Temperature Field and Primary Flow in a Heated Horizontal Tube." International Journal of Heat and Mass Transfer 12 (1969): 1535-1552.

83. Morcos, S. M. and Bergles, A. E. "Combined Forced and Free Laminar Convection in Horizontal Tubes." Heat Transfer Laboratory Report, HTL-1, ISU-ERI-Ames-74008, Iowa State University, 1974.

84. Morcos, S. M. and Bergles, A. E. "Experimental Investigation of Combined Forced and Free Laminar Convection in Horizontal Tubes." Journal of Heat Transfer 97 (1975): 212-219.

85. Porter, J. E. "Heat Transfer at Low Reynolds Number (Highly Viscous Liquids in Laminar Flow) Industrial Research Fellow Report." Transactions of the Institution of Chemical Engineers 49 (1971): 1-29.

86. Froishteter, G. B. and Smorodinskii, E. L. "Laminar Heat Transfer of Non-Newtonian Liquids in Tubes with Variable Physical Properties." Translated from Teoreticheskir Osnovy Khimicheskoi Tekhnologii 9, No. 3 (1975): 392-405.

87. Metzner, A. B.; Vaughn, R. D. and Houghton, G. L. "Heat Transfer to Non-Newtonian Fluids." AIChE Journal 3, No. 1 (1957): 92-100.

88. Charm, S. E. "Calculation of Centre-Line Temperatures in Tubular Heat Exchangers for Pseudoplastic Fluids in Streamline Flow." Industrial and Engineering Chemistry Fundamentals 1, No. 2 (1962): 79-82.

89. Charm, S. E. and Merrill, E. W. "Heat Transfer Coefficients in Straight Tubes for Pseudoplastic Food Materials in Streamline Flow." Food Research 24 (1959): 319-331.

90. Gluck, D. F. "The Effect of Turbulence Promotion on Newtonian and Non-Newtonian Heat Transfer Rates." M. Ch. E. Thesis, University of Delaware, 1959.

91. Metzner, A. B. and Gluck, D. F. "Heat Transfer to Non-Newtonian Fluids under Laminar Flow Conditions." Chemical Engineering Science 2 (1960): 185-190.

92. Oliver, D. R. and Jenson, V. G. "Heat Transfer to Pseudoplastic Fluids in Laminar Flow in Horizontal Tubes." Chemical Engineering Science 9 (1964): 115-129.

93. Junkhan, G. H. and Bergles, A. E. "Heat Transfer Laboratory Data Acquisition System." Heat Transfer Laboratory Report, HTL-12, ISU-ERI-77178, Iowa State University, December, 1976.

94. Uhl, V. W. and Root, W. L. "Heat Transfer in Hollow Cut-Flight Jacketed Units to Viscous Fluids." Chemical Engineering Progress Symposium Series 102, vol. 66 (1970): 199-206.

95. Amato, W. S. and Tien, C. "Free Convection Heat Transfer from Isothermal Spheres in Polymer Solutions." International Journal of Heat and Mass Transfer 19 (1976): 1257-1266.

96. Oliver, D. R. and Asghar, S. M. "The Laminar Flow of Newtonian and Viscoelastic Liquids in Helical Coils." Transactions of the Institution of Chemical Engineers 53 (1975): 181-186.

97. Lipson, C. and Seth, N. J. Statistical Design and Analysis of Engineering Experiements. First edition. New York: McGraw-Hill Book Company, 1973.

98. Cook, N. H. and Rabinowicz, E. Physical Measurement and Analysis. London: Addison Wesley Publishing Company, Inc., 1963.

99. Churchill, S. W. and Usagi, R. "A General Expression for the Correlation of Rates of Transfer and Other Phenomena." AIChE Journal 18, No. 6 (1972): 1121-1128.

100. Mischke, C. and Hall, J. L. ISU Cadet Program ME 0226. Department of Mechanical Engineering, Iowa State University, Ames, Iowa, 1975.

101. Churchill, S. W. and Ozoe, H. "Correlations for Laminar Forced Convection in Flows over a Uniformly Heated Plate and in Developing and Fully Developed Flow in a Tube." ASME Paper No. 72-WA/HT-14, 1973.

102. Bergles, A. E. "Laminar Flow Heat Transfer in Horizontal Tubes under Normal and Augmented Conditions." Heat Transfer Laboratory Report, HTL-11, ISU-ERI-Ames-77179, Iowa State University, 1975.

103. Hong, S. W. and Bergles, A. E. "Augmentation of Laminar Flow Heat Transfer in Tubes by Means of Twisted-Tape Inserts." Journal of Heat Transfer 98 (1976): 251-256.

104. Handbook on Methocel. Midland, Mich.: Dow Chemicals, 1975.

105. Scheve, J. L. "A Simplified Process Viscometer for Non-Newtonian Fluids." M.S. Thesis, Iowa State University, 1971.

106. A.S.M.E. Steam Tables. New York: A.S.M.E., 1967.

ACKNOWLEDGMENTS

I take this opportunity to express my gratitude to Dr. A. E. Bergles, Chairman of the Mechanical Engineering Department, for his invaluable guidance and supervision at all stages of this work.

I am thankful to Dr. R. H. Pletcher and Dr. J. L. Hall with whom I had many useful sessions of discussion. I am also thankful to Dr. G. H. Junkham and Dr. D. F. Young for their help during the course of this work.

I am also thankful to Mr. Hap Steed of the Mechanical Engineering Department and Mr. Leon Girard and associates from the Engineering Research Institute workshop for their earnest co-operation and pains they have taken to rectify the troubles encountered during the fabrication of the experimental setup. Thanks are also due to Miss Mary Smith for her neat typing of this thesis.

The financial support given by the Engineering Research Institute, the Power Affiliate Program, and the Department of Mechanical Engineering during the course of this study is greatly appreciated.

Last, but not the least, I am greatly indebted to my parents, brothers, and sisters, for their constant encouragement and affection. I am especially grateful to my parents, Mr. and Mrs. D. M. Joshi, for the inspiration, love, and motivation they provided for my higher education, since the early days of my life.

This thesis is humbly dedicated to my parents, to whom I owe all that I know.

APPENDIX A: FINITE-DIFFERENCE EQUATIONS

Dufort-Frankel Formulation

A Dufort-Frankel finite-difference formulation of the non-dimensional momentum, energy, and continuity equations, Eqs. (3.8a) to (3.10) is given here.

Momentum

$$\hat{\rho}_{i,j} U_{i,j} \frac{(U_{i+1,j} - U_{i-1,j})}{(\Delta Y_+ + \Delta X_-)} + \hat{\rho}_{i,j} V_{i,j} \frac{(U_{i,j+1} - U_{i,j-1})}{(\Delta Y_+ + \Delta Y_-)}$$

$$= - \frac{(P_{i+1} - P_{i-1})}{(\Delta X_+ + \Delta X_-)} + \left\{ \frac{1}{R_j} \frac{2}{(\Delta Y_+ + \Delta Y_-)} \right. \qquad \text{(A.1)}$$

$$\left\{ \frac{(R_{j+1} + R_j)\ (\hat{\mu}_{a,i,j+1} + \hat{\mu}_{a,i,j})}{4} \frac{(U_{i,j+1} - 0.5\ (U_{i+1,j} + U_{i-1,j}))}{\Delta Y_+} \right.$$

$$\left. \left. - \frac{(R_j + R_{j-1})(\hat{\mu}_{a,i,j} + \hat{\mu}_{a,i,j-1})}{4} \frac{(0.5\ (U_{i+1,j} + U_{i-1,j}) - U_{i,j-1})}{\Delta Y_-} \right\} \right\}$$

Energy

$$\hat{\rho}_{i,j}\, U_{i,j}\, \hat{C}_{p\,i,j}\, \frac{(T_{i+1,j} - T_{i-1,j})}{(\Delta X_+ + \Delta X_-)} + \hat{\rho}_{i,j}\, V_{i,j}\, \hat{C}_{p\,i,j} \frac{(T_{i,j+1} - T_{i,j-1})}{(\Delta Y_+ + \Delta Y_-)}$$

$$= \left\{ \frac{1}{R_j} \frac{2}{(\Delta Y_+ + \Delta Y_-)} \right\} \tag{A.2}$$

$$\left\{ \frac{(R_{j+1} + R_j)(\hat{k}_{i,j+1} + \hat{k}_{i,j})}{4} \frac{(T_{i,j+1} - 0.5\ (T_{i+1,j} + T_{i-1,j}))}{\Delta Y_+} \right.$$

$$\left. - \frac{(R_j + R_{j-1})(\hat{k}_{i,j} + \hat{k}_{i,j-1})}{4} \frac{(0.5\ (T_{i+1,j} + T_{i-1,j}) - T_{i,j-1})}{\Delta Y_-} \right\}$$

$$+ \hat{\mu}_{a,i,j} \left\{ \frac{U_{i,j+1} - U_{i,j-1}}{\Delta Y_+ + \Delta Y_-} \right\}^2$$

Continuity

$$\frac{(R_{j+1} + R_j)}{4(\Delta X_+ + \Delta X_-)} \left\{ (\hat{\rho U})_{i+1,j+1} - (\hat{\rho U})_{i-1,j+1} + (\hat{\rho U})_{i+1,j} - (\hat{\rho U})_{i-1,j} \right\}$$

$$+ \frac{(\hat{\rho VR})_{i+1,j+1} - (\hat{\rho VR})_{i+1,j}}{\Delta Y_+} = 0 \tag{A.3}$$

Comments on Dufort-Frankel Momentum Equation

In all of the above equations, non-dimensional apparent viscosity is

$$\hat{\mu}_{a,i,j} = \frac{K_{i,j}\left\{\left|\frac{(U_{i,j+1} - U_{i,j-1})}{(\Delta Y_+ + \Delta Y_-)}\right|\right\}^{n-1}}{(\mu_{a,o})_w} \qquad (3.8b)$$

where $(\mu_{a,o})_w$ is the apparent viscosity at the wall at the tube inlet.

The scheme given by Eq. (A.1) does not adhere to the Dufort-Frankel differencing in the strict sense. Equation (3.8b) shows that while evaluating $\hat{\mu}_{a,i,j+1}$ and $\hat{\mu}_{a,i,j-1}$ a term $U_{i,j}$ will be in a derivative form and it would appear that this $U_{i,j}$ should be averaged as $((U_{i+1,j} + U_{i-1,j})/2)$ to be consistent with the Dufort-Frankel differencing. This would require a much more complex solution for $U_{i+1,j}$ in Eq. (A.1) due to the non-linearity of the algebraic system. Nelson [51] has shown for the turbulent flow that Eq. (A.1) may be used and this equation will remain stable if the $\hat{\mu}_{a,i,j}$'s used are the average of $\hat{\mu}_{a,i,j-1}$, $\hat{\mu}_{a,i,j}$ and $\hat{\mu}_{a,i,j+1}$.

In Eq. (3.8b), for n = 1, the exponent of $\partial u/\partial y$ term vanishes and, hence, $\partial u/\partial y$ has no influence on the local viscosity. For n = 0.5, the exponent of $\partial u/\partial y$ is -0.5, and, therefore, it will influence the local viscosity to some extent; however, without using averages as suggested by Nelson, Eq. (A.1) was found to be stable.

For n = 0.25, the exponent of $\partial u/\partial y$ is -0.75 and, therefore, the term $\partial u/\partial y$ plays a dominant role in determining the value of local viscosity. This $\hat{\mu}_a$ dependence on $\partial u/\partial y$ is analogous to one observed in turbulent flows. At lower values of n ($n < 0.5$), Eq. (A.1) was used

without averaging for $\hat{\mu}_a$, and a substantial instability was noticed. This instability was eliminated by taking averages of viscosities, as suggested by Nelson.

Standard Explicit Finite-Difference Equations

The standard explicit form of the momentum equation used in the starting procedure (normally the first ten steps) is

$$\hat{\rho}_{i,j}\, U_{i,j}\, \frac{(U_{i+1,j} - U_{i,j})}{\Delta X_+} + \hat{\rho}_{i,j}\, V_{i,j}\, \frac{(U_{i,j} - U_{i,j-1})}{\Delta Y_-} \; *$$

$$= \left\{ \frac{2}{R_j (\Delta Y_+ + \Delta Y_-)} \right\} \tag{A.4}$$

$$\left\{ \frac{(R_j + R_{j+1})(\hat{\mu}_{a,i,j} + \hat{\mu}_{a,i,j+1})}{4} \frac{(U_{i,j+1} - U_{i,j})}{\Delta Y_+} \right.$$

$$\left. - \frac{(R_j + R_{j-1})(\hat{\mu}_{a,i,j} + \hat{\mu}_{a,i,j-1})}{4} \frac{(U_{i,j} - U_{i,j-1})}{\Delta Y_-} \right\}$$

The starred term is used when $V_{i,j}$ is positive; otherwise, to maintain stability it is replaced by

$$\hat{\rho}_{i,j}\, V_{i,j}\, \frac{(U_{i,j+1} - U_{i,j})}{\Delta Y_+}$$

The standard explicit form of the energy equation is

$$\hat{\rho}_{i,j}\, U_{i,j}\, \hat{C}_{p\ i,j} \frac{(T_{i+1,j} - T_{i,j})}{\Delta X_+} + \hat{\rho}_{i,j}\, V_{i,j}\, \hat{C}_{p\ i,j} \frac{(T_{i,j} - T_{i,j-1})}{\Delta Y_-}$$

$$= \left\{ \frac{2}{R_j\ (\Delta Y_+ + \Delta Y_-)} \right\} \tag{A.5}$$

$$\left\{ \frac{(R_j + R_{j+1})(\hat{k}_{i,j} + \hat{k}_{i,j+1})}{4} \frac{(T_{i,j+1} - T_{i,j})}{\Delta Y_+} \right.$$

$$\left. - \frac{(R_j + R_{j-1})(\hat{k}_{i,j} + \hat{k}_{i,j-1})}{4} \frac{(T_{i,j} - T_{i,j-1})}{\Delta Y_-} \right\}$$

$$+ \hat{\mu}_{a,i,j} \frac{(U_{i,j} - U_{i,j-1})^2}{\Delta Y_-}$$

$\hat{\mu}_{a,i,j}$ is calculated the same way as in the Dufort-Frankel formulation, although the averaging is not really necessary.

The continuity equation for the ordinary explicit method is

$$\frac{(R_{j+1} + R_j)}{\Delta X_+} \left\{ (\hat{\rho U})_{i+1,j+1} - (\hat{\rho U})_{i,j+1} + (\hat{\rho U})_{i+1,j} - (\hat{\rho U})_{i,j} \right\}$$

$$+ \frac{(\hat{\rho VR})_{i+1,j+1} - (\hat{\rho VR})_{i+1,j}}{\Delta Y_+} = 0 \tag{A.6}$$

APPENDIX B: TRUNCATION ERROR IN THE DUFORT-FRANKEL DIFFERENCE EQUATIONS

Consistency is studied by expanding the dependent variables in Taylor series and estimating the truncation error. A finite-difference scheme is said to be consistent if the truncation error vanishes as the mesh size approaches zero. In the following analysis a uniform grid spacing in the radial direction is assumed. The variable U at various grid points is expanded in Taylor series about the point (i,j) to give the following expressions:

$$U_{i+1,j} = U_{i,j} + \left(\frac{\partial u}{\partial x}\right)_{i,j} \Delta X_+ + \left(\frac{\partial^2 u}{\partial x^2}\right)_{i,j} \frac{\Delta X_+^2}{2} \left(\frac{\partial^3 u}{\partial x^3}\right)_{i,j} \frac{\Delta X_+^3}{6} + \cdots\cdots \tag{B.1}$$

$$U_{i-1,j} = U_{i,j} - \left(\frac{\partial u}{\partial x}\right)_{i,j} \Delta X_- + \left(\frac{\partial^2 u}{\partial x^2}\right)_{i,j} \frac{\Delta X_-^2}{2} \left(\frac{\partial^3 u}{\partial x^3}\right)_{i,j} \frac{\Delta X_-^3}{6} + \cdots\cdots \tag{B.2}$$

$$U_{i,j+1} = U_{i,j} + \left(\frac{\partial u}{\partial y}\right)_{i,j} \Delta Y_+ + \left(\frac{\partial^2 u}{\partial y^2}\right)_{i,j} \frac{\Delta Y_+^2}{2} \left(\frac{\partial^3 u}{\partial y^3}\right)_{i,j} \frac{\Delta Y_+^3}{6} + \cdots\cdots \tag{B.3}$$

$$U_{i,j-1} = U_{i,j} - \left(\frac{\partial u}{\partial y}\right)_{i,j} \Delta Y_- + \left(\frac{\partial^2 u}{\partial y^2}\right)_{i,j} \frac{\Delta Y_-^2}{2} - \left(\frac{\partial^3 u}{\partial y^3}\right)_{i,j} \frac{\Delta Y_-^3}{6} + \cdots\cdots \tag{B.4}$$

To simplify, two assumptions are made:

1) $\Delta Y_+ = \Delta Y_-$

2) $$\frac{(R_j + R_{j+1})(\hat{\mu}_{a,i,j} + \hat{\mu}_{a,i,j+1})}{4} = R_j \hat{\mu}_{a,i,j} =$$

$$\frac{(R_j + R_{j-1})(\hat{\mu}_{a,i,j} + \hat{\mu}_{a,i,j-1})}{4}$$

The second assumption is justified since by expanding $(R_j + R_{j+1})$ $(\hat{\mu}_{a,i,j} + \hat{\mu}_{a,i,j+1})$ and $(R_j + R_{j-1})$ $(\hat{\mu}_{a,i,j} + \hat{\mu}_{a,i,j-1})$ in a Taylor series around the grid point (i,j), no new term appears that will alter the truncation error.

With these assumptions, Eqs. (B.1) to (B.4) are substituted in Eq. (A.1) to give

$$\hat{\rho}_{i,j} U_{i,j} \left[\left(\frac{\partial u}{\partial y}\right)_{i,j} + \left(\frac{\partial^2 u}{\partial x^2}\right)\left(\frac{\Delta X_+ - \Delta X_-}{2}\right) + \left(\frac{\partial^3 u}{\partial x^3}\right)_{i,j} \frac{(\Delta X_+^3 + \Delta X_-^3)}{6(\Delta X_+ + \Delta X_-)} \right]$$

$$+ \hat{\rho}_{i,j} V_{i,j} \left[\left(\frac{\partial u}{\partial y}\right)_{i,j} + \frac{1}{6}\left(\frac{\partial^3 u}{\partial y^3}\right) \Delta Y^2 \right] = - \frac{dP}{dx} - \left(\frac{d^3 P}{dx^3}\right)_{i,j}$$

$$\frac{(\Delta X_+^3 + \Delta X_-^3)}{6(\Delta X_+ + \Delta X_-)} + \frac{1}{R_j}\left\{ R_j\, \hat{\mu}_{a,i,j}\left[\left(\frac{\partial^2 u}{\partial y^2}\right)_{i,j} + \left(\frac{\partial^4 u}{\partial y^4}\right)_{i,j} \frac{\Delta Y^2}{12} \right.\right.$$

$$- \frac{\partial u}{\partial x}\frac{(\Delta X_+ - \Delta X_-)}{(\Delta Y)^2} - \frac{\partial^2 u}{\partial x^2}\frac{(\Delta X_+^2 + \Delta X_-^2)}{2(\Delta Y)^2} - \frac{\partial^3 u}{\partial x^3}$$

$$\left.\left. \frac{(\Delta X_+^3 - \Delta X_-^3)}{6(\Delta Y)^2} + \cdots\cdots \right] \right\} \qquad \text{(B.5)}$$

TE_m is the truncation error of the momentum equation which is estimated as

$$TE_m = \text{Eq. (B.5)} - \text{Eq. (3.8)}$$

$$TE_m = 0\left(\frac{\Delta X_+ - \Delta X_-}{2}\right) + 0\left(\frac{\Delta X_+^3 + \Delta X_-^3}{\Delta X_+ + \Delta X_-}\right) + 0(\Delta Y^2) + 0\left(\frac{\Delta X_+ - \Delta X_-}{\Delta Y^2}\right) + 0\left(\frac{\Delta X_+^2 + \Delta X_-^2}{\Delta Y^2}\right) + 0\left(\frac{\Delta X_+^3 - \Delta X_-^3}{\Delta Y^2}\right) \qquad \text{(B.6)}$$

Now if $\Delta X_+ = \Delta X_-$, then Eq. (B.6) becomes

$$TE_m = 0(\Delta X^2) + 0(\Delta Y^2) + 0\left(\frac{\Delta X^2}{\Delta Y^2}\right) \qquad \text{(B.7)}$$

The significance of the term $0(\Delta X^2/\Delta Y^2)$ in the truncation error has

been discussed in Chapter III. Comparing Eqs. (B.6) and (B.7), the advantage in using the central-difference Dufort-Frankel finite-difference formulation is obvious. This smaller truncation error, Eq. (B.7), can be achieved, at least approximately, by not allowing two successive step sizes to differ significantly.

Hong [53] and Richtmyer and Morton [56] have suggested methods to eliminate the first two terms in Eq. (B.7). These calculations were found to be unimportant for the present calculations.

A similar analysis was done for the energy equation and TE_e. The truncation error in the energy equation reduces to

$$TE_e = O(\Delta X^2) + O(\Delta Y^2) + O(\Delta X^2/\Delta Y^2) + O(\Delta Y^4) \qquad (B.8)$$

Here again, the consistency criterion requires that for the term $\Delta X^2/\Delta Y^2$, ΔX should go to zero faster than ΔY. Fortunately $\Delta X^2/\Delta Y^2$ is associated with $\frac{\partial^2 T}{\partial X^2}\frac{\Delta X^2}{\Delta Y^2}$. For the UHF condition, in the fully developed region $\frac{\partial^2 T}{\partial X^2}$ is zero, and, hence, the term $\frac{\partial^2 T}{\partial Y^2}\left(\frac{\Delta X^2}{\Delta Y^2}\right)$ vanishes. In the thermal entrance region, the term $\frac{\partial^2 T}{\partial Y^2}$ is very small (this can be shown by order of magnitude analysis) and, therefore, it can be neglected.

Thus, the energy equation will be consistent for $\frac{\Delta X}{\Delta Y} \simeq 1$.

APPENDIX C: COMPUTATION OF PRESSURE P_{i+1}

It is seen from the momentum equation, (A.1) and (A.4), that in order to calculate $U_{i+1,j}$ at any j location, the pressure at an axial location, i+1, P_{i+1}, must be known. The integral equation of global continuity is used to obtain this pressure. The equation of global continuity is

$$\hat{\dot{m}} = \int_{\hat{A}} \hat{\rho}_{i+1,j} \, U_{i+1,j} \, d\hat{A} \tag{3.11}$$

The finite-difference approximations require a fine grid for convergence and, therefore, the difference between $\hat{\rho}_{i+1,j}$ and $\hat{\rho}_{i,j}$ is small enough to be neglected. Thus

$$\hat{\rho}_{i,j} \simeq \hat{\rho}_{i+1,j} \tag{C.1}$$

Substituting this in Eq. (3.11) yields

$$\hat{\dot{m}} = \int_{\hat{A}} \hat{\rho}_{i,j} \, U_{i+1,j} \, d\hat{A} \tag{C.2}$$

It will be seen later that excellent results were obtained using this method, which indicates the usefulness and success of this approximation.

In Eq. (C.2), $U_{i+1,j}$ is substituted from the finite-difference Dufort-Frankel momentum equation, Eq. (A.1), and then integrated by using Simpson's rule over the entire tube cross-section. With the finite-difference form of $U_{i+1,j}$, the global continuity equation, Eq. (C.2),

has a pressure term which is only a function of axial location (i.e., at a given cross-section the pressure is constant), and, hence, it can be factored out of the integration, and the following result is obtained:

$$\hat{\dot{m}} = \int_{\hat{A}} \rho_{i,j}\, U_{i+1,j}\, d\hat{A} = \int_{\hat{A}} \frac{PB}{PA}\, d\hat{A} + (P_{i+1} - P_{i-1}) \int_{\hat{A}} \frac{PC}{PA}\, d\hat{A} \tag{C.3}$$

where

$$PA = 4\, \hat{\rho}_{i,j}\, U_{i,j}\, R_{i,j}\, (\Delta Y_+ + \Delta Y_-)\, \Delta Y_+\, \Delta Y_- + (\Delta X_+ + \Delta X_-)\, \Delta Y_-$$

$$(R_{j+1} + R_j)\, (\hat{\mu}_{a,i,j+1} + \hat{\mu}_{a,i,j}) + (\Delta X_+ + \Delta X_-)\, \Delta Y_+\, (R_j + R_{j-1})$$

$$(\hat{\mu}_{a,i,j} + \hat{\mu}_{a,i,j-1})$$

$$PB = 4\, \hat{\rho}^2_{i,j}\, R_j\, \Delta Y_+\, \Delta Y_-\, (\Delta X_+ + \Delta X_-)\, V_{i,j}\, (U_{i,j+1} - U_{i,j-1})$$

$$+ 2\, \hat{\rho}_{i,j}\, (\Delta X_+ + \Delta X_-)\, \Delta Y_-\, (\hat{\mu}_{a,i,j+1} + \hat{\mu}_{a,i,j})$$

$$(U_{i,j+1} - 0.5\, U_{i-1,j})\, (R_{j+1} + R_j) + 2\, \hat{\rho}_{i,j}\, (\Delta X_+ + \Delta X_-)$$

$$\Delta Y_+\, (\hat{\mu}_{a,i,j} + \hat{\mu}_{a,i,j-1})\, (U_{i,j-1} - 0.5\, U_{i-1,j})$$

$$(R_j + R_{j-1}) + 4\, \hat{\rho}^2_{i,j}\, U_{i-1,j}\, U_{i,j}\, R_j\, (\Delta Y_+ + \Delta Y_-)\, \Delta Y_+\, \Delta Y_-$$

$$PC = -4\, \hat{\rho}_{i,j}\, R_j\, (\Delta Y_+ + \Delta Y_-)\, \Delta Y_+\, \Delta Y_-$$

Equation (C.3) is solved for the pressure P_{i+1} since all other variables are known at the i and i-1 locations. A similar procedure was

followed to compute the pressure P_{i+1} in the ordinary explicit finite-difference scheme by using the corresponding momentum equation, Eq. (A.4).

APPENDIX D: COMPUTER CODE FOR CHAPTER III

In this appendix, the computer code developed to solve the problem of heat transfer in in-tube flow of pseudoplastic fluid is given. This computer code has a main program and six subroutines, namely,

1) DELX 1: calculates the streamwise step for starting the ordinary explicit scheme
2) PRES: calculates pressure
3) UVEL: calculates velocity
4) TEMP: calculates temperature
5) POLFIT: fits the curve
6) Fluid Property subroutines

```
C THE FOLLOWING IS THE FORMAT TO BE USED FOR THE INPUT CARDS.
C ALL FORMATS ARE 6G12.5 EXCEPT THE TITLE CARD WHICH IS 72H AND THE
C INTEGER CARDS WHICH ARE 8I10.
C
C  QUANTITIES TO BE INPUT                                          WHEN USED
C-----------------------------------------------------------------------------
C "TITLE"                                                         ALWAYS
C DENS,VISC,USTART,PSTART,RAD,DELYI                               ALWAYS
C VDK,VW,DYM,PRT,DXF,DXFM                                         ALWAYS
C SIGMA                                                           ALWAYS
C RGCN,TSTART,TWALL,CPCON,HTK,QW                                  DENS.LE.0
C IEND,ICUT,NSTA,KNC,NY,LORT,NT,NS                                ALWAYS
C INPR                                                            ALWAYS
C OREX,ORET,CXCUT,CINC,CSTOP                                      ALWAYS
C CUT(K),K=1,NSTA                                                 NSTA.GT.0
C U0,DD1,VV1                                                      USTART.LE.0
C XV0,XV10,AG,SPLV                                                VISC.LT.0
C CP0,CP10,C0                                                     CPCON.LT.0
C HTK0,HTK10,B0,SPLK                                              HTK.LT.0
C TW(J),J=1,|NT|                                                  TWALL.LT.0
C TX(J),J=1,|NT|                                                  TWALL.LT.0
C
C THE FOLLOWING IS AN EXPLANATION OF THE INPUT
C
C QUANTITY     EXPLANATION
C-----------------------------------------------------------------------------
C DENS         =DENSITY(LBM/FT3) FOR CONSTANT PROPERTY FLOW
C              .LE.0 INDICATES VARIABLE PROPERTY FLOW
C VISC         =VISCOSITY(LBM/FT-SEC) FOR CONSTANT VISCOSITY
C              .LT.0 INDICATES VARIABLE VISCOSITY  (DENS MUST BE .LT.0)
C USTART       =VELOCITY(FT/SEC) FOR UNIFORM INITIAL PROFILE
C              .LE.0 INDICATES FULLY DEVELOPED PROFILE WILL BE USED
C PSTART       =INITIAL STATIC PRESSURE (LBF/FT2)
C              .LT.0 INDICATES THAT PRESSURE OR EDGE VELOCITY
C              DISTRIBUTIONS WILL BE INPUT
C RAD          =RADIUS FOR PIPE (FT)
C              =0 INDICATES FLAT PLATE
C              .LT.0 INDICATES CHANNEL  |RAD|=HALF-WIDTH
C DELYI        =Y GRID SPACE NEAREST THE WALL
C VDK          = VAN DRIEST CONSTANT K (SUGGEST USING 0.40)
C VW           = NORMAL VELOCITY COMPONENT TO WALL
C DYM          = MINIMUM Y GRID GEOMETRIC FACTOR (USED IN TURBULENT FLOW)
C              A DYM OF 1.04 (LARGER FOR FLAT PLATE) FOR INPUT IS GOOD.
C              THE ADJUSTED DYM (BECAUSE THE SPACES MUST FILL THE WHOLE
C              PIPE OR CHANNEL) SHOULD NOT BE GREATER THAN 1.15 FOR MOST
C              CASES (1.05 OR LESS FOR HIGH PRESSURE GRADIENT OR
C              HIGH HEAT TRANSFER)
C DXF          =DELX/(BOUNDARY LAYER THICKNESS) FOR D-F EQUATIONS
C              FOR LAMINAR CONSTANT PROPERTY FLOWS.
C              0.0008 TIMES THE TUBE REYNOLDS NUMBER MAY BE USED.
C              MAY NEED SMALLER DXF FOR HEAT TRANSFER.
C              .LT.0 FOR DXF INCREASES SLOWLY FROM |DXF|
C DXFM         =MAXIMUM DXF IF DXF.LT.0. OR STARTING METHOD IS USED
C              SAME AS DXF
C SIGMA        = PARAMETER FOR CONTROLING DELTA X IN PRESSURE GRADIENT
C              CASES (USUALLY = 0.003)
C RGCN         =GAS CONSTANT R FOR DENSITY=P/RT
C              .LE.0 FOR DENSITY=-RGCN
C     FOR CONSTANT DENSITY FLOW RGCN SHOULD BE NEGATIVE
C TSTART       =TEMPERATURE(DEG R) FOR UNIFORM INITIAL PROFILE
```

```
C TWALL         =WALL TEMPERATURE(DEG R) FOR CONST WALL TEMP
C               =0 INDICATES CONSTANT WALL HEAT FLUX
C               .LT.0 FOR TEMP OR HEAT FLUX INPUT ALONG WALL
C CPCON         =SPECIFIC HEAT (BTU/LBM-R)
C               .LT.0 INDICATES VARIABLE SPECIFIC HEAT
C HTK           = THERMAL CONDUCTIVITY (BTU/HR-FT-R)
C               .LE.0 INDICATES VARIABLE THERMAL CONDUCTIVITY
C QW            =WALL HEAT FLUX (BTU/HR-FT2) FOR CONSTANT HEAT FLUX
C IEND          =LAST I STATION TO BE COMPUTED
C               THIS IS A SAFETY FEATURE.  SET IEND HIGH (1000 OR MORE)
C               IF A CASE MIGHT NEED MORE STEPS.  MOST CASES TAKE ABOUT
C               400 STEPS
C IOUT          =NUMBER OF I STEPS BETWEEN OUTPUT
C               .LE.0  NOT USED
C NSTA          =NUMBER OF REX.RET. OR X STATIONS TO BE READ IN FOR OUTPUT
C               .LE.0  NOT USED
C KNC           .GT.0  READ IN ANOTHER CASE AFTER THIS ONE
C               .LE.0  THIS IS THE LAST CASE TO BE READ IN
C NY            =NUMBER (MUST BE EVEN) OF Y GRID SPACES IN PIPE OR CHANNEL
C               SUGGEST USING 50.  MORE MAY BE NEEDED FOR SOME CASES.
C NDT           =NUMBER OF DATA POINTS INPUT FOR WALL TEMPERATURE
C               .LT.0  -NDT=NUMBER FOR HEAT FLUX
C NS            =ICOUNT WHEN D-F EQUATIONS START
C               SUGGEST USING 20
C INPR          = 0 FOR PIPE, CHANNEL, OR FLAT PLATE CASES
C               = NUMBER OF INPUT STATIONS FOR WALL RADIUS FOR BODIES
C               OF REVOLUTION
C               .LT.0 FOR INPUT FORMULAS FOR RW AND DRW/DXA IN FUNCTION
C DREX          =VALUE OF REX BETWEEN OUTPUT, OR FIRST VALUE IF DINC .GT.0
C               =0  NOT USED
C               .LT.0  INPUT REX STATIONS  (NSTA.LT.0)
C DRET          SAME AS DREX, BUT FOR RET
C DXOUT         SAME AS DREX, BUT FOR X
C DINC          =GEOMETRIC PROGRESSION FACTOR FOR REX.RET. OR X OUTPUTS
C               .LE.0  NOT USED
C DSTOP         =LARGEST VALUE OF REX.RET. OR X TO BE OUTPUT
C               .LE.0  NOT USED
C OUT(K)        =VALUES OF REX.RET. OR X TO BE OUTPUT
C UO            =AVERAGE VELOCITY FOR FULLY DEVELOPED PROFILE
C DD1           =DENSITY AT INITIAL PRESSURE AND BULK TEMPERATURE
C VV1           =VISCOSITY AT INITIAL BULK TEMPERATURE
C TW(J)         =WALL TEMP OR HEAT FLUX VALUES TO BE INPUT
C TX(J)         =X VALUES FOR TW(J)
C STORE         REFERS TO DATA STORAGE ON THE DISC
C               LT.0.0 REFERS TO STORING ON THE DISC
C PRVIOU        LE0.0 MEANS THAT DATA IS TO BE READ FROM THE DISC
C XNONET        LE0.0 REFERS TO NON-UNIFORM GRID SPACING
C               GT0.0 REFERS TO UNIFORM GRID SPACING
      REAL MUE0,MUEM,MUEF,MUEW,KTM,KTF,KTW,NTF,NTM,NTW,K0,N0,KODASH,KTO,
     1NTC
      REAL KI,NI
      DIMENSION VP(72),DF(72),DELYM(72),UPLUS(72),DUT(72),DM(72),TTW(72)
     1,
     1TX(72),DUDJ(72),DUY(72),Z(72),ZZ(72),CP(72),DIFU(72),URATIO(72)
     1,FDUDY(72)
      REAL XX(72),XK(72),Y(72),YPLUS(72),POUT(72),KT(72),NT(72)
      COMMON/MVAR/U(72),UM(72),UP(72),V(72),R(72),EV(72),EK(72),D(72),
     1C(72),DELYP(72),DELYT(72),COEFP(72),COEFM(72),SMUP(72),SMUM(72),
     2SKCF(72),SKCM(72),SPMAX(72),SMMAX(72),DELXP,DELXT,DELPT,DELPP,FP,
     3PDROP,PP,PSO,SUMPO,CHPF,ICOUNT,N,NP1,NM1,JDEL,KJDEL,NS,NPSTA,PSTAR
```

```
      4T
       COMMON/MTEMP/T(72),TP(72),TM(72),H(72),HJ(72),TSTART,TCONV,JTDEL
     5 KNC=-1                                                          0060
       PRST=-1.0
       GCON=32.174
       XJCON=777.66
         GPS=0.0
         C1W=0.0
         C2W=C.0
       BU=1.0                                                          0070
       BT=1.C                                                          0080
       BXL=1.C                                                         0090
       CHPF=8.0                                                        0100
       CH=1.0                                                          0110
       FP=1.0                                                          0120
       DXCXA=1.0
       TCONV=1.0
       NNOP=1
       NNOR=1
       NPSTA=C
       XA=0.0
       TC=0.0
       CC=C.0
       CPTC=1.0
       XVTO=0.0
       HTKTO=0.0
       RCON=1.0
       LLCF=C
       HICX=0.0
       DXFT=1.0
       NTT=1
       CXCIST=0.0
       XA=0.0
       T1=C.C
       DELPF=C.0
CREADING IN THE INPUT
    10 READ(5,1001)                                                    0140
 1001 FORMAT(72H                                                       0150
      1                                 )                            0160
       WRITE(6,1900)                                                   0170
 1900 FORMAT('1')                                                      0180
 1901 FORMAT('0',///)                                                  0190
       WRITE(6,1001)                                                   0200
    20 READ(5,1002) DENS,VISC,USTART,PSTART,RAD,DELYI
 1002 FORMAT(6G12.5)
       WRITE(6,1002) DENS,VISC,USTART,PSTART,RAD,DELYI
    22 READ(5,1002)VDK,VWALL,DYM,PRT,DXF,DXFM
       WRITE(6,1002)VDK,VWALL,DYM,PRT,DXF,DXFM
       READ (5,1002) SIGMA
       WRITE(6,1002) SIGMA
       IF (DENS.GT.0.C) GC TO 40                                       0250
    30 READ(5,1002) RCON,TSTART,TWALL,CPCON,HTK,QW
       WRITE(6,1002) RCON,TSTART,TWALL,CPCON,HTK,QW
    40 READ(5,1003) IEND,IOUT,NSTA,KNC,NY,LORT,NOT,NS
 1003 FORMAT(8I10)
       WRITE(6,1003)IEND,IOUT,NSTA,KNC,NY,LORT,NOT,NS
       IF(NOT.LE.0)NTT=-1
       NOT=IABS(NOT)
       READ (5,1003)INPR
       WRITE(6,1003)INPR
```

```
      READ(5,1002)OREX,CRET,OXOUT,OINC,OSTOP
      WRITE(6,1002)OREX,CRET,OXOUT,OINC,OSTOP
      IF(NS.GT.1) DXFT=-1.0
      IF(DXF.LT.0.0) DXFT=-1.0
      DXF=ABS(DXF)
      IF(NSTA.LE.0) GO TO 50                                          0340
      READ(5,1004)(OUT(K),K=1,NSTA)                                   0350
 1004 FORMAT(6G12.5)
      WRITE(6,1004)(OUT(K),K=1,NSTA)                                  0370
      READ(5,994) KO,NC,CRIT
  994 FORMAT(3F10.8)
C FOLLOWING CARDS GIVE INSTRUCTIONS  ABOUT THE STORING OF THE OUTPUT
C ON THE DISC
      READ(5,1004) STORE,PREVIO,XNONET
      WRITE (6,1004) STORE,PREVIO,XNONET
C     NO REFERS TO POWER INDEX OF NON NEWTONIAN FLUID
C     KO REFERS TO CONSISTENCY INDEX OF NON-NEWTONIAN FLUID
C     KO REFERS TO INLET VISCOSITY FOR NEWTONIAN FLUID
C     UNITS OF KC ARE (LBF-(SEC**N)/SQ.FT)
      IF (PREVIO.GT.0.0) GO TO 50
      READ(11)  ICOUNT,NS,DELXP,DXFT,DXF,BT,BU,D0,U0,XV0,MUE0,KO,NO,CP0,
     1XCONV,UCONV,PCONV,CCONV,XMCONV,XVCONV,TCONV,CPCONV,XKCONV,DDD,
     3CPT0,HTKT0,N,NP1,NM1,NM2,JTDEL,JDEL,KTJDEL,KC,K,PP,P,DELPP,PGRAD,
     4PDROP,RAD,XRAD,XA,XMDOT,XMDOT1,VW,PSA,PSB,PSC,PSD,U,UP,UM,D,DP,
     5DM,C,TF,TM,T,HJ,H,VP,DELYM,DELYT,EK,EV,R,Y,DELYP,XDIST,HCONV,V
     6PS0,XK,XV,DELY,DMM,FTK0,PR,EXRF,REC,REDA,QBK,QPS,QPWRX,LCOP
      WRITE(6,991) ICOUNT
      WRITE(6,4030)RED,REDA,PR
 4030 FORMAT('0','REC=',G12.5,5X,'REDA=',G12.5,5X,'PR=',G12.5)
      READ(5,1002) DXFT,DXF
      GO TO 200
C
CINITIALIZING AND NONDIMENSIONALIZING                                 0380
C
   50 IF(USTART.LE.0.0) GO TO 60                                      0390
C THIS REFERS TO THE UNIFORM VELOCITY AT THE ONSET OF HEATING
      U0=USTART                                                       0400
      JDEL=1                                                          0410
   51 IF(DENS.LE.0.0) GO TO 65                                        0420
      D0=DENS                                                         0430
      DMM=D0
       DELYR=RAD/NY
      XV0=KO*GCON*((ABS(U0/DELYR))**(NO-1))
      GO TO 80                                                        0450
   60 READ (5,1002) U0,DD1
      WRITE(6,1002) U0,DD1
C     BU=-1,REFERES TO  PARABOLIC VELOCITY AT THE ONSET OF HEATING
      BU=-1.0
      N=NY+1
      DELYR=RAD/NY
      US=ABS(U0)
      IF(XNONET.LE.0.0) GO TO 961
C UNIFORM GRID SPACING CALCULATIONS
       DYM=1.0
      DO 995 J=1,N
      Y(J)=(J-1)*DELYR
      R(J)=RAD-Y(J)
  995 CONTINUE
       DELY1=DELYR
      GO TO 964
```

```
C NON-UNIFORM GRID SPACING CALCULATIONS
  961  DELY=DELYI
       DELYP(1)=DELY
       Y(1)=0.0
       DO 962 J=2,N
       DELYP(J)=DYM*DELYP(J-1)
       Y(J)=Y(J-1)+DELYP(J-1)
       R(J)=RAD-Y(J)
  962 CONTINUE
       IF(Y(N).GE.RAD) GO TO 963
       DYM=DYM+0.005
       GO TO 961
  963 YCH=RAD/Y(N)
       DO 965 J=2,N
       Y(J)=YCH*Y(J)
       R(J)=RAD-Y(J)
  965 CONTINUE
       R(1)=Y(N)
        WRITE(6,996) DYM
  996 FORMAT('0','DYM=',F10.6)
  964 DO 997 J=2,N
  997 U(J)=US*(((3*NO+1)/(NO+1))*(1.- ((R(J)/RAD)**((NO+1)/NO))))
       U(1)=0.0
       GO TO 51
   65 IF(TSTART.LE.0.0) GO TO 70                                        0480
       TO=TSTART                                                       0490
   66 IF(RGCON.LE.0.0)GO TO 72
       DO=RHO(TO)
   67 DYMS=DYM*DYM
       DYMC=DYM*DYMS
       DYM4=1.0+DYM+DYMS
       XPSB=DYM4/(Y(2)*DYMS)
       XPSC=-DYM4/(Y(2)*(1.+DYM)*DYMC)
       XPSD=1.0/(Y(2)*DYM4*DYMC)
C CALCULATION  OF  POLYNOMIAL DU/DX
       XDUDYP=XPSB*U(2)+XPSC*U(3)+XPSD*U(4)
C CALCULATION OF LINEAR DU/DX
       DUDXL=U(2)/DELYR
       IF(XNONET.LE.0.0)DUDXL=U(2)/DELYI
C
       IF(VISC.LT.0.0) GO TO 75
C
C CALCULATION OF INLET VISCOSITY
       XVO=KO*GCON*(XDUDYP**(NO-1.))
       WRITE(6,998) XVO,NO,KO,XDUDYP,CRIT
   68 IF(CPCON.LE.0.0) GO TO 76                                         0540
       CPO=CPCON                                                       0550
   69 IF(HTK.LE.0.0) GO TO 77                                          0560
       HTKO=HTK                                                        0570
       GO TO 80                                                        0580
   70 CONTINUE                                                         0590
C  70 READ TEMP PROFILE, NON-DIM, BT=-1.GO TO 66
   72 DO=-RCON
       DMM=DO
       GO TO 67
   75  KTO=KI(TO)
       KO=KTO
       NTO=NI(TO)
       NO=NTO
       XVO=KO*GCON*(XDUDYP**(NO-1.))
```

```
      XVTC=TC
      WRITE(6,998) XV0,NC,K0,XDUDYP,CRIT
      GO TO 68
   76 CPC=XCP(TO)
      CPTO=TO
      GO TO 69
   77 HTKC=CONF(TO)
      HTKTO=TO
  998  FORMAT('0',*XV0=',F10.5,5X,'NO=', F10.4,5X,'K0=',F10.7,10X,'XDUDY
     1P=',F10.5,5X,'CRITICAL=',F10.5)
CCCMPUTING THE NON-DIMENSIONALIZING CONVERSION FACTORS
   80 UCONV=U0                                                          0690
      XCONV=XV0/(D0*L0)                                                 0700
      PCONV=(D0*L0*U0)/GCON
      DCONV=D0                                                          0720
      XVCONV=XV0                                                        0730
      XMCONV=(XV0*XV0)/(G0*U0)                                          0740
      WRITE(6,1005) UCONV,XCONV,PCONV,DCONV,XVCONV,XMCONV               0750
 1005 FORMAT('0UCONV=',G12.5,  12X,'XCONV=',G12.5,12X,'PCONV=',G12.5,   0760
     112X,/,' DCONV=',G12.5,12X,'XVCONV=',G12.5,11X,'XMCONV=',G12.5)
      IF(DENS.GT.0.0) GO TO 41                                          0780
      TCONV=(U0*UC)/(GCON*XJCON*CP0)
      HCONV=(G0*L0)/(GCON*XJCON)
      CPCONV=CP0                                                        0810
      XKCONV=3600.0*XV0*CP0                                             0820
      DDC=PCONV/(TCONV*DCONV)
      XVTO=XVTO/TCONV
      CPTO=CPTO/TCONV
      HTKTO=HTKTO/TCONV
      WRITE(6,1006)TCONV,HCONV,CPCONV,XKCONV                            0830
 1006 FORMAT('0TCONV=',G12.5,12X,'HCONV=',G12.5,12X,'CPCONV=',G12.5,    0840
     1/' XKCONV=',G12.5)                                                0850
C SETTING GRID SPACING IN NON-DIMENSIONAL FORM
   41 N=NY+1                                                            0870
   39 DELY=RAD/(XCONV*NY)
   44 NP1=N+1
      NM1=N-1                                                           1000
      NM2=N-2                                                           1010
      XRAD=RAD/XCONV                                                    1030
      IF(XNONET.LE.0.0)  GO TO 43
C UNIFORM GRID SPACING
      DYM=1.
      DO 42 J=1,N
      Y(J)=(J-1)*DELY
      DELYP(J)=DELY
      DELYM(J)=DELY
      DELYT(J)=2.0*DELY
       R(J)=XRAD-Y(J)
   42 CONTINUE
      Y(N+1)=Y(N-1)
      R(N+1)=R(N-1)
      GO TO 34
C NON-UNIFORM GRID SPACING
   43 DELY=DELYI/XCONV
      DELYP(1)=DELY
      DELYM(1)=DELY
      DELYT(1)=2.0*DELY
      Y(1)=0.0
   47 DO 45 J=2,N
      DELYP(J)=DYM*DELYP(J-1)
```

```
      DELYM(J)=DELYP(J-1)
      DELYT(J)=DELYM(J)+DELYP(J)
      Y(J)=Y(J-1)+DELYP(J-1)
      R(J)=XRAD-Y(J)
   45 CONTINUE
      R(N+1)=R(N-1)
      Y(N+1)=Y(N-1)
      IF(Y(N).GE.XRAD) GO TO 46
      DYM=DYM+0.005
      GO TO 47
   46 YCH=XRAD/Y(N)
      DO 48 J=2,N
   48 Y(J)=YCH*Y(J)
      Y(N+1)=Y(N-1)
      DO 49 J=2,N
      DELYP(J)=Y(J+1)-Y(J)
      DELYM(J)=Y(J)-Y(J-1)
      DELYT(J)=Y(J+1)-Y(J-1)
      R(J)=XRAD-Y(J)
   49 CONTINUE
      DELYT(N)=2.0*DELYM(N)
      DELYP(1)=Y(2)
      DELYM(1)=DELYP(1)
      DELYT(1)=2.0*DELYP(1)
      R(1)=Y(N)
      WRITE(6,1009) DYM
 1009 FORMAT('0DYM=',G12.5)
   34 WRITE(6,1007)                                                    1440
 1007 FORMAT('0Y(J)')                                                  1450
      DO 52 J=1,N                                                      1460
   52 POUT(J)=Y(J)*XCONV                                               1470
      WRITE(6,1008)(POUT(J),J=1,N)                                     1480
 1008 FORMAT(10G12.5)                                                  1490
C
C
CINITIALIZING
C
      DYMS=DYM*DYM
      DYMC=DYM*DYMS
      DYM4=1.0+DYM+DYMS
      PSB=DYM4/(Y(2)*XCONV*DYMS)
      PSC=-DYM4/(Y(2)*XCONV*(1.0+DYM)*DYMC)
      PSD=1.0/(Y(2)*XCONV*DYM4*DYMC)
      PSA=-PSB-PSC-PSC
C
C     COMPARISON OF LINEAR AND POLYNIMIAL FIT FOR VELOCITY PROFILE
      DUDXP=(PSB*U(2)+PSC*U(3)+PSD*U(4))
      XVS=KC*GCON*(DUDXP**(NO-1))
      PER=100.*(XV0-XVS)/XV0
C GRID SPACING WAS REFINED UNTIL  DU/DX BY POLYNOMIAL AND LINEAR FIT
C AGREED TO WITHIN 0.5%
      WRITE(6,79) XV0,XVS,PER,DUDXL,DUDXP
   79 FORMAT('0',*XV0=',G12.5,5X,'XVS=',G12.5,5X,'PERCENTAGE=',G12.5,/,
     25X,'DUDXL=',G12.5,5X,'DUDXP=',G12.5)
C
      VW=VWALL/UCONV
   85 IF(BU.LE.0.0) GO TO 86
      U(1)=0.0                                                         1550
      UM(1)=0.0                                                        1560
      DO 87 J=2,N                                                      1570
```

```
      U(J)=1.0                                                          1580
      UM(J)=1.0                                                         1590
   87 CONTINUE                                                          1600
   86 JDEL=N
      KJDEL=N
      DO 63 J=1,NP1
C
C     DIMENSIONLESS  PARABOLIC VELOCITY PROFILE
C
      XN1=NO+1
      U(J)=((3*NO+1)/XN1)*(1.-((1.-(Y(J)/XRAD))**(XN1/NO)))
      UM(J)=U(J)
   63 CONTINUE
   61 IF(DENS.GT.0.0) GO TO 99
      IF(ET.LE.0.0) GO TO 88                                            1620
      DO 89 J=1,NP1                                                     1630
      T(J)=TSTART/TCONV                                                 1640
      TM(J)=T(J)                                                        1650
   89 CONTINUE                                                          1660
C IMPOSING THE WALL HEATING BOUNDARY CONDITION
      IF(TWALL.LE.0.0) GO TO 90                                         1670
      T(1)=TWALL/TCONV                                                  1680
      TM(1)=T(1)                                                        1690
      GO TO 88                                                          1700
   90 IF(TWALL.LT.0.0) GO TO 81
      T(1)=-(PSB*T(2)+PSC*T(3)+PSD*T(4)+QW/(HTKO*TCONV))/PSA
      TM(1)=T(1)
      GO TO 88
   81 READ(5,1002)(TTW(J),J=1,NOT)
      WRITE(6,1002)(TTW(J),J=1,NOT)
      READ(5,1002)(TX(J),J=1,NOT)
      WRITE(6,1002)(TX(J),J=1,NOT)
      CALL POLFIT(NOT,TX,TTW,GXDIST,T1)
      IF(NTI.LE.0) GO TO 82
      T(1)=T1/TCONV
      TM(1)=T1/TCONV
      GO TO 88
   82 T(1)=-(PSB*T(2)+PSC*T(3)+PSD*T(4)+T1/(HTKO*TCONV))/PSA
      TM(1)=T(1)
C PROPERTY CALCULATION AT THE TUBE INLET
   88 DO 91 J=1,NP1                                                     1730
      V(J)=VW
      TJ=T(J)*TCONV
      D(J)=RHO(TJ)/DCONV
      VP(J)=VW
      DM(J)=D(J)                                                        1770
      XK(J)=HTKO/XKCONV
      C(J)=1.0                                                          1800
   91 CONTINUE                                                          1810
      DO 59 J=1,NM1
      NT(J)=NO
      KT(J)=KO
      TJ=T(J)*TCONV
      IF(ET.LE.0.0) KT(J)=KI(TJ)
      IF(ET.LE.0.0) NT(J)=NI(TJ)
      IF (J.EQ.1) GO TO   54
      URATIO(J)=U(J)/U(N)
      IF(URATIO(J).LT.CRIT) GO TO 53
      FDLDY(J)=FDLDY(J-1)
      GO TO 58
```

```
C  VISCOSITY CALCULATION
  53  DIFU(J)=ABS(U(J+1)-U(J-1))
      FDUDY(J)=DIFU(J)/DELYT(J)
      IF(DIFU(J).LE.1.0E-06) FDUDY(J)=FDUDY(J-1)
   54 IF(J.EQ.1) FDUDY(J)=(PSB*U(2)+PSC*U(3)+PSD*U(4))*XCONV
   58 XV(J)=(KT(J)*GCON/XVCONV)*((FDUDY(J)*UCONV/XCONV)**(NT(J)-1.))
   59 CONTINUE
      FDUDY(NP1)=FDUDY(NM1)
      FDUDY(N)=FDUDY(NM1)
      XV(N)=XV(NM1)
      XV(NP1)=XV(NM1)
      IF(RCON.LE.0.0) GO TO 95                                          1820
   92 IF(HTK.LE.0.0) GO TO 96                                           1830
   94 IF(CPCON.LE.0.0) GO TO 98                                         1850
      GO TO 101                                                         1860
   95 DO 36 J=1,NP1
      D(J)=1.0
   36 DM(J)=1.0
      GO TO 92
   96 DO 55 J=1,NP1
      TJ=T(J)*TCONV
   55 XK(J)=CONF(TJ)/XKCONV
      GO TO 94
   98 DO 84 J=1,NP1
      TJ=T(J)*TCONV
      CP(J)=XCP(TJ)
      C(J)=CP(J)/CP0
   84 CONTINUE
      GO TO 101
   99 DO 100 J=1,NP1                                                    1950
      DP(J)=1.0                                                         1960
      D(J)=1.0                                                          1970
      DM(J)=1.0                                                         1980
      XV(J)=1.0                                                         1990
      EK(J)=0.0
      C(J)=1.0
      V(J)=VW
      VP(J)=VW
  100 CONTINUE                                                          2020
  101 EXRF=0.5
      P=PSTART/PCONV
      PM=P
      PSC=P
      U(N+1)=U(N-1)
C  AVERAGING THE VISCOSITY
      DO 108 J=2,NM1
      EV(J)=(XV(J-1)+XV(J)+XV(J+1))/3.
  108 CONTINUE                                                          2260
      EV(1)=XV(1)
      EV(N)=EV(N-1)
       EV(NP1)=EV(NM1)
      IF(DENS.GT.0.0) GO TO 115                                         2280
      DO 109 J=1,N
      EK(J)=XK(J)                                                       2320
  109 CONTINUE                                                          2330
      EK(N+1)=EK(N-1)                                                   2340
C CALCULATION OF MASS FLOW RATE
  115 ICOUNT=0                                                          2470
      SUMPO=0.0                                                         2510
      DO 120 J=1,NM2,2
```

```
      YA1=DELYP(J)
      YB1=DELYP(J+1)
      YAB=YA1+YB1
      W2=YAB/YB1*(YAE/3.0-YA1/2.0)
      W1=YAE**2.0/(2.0*YA1)-W2*YAB/YA1
      W0=YAB-W1-W2
      SUM1=D(J)*U(J)*R(J)
      SUM2=D(J+1)*U(J+1)*R(J+1)
      SUM3=D(J+2)*U(J+2)*R(J+2)
  120 SUMP0=W0*SUM1+W1*SUM2+W2*SUM3+SUMP0
      JDEL=2                                                          2570
      JTDEL=2
      DELXP=1.0E-50
      XDIST=0.0                                                       2610
      IPRINT=0                                                        2620
      PDROP=0.0                                                       2630
      K=1                                                             2640
      XDOUT=0.0                                                       2650
      TXOUT=OXOUT/XOONV                                               2660
      TSTOP=OSTOP/XOONV                                               2670
C
C     CALCULATION OF EFFECTIVE VISCOSITY
      KODASH=KO*(((3*NO+1)/(4*NO))**NO)
      MUEO=AES(KODASH*OOONV*((8*UO/(2*RAD))**(NO-1)))
      REO=(2.0*DO*UO*RAD)/XVO                                         2680
      REOA=REO*XVO/MUEO
      IF(OH.OE.0.0) GO TO 117                                         2690
      XMDOT=2.0*SUMP0*DOONV*UOONV*XOONV                               2700
      GO TO 118                                                       2710
  117 XMDOT=6.28319*SUMP0*XMOONV                                      2720
  118  WRITE(6,1030) REO,REOA,XMDOT
 1030  FORMAT('0REO=',G12.5,12X,'REYNOLDS NO EFF.=',G12.5,/,
     1'0MASS FLOW=',G12.5)
      XMDOT1=XMDOT                                                    2750
      IF(DENS.GT.0.0) GO TO 116                                       2760
      PR=XVO*OPO*3600.0/HTKO
      PRA=PR*MUEO/XVO
      WRITE(6,1031)PR,PRA,MUEO
 1031  FORMAT('0',*PR=',G12.5,12X,'PRANDTL NO. EFF.=',G12.5,5X,'MUEO=',G
     112.5)
  116 WRITE(6,1016)
      DO 800 J=1,N
      HJ(J) = C(J)*T(J)+U(J)*U(J)/2.
      TH(J)=HJ(J)
  800 CONTINUE
 1016 FORMAT(////,'1**** BEGINNING OF COMPUTATION LOOP ****')         2820
C
CBEGINNING COMPUTATION LOOP
C
  200 ICOUNT=ICOUNT+1                                                 2840
      IP1=ICOUNT+1
CCALCULATING DELX
      DELXM=DELXP                                                     2850
      IF(DXFT.GE.0.0) GO TO 204
  201 IF(ICOUNT.GE.NS) GO TO 202
      CALL DELX1
      DXF=DELXP/Y(JDEL)
      GO TO 205
  202 IF(DXF.LT.(DXFM+0.02)) GO TO 203
      NS=IP1
```

```
      GO TO 201
  203 IF(ICOUNT.EQ.NS) WRITE(6,1017) ICOUNT
 1017 FORMAT(///,'0*** D-F EQUATIONS STARTED AT ICOUNT EQUAL TO',I6)
      IF(DXF.GE.0.05) GO TO 206
      DXF=1.1*DXF
      GO TO 204
  206 JDELM=MAX0(JDEL,JTDEL)
      JDELM=2.0*JDELM
      IF(ICOUNT.GE.JDELM.OR.BU.LE.0.0) DXF=DXF+0.02*DXFM
      IF(DXF.GE.DXFM)DXF=1.0
  204 DELXP=DXF*Y(JDEL)
  205 PGRAD=ABS(DELPP/DELXM)
      IF(PGRAD.EQ.0.0) PGRAD=1.0E-50
      PGRAD=D(N)*U(N)*L(N)*SIGMA/PGRAD
      DELXP=AMIN1(DELXP,PGRAD)
      DELXT=DELXP+DELXM
      XDIST=XDIST+DELXP                                              2880
      DXDIST=XDIST*XCONV
      XA=XA+DELXP*XCONV/DXDXA
C CALCULATING PRESSURE GRADIENT
  220 XMDOT1=XMDOT1+D(1)*VW*XRAD*DELXP*6.28319*XMCONV
      SUMP0=XMDOT1/(6.28319*XMCONV)
  221 CALL PRES
C CALCULATION OF UP(J)                                               3460
  240 CALL UVEL
  250 JDEL10=JDEL+10                                                 3600
      KC=MINO(N,JDEL10)                                              3610
      IF(JDEL.GE.N)KJDEL=N
C CALCULATION OF TP(J)                                               4010
  300 IF(DENS.GT.0.0) GO TO 360
      CALL TEMP
      JTDE10=JTDEL+10                                                4830
      KCT=MINO(N,JTDE10)                                             4840
      IF(TWALL)330,320,310                                           4850
  310 TP(1)=TWALL/TCONV                                              4860
      H(1)=C(1)*TP(1)
      GO TO 340                                                      4900
  320 CONTINUE                                                       4910
      TP(1)=-(PSB*TP(2)+PSC*TP(3)+PSD*TP(4)+QW/(XK(1)*XKCONV*TCONV))/PSA
      H(1)=C(1)*TP(1)
      GO TO 340
  330 CALL POLFIT (NDT,TX,TTW,DXDIST,T1)
      IF(NTT.LE.0) GO TO 331
      TP(1)=T1/TCONV
      H(1)=C(1)*TP(1)
      GO TO 340
  331 QW=T1
      GO TO 320
C CALCULATION OF DP(J)                                               4950
  340 IF(RCON.GT.0.0) GO TO 350                                      4960
      DO 341 J=1,NP1
  341 DP(J)=1.0
      GO TO 360
  350 DO 352 J=1,NP1
      TJ=T(J)*TCONV
      DP(J)=RHO(TJ)/DCONV
  352 CONTINUE                                                       5000
C CALCULATION OF VF(J)                                               5040
  360 IF(ICOUNT.GE.NS) GO TO 400
      DO 401 J=1,N
```

```
      DM(J)=D(J)
      UM(J)=U(J)
  401 CONTINUE
  400 DPJP=DP(1)                                                    5050
      DJP=D(1)                                                      5060
      DMJP=DM(1)                                                    5070
      RJP=R(1)                                                      5080
      UPJP=UP(1)                                                    5100
      UMJP=UM(1)                                                    5120
      VP(1)=VW
      KD=KC-1                                                       5140
  405 DO 410 J=1,NM2                                                5150
      DPJ=DPJP                                                      5160
      DPJP=DP(J+1)                                                  5170
      DMJ=DMJP                                                      5200
      DMJP=DM(J+1)                                                  5210
      RJ=RJP                                                        5220
      RJP=R(J+1)                                                    5230
      UPJ=UPJP                                                      5260
      UPJP=UP(J+1)                                                  5270
      UMJ=UMJP                                                      5300
      UMJP=UM(J+1)                                                  5310
      VV1=((RJP+RJ)*DELYP(J))/(DPJP*RJP*DELXT*4.0)
      VV2=VV1*DPJP*UPJP-VV1*DMJP*UMJP+VV1*DPJ*UPJ-VV1*DMJ*UMJ
      VP(J+1)=DPJ*VP(J)*RJ/(DPJP*RJP)-VV2
  410 CONTINUE                                                      5350
      VP(N)=0.0                                                     5360
C INCREMENTING                                                      5370
  451 IF(DENS.GT.0.0) GO TO 460                                     5380
      DO 452 J=1,N                                                  5390
       TM(J) = HJ(J)
      T(J)=TP(J)                                                    5410
       HJ(J)=H(J)
      DM(J)=D(J)                                                    5420
      D(J)=DP(J)                                                    5430
  452 CONTINUE                                                      5440
      T(NP1)=TP(NP1)
       HJ(NP1)=H(NP1)
  460 DO 462 J=1,N                                                  5450
      UM(J)=U(J)                                                    5460
      U(J)=UP(J)                                                    5470
      V(J)=VP(J)                                                    5480
  462 CONTINUE                                                      5490
      U(N+1)=UP(N+1)
      PM=P                                                          5500
      P=PP                                                          5510
C CALCULATING NEW PROPERTIES                                        5520
  430 TW=XV(1)*U(2)*FCONV/DELYM(2)
      TWP=XV(1)*(PSB*U(2)+PSC*U(3)+PSD*U(4))*XCONV*PCONV
      IF(TW.LE.0.0)GO TO 600                                        5550
  464 CONTINUE                                                      5560
      UST=TW*GCON/(D(1)*DCONV)
      UST=SQRT(UST)                                                 5580
      DO 463 J=1,N
      UPLUS(J)=U(J)*UCONV/UST                                       5600
      YPLUS(J)=(Y(J)*D(1)/(XV(1)*UCONV))*UST
  463 CONTINUE                                                      5620
  470 IF(DENS.GT.0.0) GO TO 441
      DTDYW=(T(2)-T(1))*TCONV/(DELYM(2)*XCONV)
      DTDYP=(PSA*T(1)+PSB*T(2)+PSC*T(3)+PSD*T(4))*TCONV
```

```
      DHDYW=(H(2)-H(1))*HCONV/(DELYM(2)*XCONV)
      DHDYP=(PSA*H(1)+PSB*H(2)+PSC*H(3)+PSD*H(4))*HCONV
       G2W=-XK(1)*DHDYP*XKCONV/(C(1)*CPCONV)
       GFS=GFS+(G2W+G1W)*3.14159*RAD*DELXP*XCONV
       G1W=G2W
      DTTA=T(1)*TCONV-TC
      IF(DTTA.EQ.0.0) DTTA=(1.0E-50)
      HHA=-XK(1)*DTDYW*XKCONV/DTTA
      HDX=HHA*DELXP*XCONV
      HIDX=HICX+HDX
      HAVE=HIDX/(XDIST*XCONV)
      IF(CFCON.GT.0.0) GO TO 472                                        5740
      DO 471 J=1,NP1
      TJ=T(J)*TCONV
      CP(J)=XCP(TJ)
      C(J)=CF(J)/CP0
  471 CONTINUE
  472 DO 479 J=1,NM1
      NT(J)=NC
      KT(J)=KC
      TJ=T(J)*TCONV
      IF (VISC.LE.0.0) NT(J)=NI(TJ)
      IF (VISC.LE.0.0) KT(J)=KI(TJ)
      IF (J.EQ.1) GO TO  476
      URATIO(J)=U(J)/U(N)
      IF(URATIO(J).LT.CRIT) GO TO 473
      FDUDY(J)=FDUDY(J-1)
      GO TO 478
  473 DIFU(J)=ABS(U(J+1)-U(J-1))
      FDUDY(J)=DIFU(J)/DELYT(J)
      IF(DIFU(J).LE.1.0E-06) FDUDY(J)=FDUDY(J-1)
  476 IF(J.EQ.1) FDUDY(J)=(PSB*U(2)+PSC*U(3)+PSD*U(4))*XCONV
  478 XV(J)=(KT(J)*GCON/XVCONV)*((FDUDY(J)*UCONV/XCONV)**(NT(J)-1.))
  479 CONTINUE
      FDUDY(N)=FDUDY(NM1)
      FDUDY(NP1)=FDUDY(NM1)
      XV(N)=XV(NM1)
      XV(NP1)=XV(NM1)
  474 IF(HTK.GT.0.0) GO TO 441
      DO 475 J=1,NP1
      TJ=T(J)*TCONV
      XK(J)=CONF(TJ)/XKCONV
  475 CONTINUE
      GO TO 441
  441  DO 443  J=2,NM1
  443 EV(J)=(XV(J-1)+XV(J)+XV(J+1))/3.
      EV(1)=XV(1)
       EV(NP1)=EV(NM1)
      EV(N)=EV(N-1)
      IF (DENS.GT.0.0) GO TO 442
      DO 444 J=1,NP1
  444 EK(J)=XK(J)
  442 CONTINUE
CFINDING OUTPUT STATIONS                                                6080
  500 IF(ICOUNT.GE.IEND) GO TO 600                                      6090
      IF(IOUT.LE.0) GO TO 502                                           6100
      IF((ICOUNT-IOUT).GE.IPRINT) GO TO 505                             6110
  502 IF(CXOUT)503,510,505                                              6120
  503 IF((XDIST*XCONV).GE.OUT(K)) GO TO 504                             6130
      GO TO 200                                                         6140
```

```
  504 IF(NSTA.LE.K) GO TO 600                                          6150
      K=K+1                                                            6160
      GO TO 605                                                        6170
  505 IF(XDIST.GE.TSTOP) GO TO 600                                     6180
      IF(XDIST.GE.(XDOUT+TXOUT)) GO TO 506                             6190
      GO TO 200                                                        6200
  506 IF(CINC.LE.0.0) GO TO 605                                        6210
      TXOUT=CINC*TXOUT                                                 6220
      GO TO 605                                                        6230
  510 IF(CREX) 615,511,615                                             6240
  511 IF(CRET) 615,200,615                                             6250
COUTPUT                                                              6260
  600 PRST=1.0                                                         6270
      GO TO 610                                                        6280
  605 PRST=-1.0                                                        6290
  610 IPRINT=ICOUNT                                                    6300
      XDOUT=XDIST                                                      6310
  615 DN=D(N)                                                          6320
      UN=U(N)                                                          6330
      SUM1=0.0                                                         6340
      SUM2=0.0                                                         6350
      SUM3=0.0                                                         6360
      SUM4=0.0                                                         6370
      SUM5=0.0                                                         6380
      SUM6=0.0
      DO 620 J=1,NM2,2                                                 6390
      YA1=DELYP(J)                                                     6400
      YB1=DELYP(J+1)                                                   6410
      YAB=YA1+YB1                                                      6420
      W2=YAB/YB1*(YAB/3.0-YA1/2.0)                                     6430
      W1=YAB**2.0/(2.0*YA1)-W2*YAB/YA1                                 6440
      W0=YAB-W1-W2                                                     6450
      UOUN1=U(J)/UN                                                    6460
      UOUN2=U(J+1)/UN                                                  6470
      UOUN3=U(J+2)/UN                                                  6480
      UMR1=UOUN1*R(J)                                                  6490
      UMR2=UOUN2*R(J+1)                                                6500
      UMR3=UOUN3*R(J+2)                                                6510
      DOUN1=UOUN1*D(J)/DN                                              6520
      DOUN2=UOUN2*D(J+1)/DN                                            6530
      DOUN3=UOUN3*D(J+2)/DN                                            6540
      Y1=(1-DOUN1)
      Y2=(1-DOUN2)
      Y3=(1-DOUN3)
      YY1=DOUN1*(1-UOUN1)
      YY2=DOUN2*(1-UOUN2)
      YY3=DOUN3*(1-UOUN3)
      YW1=6.28319*D(J)*U(J)*R(J)*C(J)
      YW2=6.28319*D(J+1)*U(J+1)*R(J+1)*C(J+1)
      YW3=6.28319*D(J+2)*U(J+2)*R(J+2)*C(J+2)
      IF(DENS.GT.0.0) GO TO 619
      UT1=2.0*R(J)*U(J)*T(J)*D(J)*C(J)
      UT2=2.0*R(J+1)*U(J+1)*T(J+1)*D(J+1)*C(J+1)
      UT3=2.0*R(J+2)*U(J+2)*T(J+2)*D(J+2)*C(J+2)
      SUM6=SUM6+W0*UT1+W1*UT2+W2*UT3
  619 CONTINUE
      SUM1=SUM1+W0*Y1+W1*Y2+W2*Y3                                      6640
      SUM2=SUM2+W0*YY1+W1*YY2+W2*YY3                                   6650
      SUM3=SUM3+W0*YW1+W1*YW2+W2*YW3                                   6660
      SUM4= SUM4+W0*UOUN1+W1*UOUN2+W2*UOUN3                            6670
```

```
      SUM5=SUM5+W0*UMR1+W1*UMR2+W2*UMR3                                  6680
  620 CONTINUE                                                           6690
      DST=SUM1                                                           6700
      THETA=SUM2                                                         6710
  621 XMDOT=SUM3                                                         6760
      UMEAN=SUM5*UN*CONV*2.0/(XRAD*XRAD)
C
      TM=SUM6*TCONV*3.14159/XMDOT
  623 REX=DO*UMEAN*XDIST*XCONV/XVO
      RED=2.0*DO*UMEAN*RAD/XVO
      RECA=RED*XVO/MLEO
        RET=RECA
      IF(FRST.GE.0.0) GO TO 627
      IF(OREX) 661,660,663                                               6800
  660 IF(CRET) 665,627,667                                               6810
  661 IF(REX.GE.COUT(K)) GO TO 662                                       6820
      GO TO 200                                                          6830
  662 IF(NSTA.LE.K) GO TO 624                                            6840
      K=K+1                                                              6850
      GO TO 625                                                          6860
  663 IF(REX.GE.CSTOP) GO TO 624                                         6870
      IF(REX.GE.(POREX+OREX)) GO TO 664                                  6880
      GO TO 200                                                          6890
  664 IF(CINC.LE.0.0) GO TO 625                                          6900
      OREX=CINC*OREX                                                     6910
      GO TO 625                                                          6920
  665 IF(RET.GE.COUT(K)) GO TO 666                                       6930
      GO TO 200                                                          6940
  666 IF(NSTA.LE.K) GO TO 624                                            6950
      K=K+1                                                              6960
      GO TO 625                                                          6970
  667 IF(RET.GE.CSTOP) GO TO 624                                         6980
      IF(RET.GE.(PORET+ORET)) GO TO 668                                  6990
      GO TO 200                                                          7000
  668 IF(CINC.LE.).0) GO TO 625                                          7010
      ORET= CINC*CRET                                                    7020
      GO TO 625                                                          7030
  624 PRST=1.0                                                           7040
      GO TO 626                                                          7050
  625 PRST=-1.0                                                          7060
  626 POREX=REX                                                          7070
      PORET=RET                                                          7080
      IPRINT=ICOUNT                                                      7090
  627 OXMDOT=XMDOT*XMCONV                                                7100
      IF(FP.LE.0.0.OR.INFR.NE.0) GO TO 628
      IF((CXMDOT.LE.(0.95*XMDOT1).OR.CXMDOT.GE.(1.05*XMDOT1)))PRST=1.0
  628 CONTINUE
      OXCO=OXDIST/(2.0*RAD)                                              7140
      ODELX=DELXP*XCONV                                                  7150
      OP=P*PCONV                                                         7160
      OPORCP=-PORCP*PCONV                                                7170
      OPORX=DELPP*PCONV/ODELX                                            7180
      ODEL=Y(JDEL)*XCONV                                                 7190
      ODST=DST*XCONV                                                     7200
      OTHETA=THETA*XCONV                                                 7210
  622 F=CPORCP*4.0*GCON*RAD/(OXDIST*DO*UMEAN*UMEAN)
      CF=TW/(0.5*D(N)*U(N)*U(N)*PCONV)
      DMM=RHO(IMM)
      CFM=TWP*GCON/(0.5*DMM*UMEAN*UMEAN)
      US2=TW*GCON/(D(1)*DCONV)
```

```
      IF(TW.GE.0.0) US=SQRT(US2)
      WRITE(6,1901)                                                    7260
      WRITE(6,1001)                                                    7270
      WRITE(6,1051) RAD,RED,CXMDOT                                     7280
      WRITE(6,1052) CXDIST,DXDD,DDELX                                  7290
      WRITE(6,1053) DP,DPDROP,DPWRX                                    7300
      WRITE(6,1054) DDEL,DDST,RECA
      WRITE(6,1055) TW,F,CF                                            7320
      WRITE(6,1056) US,JDEL,ICOUNT                                     7330
 1051 FORMAT('     RADIUS=',G12.5,14X,'RED=',G12.5,8X,'MASS FLOW=',G12.5)  7340
 1052 FORMAT('          X=',G12.5,14X,'X/D=',G12.5,8X,'      DELX=',G12.5)  7350
 1053 FORMAT(' ',8X,'P=',G12.5,13X,'P0-P=',G12.5,8X,'DELP/DELX=',G12.5)  7360
 1054 FORMAT('        DEL=',G12.5,10X,'DELSTAR=',G12.5,12X,' REDA=',
     1G12.5)
 1055 FORMAT('  TAU WALL=',G12.5,16X,'F=',G12.5,15X,'CF=',G12.5)         7380
 1056 FORMAT('      USTAR=',G12.5,13X,'JDEL=',I7,16X,'ICOUNT=',I7)       7390
      ZZZ=CF*SQRT(REX)                                                 7400
      WRITE(6,2000) REX,RET,ZZZ                                        7410
 2000 FORMAT('        REX=',G15.5,11X,'RET=',G12.5,14X,'ZZZ=',G12.5)     7420
      XB=XV0*XDIST*XCONV/(RAD*RAD*D0*UMEAN)
      DPD1=DPDROP/(D0*UMEAN*UMEAN)*32.174                              7740
      DPD2=2.0*DPD1                                                    7750
      WRITE(6,1080)UMEAN,DPD2,XB                                       7760
 1080 FORMAT('      UMEAN=',G12.5,13X,'DPD2=',G12.5,15X,'XB=',G12.5)     7770
      WRITE(6,2001) TWP,VWALL,XMDOT1
 2001 FORMAT('        TWP=',G12.5,15X,'VW=',G12.5,12X,'MDOT1=',G12.5)
      WRITE(6,2002) CFM
 2002 FORMAT('        CFM=',G12.5)
      WRITE(6,1060)                                                    7450
 1060 FORMAT('0**U(J)**')                                              7460
      DO 630 J=1,KC                                                    7470
  630 PCUT(J)=U(J)*UCONV                                               7480
      WRITE(6,1061)(PCUT(J),J=1,KC)                                    7490
 1061 FORMAT(' ',10G13.5)
      WRITE(6,1062)                                                    7510
 1062 FORMAT('0**V(J)**')                                              7520
      DO 631 J=1,N                                                     7530
  631 PCUT(J)=V(J)*UCONV                                               7540
      WRITE(6,1061)(PCUT(J),J=1,N)                                     7550
       WRITE(6,1063)
 1063 FORMAT('0**DU/DY**')
      DO  632 J=1,N
  632 PCUT(J)=FDUDY(J)*UCONV/XCONV
      WRITE(6,1061) (PCUT(J),J=1,N)
  650 IF(DENS.GT.0.0) GO TO 700                                        7780
C
CADDITIONAL OUTPUT FOR HEAT TRANSFER CASES
C
      IF(VISC.LE.0.0) GO TO 3000
C
C CALCULATION OF THE CONSTANT PROPERTY RESULTS
C
      MUEM=MUE0
      XVMM=XV0
      XKMM=HTK0
      CPMM=CP0
      KTM=KC
      NTM=NC
      GO TO 3001
C
```

```
C CALCULATION OF THE VARIABLE PROPERTY RESULTS
C
 3000 XKMM=CONF(TMM)
      T1=T(1)*TCONV
      TFLM=(TMM+T1)/2.
      XKF=CONF(TFLM)
      CPMM=XCP(TMM)
      KTM=KI(TMM)
      KTW=KI(T1)
      KTF=KI(TFLM)
      NTM=NI(TMM)
      NTW=NI(T1)
      NTF=NI(TFLM)
       FCUDY1=FOUDY(1)*UCONV/XCONV
      XVMM=KTM*GCON*(FCUDY1**(NTM-1))
      XVMW=KTW*GCON*(FCUDY1**(NTW-1))
      XVMF=KTF*GCON*(FCUDY1**(NTF-1))
      MUEM=KTM*GCON*(((3*NTM+1)/4/NTM)**NTM)*((4*UMEAN/RAD)**(NTM-1))
      MUEW=KTW*GCON*(((3*NTW+1)/4/NTW)**NTW)*((4*UMEAN/RAD)**(NTW-1))
      MUEF=KTF*GCON*(((3*NTF+1)/4/NTF)**NTF)*((4*UMEAN/RAD)**(NTF-1))
C
C THE CALCULATION OF HEAT TRANSFER PARAMETERS
C
 3001 PRMM=XVMM*CPMM*3600.0/XKMM
       PRAMM=PRMM*MUEM/XVMM
      REXMM=DMM*UMEAN*DXDIST/XVMM
      RETMM=DMM*UMEAN*THETA*XCONV/XVMM
      REDMM=2.0*DMM*UMEAN*RAD/XVMM
       REDAMM=REDMM*XVMM/MUEM
      QWALL=-XK(1)*DTDYP*XKCONV
      RECF=PR**EXRF
      TAW=TMM+RECF*UMEAN*UMEAN/(2.0*CPMM*GCON*XJCON)
      DTTM=T(1)*TCONV-TAW
      IF(DTTM.EQ.0.0) DTTM=(1.0E-50)
      DTTAW=T(1)*TCONV-TAW
      IF(DTTAW.EQ.0.0) DTTAW=(1.0E-50)
      GZB=XMDOT1*CPMM*3600./(XKMM*DXDIST)
      XPLUS= DXDIST/(RAD*REDAMM*PRAMM)
      DXPLUS= DXDIST/(RAD*REDMM*PRMM)
      HHH=-XK(1)*DTDYP*XKCONV/DTTM
      STMTP=HHH/(DMM*UMEAN*CPMM*3600.0)
      XNUD=HHH*RAD*2.0/(XK(N)*XKCONV)
      XNUDMM=HHH*2.0*RAD/XKMM
      XNUXMM=HHH*DXDIST/XKMM
      XNDTAW=XNUDMM*DTTM/DTTAW
      XNUDA=HAVE*RAD*2.0/XKMM
      XVN=XV(N)*XVCONV
      XV1=XV(1)*XVCONV
      CPN=C(N)*CPCONV
      CP1=C(1)*CPCONV
      XKN=XK(N)*XKCONV
      XK1=XK(1)*XKCONV
       QBK=DXMDOT*3600.*(CPMM*TMM-CP0*TSTART)
      FACTM=((3*NTM+1)/(4*NTM))**(1./3.0)
      XNUDM=XNUDMM/FACTM
      WRITE(6,1071) TMM,TAW,DMM
      WRITE(6,1072) XVMM,CPMM,XKMM
      WRITE(6,1073) XVN,CPN,XKN
      WRITE(6,1074) XV1,CP1,XK1
      WRITE(6,1075) PRMM,PRAMM,DTTM
```

```
      WRITE(6,1076) DTTAW,DTDYW,DTDYP
      WRITE(6,1077) DHDYW,DHDYP,QWALL
      WRITE(6,1078) XNUC,XNUDMM,XNUDA
      WRITE(6,1079) JTDEL,HAVE,MUEM
      WRITE(6,1090) REC,REDMM,REDAMM
      WRITE(6,1091) GZB,XPLUS,OXPLUS
      WRITE(6,1092) XNUTAW,XMNUM,FACTM
      WRITE(6,1093) KTM,PTM,MUE0
      WRITE(6,1094)QPS,QEK
 1071 FORMAT('0     TMEAN=',G12.5,14X,'TAW=',G12.5,10X,'RHOMEAN=',G12.5)
 1072 FORMAT('     XVMEAN=',G12.5,11X,'CPMEAN=',G12.5,12X,'KMEAN=',G12.5)
 1073 FORMAT('     XVEDGE=',G12.5,11X,'CPEDGE=',G12.5,12X,'KEDGE=',G12.5)
 1074 FORMAT('     XVWALL=',G12.5,11X,'CPWALL=',G12.5,12X,'KWALL=',G12.5)
 1075 FORMAT('     PRMEAN=',G12.5,13X,'PRAMM=',G12.5,12X,'DTTM=',G12.5)
 1076 FORMAT('      DTTAW=',G12.5,12X,'DTDYW=',G12.5,11X,'DTDYP =',G12.5)
 1077 FORMAT('      DHDYW=',G12.5,12X,'DHDYP=',G12.5,11X,'QWALL =',G12.5)
 1078 FORMAT('     XNUC=',G12.5,12X,'XNUDMM=',G12.5,12X,'XNUDA=',G12.5)
 1079 FORMAT('     JTDEL=',I7    ,17X,'HAVE =',G12.5,11X,'MUEM  =',G12.5)
 1090 FORMAT('      REC=',G12.5,12X,'REDMM=',G12.5,12X,'REDAMM=',G12.5)
 1091 FORMAT('      GZB=',G12.5,12X,'XPLUS=',G12.5,12X,'OXPLUS=',G12.5)
 1092 FORMAT('  NUDMMTAW=',G12.5,13X,'XMNUM=',G12.5,12X,'FACTM=',G12.5)
 1093 FORMAT('      KTM=',G12.5,14X,'PTM=',G12.5,10X,'MUE0=',G12.5)
 1094 FORMAT('      QSLM=',G12.5,14X,'QBK=',G12.5)
      WRITE(6,1067)                                                    7840
 1067 FORMAT('0**T(J)***')                                             7850
      DO 652 J=1,N
  652 POUT(J)=T(J)*TCONV                                               7870
      WRITE(6,1061)(POUT(J),J=1,N)
      WRITE(6,1068)                                                    7890
 1068 FORMAT('0**H(J)***')
      KCO=MAX0(KC,KCT)                                                 7910
      DO 654 J=1,KCO                                                   7920
  654 POUT(J)=H(J)*HCONV                                               7930
      WRITE(6,1061)(POUT(J),J=1,KCO)                                   7940
      DO 656 J=1,N
  656 POUT(J)=EV(J)*XVCONV
      WRITE(6,1069)                                                    7970
 1069 FORMAT('0** EV(J)***')
      WRITE(6,1061)(POUT(J),J=1,N)
      IF (VISC.GE.0.0) GO TO 700
 3003 CPF=XCP(IFLM)
      GZF=XMDOT1*CPF/(XKF*OXDIST)
      DMF=RHO(IFLM)
      REDEF=2.*DMF*UMEAN*RAD/MUEF
      XNUDF=PHH*RAD*2./XKF
      RATIO=KTM/KTW
      VISCR=(KTW/KTM)**0.14
      FACTW=((3*NTW+1)/(4*NTW))**(1./3.)
      FACTF=((3*NTF+1)/(4*NTF))**(1./3.)
      XMNUDF=XNUDF*VISCR/FACTW
      XMNUDE=XNUDMM*VISCR/FACTW
      XMNAM=XNUDMM/FACTW
      PRF=3600.*MUEF*CPF/XKF
      CPW=XCP(T1)
      XKW=CONF(T1)
      PRW=3600.0*MUEW*CPW/XKW
      XPF=OXDIST/(RAD*RECEF*PRF)
       RHOW=RHO(T1)
      D3=(2*RAD)**3
      RHOF=RHO(IFLM)
```

```
      BETAF=BETA(TFLM)
      BETAW=BETA(T1)
      GRF=GCON*BETAF*DTTM*D3*RHOF*RHOF/MUEF/MUEF
      GRW=GCON*BETAW*DTTM*D3*RHOW*RHOW/MUEW/MUEW
      WRITE(6,3009) GZF,REDEF,XNUDF,VISCR,FACTW,FACTF,XMNUDF,XMNUDB,
     1PRF,PRW,XPF,GRF,GRW,XMNNN
 3009 FORMAT('0',10X,'VARIABLE PROPERTY RESULT',/,10X,'****************
     1**********',/,
     2'0GZF=',G12.5,14X,'REDF=',G12.5,10X,'NUDF=',G12.5,/,
     4'0VISCR=',G12.5,11X,'FACTW=',G12.5, 9X,'FACTF=',G12.5,/,
     5'0MNUDF=',G12.5,11X,'MNUDB=',G12.5,10X, 'PRF=',G12.5,/,
     6'0PRW=',G12.5, 9X,'X-PLUS -F=',G12.5,/,'0GRF=',G12.5, 7X,'GRW=',
     7G12.5,5X,'CGR. XNUMM=',F10.4,/)
      WRITE(6,2009)KTF,KTW,NTF,NTW,RATIO
 2009 FORMAT(' KTF=',F10.6,11X,'KTW=',F10.5,16X,'NTF=',F10.4,16X,'NTW=',
     1F10.4,//,10X,'K-BULK/K-WALL=',F10.4)
      WRITE(6,3011)XVMM,XVMF,XVMW,MUEM,MUEF,MUEW
 3011 FORMAT('0',5X,'XVMM=',G12.5,10X,'XVMF=',G12.5,10X,'XVMW=',G12.5,//
     1          ,4X,'MUMM=',G12.5,10X,'MUMF=',G12.5,10X,'MUMW=',G12.5)
  700 IF(PRST.LE.0.0) GO TO 200                                          8050
      IF(STORE.GT.0.0) GO TO 701
      WRITE(10) ICOUNT,NS,DELXP,DXFT,DXF,BT,BU,C0,U0,XV0,MUE0,K0,N0,CP0,
     1XCONV,UCONV,PCONV,DCONV,XMCONV,XVCONV,TCONV,CPCONV,XKCONV,DDD,
     3CPT0,HTKT0,N,NP1,NM1,NM2,JTDEL,JDEL,KTJDEL,KC,K,PP,P,DELPP,PGRAD,
     4PDRCP,RAD,XRAD,XA,XMDOT,XMDOT1,VW,PSA,PSB,PSC,PSD,U,UP,UM,D,DP,
     5DM,C,TP,TM,T,HJ,H,VP,DELYM,DELYT,EK,EV,R,Y,DELYP,XDIST,HCONV,V
     6PSC,XK,XV,DELY,DMM,HTK0,PR,EXRF,RED,REDA,GBK,QPS,CPWRX,LCOP
      LCOP=LCOP+1
      WRITE(6,991) ICOUNT
      WRITE(6,980) LCOP,DXFT,DXF
  701 IF (KNC.GT.0) GO TO 5                                              8060
  980 FORMAT('0','LOOP=',I8,5X,'DXFT=',F10.4,5X,'DXF=',F10.5)
  991  FORMAT('0','ICOUNT=',I6)
      STOP                                                               8070
      END                                                                8080
C
C
      SUBROUTINE DELX1
C
CCALCULATES DELX FOR STANDARD EXPLICIT EQUATIONS USED AS STARTING
CMETHOD
C
C THIS SUBROUTINE CALCULATES THE X STEPS FOR THE ORDINARY EXPLICIT
C METHOD BASED ON THE STABILITY REQUIRMENTS
C
      COMMON/MVAR/U(72),UM(72),UP(72),V(72),R(72),EV(72),EK(72),D(72),
     1C(72),DELYP(72),DELYT(72),COEFP(72),COEFM(72),SMUP(72),SMUM(72),
     2SKCP(72),SKCM(72),SPMAX(72),SMMAX(72),DELXP,DELXT,DELPT,DELPP,FP,
     3PDRCP,PP,PS0,SUMP0,CHPF,ICOUNT,N,NP1,NM1,JDEL,KJDEL,NS,NPSTA,PSTAR
     4T
      SMUP(1)=EV(1)+EV(2)
      SKP=EK(1)+EK(2)
      CC3=0.0
      DO 5 J=2,NM1
      SMUM(J)=SMUP(J-1)
      SMUP(J)=EV(J)+EV(J+1)
      SKM=SKP
      SKP=EK(J)+EK(J+1)
      SKCM(J)=SKM/C(J)
      SKCP(J)=SKP/C(J)
```

```
      SPMAX(J)=AMAX1(SMUP(J),SKCP(J))
      SMMAX(J)=AMAX1(SMUM(J),SKCM(J))
      CC1=2.0*D(J)*U(J)*R(J)*DELYT(J)
      COEFP(J)=(R(J)+R(J+1))/(CC1*DELYP(J))
      COEFM(J)=(R(J)+R(J-1))/(CC1*DELYP(J-1))
      CC2=(ABS(V(J)))/(U(J)*DELYP(J-1))+COEFP(J)*SPMAX(J)+COEFM(J)*
     1SMMAX(J)
      CC3=AMAX1(CC2,CC3)
    5 CONTINUE
      DELXP=0.5/CC3
      RETURN
      END
C
C
      SUBROUTINE PRES
C
C THIS SUBROUTINE CALCULATES THE AXIAL PRESSURE GRADIENT
C
C
      COMMON/MVAR/U(72),UM(72),UP(72),V(72),R(72),EV(72),EK(72),D(72),
     1C(72),DELYP(72),DELYT(72),COEFP(72),COEFM(72),SMUP(72),SMUM(72),
     2SKCP(72),SKCM(72),SPMAX(72),SMMAX(72),DELXP,DELXT,DELPT,DELPP,FP,
     3PDRCP,FP,PSO,SUMPC,CHPF,ICOUNT,N,NP1,NM1,JDEL,KJDEL,NS,NPSTA,PSTAR
     4T
      DIMENSION SUM1(60),SUM2(60)
      NM2=N-2
      IF(ICOUNT.GE.NS) GO TO 220
CSTANDARD EXPLICIT EQUATIONS
      U(1)=U(2)/(1.0+(1.0-U(2)/U(3))*DELYP(1)/DELYP(2))
      IF(U(1).EQ.0.0) U(1)=(1.0E-50)
      AXX=0.0
      BXX=0.0
      CXX=0.0
      DXX=0.0
      UD1=0.0
      CM1=0.0
      DO 5 J=1,NM2,2
      YA1=DELYP(J)
      YB1=DELYP(J+1)
      YAB=YA1+YB1
      W2=YAB/YB1*(YAB/3.0-YA1/2.0)
      W1=YAB**2.0/(2.0*YA1)-W2*YAB/YA1
      WC=YAB-W1-W2
      AX1=R(J)/U(J)
      AX2=R(J+1)/U(J+1)
      AX3=R(J+2)/U(J+2)
      IF(J.EQ.1) GO TO 6
      UD1=(U(J)-U(J-1))/(DELYP(J-1)*U(J))
      CM1=(R(J-1)+R(J))*(EV(J-1)+EV(J))*(U(J)-U(J-1))/(2.0*DELYP(J-1))
    6 UD2=(U(J+1)-U(J))/(DELYP(J)*U(J+1))
      UD3=(U(J+2)-U(J+1))/(DELYP(J+1)*U(J+2))
      IF(V(J).LT.0.0) UD1=(U(J+1)-U(J))/(DELYP(J)*U(J))
      IF(V(J+1).LT.0.0) UD2=(U(J+2)-U(J+1))/(DELYP(J+1)*U(J+1))
      IF(V(J+2).LT.0.0) UD3=(U(J+3)-U(J+2))/(DELYP(J+2)*U(J+2))
      BX1=DELXP*V(J)*C(J)*R(J)*UD1
      BX2=DELXP*V(J+1)*C(J+1)*R(J+1)*UD2
      BX3=DELXP*V(J+2)*C(J+2)*R(J+2)*UD3
      CP1=(R(J)+R(J+1))*(EV(J)+EV(J+1))*(U(J+1)-U(J))/(2.0*DELYP(J))
      CP2=(R(J+1)+R(J+2))*(EV(J+1)+EV(J+2))*(U(J+2)-U(J+1))/(2.0*
     1DELYP(J+1))
```

```
      CP3=(R(J+2)+R(J+3))*(EV(J+2)+EV(J+3))*(U(J+3)-U(J+2))/(2.0*
     1DELYP(J+2))
      CX1=DELXP*(CP1-CM1)/(DELYT(J)*U(J))
      CX2=DELXP*(CP2-CP1)/(DELYT(J+1)*U(J+1))
      CX3=DELXP*(CP3-CP2)/(DELYT(J+2)*U(J+2))
      DX1=D(J)*R(J)*L(J)
      DX2=D(J+1)*R(J+1)*L(J+1)
      DX3=D(J+2)*R(J+2)*L(J+2)
      AXX=W0*AX1+W1*AX2+W2*AX3+AXX
      BXX=W0*BX1+W1*BX2+W2*BX3+BXX
      CXX=WC*CX1+W1*CX2+W2*CX3+CXX
    5 DXX=WC*DX1+W1*DX2+W2*DX3+DXX
      DELPP=(DXX-SUMPC-BXX+CXX)/AXX
      U(1)=0.0
      GO TO 10
C*****CRUFORT-FRANKEL EQUATIONS
  220 SUMP1=0.0                                                    2910
      SUMP2=0.0                                                    2920
      DELXM=DELXT-DELXP
      DEN=(R(1)+R(2))*(EV(1)+EV(2))+2.0*R(1)*EV(1)
      SUM1(1)=2.0*(R(1)+R(2))*(EV(1)+EV(2))*U(2)*D(1)*R(1)/DEN
      SUM2(1)=8.0*R(1)*R(1)*D(1)*(DELYP(1)**2.0)/(DELXT*DEN)
      RJP=R(2)                                                     2930
      RJ=R(1)                                                      2940
      UJP=U(2)                                                     2950
      UJ=U(1)                                                      2960
      EVJP=EV(2)                                                   2970
      EVJ=EV(1)                                                    2980
      DELYPJ=DELYP(1)                                              2990
      DO 221 J=2,N
      RJM=RJ                                                       3010
      RJ=RJP                                                       3020
      RJP=R(J+1)                                                   3030
      UJM=UJ                                                       3040
      UJ=UJP                                                       3050
      UJP=U(J+1)                                                   3060
      EVJM=EVJ                                                     3070
      EVJ=EVJP                                                     3080
      EVJP=EV(J+1)                                                 3090
      DELYMJ=DELYPJ                                                3100
      DELYPJ=DELYP(J)                                              3110
      DELYTJ=DELYMJ+DELYPJ                                         3120
      VJ=V(J)                                                      3130
      UMJ=UM(J)                                                    3140
      DJ=D(J)                                                      3150
      PA=-4.0*DJ*RJ*DELYPJ*DELYMJ*DELXT*VJ*(UJP-UJM)
      PC=2.*(RJP+RJ)*DELYMJ*(EVJP+EVJ)*(UJP*DELXT-UMJ*DELXP)
      PD=2.*(RJM+RJ)*DELYPJ*(EVJM+EVJ)*(UJM*DELXT-UMJ*DELXP)
      PE=4.0*UMJ*DJ*LJ*RJ*DELYTJ*DELYPJ*DELYMJ
      PF=4.0*DJ*UJ*RJ*DELYTJ*DELYMJ*DELYPJ
      PG=2.*(RJP+RJ)*DELYMJ*(EVJP+EVJ)*DELXM
      PH=2.*(RJM+RJ)*DELYPJ*(EVJM+EVJ)*DELXM
      PPP=4.0*RJ*DELYTJ*DELYMJ*DELYPJ
      SUM1(J)=((PA+PC+PD+PE)*DJ*RJ)/(PF+PG+PH)
      SUM2(J)=(PPP*DJ*RJ)/(PF+PG+PH)
  221 CONTINUE
      DO 50 J=1,NM2,2
      YA1=DELYP(J)
      YB1=DELYP(J+1)
      YAB=YA1+YB1
```

```
      W2=YAB/YB1*(YAB/3.0-YA1/2.0)
      W1=YAB**2.0/(2.0*YA1)-W2*YAB/YA1
      W0=YAB-W1-W2
      SUMP1=W0*SUM1(J)+W1*SUM1(J+1)+W2*SUM1(J+2)+SUMP1
   50 SUMP2=W0*SUM2(J)+W1*SUM2(J+1)+W2*SUM2(J+2)+SUMP2
      DELPT=(SUMP1-SUMP0)/SUMP2                                          3370
      DELPP=DELXP*DELPT/DELXT                                            3380
   10 CONTINUE
      PDROP=PDROP+DELPP                                                  3390
      PP=PS0+PDROP                                                       3400
      RETURN
      END
C
C
      SUBROUTINE UVEL
C
C THIS SUBROUTINE APPLIES THE FINITE DIFFERENCE FORMS OF THE
C MOMENTUM EQUATION TO CALCULATE THE AXIAL VELOCITY COMPONENTS U(I+1,J)
C FOR EACH  J AT I+1
C
C
      COMMON/MVAR/U(72),UM(72),UP(72),V(72),R(72),EV(72),EK(72),D(72),
     1C(72),DELYP(72),DELYT(72),COEFP(72),COEFM(72),SMUP(72),SMUM(72),
     2SKCP(72),SKCM(72),SPMAX(72),SMMAX(72),DELXP,DELXT,DELPT,DELPP,FP,
     3PDROP,FP,PS0,SUMF0,CHPF,ICOUNT,N,NP1,NM1,JDEL,KJDEL,NS,NPSTA,PSTAR
     4T
      IF(ICOUNT.GE.NS) GO TO 40
      IF(NPSTA.LT.0.AND.FSTART.LT.0.0) GO TO 30
CSTANDARD EXPLICIT EQUATIONS
      IF(FP.LE.0.0) GO TO 20
      UP(N)=U(N)+(DELXP/(D(N)*U(N)))*(4.00*EV(N)*(U(NM1)-U(N))/(DELYP(N)
     1*DELYP(N))-DELPP/DELXP)
      GO TO 30
   20 UP(N)=1.0
   30 UDEL=0.9995*UP(N)
      UP(1)=0.0
      UJ=U(1)
      UJP=U(2)
      DO 35 J=2,N
      IF(JDEL.EQ.N) GO TO 33
      IF(UP(J-1).LE.0.99*UP(N)) KJDEL=J
      IF(UP(J-1).GE.UDEL) GO TO 32
      JDEL=J
      IF(J.EQ.N) KJDEL=N
   33 IF(J.EQ.N) GO TO 35
      UJM=UJ
      UJ=UJP
      UJP=U(J+1)
      IF(V(J).LE.0.0) GO TO 31
      UP(J)=UJ-DELXP*V(J)*(UJ-UJM)/(DELYP(J-1)*UJ)-DELPP/(D(J)*UJ)+
     1DELXP*(COEFP(J)*SMUP(J)*(UJP-UJ)-COEFM(J)*SMUM(J)*(UJ-UJM))
      GO TO 35
   31 UP(J)=UJ-DELXP*V(J)*(UJP-UJ)/(DELYP(J)*UJ)-DELPP/(D(J)*UJ)+
     1DELXP*(COEFP(J)*SMUP(J)*(UJP-UJ)-COEFM(J)*SMUM(J)*(UJ-UJM))
      GO TO 35
   32 UP(J)=UP(N)
   35 CONTINUE
      GO TO 250
COUFORT-FRANKEL EQUATIONS
   40 IF(NPSTA.LT.0.AND.FSTART.LT.0.0) GO TO 245
```

```
      IF(FR.LE.0.0) GO TO 244
  240 DN=D(N)
      DELYMN=DELYF(N)
      UN=U(N)
      EVN=EV(N)
      EVNM=EV(N-1)
      UP(N)=((-(1.0*DELYMN*DELYMN*(DELPT))+(1.0*DELXT*(EVNM+EVN)*U(N-1))
     1-(0.5*DELXT*(EVNM+EVN)*UM(N))
     2+(1.0*DELYMN*DELYMN*UM(N)*UN*UN))/((1.0*DELYMN*DELYMN*DN*UN)
     3+(0.5*DELXT*(EVNM+EVN))))
      GO TO 245                                                          3570
  244 UP(N)=1.00                                                         3580
  245 UDEL=0.9999*UP(N)                                                  3590
      UP(1)=0.0                                                          3620
      RJP=R(2)                                                           3630
      RJ=R(1)                                                            3640
      UJP=U(2)                                                           3650
      UJ=U(1)                                                            3660
      EVJP=EV(2)                                                         3670
      EVJ=EV(1)                                                          3680
      DELYPJ=DELYF(1)                                                    3690
      DELXM=DELXT-DELXP
  251 DO 255 J=2,N                                                       3700
      IF(JDEL.EQ.N) GO TO 254
      IF(UP(J-1).LE.0.99*UP(N)) KJDEL=J
      IF(UP(J-1).GE.UDEL) GO TO 253                                      3710
      JDEL=J                                                             3720
      IF(J.EQ.N) KJDEL=N
  254 IF(J.EQ.N) GO TO 255
      RJM=RJ                                                             3740
      RJ=RJP                                                             3750
      RJP=R(J+1)                                                         3760
      UJM=UJ                                                             3770
      UJ=UJP                                                             3780
      UJP=U(J+1)                                                         3790
      EVJM=EVJ                                                           3800
      EVJ=EVJP                                                           3810
      EVJP=EV(J+1)                                                       3820
      DELYMJ=DELYPJ                                                      3830
      DELYPJ=DELYF(J)                                                    3840
      DELYTJ=DELYMJ+DELYPJ                                               3850
      VJ=V(J)                                                            3860
      UMJ=UM(J)                                                          3870
      DJ=D(J)                                                            3880
  252 UA=-4.0*DJ*RJ*DELYPJ*DELYMJ*DELXT*VJ*(UJP-UJM)
      UB=-4.0*RJ*DELYTJ*DELYMJ*DELYPJ*DELPT
      UC=2.*(RJP+RJ)*DELYMJ*(EVJP+EVJ)*(UJP*DELXT-UMJ*DELXP)
      UD=2.*(RJM+RJ)*DELYPJ*(EVJM+EVJ)*(UJM*DELXT-UMJ*DELXP)
      UE=4.0*UMJ*DJ*UJ*RJ*DELYTJ*DELYPJ*DELYMJ
      UF=4.0*DJ*UJ*RJ*DELYTJ*DELYMJ*DELYPJ
      UG=2.*(RJP+RJ)*DELYMJ*(EVJP+EVJ)*DELXM
      UH=2.*(RJM+RJ)*DELYPJ*(EVJM+EVJ)*DELXM
      UP(J)=(UA+UB+UC+UD+UE)/(UF+UG+UH)                                  3970
      GO TO 255                                                          3980
  253 UP(J)=UP(N)                                                        3990
  255 CONTINUE                                                           4000
  250 CONTINUE
      UP(N+1)=UP(N-1)
      RETURN
      END
```

```
C
C
      SUBROUTINE TEMP
C
C THIS SUBROUTINE APPLIES THE FINITE DIFFERENCE FORMS OF THE ENERGY
C EQUATION TO CALCULATE THE TEMPERATURES T(I+1,J) FOR EACH J AT I+1
C
C
      COMMON/MVAR/U(72),UM(72),UP(72),V(72),R(72),EV(72),EK(72),D(72),
     1C(72),DELYP(72),DELYT(72),COEFP(72),COEFM(72),SMUP(72),SMUM(72),
     2SKCP(72),SKCM(72),SPMAX(72),SMMAX(72),DELXP,DELXT,DELPT,DELPP,FP,
     3PDRCP,PP,PSO,SUMPC,CHPF,ICOUNT,N,NP1,NM1,JDEL,KJDEL,NS,NPSTA,PSTAR
     4T
      COMMON/MTEMP/T(72),TP(72),TM(72),H(72),HJ(72),TSTART,TCONV,JTDEL
      JD=MINO(JDEL,20)
      IF(ICOUNT.GE.NS) GO TO 80
CSTANDARD EXPLICIT EQUATIONS
      IF(FP.LE.0.0.AND.PSTART.GE.0.0) GO TO 50
       H(N)= HJ(N)+DELXP*4.*EK(N)*(HJ(NM1)-HJ(N))/(DELYP(N)*DELYP(N)*
     1D(N)*U(N))
      GO TO 60
   50 TP(N)=TSTART/TCONV
       H(N)=TP(N)*C(N)+U(N)*U(N)/2.
 60    TDEL=HJ(N)
      JTD=0.5*JTDEL
      JTD=MAX0(JTD,JD)
      DO 70 J=2,NM1
       TTEST=ABS(HJ(J-1)-TDEL)
      IF(TTEST.LE.0.001*TDEL) GO TO 65
   90 CONTINUE
      JTDEL=J
       TTV=DELXP*V(J)*(HJ(J)-HJ(J-1))/(DELYP(J-1)*U(J))
       RJP=(R(J+1)+R(J))/2.
       RJM=(R(J)+R(J-1))/2.
       EKP=(EK(J+1)+EK(J))/2.
       EKM=0.5*(EK(J)+EK(J-1))
        CJP= 0.5*(C(J+1)+C(J))
       CJM=0.5*(C(J)+C(J-1))
       EVP=0.5*(EV(J+1)+EV(J))
       EVM=(EV(J)+EV(J-1))/2.
       UJP=0.5*(U(J+1)+U(J))
       UJM=0.5*(U(J)+U(J-1))
       TAA=RJP*EKP*(HJ(J+1)-HJ(J))/(CJP*DELYP(J))
       TAB=(EVP-EKP/CJP)*UJP*(U(J+1)-U(J))/DELYP(J)
       TBA=RJM*EKM*(HJ(J)-HJ(J-1))/(CJM*DELYP(J-1))
       TBB=(EVM-EKM/CJM)*UJM*(U(J)-U(J-1))/DELYP(J-1)
       H(J)= HJ(J)-TTV+2.0*DELXP*(TAA+TAB-TBA-TBB)/(R(J)*D(J)*U(J)*
     1(DELYP(J)+DELYP(J-1)))
      GO TO 67
 65    H(J)=H(N)
 67    TP(J)= (H(J)-UP(J)*UP(J)/2.)/C(J)
   70 CONTINUE
       TP(N)=(H(N)-UP(N)*UP(N)/2.)/C(N)
      GO TO 371
CCRANK-FRANKEL EQUATIONS
   80 CONTINUE
      IF(FP.LE.0.0.AND.PSTART.GE.0.0) GO TO 312
       EKFP= (EK(N)+EK(N-1))/2.0
       DPF1=4.0*EKFP*DELXT/(DELYP(N)*DELYP(N)*D(N))
       H(N)=(DPF1*HJ(NM1)+TM(N)*(1.-.5*DPF1))/(1.+.5*DPF1)
```

```
      GO TO 313                                                          4340
  312 TP(N)=TSTART/TCONV                                                 4350
       H(N)= C(N)*TP(N)+UP(N)*UP(N)/2.
  313   TDEL=P(N)
      JTO=0.5*JTDEL
      JTD=MAX0(JTO,JC)
      RJP=R(2)                                                           4370
      RJ=R(1)                                                            4380
       TJP=HJ(2)
       TJ=HJ(1)
      UJP=U(2)                                                           4410
      UJ=U(1)                                                            4420
      EKJP=EK(2)                                                         4430
      EKJ=EK(1)                                                          4440
      DELYPJ=DELYP(1)                                                    4450
  301 DO 305 J=2,N
       TTEST=ABS(HJ(J-1)-TDEL)
      IF(TTEST.LE.0.0001*TDEL) GO TO 302
   91 CONTINUE
      JTDEL=J                                                            4490
      IF(J.EQ.N) GO TO 305
      RJM=RJ                                                             4500
      RJ=RJP                                                             4510
      RJP=R(J+1)                                                         4520
      TJM=TJ                                                             4530
      TJ=TJP                                                             4540
       TJP=HJ(J+1)
      UJM=UJ                                                             4560
      UJ=UJP                                                             4570
      UJP=U(J+1)                                                         4580
      EKJM=EKJ                                                           4590
      EKJ=EKJP                                                           4600
      EKJP=EK(J+1)                                                       4610
      DELYMJ=DELYPJ                                                      4620
      DELYPJ=DELYP(J)                                                    4630
      DELYTJ=DELYPJ+DELYMJ                                               4640
      TMJ=TM(J)                                                          4650
      DJ=D(J)                                                            4660
       CJP=C(J+1)
      CJ=C(J)                                                            4670
       CJM=C(J-1)
      VJ=V(J)                                                            4680
       EVJP=EV(J+1)
      EVJ=EV(J)                                                          4690
       EVJM=EV(J-1)
       TA=2.*TMJ*DJ*UJ*RJ*DELYTJ*DELYPJ*DELYMJ
        TC= 2.*VJ*(TJM-TJP)*DJ*RJ*DELXT*DELYMJ*DELYPJ
       TB= (0.5*(EVJP+EVJ)-(EKJP+EKJ)/(CJP+CJ))*(RJP+RJ)*(UJP+UJ)*
     1(UJP-UJ)*DELXT*DELYMJ
       TD= (0.5*(EVJ+EVJM)-(EKJ+EKJM)/(CJ+CJM))*(RJ+RJM)*(UJ+UJM)*
     1(UJ-UJM)*DELXT*DELYPJ
       TE=((RJP+RJ)*(EKJP+EKJ)/(CJP+CJ))*(TJP-.5*TMJ)*DELYMJ*DELXT*2.
       TF= ((RJ+RJM)*(EKJ+EKJM)/(CJ+CJM))*(.5*TMJ-TJM)*DELYPJ*DELXT*2.
       TG= 2.*DJ*UJ*RJ*DELYTJ*DELYPJ*DELYMJ
       TH = DELYMJ*DELXT*(RJP+RJ)*(EKJP+EKJ)/(CJP+CJ)
       TI=DELYPJ*DELXT*(RJ+RJM)*(EKJ+EKJM)/(CJ+CJM)
       H(J)= (TA+TC+TB-TD+TE-TF)/(TG+TH+TI)
      GO TO 303
  302   H(J)=H(N)
  303   TP(J)= (H(J)-UP(J)*UP(J)/2.)/C(J)
```

```
  305 CONTINUE                                                          4820
      TP(N)=(H(N)-UP(N)*UP(N)/2.)/C(N)
  371 CONTINUE
      TP(NP1)=TP(NM1)
      H(NP1)= H(NM1)
      RETURN
      END
C
C
      SUBROUTINE POLFIT(N,X,Y,AX,AY)                                    6760
C
C
CLOSED TO CURVE FIT BOUNDARY CONDITIONS
C     INTERPOLATOR SUBROUTINE                                           6770
C       AX=X-INTERCEPT OF DESIRED POINT                                 6780
C       AY=Y-INTERCEPT OF DESIRED POINT                                 6790
C        X=X-INTERCEPTS OF THE DATA POINTS                              6800
C        Y=Y-INTERCEPTS OF THE DATA POINTS                              6810
C        N=NUMBER OF DATA POINTS                                        6820
       DIMENSION X(N),Y(N)                                              6830
      IF(AX.LT.X(1))GO TO 10                                            6840
      DO 14 I=2,N                                                       6850
       JJ=I                                                             6860
      IF(AX-X(I))12,13,14                                               6870
  14  CONTINUE                                                          6880
      XONE=X(N-2)                                                       6890
      XTWO=X(N-1)                                                       6900
      XTHREE=X(N)                                                       6910
      M=N                                                               6920
      WRITE(6,15)                                                       6930
  15  FORMAT(/     * ****WARNING****  Y IS EXTRAPOLATED*)               6940
      GO TO 16                                                          6950
  13   AY = Y(JJ)                                                      6960
      RETURN                                                            6970
  12   IF(JJ.EQ.2) I=3                                                 6980
      XONE=X(I-2)                                                       6990
      XTWO=X(I-1)                                                       7000
      XTHREE=X(I)                                                       7010
      M=I                                                               7020
      GO TO 16                                                          7030
  10  XONE=X(1)                                                         7040
      XTWO=X(2)                                                         7050
      XTHREE=X(3)                                                       7060
      M=3                                                               7070
      WRITE(6,15)                                                       7080
  16  AL1=(AX-XTWO)*(AX-XTHREE)/((XONE-XTWO)*(XONE-XTHREE))             7090
      AL2=(AX-XTHREE)*(AX-XONE)/((XTWO-XTHREE)*(XTWO-XONE))             7100
      AL3=(AX-XONE)*(AX-XTWO)/((XTHREE-XONE)*(XTHREE-XTWO))             7110
      AY=AL1*Y(M-2)+AL2*Y(M-1)+AL3*Y(M)                                 7120
      RETURN                                                            7130
      END                                                               7140
C
C
C  FLUID PROPERTY SUBROUTINES
C
C
      FUNCTION RHO(T)
C     DENSITY OF THE CONSTANT PROPERTY NON-NEWTONIAN FLUID
C       UNITS LBM/FT/FT/FT
C
```

```
      DATA X1,X2,X3,X4/62.422,-0.21862,-0.21785,0.01077/
      ETA=(T-50.0)/50.0
      RHO=(X1+X2*ETA+X3*ETA*ETA+X4*(ETA**3.0))*1.0012
      RETURN
      END
      FUNCTION BETA(T)
C     THIS REFERS TO COEFFICIENT OF THERMAL EXPANSION  FOR THE FLUID
C                          UNITS 1/F
      DATA X1,X2,X3,X4 /-0.21862,-0.43570,0.03231,64.422/
      DATA X5,X6/-0.21785,0.01077/
      ETA=(T-50.0)/50.0
      VOL=X1+X2*ETA+X3*(ETA**2.0)
      DVOL=X4+X1*ETA+X5*ETA*ETA+X6*(ETA**3.0)
      BETA=-(VOL/(50.0*DVOL))
       RETURN
      END
      FUNCTION  CONF(T)
C  CONDUCTIVITY OF THE NON-NEWTONIAN FLUID
C          UNITS  BTU/(HR.FT.F)
      CONF=0.355
       RETURN
       END
      FUNCTION XCP(T)
C  THIS FUNCTION REFERS TO SPECIFIC HEAT OF THE NON-NEWTONIAN FLUID
C   UNITS ARE  BTU/LBM/F
      XCP=1.0
       RETURN
       END
      REAL FUNCTION NI(T)
C  THIS FUNCTION REFERS TO FLOW BEHAVIOUR INDEX OF THE NON-NEWTONIAN FLUID
      NI=0.5
       RETURN
       END
      REAL FUNCTION KI(T)
C      KI IS CONSISTENCY INDEX
C  UNITS OF KI ARE LBF.(SEC**N)/SQ.FT
      ETA=T-460.
      KI=0.13684*EXP(-0.(29207*ETA)
      RETURN
       END
```

APPENDIX E: NUMERICAL PREDICTIONS - CONSTANT PROPERTY

The data listed here represent numerical solutions for thermally developing, laminar in-tube flow with constant wall heat flux. Fluid properties are assumed to be independent of temperature.

Table E.1. Flow behavior index, n = 1.0

Gz	$X^+ x10^3$	Nu	$\frac{Nu}{(\Delta)}^{1/3}$
14721.6	0.1067	35.26	35.26
7515.8	0.209	27.68	27.68
6208.7	0.253	25.89	25.89
3611.0	0.435	21.90	21.90
3129.1	0.502	21.08	21.08
2029.5	0.774	18.43	18.43
1546.1	1.02	16.76	16.76
773.4	2.03	13.00	13.00
581.6	2.70	11.73	11.73
387.1	4.06	10.76	10.76
313.1	5.02	9.44	9.44
216.7	7.25	8.36	8.36
151.0	10.40	7.46	7.46
102.3	15.36	6.65	6.65
77.7	20.22	6.12	6.12
51.4	30.56	5.42	5.42
39.0	40.30	5.10	5.10
31.4	50.03	4.90	4.90
22.4	70.11	4.66	4.66
15.6	100.53	4.48	4.48
10.4	150.40	4.39	4.39
7.8	200.30	4.365	4.365
6.3	250.00	4.36	4.36

The numerically calculated pressure gradient for these results at each station is

$$\frac{dp}{dx} = -0.041 \quad lb_f/ft^2/ft$$

Table E.2. Flow behavior index, n = 0.75

Gz	$X^+ x10^3$	Nu	$\frac{Nu}{(\Delta)}^{1/3}$
15584.0	0.100	38.18	37.18
10129.0	0.155	32.28	31.43
7731.1	0.204	29.10	28.33
4789.3	0.329	24.35	23.71
2921.9	0.538	20.38	19.84
2099.5	0.750	18.13	17.66
1810.1	0.869	17.22	16.77
1479.9	1.07	16.04	15.62
1030.8	1.53	14.18	13.81
759.4	2.07	12.79	12.46
515.6	3.05	11.24	10.94
308.2	5.10	9.45	9.20
223.6	7.04	8.54	8.31
193.7	8.13	8.17	7.95
156.5	10.00	7.66	7.45
78.4	20.00	6.29	6.13
52.3	30.00	5.68	5.53
39.2	40.00	5.33	5.19
31.4	50.10	5.10	4.97
22.4	70.00	4.84	4.71
19.6	80.00	4.76	4.63
15.7	100.00	4.65	4.53
10.47	150.00	4.54	4.42
7.85	200.00	4.51	4.40

The numerically calculated pressure gradient for these results at each station is

$$\frac{dp}{dx} = -35.34 \quad lb_f/ft^2/ft$$

Table E.3. Flow behavior index, n = 0.5

Gz	$X^+ x10^3$	Nu	$\frac{Nu}{(\Delta)}^{1/3}$
11868.0	0.133	36.09	33.50
7867.5	0.200	30.76	28.56
3582.8	0.439	22.99	21.34
2139.6	0.736	19.14	17.77
1503.4	1.05	16.92	15.71
995.5	1.58	14.69	13.63
774.3	2.03	13.49	12.52
505.8	3.11	11.69	10.85
314.4	5.00	9.96	9.25
223.4	7.05	8.94	8.30
156.4	10.00	8.01	7.44
104.8	15.02	7.14	6.62
78.3	20.09	6.59	6.12
52.2	30.21	5.96	5.53
39.3	40.00	5.60	5.19
31.44	50.00	5.36	4.98
26.20	60.00	5.20	4.82
17.5	90.00	4.94	4.58
15.7	100.60	4.89	4.54
13.1	120.11	4.83	4.49
11.3	139.00	4.80	4.45
10.5	150.07	4.79	4.44
9.3	169.52	4.77	4.43

The numerically calculated pressure gradient for these results at each station is

$$\frac{dp}{dx} = -11.92 \quad lb_f/ft^2/ft$$

Table E.4. Flow behavior index, n = 0.25

Gz	$X^+ x10^3$	Nu	$\frac{Nu}{(\Delta)}^{1/3}$
3032.4	0.518	24.67	20.47
2169.6	0.724	21.20	17.59
1555.2	1.01	18.23	15.13
1033.4	1.52	15.73	13.05
781.5	2.01	14.64	12.15
390.7	4.02	11.79	9.78
313.5	5.01	11.11	9.22
223.4	7.03	10.03	8.32
156.61	10.03	8.93	7.41
104.4	15.04	8.00	6.64
78.4	20.04	7.33	6.08
52.3	30.03	6.65	5.52
31.4	50.09	5.98	4.96
22.4	70.02	5.71	4.74
15.7	100.00	5.47	4.54
13.1	120.00	5.39	4.47
10.05	150.00	5.35	4.44
9.9	159.00	5.34	4.43

The numerically calculated pressure gradient for these results at each station is

$$\frac{dp}{dx} = -3.06 \quad lb_f/ft^2/ft$$

APPENDIX F: ANALYSIS OF FULLY DEVELOPED NEWTONIAN HEAT TRANSFER

This appendix outlines a numerical scheme to predict Nusselt number for a fully developed Newtonian flow with temperature-dependent viscosity.

Numerous highly viscous Newtonian fluids such as lubricating oils, transformer oils, etc. are commonly used in industry. In these fluids, viscosity exhibits a strong temperature-dependence. This viscosity variation has a strong influence on the heat transfer rates at the wall. Free convection arising due to temperature-dependent density is small for the highly viscous liquids.

In the fully developed case, the local velocity and temperature profile does undergo changes due to temperature-dependent μ; however, these changes are small and can be neglected. The temperature difference $(t_w - t_b)$ is constant and flow can be considered to be "locally fully developed."

Problem Formulation

Statement of the problem

The purpose of this analysis is to investigate Nusselt number for a laminar flow of Newtonian fluid inside a circular tube subjected to a uniform wall heat flux boundary condition. The fluid velocity and temperature profiles are fully developed. All the fluid properties excluding μ are assumed to be independent of temperature. Since the majority of the fluids under consideration exhibit an exponential

viscosity-temperature dependence, the following relation is selected:

$$\mu = a \exp(-bt) \tag{F.1}$$

Governing equations

The equations are formulated subject to the following assumptions:

1) fully developed velocity and temperature profiles,

2) negligible axial conduction and viscous dissipation, and

3) all fluid properties other than μ are constant.

With these assumptions, the momentum and energy equations are reduced to

$$\frac{1}{r}\frac{\partial}{\partial r}\left(r\mu\frac{\partial u}{\partial r}\right) = g_c\frac{dp}{dx} \tag{F.2}$$

$$u\rho c_p\frac{dt_b}{dx} = \frac{k}{r}\frac{\partial}{\partial r}\left(r\frac{\partial t}{\partial r}\right) \tag{F.3}$$

and boundary conditions are

$$-k\left(\frac{\partial t}{\partial r}\right)_w = q_w'' \; ; \quad u_w = 0; \; \left(\frac{\partial t}{\partial r}\right)_c = 0 \quad \text{and} \quad \left(\frac{\partial u}{\partial r}\right)_c = 0$$

Equations (F.2) and (F.3) are rewritten in nondimensionalized form as

$$\frac{1}{R}\frac{\partial}{\partial R}\left(R\hat{\mu}\frac{\partial U}{\partial R}\right) = \frac{dP}{dX} \tag{F.4}$$

and

$$\frac{\hat{k}}{R}\frac{\partial}{\partial R}\left(R\frac{\partial T}{\partial R}\right) = \hat{\rho}U\hat{C}_p\frac{dT_b}{dX} \tag{F.5}$$

where

$$\hat{\mu} = \frac{a \exp(-bt)}{\mu_o}$$

and boundary conditions are

$$-\hat{k}\left(\frac{\partial T}{\partial R}\right)_w = \hat{Q}_w \ , \quad U_w = 0 \ , \quad \left(\frac{\partial T}{\partial R}\right)_c = 0$$

and

$$\left(\frac{\partial U}{\partial R}\right)_c = 0$$

Other nondimensionalized parameters are defined in the list of nomenclature.

These two equations can be integrated by an iterative procedure in which the temperature distribution for constant properties is used as a first approximation. Then using the prescribed μ-t variation, the momentum equation is integrated numerically to yield a second approximation for the velocity distribution. This velocity distribution is employed in a numerical integration of the energy equation to yield a second approximation for the temperature distribution. The procedure is repeated until the velocity and temperature distributions do not change. Then the mean velocity, bulk temperature, etc. are calculated.

Integral equations

Equation (F.4) was integrated twice, and the constants were evaluated using the nondimensional boundary condition, which results in the following integral form:

$$U_j = -\frac{1}{2}\frac{dP}{dX}\left(\int_{R_w}^{R_j} \frac{R}{\hat{\mu}}\, dR\right) \tag{F.6}$$

The integral form of Eq. (F.5) is

$$T_j = T_c + \frac{\hat{\rho}\hat{C}_p}{\hat{k}}\left(\frac{dT_b}{dX}\right)\left\{\int_0^{R_j} \frac{1}{R_j}\left(\int_0^{R_j} U_j R_j\, dR\right)\, dR\right\} \tag{F.7}$$

Since there are two equations and three unknowns, velocity, temperature, and pressure, one more equation is needed to solve this problem. The third equation is obtained from global continuity:

$$\hat{\dot{m}} = \int_A \rho u dA \tag{F.8}$$

which can be written in nondimensional form as

$$\hat{\dot{m}} = 2\pi\hat{\rho}\int_0^{R_w} R_j U_j dR \tag{F.9}$$

Now, U_j is given by Eq. (F.6) so that Eq. (F.9) can be solved explicitly for dP/dX:

$$\frac{dP}{dX} = (\dot{m}/\rho\pi)\Bigg/\left\{\int_0^{R_w} R_j\left(\int_0^{R_j} (R_j/\mu_j)dR\right) dR\right\} \tag{F.10}$$

Method of Solution

Equations (F.6), (F.7), and (F.10) were solved iteratively. A uniform grid spacing along the tube was utilized to accomplish the numerical integration depicted in Fig. F.1. Simpson's rule was used for numerical integration. The flow chart of the numerical procedure is shown in Fig. F.2. Subscripts 1 and 2 are used to denote values of 1st and 2nd iteration steps. An iteration by a shooting method was employed at various steps to correctly predict appropriate temperature at the tube centerline so that $(\partial T/\partial R)_c = 0$ and, near the wall $\hat{k}(dT/dR)_w = \hat{Q}_w$. The bulk temperature was computed as

$$T_b = \frac{\int_0^{R_w} T_j U_j R_j dR}{\int_0^{R_w} U_j R_j dR} \qquad \text{(F.11)}$$

From this, the Nusselt number, (μ/μ_w), wall temperature, etc. were computed.

Computer code for this analysis is given at the end of this appendix.

Results and Discussion

In this analysis, results were obtained for various values of heat fluxes. The predictions are obtained for several viscosity ratios up to $\mu/\mu_w = 8$, and these predictions are tabulated in Table F.1. In Fig. 4.7, predictions of Nu_∞ are plotted against X^+, for $X^+ > 1x10^{-1}$.

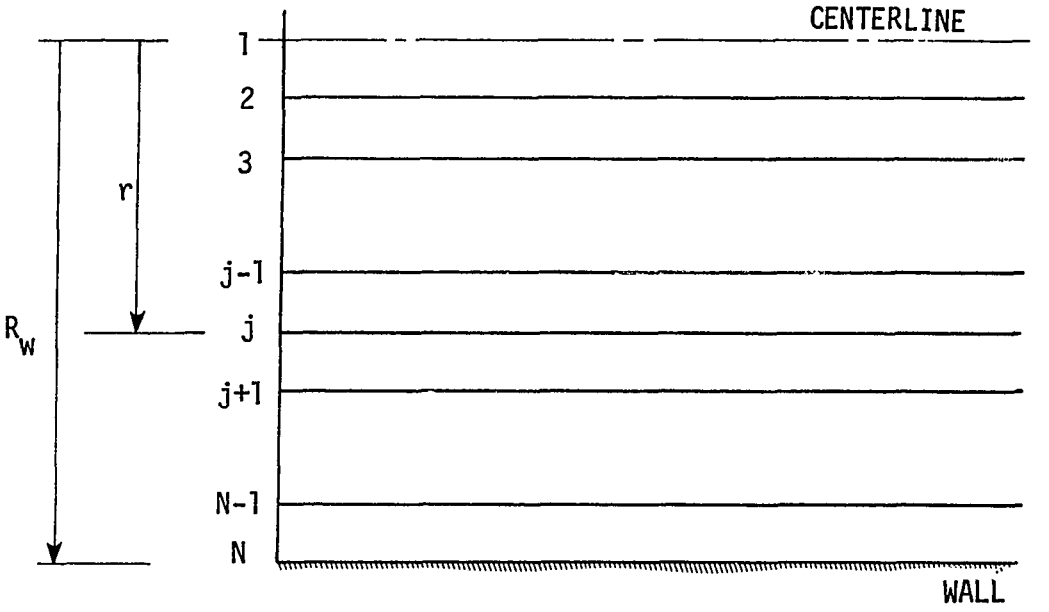

Fig. F.1 The finite-difference grid for fully developed flow inside a circular tube.

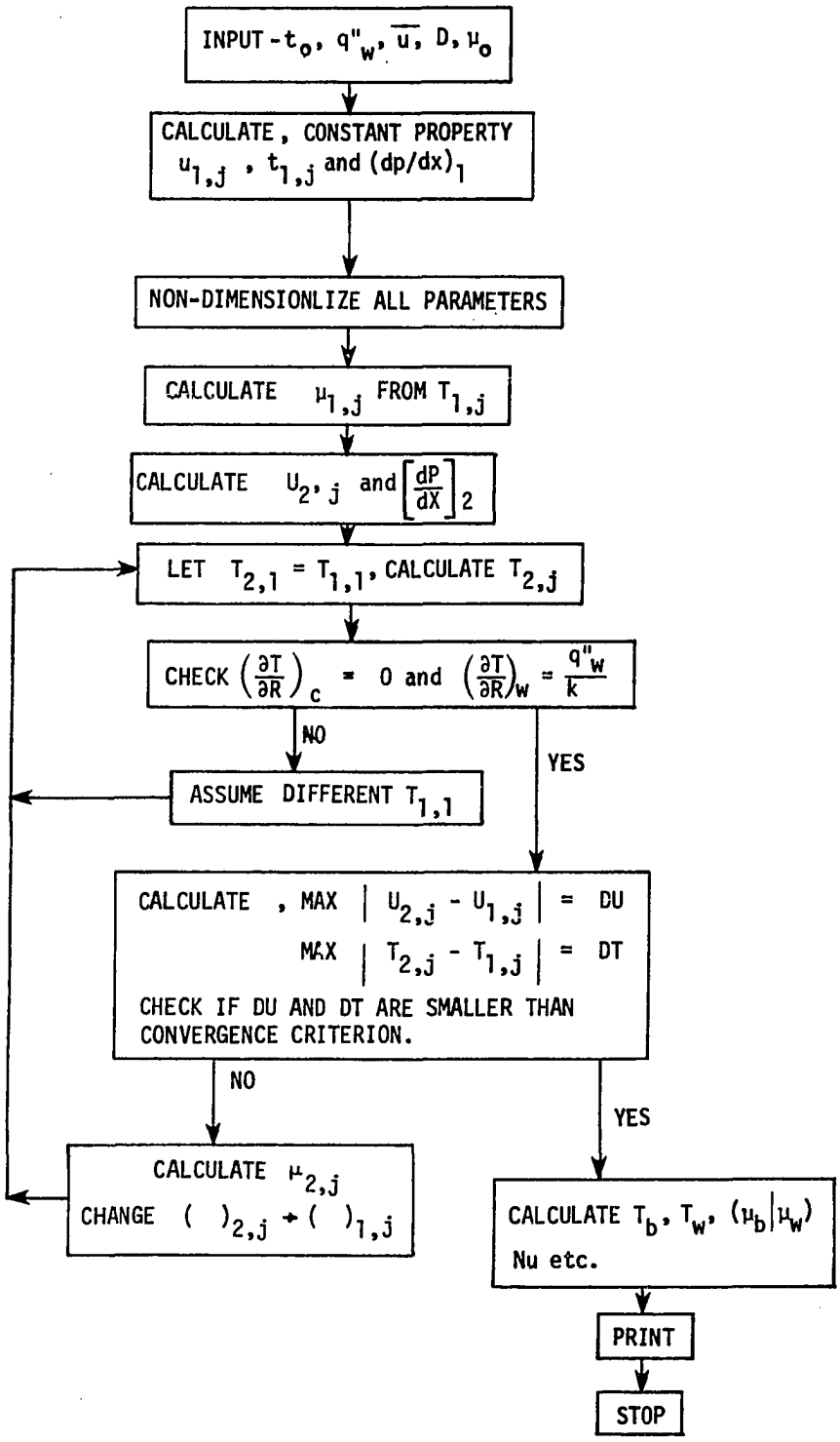

Fig. F2 A flow chart of the computer program.

Table F.1. The Newtonian fully developed predictions

q''_w Btu/hrft^2	$\gamma\Delta T$	μ/μ_w	Nu	$(\frac{Nu}{Nu_{cp}})_\infty$
250.0	1.18	1.65	4.69	1.08
500.0	2.35	2.58	4.97	1.14
750.0	3.53	3.87	5.22	1.20
800.0	3.77	3.98	5.29	1.21
850.0	4.00	4.51	5.31	1.23
1200.0	5.65	7.55	5.59	1.28

In Fig. 4.10, a log-linear relationship is seen between $(Nu/Nu_{cp})_\infty$ and (μ/μ_w). The slope of this log-linear plot is 0.14. Hence,

$$(\frac{Nu}{Nu_{cp}})_\infty = (\mu/\mu_w)^m \qquad (F.12)$$

and $$m = 0.14$$

Yang [32] and Deissler [33] have performed a similar analysis. Yang has obtained m = 0.11 while Deissler has computed m = 0.14. Thus, the present analysis is in excellent agreement with Deissler's prediction, and does not differ significantly from Yang's predictions. Shannon and Depew [34] have shown that for $\mu/\mu_w < 5$, Eq. (F.12) holds, and for $\mu/\mu_w > 5$, $(Nu/Nu_{cp})_\infty$ has an asymptotic value of 1.5. No such asymptotic relation was found in the present analysis.

The predictions of all the analyses described so far are of the

form as given in Eq. (F.12). For a constant wall heat flux boundary condition, t_w is unknown and, hence, an iterative procedure needs to be followed to estimate μ_w and Nu_∞. To avoid this iteration, a new parameter $\gamma\Delta T$ was introduced as

$$\gamma\Delta T = \frac{q''_w D}{2k} \left(-\frac{1}{\mu}\frac{d\mu}{dT}\right) \qquad (4.7)$$

$$= \frac{q''_w D}{2k} (b)$$

For a known fluid and q''_w, $\gamma\Delta T$ is calculated explicitly. A plot of $(Nu/Nu_{cp})_\infty$ against $\gamma\Delta T$ is shown in Fig. 4.13 and this curve is correlated as

$$\left(\frac{Nu}{Nu_{cp}}\right)_\infty = 10 + 0.069\ \gamma\Delta T - 0.0033\ (\gamma\Delta T)^2 \qquad (4.14)$$

With this correlation, $(Nu/Nu_{cp})_\infty$ is computed explicitly. Thus, iterations are avoided and the design procedure is greatly simplified.

Computer code

In this section a computer code utilized for the fully developed Newtonian analysis is given.

```
C  THIS PROGRAM IS DEVELOPED TO SOLVE THE FULLY DEVELOPED NEWTONIAN
C  FLOW INSIDE  A  CIRCULAR TUBE. SUBJECTED TO THE CONSTANT WALL HEAT
C  FLUX BOUNDARY CONDITION. THE NUSSELT NUMBER IS DESIRED  AT THE
C  DISTANCE L FROM THE INLET OF THE HEATED TUBE
C
C  IN THIS PROGRAM VISCOSITY IS THE ONLY TEMPERATURE DEPENDENT FLUID
C  PROPERTY
C
C THIS PROBLEM IS SOLVED BY THE ITERATION OF THE MOMENTUM AND
C ENERGY EQUATION
C
C-----------------------------------------------------------------------
C
C AC            CROSS-SECTIONAL AREA OF THE TUBE  FT*FT
C AS            SURFACE AREA OF THE TUBE          FT*FT
C L             LENGTH  FT
C NY            NUMBER( MUST BE EVEN ) OF Y GRID SPACES IN THE TUBE
C QW            WALL HEAT FLUX    BTU/HR/FT/FT
C XM            MASS FLOW RATE
C
C  FOLLOWING QUANTITIES ARE EVALUATED AT THE INLET OF THE TUBE
C
C CP0           SPECIFIC HEAT  BTU/LBM/F
C D0            DENSITY    LBM/FT/FT/FT
C HTK0          THERMAL CONDUCTIVITY  BTU/HR/FT/F
C T0            TEMPERATURE    F (RANKIN)
C XV0             VISCOSIT    LBM/FT/SEC
C
C-----------------------------------------------------------------------
C
C
C               ********* MAIN PROGRAM *********
C
C
      DIMENSION T(101,2),SUM(101),SUMUP(102),DIFT(101),C(101),
     1SUMH(101),DIFU(101)
      COMMON/VEL/EV(101),U(101,2),R(101),DELY,DPDX,N,XMASS,PI
      COMMON/SHOT/X(20),Y(20),XR,I
       COMMON/ SHOB/ XE(20),YB(20),XRB,ITB
      REAL L
      READ (5,1002) D0,XV0,U0,CP0,T0,RAD
1     READ(5,1003,END=800) QW,L,HTK0,NY
      WRITE(6,1002) D0,XV0,U0,CP0,T0,RAD
      WRITE(6,1003) QW,L,HTK0,NY
 1002 FORMAT(6G12.6)
 1003 FORMAT(2F10.2,F10.6,I5)
      GCON=32.2
       PI=3.1462
      XJCONV=778.26
      CWS=1.1
      CTS=0.05
      CUD=0.2
      AS=2.0*PI*RAD*L
      AC=PI*RAD*RAD
      XM=D0*U0*AC
      TM=(QW*AS/XM/CP0/3600.)+T0
      DTDX=2.0*PI*QW*RAD/XM/CP0/3600.
      WRITE(6,1004) XM,TM,DTDX
1004  FORMAT('0',5X,'XMV=',F10.4,5X,'TBULK=',F10.3,5X,'DTDX=',F10.4)
C
```

```
C      SETTING THE Y-GRID SPACING
C
       N=NY+1
       NM=N-1
       NL=N-2
        NK=N-4
       NB=N-6
       DELY=RAD/NY
       DELY1=DELY*2.
       DO 10 J=1,N
       R(J)=(J-1)*DELY
 10    CONTINUE
C
C CONSTANT PROPERTY PROFILES
C
       XA=GW/CO/1800./CPO/RAD/UO
       XZ=7.0*QW*RAD/HTKO/24.
       XC=DO*CPO*LO*1800./HTKO
       C=TW-XA*L-XZ
       DO 20 J=1,N
       U(J,1)=2.*UO*(1.-(R(J)*R(J)/RAD/RAD))
       C1=XC*R(J)*R(J)
       T(J,1)=C+(XA*(L+C1 -(C1*R(J)*R(J)/RAD/RAD/4.)))
 20    CONTINUE
       U(N,1)=0.0
       WRITE(6,1010)
1010   FORMAT('0',10X,'**VELOCITY DISTRIBUTION**')
       WRITE(6,1100) (U(J,1),J=1,N,2)
       WRITE(6,1020)
 1020  FORMAT('0',10X,'TEMPERATURE-DISTRIBUTION')
       WRITE(6,1100) (T(J,1),J=1,N,2)
 1100  FORMAT(' ',10G13.5)
C
C     CALCULATION OF PRESSURE DROP
C
       DPDX=-8.0*VISC(TM)*UO/GCON/RAD/RAD
       H=GW/(T(N,1)-TM)
       XNUD=2.0*H*RAD/HTKO
       DTDYA=-QW/HTKO
       WRITE(6,1030) DPDX,H,XNUD,DTDYA
 1030  FORMAT('0', 10X,'CONSTANY PROPERTY RESULTS',/,
      1            10X,'DPDX=',G13.5,'LBF/SQ.FT/FT',5X,'H=',F10.3,'BTU/HR.
     1SQ FT.F',5X,'NUD=',F8.3,5X,'DTDYA=',F10.3,'F/FT')
       PSB=3./DELY1
       PSC=-1.5/DELY1
       PSD=1.0/3.0/DELY1
       PSA=-PSB-PSC-PSC
C POLYNOMIAL FIT FOR THE DU/DX
       DUDYP=PSB*U(NL,1)+PSC*U(NK,1)+PSD*U(NB,1)
C LINEAR FIT FOR THE DU/DX
       DUDYL=U(NL,1)/DELY1
       PER=(DUDYP-DUDYL)*100./DUDYP
C
C THE GRID SPACING WAS REFINED UNTIL DU/DX BY POLYNOMIAL FIT AND THE
C LINEAR FIT AGREED TO WITHIN 0.5%
C
       WRITE(6,1040) DUDYP,DUDYL,PER
 1040   FORMAT('0',5X,'DUDYP=',F10.3,'1/SEC',5X,'DUDYL=',F10.3,'1/SEC',
      15X,'PERCENTAGE=',F10.2)
C
```

```
C A SIMILAR POLYNOMIAL AND LINEAR FIT IS OBTAINED FOR THE DT/DY
C
      DTDYP=PSA*T(N,1)+PSB*T(NL,1)+PSC*T(NK,1)+PSD*T(NB,1)
      DTDYL=(T(NL,1)-T(N,1))/DELY1
      PER=(DTDYP-DTDYL)*100./DTDYP
      WRITE(6,1050) DTDYP,DTDYL,PER
 1050 FORMAT('0',*DTDYP=',F10.3,'F/FT',5X,'DTDYL=',F10.3,'F/FT',5X,'
     1PERCENTAGE=',F10.2)
C
C CONVERSION FACTORS  FOR NON-DIMENSIONALIZING
C
      DCONV=D0
      XVCONV=XV0
      UCONV=U0
      XCONV=XV0/D0/U0
      PCONV=D0*U0*U0/GCON
      XMCONV=XV0*XV0/D0/L0
      TCONV=L0*U0/GCON/XJCONV/CP0
      CPCONV=CP0
      XKCONV=3600.*XV0*CP0
      XRAD=RAD/XCONV
      WRITE(6,1060) DCONV,XVCONV,UCONV,XCONV,PCONV,XMCONV,TCONV,CPCONV,
     1 XKCONV,XRAD
 1060 FORMAT('0',5X,'DCONV=',G13.5,5X,'XVCONV=',G13.5,5X,'UCONV=',G13.5,
     15X,'XCONV=',G13.5,
     15X,'PCONV=',G13.5,/,5X,'XMCONV=',G13.5,5X,'TCONV=',G13.5,5X,'CPCON
     1V',G13.5,5X,'XKCONV=',G13.5,5X,'XRAD=',G13.5)
C
C CALCULATION OF THE TEMPERATURE DEPENDENT VISCOSITY
C
      DO 40 J=1,N
      TJ=T(J,1)
      EV(J)=VISC(TJ)/XV0
      T(J,1)=T(J,1)/TCON
       U(J,1)=U(J,1)/UCONV
      R(J)=R(J)/XCONV
  40  CONTINUE
      XMASS=XM/XMCONV
      DELY=DELY/XCONV
      LOOP=0
      PRST=0.0
      ITERT=0
      LI=0
      ITE=0
       PRST=0.0
C
C CALCULATION OF VELOCITY PROFILE
C
      CALL UVEL
C
       DO 50 J=1,N,2
 50   O(J)=U(J,2)*UCONV
      WRITE (6,1010)
      WRITE(6,1100) (O(J),J=1,N,2)
      WRITE(6,1105)
 1105 FORMAT('0',20X,'***COMPUTATIONAL LOOP BEGINS ***')
C
C SIMPSONS RULE OF INTEGRATION FOR THE CALCULATION OF MASS FLOW
C
 140  SUM(1)=0.0
```

```
      DO 150 J=3,N,2
      SUM(J)=SUM(J-2)+(DELY*(U(J-2,2)*R(J-2)+4.*U(J-1,2)*R(J-1)+R(J)*
     1U(J,2))/3.0)
      SUM(J-1)=(SUM(J)+SUM(J-2))/2.0
  150 CONTINUE
      XM1=SUM(101)*XCONV*XCONV*UCONV*DO*2.*PI
      CMC=ABS((XM1-XM)*100.0/XM)
      IF (CMC.GE.5.0) GO TO 699
C
C       TEMPERATURE CALCULATION
C
      CC=XKCONV*DTDX*XCONV/TCONV/HTK0
C ASSUME CENTERLINE TEMPERATURE  T(1,2)
C BASED ON THIS COMPUTE T(J,2)
        T(1,2)=T(1,1)
      SUMUP(1)=0.0
      SUMUP(3)=((DELY/3.0)*((4.*SUM(2)/R(2))+(SUM(3)/R(3))))
      T(3,2)= T(1,2)+SUMUP(3)*CO
      T(2,2)=(T(1,2)+T(3,2))/2.
      DO 200  J=5,N,2
      SUMUP(J)=SUMUP(J-2)+(((SUM(J-2)/R(J-2))+(4.*SUM(J-1)/R(J-1))
     1+(SUM(J)/R(J))) *(DELY/3.))
      T(J,2)=T(1,2)+SUMUP(J)*CO
      T(J-1,2)=(T(J-2,2)+T(J,2))/2.0
  200 CONTINUE
C CHECK THAT THE SLOPE OF THE TEMPERATURE PROFILE IS ZERO AT THE
C CENTERLINE OF THE TUBE
      DTDY2=TCONV*(T(N,2)*PSA+T(NL,2)*PSB+T(NK,2)*PSC+T(NB,2)*PSD)
      TC=(DTDYP-DTDY2)/DTDYP
      TDR=ABS(TD)
      SC=(T(1,2)-T(3,2))*100./T(1,2)
      SC1=ABS(SC)
      DO 250 J=1,N,2
  250 O(J)=T(J,2)*TCONV
      WRITE(6,1020)
      WRITE(6,1100) (O(J), J=1,N,2)
      TC=T(1,2)*TCONV
      IF((SC1.LE.CTS).AND.(TDR.LE.CWS)) PRST=1.0
      IF (PRST.GE.1.0) GO TO 300
  300 ITERT=ITERT+1
      I=ITERT
      Y(I)=TC
      X(I)=TC
      WRITE(6,1110) ITERT,SC,DTDY2,TD,TC,PRST,LOOP,XM1
 1110 FORMAT('0',5X,'ITERATION=',I5,10X,'(DT/DY) CENT=',G13.5,5X,'(DT/DY
     1) WALL=',G13.3,5X,/,5X,' WALL SLOPE DIFF=',G13.3,5X,'NEW TC=',F10.
     13,5X,'PRST=',F10.3,5X,'LOOP=',I5,2X,'XM1=',F10.5)
      IF(PRST.GE.1) GO TO 350
      WRITE(6,1010)
C
C COMPUTE THE TEMPERATURE DIFFERENCE BETWEEN TWO CONSECUTIVE
C TEMPERATURE PROFILES
C
      DO 310 J=1,N,4
      DIFT(J)=(T(J,2)-T(J,1))*TCONV
  310 CONTINUE
      WRITE(6,1120)
 1120 FORMAT('0',9X,'**DIFT(J)**')
      WRITE(6,1100) (DIFT(J),J=1,N,4)
C
```

```
C UPDATE THE VARIABLES
C
      DO 330 J=1,N
      T(J,1)=T(J,2)
      U(J,1)=U(J,2)
 330  CONTINUE
      IF(ITERT.GE.20) GO TO 699
      IF (LOOP.GE.30 ) GO TO 699
      IF(I.GE.2) GO TO 335
      T(1,1)=(T(1,1)*TCONV-10.0)/TCONV
      GO TO 140
 335  XT=TC
C
C USE THE SHOOTING METHOD TO CORRECTLY GUESS THE CENTERLINE TEMPERATURE
C THIS IS DONE ONLY AFTER THE SECND ITERATION
C
      CALL  SHOOT
C
      T(1,1)=XR/TCONV
      XC=ABS((XR-XT)*100./XR)
      IF (XC.LE.0.50)      PRST=1.
       IF (PRST.GE.1.) GO TO 350
      GO TO 140
 350  DO 400 J=1,N,2
      DIFT(J)=(T(J,2)-T(J,1))*TCONV
 400  CONTINUE
      WRITE(6,1150)
C
C VARIFY THAT THE SLOPE OF THE TEMPERATURE PROFILE AT THE TUBE CENTRE
C IS ZERO AND THE DIFFERENCE BETWEEN TWO CONSECUTIVE TEMPERATURE
C PROFILES IS VERY SMALL
C THIS CONFIRMS THAT THE TEMPERATURE PROFILE IS O.K.
C
 1150 FORMAT(' ',5X,'**TEMPERATURE PROFILE O.K.**',/)
      WRITE(6,1120)
      WRITE(6,1100) (DIFT(J),J=1,N,2)
C
C SIMPSONS RULE OF INTEGRATION TO COMPUTE BULK TEMP. TB
C
      SUMH=0.0
      DO 450 K=1,NL,2
      J=(N-K)+1
      SUMH=SUMH+(DELY*(T(J-2,2)*U(J-2,2)*R(J-2)+4.*U(J-1,2)*T(J-1,2)*R(
     1J-1)+U(J,2)*T(J,2)*R(J))/3.0)
 450  CONTINUE
      TB=2.0*SUMH*TCONV/XRAD/XRAD
C
C CALCULATION OF THE HEAT TRANSFER PARAMETERS
C
       TW1=T(N,2)*TCONV
      DELTA=TW1-TE
      H1=QW/DELTA
      XNUD=H1*2.*RAD/HTKO
      WRITE(6,1200) TW1,TB,DELTA,H1,XNUD
 1200 FORMAT('0',5X,'TW1=',F10.2,5X,'TB=',F10.2,5X,'DELTA=',F10.2,5X,
     1'H1=',F10.3,'BTU/HR/FT/F',5X,'NUD=',F10.3)
      PR=3600.*VISC(TB)*CPO/HTKO
      RE=DO*2.0*RAD*UO/VISC(TB)
      GZ=3600.0*XM*CPO/HTKO/L
       VRATI=VISC(TB)/VISC(TW1)
```

```
      PD=DPDX*PCONV/XCONV
      WRITE(6,1230) RE,GZ,PR,VRATI,PD
 1230 FORMAT('0',5X,'RED=',F10.3,5X,'GZ=',F10.3,5X,'PR=',F10.3,
     15X,'VISC  RATIO=',F10.3,5X,'DPDX=',F10.4)
      DO 470 J=1,N
      T(J,1)=T(J,2)
      U(J,1)=U(J,2)
      TJ=T(J,1)*TCONV
      EV(J)=VISC(TJ)/AVO
  470 CONTINUE
C
C CHECKING THE CALCULATED BULK TEMPERATURE WITH COMPUTED BULK TEMPERATU-
C RE FOR A GIVEN WALL HEAT FLUX QW, AND LENGTH L FROM THE INLET
C
      DTC=ABS(TE-TM)
      IF(DTB.LE.0.5) GO TO 1245
      ITE=ITB+1
      IF(ITB.GE.5) GO TO 699
       IF (ITB.GE.2) GO TO 475
      XB(1)=T(1,1)*TCONV
      YB(1)=TE-TM
      WRITE(6,1238) YB(1),XB(1)
 1238  FORMAT('0',2X,'TE-TM=',F10.2,2X,'T CENTRE=',F10.2)
      T(1,1)=(XB(1)+12.)/TCONV
       GO TO 140
  475  YB(ITE)=TE-TM
      XB(ITB)=T(1,1)*TCONV
      XTE=XB(ITB)
      WRITE(6,3000) YB(ITB),XTB,ITB
 3000 FORMAT('0',2X,'TE-TM=',F10.2,2X,'TCENTRE=',F10.2,2X,'ITERATION FOR
     1  THE BULK TEMP=',I5)
C
C USE OF SHOOTING METHOD TO OBTAIN CORRECT  GUESS FOR THE CENTRELINE
C TEMPERATURE SO THAT CORRECT BULK TEMPERATURE IS OBTAINED
C
      CALL SHOTB
      XCE=ABS((XTE-XRB)*100./XRB)
      IF(XCB.LE.0.5.AND.DTB.LE.0.5)  PBST=1
      WRITE(6,4000) XRB,XCB,PBST
 4000  FORMAT('0',2X,'XRB=',F10.2,2X,'XCB=',F10.2,2X,'PBST=',F10.2)
       IF (PEST.GE.1)  GO  TO 1245
      T(1,1)=XRB/TCONV
      ERR=XTE-XRB
      WRITE(6,1239) ITB,ERR
1239  FORMAT('0',5X,'ITERATION=',I5,5X,'TB-TM=',F10.2)
       GO TO 140
C
C WITH NEW TEMPERATURE, COMPUTE NEW VISCOSITY AND, HENCE, NEW VELOCITY
C
1245  VB=VISC(TB)
      DPDX=-6.*VB*UO/GCON/RAD/RAD
      DPDX=DPDX*XCONV/PCONV
C
      CALL VEL
C
      ERS=0.0
C
C CHECK THE DIFFERENCE BEWTEEN TWO CONSECUTIVE VELOCITY PROFILES
C IF THE DIFFERENCE IS SMALL TAKE THE PRINT OUT
C
```

```
      DO 500 J=1,N,2
      DIFU(J)=(U(J,2)-U(J,1))*UCONV
      DIU=DIFU(J)
      IF (DIU.GE.CRS) DIU=CRS
  500 CONTINUE
      IF(CRS.LE.CUD) GO TO 600
      WRITE(6,1250)
 1250 FORMAT(' ',**DIFU(J)**')
      WRITE(6,1100) (DIFU(J), J=1,N,4)
      LOOP=LOOP+1
      IF (LOOP.GE.30 ) GO TO  699
      GO TO 140
  600 WRITE(6,1250)
      WRITE(6,1100) (DIFU(J),J=1,N,2)
      WRITE(6,1010)
  699 DO 700 J=1,N,2
  700 O(J)=U(J,2)*UCONV
      WRITE(6,1100) (O(J),J=1,N,2)
      IF (PRST.GE.1.) LT=LT+1
      IF((PRST.GE.1.).AND.(LT.LT.3)) GO TO 140
      GO TO 1
  800 STOP
      END
C
C
      SUBROUTINE  UVEL
C     CALCULATION OF VELOCITY
C SIMPSONS RULE IS USED FOR THE INTEGRATION
C
      COMMON/VEL/EV(101),U(101,2),R(101),DELY,DPDX,N,XMASS,PI
      DIMENSION SUMU(101),YS(101),SUMP(101)
      WRITE(6,2000)
 2000 FORMAT('0',10X,'INSIDE VELOCITY LOOP',/,10X,'**EV(J)**')
      WRITE(6,2001) (EV(J), J=1,N,2)
 2001 FORMAT(' ',10G13.5)
      SUMU(1)=0.0
       NL=N-2
      DO  50  K=1,NL,2
      J=N-K+1
      SUMU(K+2)=SUMU(K)+(DELY*((R(J-2)/EV(J-2))+(4.*R(J-1)/EV(J-1))+
     1(R(J)/EV(J)))/3.0)
      SUMU(K+1)=(SUMU(K)+SUMU(K+2))/2.0
   50 CONTINUE
      DO 60 K=1,N
   60 YS(K)=SUMU(K)
      DO 70 K=1,N
      J=N-K+1
   70 SUMU(J)=YS(K)
      SUMP(1)=0.0
      DO 80 J=3,N,2
      SUMP(J)=SUMP(J-2)+((DELY/3.)*(SUMU(J-2)*R(J-2)+4.*SUMU(J-1)*R(J-1)
     1+SUMU(J)*R(J)))
      SUMP(J-1)=(SUMP(J)+SUMP(J-2))/2.0
   80 CONTINUE
      DPDX=-XMASS/(SUMP(101)*PI)
      U(1,2)=-SUMU(1)*DPDX/2.
      DO 90 J=3,N,2
      U(J,2)=-SUMU(J)*DPDX/2.0
      U(J-1,2)=(U(J,2)+U(J-2,2))/2.
   90 CONTINUE
```

```
      U(N,2)=0.0
      WRITE(6,2004)
 2004 FORMAT('0', 5X,'OUT OF VELOCITY LOOP')
      RETURN
      END
C
C
      SUBROUTINE  SHOTB
C SHOOTING METHOD FOR THE BULK TEMPERATURE
C
       COMMON/ SHUB/ XE(20),YB(20),XRB,ITB
      IT=ITE-1
      SLE=( YB(IT)-YE(ITE))/(XB(IT)-XB(ITB))
      XRE=XE(ITB)-(YE(ITE)/SLB)
      RETURN
      END
C
C
C SHOOTING METHOD FOR THE CENTRELINE TEMERATURE
      SUBROUTINE SHOOT
C
      COMMON/SHUT/X(20),Y(20),XR,I
      IL=I-1
      SL=(Y(IL)-Y(IL))
      SL=(Y(IL)-Y(I))/(X(IL)-X(I))
      XR=X(IL)-(Y(IL)/SL)
      RETURN
       END
C
C
C   FLUID VISCOSITY -TEMPERATURE DEPENDENCE
C
C
       FUNCTION VISC(T)
C  UNITS LBM/FT/SEC
      DATA X1,X2/0.24524E-02,-0.19722E-01/
      ETA=T-460.
      VISC=32.2*X1*EXP(X2*ETA)
      RETURN
       END
```

APPENDIX G: VARIABLE PROPERTY NUMERICAL PREDICTIONS

In this appendix, variable property numerical predictions are tabulated. The predictions are obtained for

1) Constant wall heat flux boundary condition
2) Hydrodynamically developed and thermally developing flow
3) All fluid properties, other than K and ρ, were assumed to be independent of temperature.

Table G.1. Flow behavior index, n = 1

q''_w = 500 Btu/hr ft^2, $\gamma\Delta T$ = 2.35					q''_w = 800 Btu/hr ft^2, $\gamma\Delta T$ = 3.77				
$X^+ \times 10^3$	Nu	$\frac{Nu}{Nu_{cp}}$	$\frac{K}{K_w}$	f	$X^+ \times 10^3$	Nu	$\frac{Nu}{Nu_{cp}}$	$\frac{K}{K_w}$	f
0.103	36.70	1.020	1.133	1.83	0.107	36.70	1.025	1.221	3.52
0.203	28.67	1.031	1.173	1.82	0.202	29.15	1.045	1.286	3.49
0.512	20.86	1.033	1.246	1.81	0.510	21.33	1.053	1.410	3.44
1.00	16.67	1.039	1.316	1.78	1.03	16.97	1.062	1.540	3.37
2.01	13.32	1.045	1.411	1.74	2.03	13.70	1.078	1.708	3.26
5.00	10.00	1.060	1.581	1.65	5.00	10.39	1.094	2.026	2.99
9.95	8.16	1.092	1.755	1.54	9.90	8.52	1.130	2.367	2.69
19.73	6.78	1.101	1.969	1.39	15.56	7.55	1.146	2.649	2.44
48.20	5.59	1.131	2.281	1.10	150.00	5.29	1.213	3.977	-
84.11	5.19	1.133	2.441	0.88	-	-	-	-	-
150.00	4.97	1.140	2.577	-	-	-	-	-	-

Table G.2. Flow behavior index, n = 0.75

q''_w = 1000 Btu/hr ft^2, $\gamma\Delta T$ = 1.34					q''_w = 2000 Btu/hr ft^2, $\gamma\Delta T$ = 2.62				
$X^+ \times 10^3$	Nu	$\frac{Nu}{Nu_{cp}}$	$\frac{K}{K_w}$	f	$X^+ \times 10^3$	Nu	$\frac{Nu}{Nu_{cp}}$	$\frac{K}{K_w}$	f
0.104	37.85	1.007	1.0754	11.05	0.1050	38.66	1.030	1.153	10.95
0.200	29.65	1.012	1.097	11.03	0.202	30.35	1.038	1.199	10.87
0.506	21.52	1.020	1.137	10.95	0.508	22.15	1.051	1.282	10.71
1.01	17.04	1.042	1.175	10.86	1.02	17.66	1.080	1.366	10.54
2.01	13.61	1.054	1.224	10.73	2.02	14.20	1.102	1.473	10.30
5.01	10.18	1.062	1.310	10.38	5.02	10.69	1.117	1.672	9.65
10.04	8.27	1.080	1.394	9.95	10.08	8.75	1.145	1.871	8.91
20.14	6.46	1.088	1.527	9.34	20.22	7.25	1.155	2.123	7.88
50.61	5.58	1.096	1.629	8.14	51.20	5.94	1.172	2.475	6.08
102.30	5.10	1.099	1.696	6.88	104.40	5.44	1.172	2.636	4.46
150.00	5.00	1.111	-	6.63	150.00	5.33	1.184	-	3.91

Table G.2. (continued)

q''_w = 3000 Btu/hr ft^2, $\gamma\Delta T$ = 3.86					q''_w = 4000 Btu/hr ft^2, $\gamma\Delta T$ = 5.08				
$X^+ \times 10^3$	Nu	$\frac{Nu}{Nu_{cp}}$	$\frac{K}{K_w}$	f	$X^+ \times 10^3$	Nu	$\frac{Nu}{Nu_{cp}}$	$\frac{K}{K_w}$	f
0.105	39.40	1.051	1.233	10.83	0.106	40.09	1.071	1.316	10.72
0.203	31.01	1.064	1.305	10.71	0.204	31.65	1.088	1.416	10.56
0.510	22.78	1.082	1.437	10.49	.511	23.39	1.114	1.601	10.27
1.02	18.27	1.118	1.571	10.25	1.021	18.86	1.155	1.792	9.97
2.02	14.79	1.147	1.747	9.91	2.03	15.35	1.194	2.047	9.55
5.04	11.18	1.172	2.088	9.01	5.05	11.64	1.223	2.565	8.43
10.12	9.19	1.203	2.441	8.02	10.11	9.60	1.257	3.114	7.26
20.34	7.61	1.212	2.915	6.72	20.41	7.95	1.268	3.896	5.79
51.75	6.26	1.230	3.585	4.66	52.30	6.49	1.278	5.076	3.65
104.90	5.72	2.235	3.894	3.08	107.90	5.92	1.279	5.62	2.19
150.00	5.64	1.253	-	2.74	150.60	5.85	1.300	-	2.02

Table G.3. Flow behavior index, n = 0.5

q''_w = 1000 Btu/hr ft^2, $\gamma\Delta T$ = 1.34					q''_w = 2000 Btu/hr ft^2, $\gamma\Delta T$ = 2.62				
$X^+ \times 10^3$	Nu	$\frac{Nu}{Nu_{cp}}$	$\frac{K}{K_w}$	f	$X^+ \times 10^3$	Nu	$\frac{Nu}{Nu_{cp}}$	$\frac{K}{K_w}$	f
0.156	24.57	1.017	1.083	3.69	0.156	35.56	1.029	1.168	3.61
0.303	27.15	1.036	1.107	3.67	0.307	27.98	1.068	1.218	3.58
0.511	22.66	1.039	1.129	3.65	0.518	23.48	1.092	1.264	3.55
1.02	17.98	1.051	1.165	3.62	1.03	18.79	1.105	1.340	3.50
2.02	14.40	1.066	1.211	3.58	2.03	15.28	1.140	1.433	3.45
5.03	10.83	1.087	1.289	3.51	5.05	11.51	1.160	1.612	3.24
10.08	8.81	1.100	1.366	3.35	10.09	9.44	1.180	1.787	3.00
20.15	7.27	1.108	1.458	3.14	20.28	7.82	1.194	2.009	2.65
50.77	5.95	1.112	1.58	2.74	50.90	6.42	1.202	2.312	2.05
102.60	5.48	1.123	1.63	2.31	104.39	5.87	1.209	2.458	1.50
150.00	5.36	1.123	-	2.24	150.00	5.77	1.210	-	1.33

Table G.3. (continued)

q''_w = 3000 Btu/hr ft^2, $\gamma\Delta T$ = 3.87					q''_w = 4000 Btu/hr ft^2, $\gamma\Delta T$ = 5.12				
$X^+ x10^3$	Nu	$\frac{Nu}{Nu_{cp}}$	$\frac{K}{K_w}$	f	$X^+ x10^3$	Nu	$\frac{Nu}{Nu_{cp}}$	$\frac{K}{K_w}$	f
0.156	36.47	1.073	1.254	3.54	0.159	37.35	1.105	1.343	3.47
0.309	28.86	1.106	1.331	3.50	0.311	20.71	1.143	1.449	3.42
1.00	19.80	1.151	1.517	3.39	1.00	20.62	1.199	1.705	3.28
2.01	16.16	1.193	1.666	3.32	2.03	16.92	1.255	1.915	3.20
5.04	12.16	1.222	1.968	3.02	5.06	12.74	1.287	2.364	2.84
10.11	10.02	1.254	2.267	2.71	10.16	10.50	1.313	2.825	2.47
20.39	8.25	1.262	2.682	2.26	20.49	8.64	1.320	3.496	1.96
51.96	6.72	1.266	3.280	1.57	52.42	6.95	1.320	4.560	1.23
106.70	6.15	1.266	3.545	1.03	102.51	6.41	1.320	4.948	0.77
150.00	6.04	1.266	-	0.96	150.00	6.30	1.321	-	-

APPENDIX H: THE PREPARATION OF PSEUDOPLASTIC FLUIDS

In this study, the working fluids were two aqueous solutions; 0.9 percent and 1.0 percent by weight of polymer XD - 7630.02 (hydroxyethylmethylcellulose, HEMC, Dow Chemicals) were prepared in the laboratory. These aqueous solutions were selected because

1. They are definitely pseudoplastic fluids.
2. They are fairly stable.
3. There is no health or fire hazard associated with their use.
4. They are relatively easy to obtain and prepare in large quantities.
5. These fluids, with 0.9 percent and 1.0 percent concentration, are quite viscous (100-200 cps), yet they could still be handled by the gear pump installed in the test loop.

In the following section, a method is described to prepare the 0.9 percent HEMC solution [104].

Method of Preparation

In a large glass tank 80 lbs (about 10 U.S. gallons) of distilled water was precisely measured. In this water at room temperature, 0.72 lbs of polymer powder was gradually added. During addition, the water was mildly agitated with the help of an aluminum rod to disperse the powder uniformly throughout the entire solution and to avoid any globule formation. This surface treated powder readily dispersed in the water and gave a milky white solution.

This solution had a pH value of about 5.0, which was estimated by using pH paper. A one molar solution of NaOH was added (in drops) to this polymer solution to raise its pH value. The polymer solution was agitated while the alkaline solution was added as to bring about a uniform dispersion. As the pH value of the solution started rising, the solution became more and more viscous, and at about 8.5 pH a crystal-clear, highly viscous solution was obtained.

A similar procedure was followed to prepare the 1.0 percent solution. It is important to emphasize here that these two solutions are quite close in their concentration. However, these two solutions have a distinctly different flow curve and they exhibit different ranges of K and n.

APPENDIX I: FLUID FLOW CURVES

The fluid flow curve is a plot of shear stress, τ, against shear rate, du/dy. The constitutive equation of the pseudoplastic fluid is

$$\tau = K(du/dy)^n \tag{1.2}$$

This equation can be rewritten as

$$\log \tau = \log K + n \log (du/dy) \tag{I.1}$$

This is a log-linear equation with consistency index K as the intercept on the τ axis at unit value of du/dy, and n is the slope of this straight line.

For the pseudoplastic fluids, the constitutive equation is also written as [1]

$$\tau = K' (8\bar{u}/D)^n \tag{I.2}$$

$8\bar{u}/D$ is the slope of the velocity profile at the wall for Newtonian fluids. Furthermore

$$K' = K \left(\frac{3n+1}{4n}\right)^n \tag{I.3}$$

The log-linear Eq. (I.2) was used to obtain the fluid flow curve. The actual test section with those pressure taps was effectively utilized to estimate this fluid flow curve. For in-tube hydrodynamically developed flow

$$\tau_w = \frac{D\Delta P}{4L} \tag{I.4}$$

and $(8\bar{u}/D)$ was evaluated from the known fluid flow rate and tube geometry. This simple straight tube viscometer was used by Oliver [68], and Scheve [105] demonstrated the effectiveness of such a viscometer (rheometer) for non-Newtonian fluids.

Experimental Procedure

The experimental setup here is essentially the same as that described in Chapter VI and shown in Fig. 6.1. The test section I (Fig. 6.3) was used as a tube "viscometer." This test section has a hydrodynamic entrance length, AB (3.5 ft) and a measuring length BC (5.98 ft) across which the pressure drop was measured by a mercury manometer.

The fluid was circulated through the test loop with a gear pump. The fluid flow rate through the test section was precisely adjusted by a needle valve placed upstream of the hydrodynamic entrance length, AB. The inlet temperature of the fluid was adjusted by monitoring heat input in the top surge tank and preheater and the cooling in the heat exchanger. The test section was heavily insulated, and hence, within about 15 minutes, all thermocouples on the test section and fluid inlet and outlet thermocouples read within 0.5°F, and, thus, throughout the test section an isothermal condition was established. Normally it took about half an hour to establish steady thermal and hydrodynamic conditions. Once this steady-state was reached,

1) Pressure drop was recorded from the mercury manometer and τ_w was estimated from Eq. (I.4).
2. Fluid flow rate was measured by a weigh tank, and $(8\bar{u}/D)$ was calculated.

These data were obtained for various flow rates at t = 65.0, 100,0, 115.0, and 130.0°F. The data are presented in Figs. I.1 and I.3.

Fluid Degradation

The pseudoplastic fluids are basically polymer solutions. Due to the circulation through the test loop via the gear pump as well as various heating and cooling processes in the test loop, the fluid polymer chains tend to break down with time. This fluid degradation with time, which is also known as aging, caused a noticeable change in values of K and n with time. In general, K decreased while n increased with time. As mentioned in Chapter VI, to account for this aging, the following procedure was developed.

For solution I (0.9 percent HEMC), 19 heat transfer runs were made. The K and n values for each temperature were estimated at

Time I: before the start of heat transfer experiments

Time II: after 10 heat transfer runs (about 48 hours)

Time III: after 19 heat transfer runs (about 75 hours).

As shown in Fig. I.1, a significant effect of degradation was observed. To all these data linear regression correlations (95 percent confidence) were fit as

$$\tau_w = K' \, (8\bar{u}/D)^n \qquad (I.2)$$

These correlations are tabulated in Table I.1. The correlation coefficients of these correlations are of the order of 0.99, exhibiting an excellent pseudoplastic (log-linear) relationship.

The arithmetic averages of correlations for Times I and II were used to reduce data for Runs 1 to 10 and similar averages of correlations for

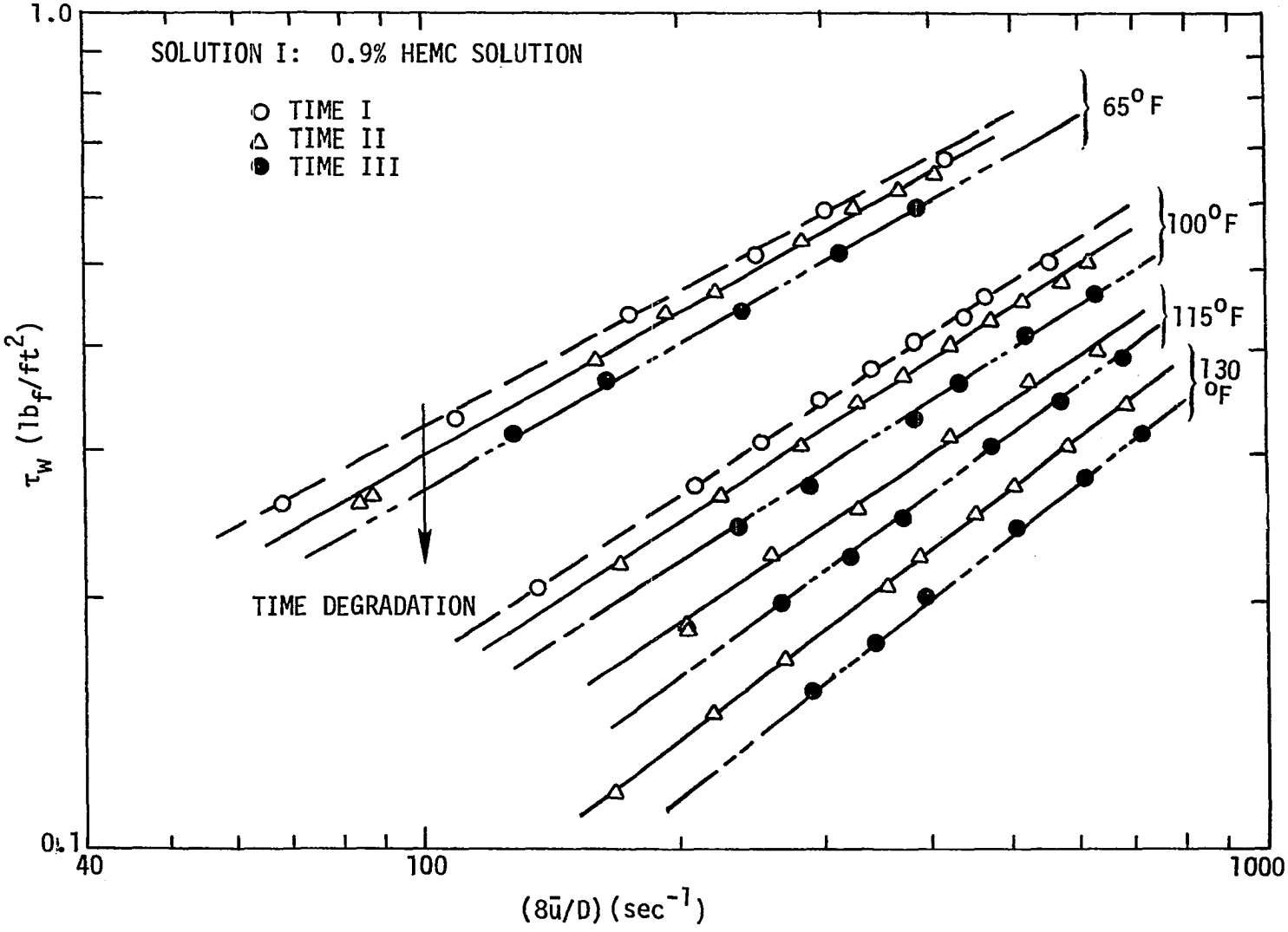

Fig. I.1 Flow curve for 0.9% HEMC solution.

Table I.1. Correlations for Solution I (0.9 percent HEMC)

Situation	65°F		100°F		115°F		130°F	
	$K' \times 10^2$	n	$K' \times 10^2$	n	$K' \times 10^2$	n	$K' \times 10^2$	n
Time I (before the start of heat transfer runs)	2.7086	0.54	0.8602	0.65	--	--	--	--
Time II (after 10 heat transfer runs)	1.9350	0.59	0.8009	0.65	0.40369	0.70	0.2440	0.76
Time III (after 19 heat transfer runs)	1.8610	0.58	0.5582	0.69	0.344	0.73	0.1644	0.80

Correlation: $\tau_w = K' (8\bar{u}/D)^n$; the correlation coefficients were of the order of 0.99 in all of the above correlations.

Times II and III were taken to reduce data for runs 10 to 19. These arithmetic averages are plotted in Fig. I.2. and tabulated in Table I.2.

A similar procedure was followed for Solution II (1.0 percent HEMC solution). For this solution 9 heat transfer runs were made and, hence, K and n data were obtained at

Time I: before start of heat transfer runs

Time II: after 9 heat transfer runs (about 48 hours).

Data for Times I and II are plotted in Fig. I.3 and correlations from these data are tabulated in Table I.3. The average results for Times I and II are plotted in Fig. I.4 and are tabulated in Table I.4.

The details of these data and calculations are documented in ISU Heat Transfer Laboratory files.

Philosophy of time averaging

As noted in the preceding discussion, the K and n results at various times were correlated, and averages of the correlations were taken to account for the degradation with time. These K and n plots were used to calculate various viscosities such as apparent viscosity μ_a and effective viscosity, μ_{eff}.

$$\mu_{eff} = \tau_w/(8\bar{u}/D) \tag{3.28}$$

$$= K' (8\bar{u}/D)^n/(8\bar{u}/D)$$

$$= K' (8\bar{u}/D)^{n-1} \tag{I.11}$$

and

$$\mu_a = K \left(\frac{du}{dy}\right)^{n-1} \tag{1.3}$$

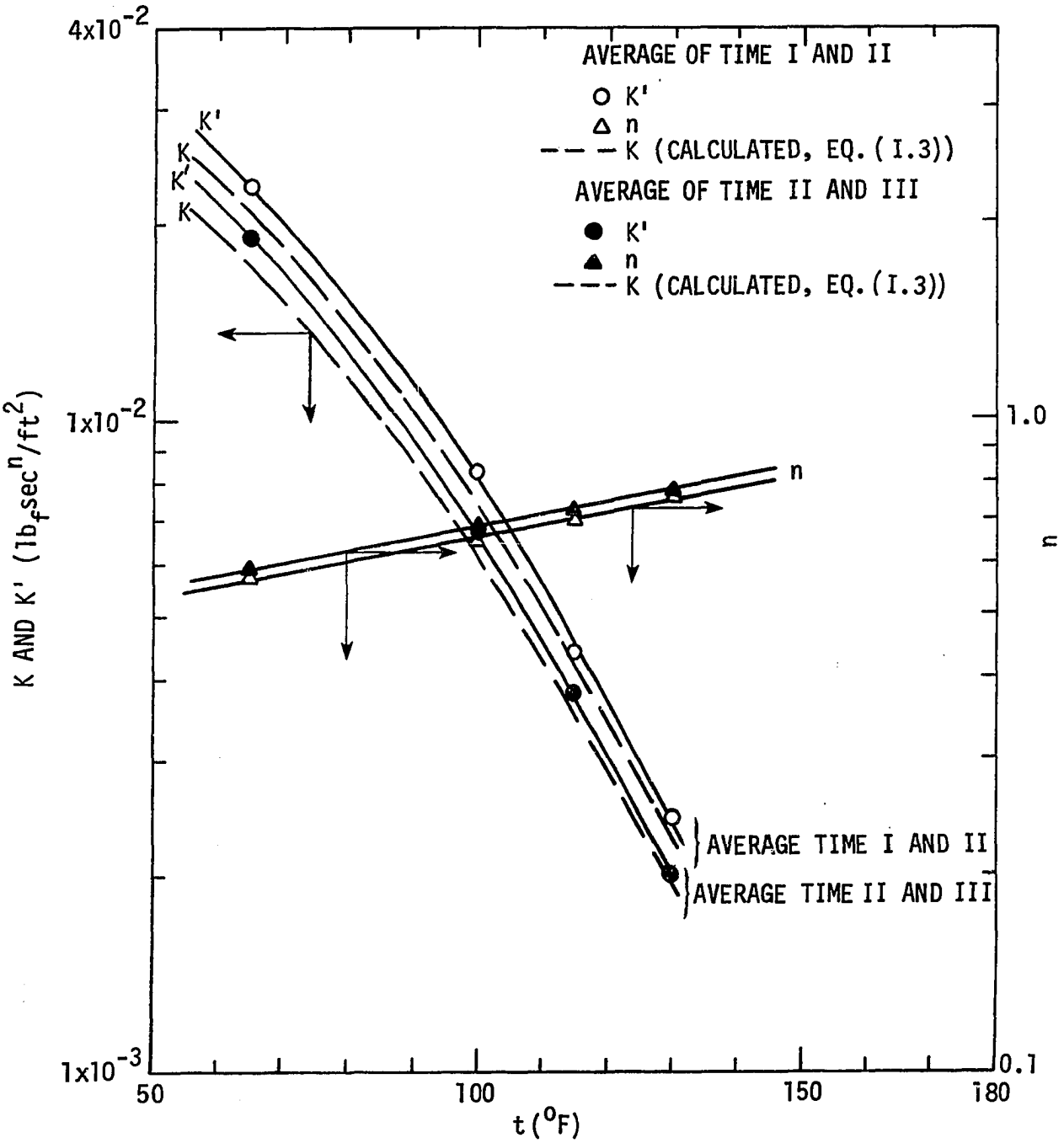

Fig. I.2 Average values for Solution I (0.9% HEMC).

Table I.2. Averages of K' and n for Solution I (0.9 percent HEMC)

	$t_{°F}$	K' (lb_f sec^n/ft^2)	n	Correlations
Average of Time I and II (Runs 1 to 10)	65.0	2.2894	0.57	$K' = 0.057151$
	100.0	0.8300	0.65	$\exp(-3.63573 \times 10^{-3}t$
	115.0	0.4369	0.70	$-1.596 \times 10^{-4}t^2)$ (I.5)
	130.0	0.244	0.76	Max. error: 3.0 percent
				$n = 0.425913 \exp(0.004366t)$
				Max. error: 1.5 percent (I.6)
Average of Time II and III (Runs 11 to 19)	65.0	1.9877	0.59	$K' = 0.047635$
	100.0	0.6686	0.67	$\exp(-3.915 \times 10^{-2}t$
	115.0	0.3877	0.72	$-1.575 \times 10^{-4}t^2)$ (I.7)
	130.0	0.2003	0.78	Max. error: 1.5 percent
				$n = 0.444659 \exp(0.004236t)$
				Max. error: 1.3 percent

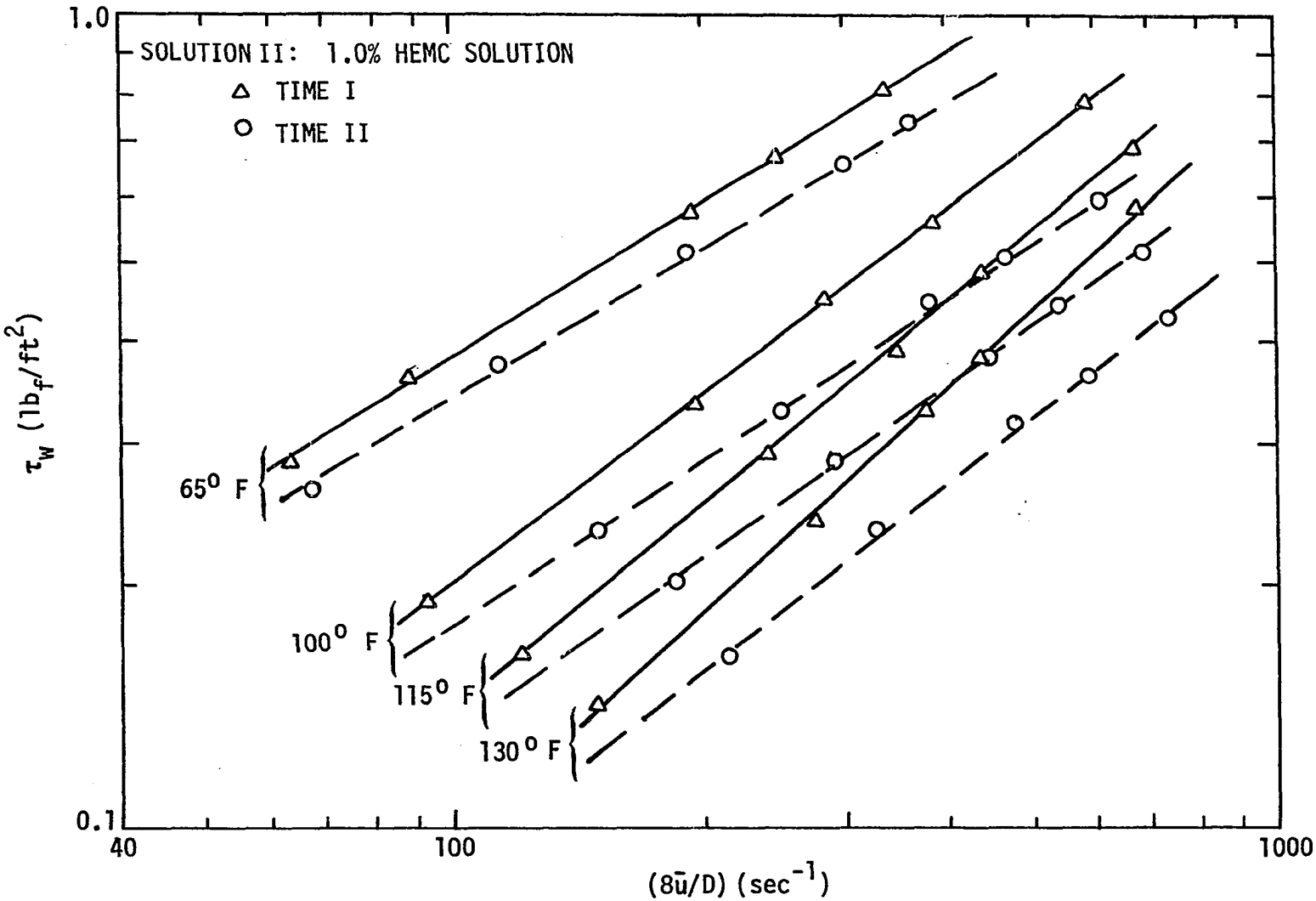

Fig. I.3 Flow curve for 1.0% HEMC solution.

Table I.3. Correlations for Solution II (1.0 percent HEMC)

Situation	65°F		100°F		115°F		130°F	
	$K' \times 10^2$	n	$K' \times 10^2$	n	$K' \times 10^2$	n	$K' \times 10^2$	n
Time I (before the start of heat transfer runs)	2.1470	0.62	0.5973	0.76	0.3204	0.82	0.1327	0.93
Time II (after 9 heat transfer runs)	1.9960	0.61	0.7583	0.68	0.4861	0.71	0.2670	0.77

Correlation: $\tau_w = K' (8\bar{u}/D)^n$; the correlation coefficients in all of the above correlations were of the order of 0.99.

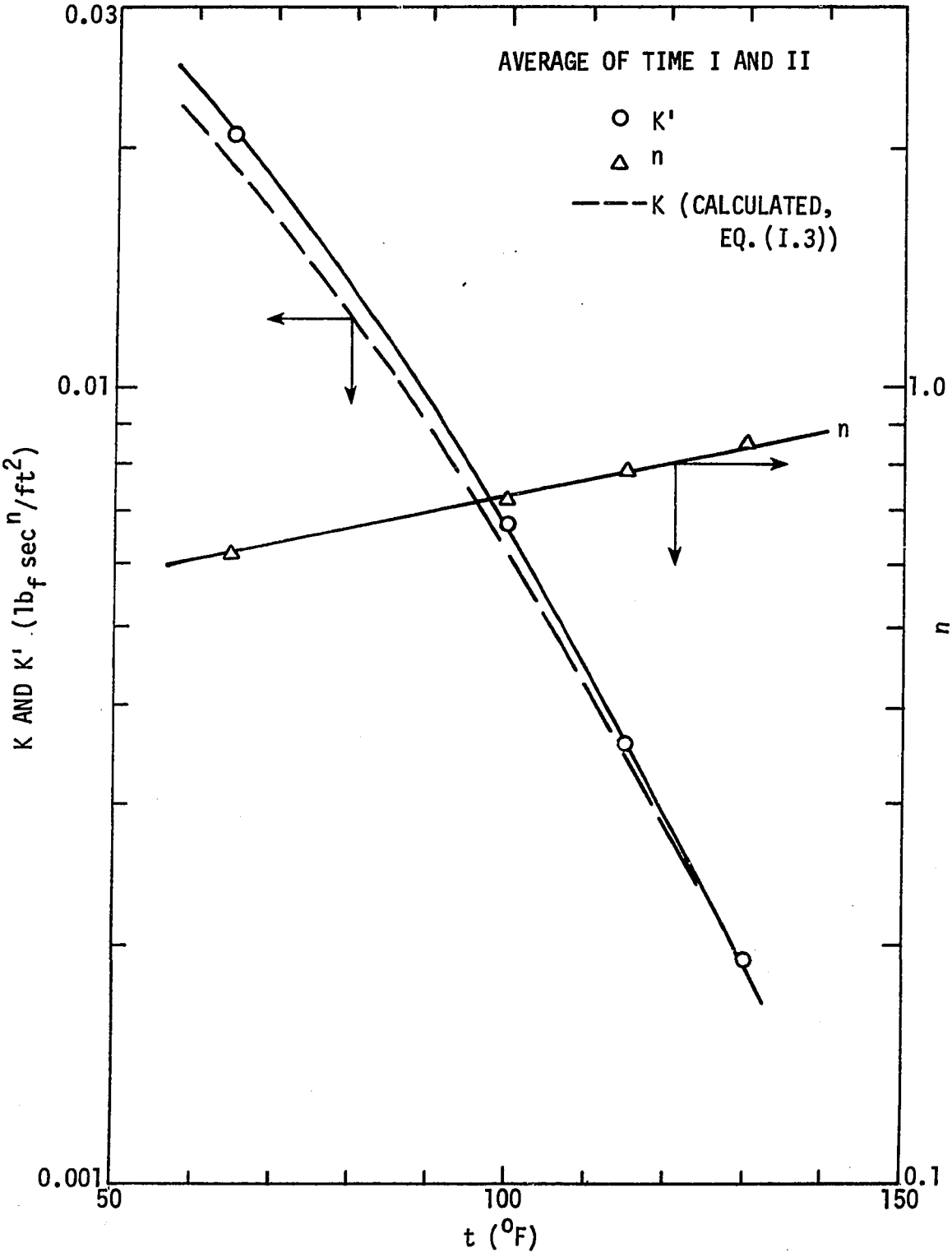

Fig. I.4 Average values for Solution II (1.0% HEMC).

Talbe I.4. Averages of K' and n for Solution II (1.0 percent HEMC)

	t °F	K' lb_f sec^n/ft^2	n	Correlations
Average of time I and II	65.0	2.0701	0.62	$K' = 0.070103$
	100.0	0.6729	0.72	$\exp(-0.966 \times 10^{-2} t$
	115.0	0.3559	0.78	$-1.3951 \times 10^{-4} t^2)$ (I.9)
	130.0	0.1908	0.85	Max. error: 2.0 percent
				$n = 0.450709$
				$\exp(0.004805t)$
				Max. error: 1.2 percent (I.10)

For the given fluid, μ_{eff} is dependent on temperature, $(8\bar{u}/D)$, and time (or, more strictly speaking, time and flow conditions). In order to evaluate the relative effect of time and temperature variation on μ_{eff}, for a given τ_w and temperature, the change in μ_{eff} with time was evaluated. This is plotted in Fig. I.5, for solution II at τ_w = 0.4 and 0.25 lb_f sec^n/ft^2. Similarly, at these shear stress values, at a given time level, the change in μ_{eff} due to temperature was evaluated. This is also plotted in Fig. I.5. This figure distinctly demonstrates the dominance of the temperature effect over the time effect. The change in μ_{eff} due to time effects was linear and, hence, the time averages were taken to account for these effects.

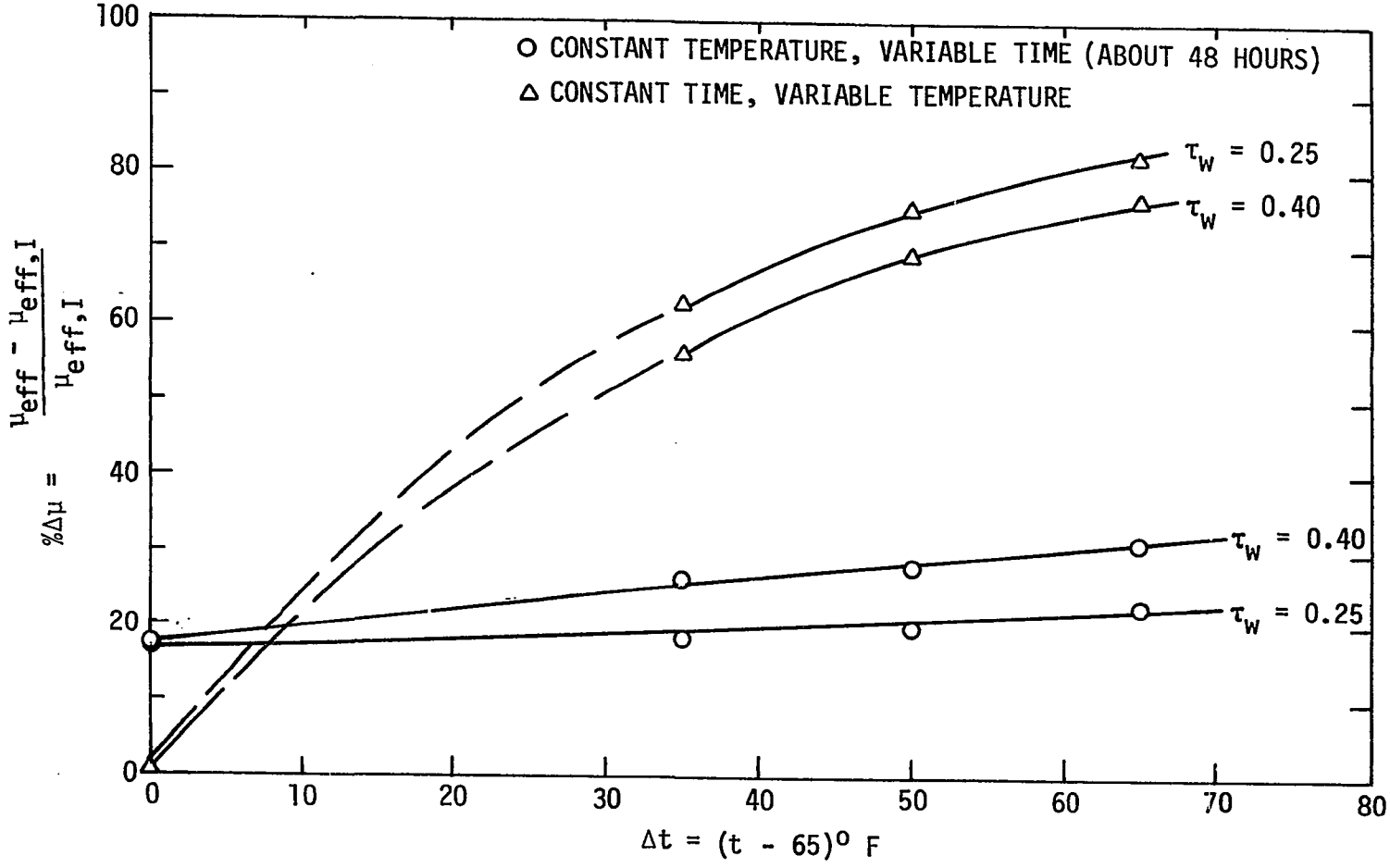

Fig. I.5 Plot of percentage change in effective viscosity against temperature difference.

APPENDIX J: WORKING FLUID PROPERTIES

In this experiment, 0.9 percent and 1.0 percent by weight aqueous solutions of polymer HEMC (XD-7630.02) were used as the working fluids. These are very weak solutions, and, therefore, all fluid properties other than density, consistency index, and flow behavior index could be assumed to be the same as the water solvent [39,94,95,96].

The working fluid properties are dependent on two state variables, namely, pressure and temperature. Since the pressure variations in the system were too small to affect fluid properties, they were adequately represented by functions of temperature alone.

In the following discussion, the properties common to both working fluids, ρ, β, c_p, and k, are given first. The determination of the consistency index is described in Appendix I.

Fluid Properties

Density

The Handbook on Methocel [104] gives the specific gravity of both these fluids as 1.0012. The density and other properties of distilled water are taken from ASME Steam Tables [106].

t (°F)	ρ (lb_m/ft^3)
50.0	62.50
100.0	62.07
150.0	61.27
200.0	60.17

The equation for these data are

$$\rho = 1.0012\ (62.422 - 0.21862\eta - 0.21785\eta^2 + 0.001077\ \eta^3)\ lb_m/ft^3 \qquad (J.1)$$

where

$$n = \frac{t - 50°F}{50°F}$$

Temperature range: 50-200°F

Maximum error: 0.02 percent

Isobaric thermal expansion coefficient

The isobaric thermal expansion coefficient is defined by the equation

$$\beta = -\frac{1}{\rho}\left(\frac{\partial \rho}{\partial t}\right) \qquad (J.2)$$

using Eq. (J.1), β is written as

$$\beta = \frac{-0.21862 - 0.43570\eta + 0.03231\ \eta^2}{50(62.422 - 0.21862\eta - 0.21785\ \eta^2 + 0.01077\ \eta^3)}\ \frac{1}{°F} \qquad (J.3)$$

where

$$\eta = \frac{t - 50.0°F}{50.0°F}$$

Isobaric specific heat

The variation in c_p with temperature is very small and, therefore, c_p was assumed to be constant:

$$c_p = 1.0 \text{ Btu/lb}_m/^\circ\text{F} \tag{J.4}$$

Temperature range: 50-180°F

Maximum error: 0.2 percent

Thermal conductivity

The data points are

t °F	k (Btu/hr ft °F)
50	0.3392
100	0.3633
150	0.3806

They are described by the following equation

$$k = 0.3392 + 0.0275\eta - 0.0034\,\eta^2 \frac{\text{Btu}}{\text{hr ft } ^\circ\text{F}} \tag{J.5}$$

where

$$\eta = \frac{t - 50.0^\circ\text{F}}{50.0^\circ\text{F}}$$

Temperature range: 50-200°F

Maximum error: 0.13 percent

Consistency Index and Flow Behavior Index

The graphical data given in Appendix I are described by the following equations:

Solution I (0.9 percent HEMC, Runs 1 to 10)

$$K' = 0.057151 \exp (-3.63573 \times 10^{-3}t - 1.596 \times 10^{-4}t^2) \quad (I.5)$$

Maximum error: 3.0 percent

$$n = 0.425913 \exp (0.004366t) \quad (I.6)$$

Maximum error: 1.5 percent

The correlation for calculated K, Eq. (I.3), is similar to that for K', Eq. (I.5); however, a log-linear expression was fitted to small portions of the K-t curve (Fig. I.3).

for 55 to 65°F

$$K = 0.088962 \exp (-0.022326t)$$

for 65 to 75°F

$$K = 0.109202 \exp (-0.025479t)$$

for 75 to 85°F

$$K = 0.138329 \exp (-0.028632t)$$

for 85 to 95°F

$$K = 0.180966 \exp (-0.031793t)$$

for 95 to 105°F

$$K = 0.244018 \exp (0.034939t)$$

for 105 to 120°F

$$K = 0.369801 \exp (-0.038874t)$$

for 120 to 135°F

$$K = 0.65217 \exp(-0.043602t) \qquad (J.6)$$

All these equations have accuracy of 0.1 percent with the actual K-t relationship. These equations are of the form

$$K = a \exp(-bt) \qquad (2.40)$$

hence,

$$\gamma = -\left(\frac{1}{K}\frac{dK}{dt}\right) = b = \text{constant}$$

This is a useful form to compare experimental results with analytical predictions developed in Chapters III and IV.

Solution I (0.9 percent HEMC, Runs 10 to 19)

$$K' = 0.047635 \exp(-3.915 \times 10^{-2}t - 1.575t^2) \qquad (I.7)$$

Maximum error: 1.5 percent

$$\eta = 0.444659 \exp(0.004236t) \qquad (I.8)$$

Maximum error: 1.3 percent

The correlations for K are given below.

for 55 to 70°F

$$K = 0.077219 \exp(-0.023113t)$$

for 70 to 85°F

$$K = 0.107085 \exp(-0.027784t)$$

for 85 to 95°F

$$K = 0.148708 \exp(-0.031678t)$$

for 95 to 110°F

$$K = 0.215591 \exp(-0.03556t)$$

for 110 to 120°F

$$K = 0.33017862 \exp(-0.039459t)$$

for 120 to 135°F

$$K = 0.52674 \exp(-0.043329t)$$

for 135 to 150°F

$$K = 0.989871 \exp(-0.048001t) \qquad (J.7)$$

All these equations have accuracy of 0.1 percent with the actual K-t relation.

Solution II (1.0 percent HEMC, Runs 1 to 9)

$$K' = 0.0701034 \exp(-0.6604 \times 10^{-3}t - 1.395 \times 10^{-4}t^2) \qquad (I.9)$$

$$n = 0.450709 \exp(0.004805t)$$

The correlations for K are given below.

for 55 to 70°F

$$K = 0.105895 \exp(-0.0265t)$$

for 70 to 95°F

$$K = 0.188437 \exp(-0.03403t)$$

for 95 to 110°F

$$K = 0.261398 \exp(-0.03745t)$$

for 110 to 130°F

$$K - 0.444107 \exp(-0.0422419t) \qquad (J.8)$$

All these equations have accuracy of 0.1 percent with the actual K-t relationship.

APPENDIX K: SAMPLE CALCULATIONS

Run No. 13 for solution I (0.9 percent HEMC) is used here to illustrate the data reduction procedure. In the following discussion, all fluid properties were evaluated at bulk temperature unless mentioned otherwise.

Experimental Parameters

Physical dimensions and properties of the tube

Inside tube diameter, D = 0.401 in.

Outside tube diameter, D1 = 0.441 in.

Total heated length, L = 71.8 in.

Length up to measuring station No. 4, L_S = 60.4 in.

Thermal conductivity of the tube, k1 = 9.4 Btu/hr ft °F

Length between the pressure taps = 73.9 in.

Measured quantities

The tube wall thermocouples readings at the measuring station were numbered 1 to 3. These thermocouples were 120° apart. The two thermocouples placed in the flow at the inlet and outlet section were Numbers 13 and 14.

The measured data were as follows:

t_1 = 146.76°F

t_2 = 147.01°F

t_3 = 146.52°F

t_{13} = 65.57°F

t_{14} = 98.10°F

Fluid flow rate (measured by weigh tank) = 78.10 lb_m/hr

Voltage across the test section, V_T = 7.98 volts

Voltage across the shunt, V_S = 41.007 mv

Pressure drop = 1.25 in. of mercury

Room temperature = 79.0°F

Experimental Calculations

Heat flux calculations

The heat loss through the insulation was estimated to be 1.5 percent [53,54,83], and, therefore, the net heat supplied to the fluid was

$$I = 2.4\ V_S$$

$$= 2.4 \times 51.007 = 98.42 \text{ amps}$$

The heat loss through the insulation was estimated to be 1.5 percent, and, therefore, the net heat supplied to the fluid was

$$Q = 0.985\ V_T I$$

$$= 0.985 \times 7.98 \times (98.42) \times 3.4129$$

$$= 2640.14 \text{ Btu/hr}$$

The average heat flux, q''_w, based on the inside tube surface area was

$$q''_w = \frac{Q}{\pi DL}$$

$$= \frac{2640.14 \times 144}{TC \times 0.401 \times 71.8}$$

$$= 4205.73 \frac{Btu}{hr\ ft^2}$$

The rate of volumetric heat generation was calculated as

$$q''_v = \frac{Q}{\frac{\pi}{4}(D_1^2 - D^2)\, L}$$

$$= \frac{4 \times 2640.14 \times 144 \times 12}{\pi[(0.441)^2 - (0.401)^2] \times 71.8}$$

$$= 2.402 \times 10^6 \text{ Btu/hr ft}^3$$

The temperature drop across the tube wall was calculated [54,83] as

$$t_w = \frac{q''_v}{8\, kl}\left[(D1)^2 \ln (D1/D) - \frac{1}{2}((D1)^2 - D^2)\right]$$

$$= \frac{2.402 \times 10^6}{8 \times 9.4 \times 144}\left[(0.441)^2 \ln \left(\frac{0.441}{0.401}\right)\right.$$

$$\left. - \frac{1}{2}(0.441)^2 - (0.401)^2\right]$$

$$= 0.37°F$$

The above temperature drop was applied uniformly around the circumference of the tube so as to obtain the following inside wall temperatures:

$t_1 = 146.39°F$

$t_2 = 146.64°F$

$t_3 = 146.15°F$

Simpson's rule was used to compute average wall temperature as

$t_w = 146.39°F$

Fluid bulk temperature

The fluid flow rate was measured by using a weigh tank:

$$\dot{m} = 78.18 \text{ lb}_m/\text{hr}$$

An energy balance over the tube length from the onset of heating up to measuring station yields

$$Q \frac{L_S}{L} = \dot{m} c_p \ (t_b - t_o)$$

hence,
$$t_b = \frac{Q}{\dot{m} c_p} \left(\frac{L_S}{L}\right) + t_o$$

$$= \frac{2640.10}{78.10 \times 1} \left(\frac{60.4}{71.8}\right) + 65.57$$

$$= 93.98°F$$

Nusselt number

The circumferentially averaged heat transfer coefficient was calculated as

$$\bar{h} = \frac{q''_w}{t_w - t_b}$$

$$= \frac{4205.14}{146.39 - 93.98}$$

$$= 80.25 \text{ Btu/hr ft}^2 \text{ °F}$$

The above calculated $\bar{h}$ and the thermal conductivity k of the solution at bulk temperature were used to calculate the Nusselt number:

$$Nu = \frac{\bar{h}D}{k}$$

$$= \frac{80.25 \times 0.401}{0.361 \times 12}$$

$$= 7.43$$

Effective viscosity

K' and n were evaluated from the respective property correlations. K was calculated as

$$K = K' \, (4n/3n+1)^n$$

At this station

$$K' = 8.20 \times 10^{-3} \quad \text{and} \quad K'_w = 9.19 \times 10^{-4} \ (lb_f \ sec^n)/ft^2$$

$$n = 0.66 \quad \text{and} \quad n_w = 0.83$$

$$K = 7.57 \times 10^{-3} \quad \text{and} \quad K_w = 8.79 \times 10^{-4} \ (lb_f \ sec^n)/ft^2$$

$$\frac{K}{K_w} = 8.62$$

$$\mu_{eff} = K' \, (8\bar{u}/D)^{n-1}$$

$$= 32.2 \times 8.20 \times 10^{-3} \left(\frac{8 \times 0.398 \times 12}{0.401}\right)^{0.66-1}$$

$$= 0.057 \ lb_m/ft \ sec$$

similarly, $(\mu_{eff})_w = 0.013 \ lb_m/ft \ sec$

Dimensionless numbers

Reynolds number,

$$Re = \left(\frac{\rho \bar{u} D}{\mu_{eff}}\right) = \frac{62.28 \times 0.398 \times 0.401}{12 \times 0.057}$$

$$= 14.6$$

similarly, $(Re)_w = 61.8$

Prandtl number,

$$Pr = \frac{\mu_{eff} c_p}{k} = \frac{0.057 \times 1 \times 3600}{12 \quad 0.361}$$

$$= 564.5$$

similarly, $Pr_w = 127.0$

Dimensionless distance,

$$X^+ = \frac{2(x/D)}{RePr} = \frac{2(60.4/0.401)}{14.6 \times 564.5}$$

$$= 3.65 \times 10^{-2}$$

similarly, $X_w^+ = 3.84 \times 10^{-2}$

Graetz number,

$$Gz = \frac{\dot{m} c_p}{k \times} = \frac{78.18 \times 1}{0.361 \times (60.4 \times 12)}$$

$$= 43.1$$

Comparison with numerical solution

As mentioned in Appendix J, the present K-t curve was of the type

$$K = a \exp(-bt - ct^2)$$

but a curve of the type

$$K = a \exp(-bt)$$

was fit to each 15-20°F interval, and from these equations γ was evaluated at fluid bulk temperature (see Appendix J).

$$\gamma\Delta T = \frac{q''_w D}{2k} \left[-\frac{1}{k}\frac{dK}{dt}\right]$$

$$= \frac{4205.73 \times 0.401}{2 \times 12 \times 0.361} (0.0355)$$

$$= 6.17$$

$$C_K = C_1\gamma\Delta T - C_2(\gamma\Delta T)^2$$

$$= (0.12392 - 0.05420n)\gamma\Delta T - (0.010133 - 0.0068n)\ (\gamma\Delta T)^2$$

with $n = 0.66$, $C_K = 0.33$

$$\left(\frac{Nu}{Nu_{cp}}\right)_{max} = 1.0 + C_k = 1.0 + 0.33$$

$$= 1.33$$

The exponent of the viscosity correction was calculated as

$$m = 0.58 - 0.44\eta$$

$$= 0.58 - 0.44 \times 0.66$$

$$= 0.29$$

Then $$\left(\frac{K}{K_w}\right)_{crit} = (1.33)^{1/0.29}$$

$$= 2.68$$

Hence, $$(K/K_w) > (K/K_w)_{crit}$$

The consistency correction was thus calculated as follows:

The exponent of the consistency correction at wall

$$m_w = 0.58 - 0.44n_w$$

$$= 0.58 - 0.44 \times 0.83$$

$$= 0.22$$

The consistency correction is then

$$(C_c)^m = (K/K_w)^m_{crit}$$

$$= (2.68)^{0.22}$$

$$= 1.24$$

The non-Newtonian correction is

$$(\Delta_w)^{1/3} = \left(\frac{3n+1}{4n}\right)^{1/3}_w$$

$$= 1.02$$

Now, Nusselt number, Nu = 7.43

The corrected non-Newtonian Nusselt number is

$$\frac{Nu}{(\Delta_w)^{1/3}} = \frac{7.43}{1.02}$$

$$= 7.31$$

Finally, the consistency corrected non-Newtonian Nusselt number is

$$\frac{Nu}{(\Delta_w)^{1/3}(C_c)^m} = \frac{7.31}{1.24}$$

$$= 5.91$$

This value is at $X^+ = 3.65 \times 10^{-2}$; the corresponding numerically calculated value at this X^+ is 6.12, thus, showing 0.35 percent error.

Friction factor

The reynolds number at the middle section of the tube is given by

$$Re_M = \frac{\rho D \bar{u}}{\mu_{eff}} = 11.7$$

and fluid properties were evaluated at

$$t_{am} = \frac{t_o + t_e}{2}$$

The pressure taps on the metal tube were 73.9 in. apart, 1.05 in. outside the 71.8 in. heated length at each end. It was therefore necessary to calculate isothermal pressure drops, which need to be subtracted from the total pressure drop.

At inlet, $t_o = 65.67$

$$Re_o = (\rho D \bar{u}/\mu_{eff})_o$$

$$= \frac{62.41 \times 0.401 \times 0.396}{0.0918 \times 12}$$

$$= 9.0$$

$$f_o = 64/Re_o$$

$$= 64/9$$

$$= 7.11$$

At exit, $t_e = 98.10$

$$Re_e = (\rho D \bar{u}/\mu_{eff})_e$$

$$= \frac{62.09 \times 0.401 \times 0.399}{0.0519 \times 12}$$

$$= 16.0$$

$$f_e = 64/Re_e$$

$$= 64/16$$

$$= 4.0$$

The isothermal pressure drops across the unheated inlet and outlet segments were calculated as

$$\Delta p_o = \left(\frac{fL\ \rho\bar{u}^2}{2gD}\right)_o$$

$$= \frac{7.11 \times 1.05 \times 62.41 \times (0.397)^2 \times 12}{12 \times 32.2 \times 0.401 \times 2}$$

$$= 2.84\ lb_f/ft^2$$

$$\Delta p_e = \left(\frac{fL\ \rho\bar{u}^2}{2gD}\right)_e$$

$$= \frac{4 \times 1.05 \times 62.09 \times (0.399)^2 \times 12}{12 \times 2 \times 32.2 \times 0.40}$$

$$= 1.61\ lb_f/ft^2$$

The total measured pressure drop as calculated from the differential mercury head, ΔH, is given by

$$\Delta p_t = \frac{g}{g_c} \Delta H\ (\rho_{Hg} - \rho_{HEMC})_{room\ temp}$$

$$= \frac{1.25}{12} (847.37 - 62.32)$$

$$= 81.78\ lb_f/ft^2$$

Finally, the pressure drop across the heated section is

$$\Delta p_h = \Delta p_t - \Delta p_o - \Delta p_e$$

$$= 81.78 - 2.84 - 1.61$$

$$= 77.33 \text{ lb}_f/\text{ft}^2$$

$$= 0.537 \text{ psi}$$

$$f = \left(\frac{2g_c D\Delta P_h}{\rho \bar{u}^2 L_T}\right)_{am}$$

$$= \frac{2 \times 32.2 \times 0.401 \times 77.33}{62.24 \times (0.398)^2 \times 71.8}$$

$$= 2.98$$

A listing of the FORTRAN IV computer program utilized to facilitate the data reduction is given in Appendix L. The experimental results for heat transfer and friction factor are tabulated in Appendix M.

APPENDIX L: COMPUTER PROGRAM FOR EXPERIMENTAL DATA REDUCTION

```
C      COMPUTICNAL PROCEDURE  FOR THE DATA REDUCTION FOR A NON-NEWTONIAN
C      FLUID FLCW IN A PLAIN TUBE.
       REAL NUB. NUF. NUC. N. MUEF. MUEB. MUEW. KAW. KAB.K.M.LO.LI
       REAL MUEI.MUEM.MUEC .NUL
C
       DIMENSICN  TEMP(5). TWI(5)
C
C      D1 IS INTERNAL CIAMETER OF THE TUBE
C
C      D2 IS CUTER DIAMETER CF THE TUBE
C
C      TL IS TUTAL HEATED LENGTH
C
C      TL1. TL2. TL3. AND TL4 DENOTE THE DISTANCES OF HEAT TRANSFER
C      SECTICN FRCM THE CNSET OF HEATING.
C
C      THLTB CENOTE  THE THERMAL CONDUCTIVITY OF THE TUBE
C
C
       DATA D1. D2. TL1. TL2. TL3. TL4. THCTB/0.04221.0.046875.0.4063
      1.0.994E.2.4688.3.5688.9.64/
       DATA TL5.TL6.TL7.TL8.TL/5.4792.6.9792.7.8125.8.6432.8.9896/
C
C     LI AND LO DENOTES LENGTH BETWEEN  PRESSURE TAP  AND HEATED SECTION AT
C      INLET AND CUTLET RESPECTIVELY
       DATA LI.LC/ 0.10417.0.02083/
C
C
       DATA PI.GC.PCF/3.141593.32.174.3.4129/
C
       D12=D1*D1
       D13=D12*D1
       D22=D2*D2
       AREA=PI*D12/4.0
C
C      CALCULATICN CF THE ELECTRICAL HEAT INPUT
C
 1     READ(5.2.END=500) NR.NS.FLI.M.VLT.VLS.H2.ROOMT
 2     FCRMAT(2I5.6F10.4)
       AMP = 2.4 * VLS
       RT = VLT/AMP
       WAT = 0.985 * VLT* AMP
       QTCT = WAT * PCF
       QFLUX = QTCT/(PI * D1 * TL)
       FLCW = M * 60.C
C      VOLUMETRIC HEAT GENERATION IS DENOTED BY QPUV
       QPUV = 4* QTOT / (PI * (D22-D12) * TL)
       DTW = QPUV * (D22*ALOG(D2/D1)-((D22-D12)/2.))/(8.0*THCTB)
       WRITE(6.501) NR.NS.FLOW.FLI.VLT.VLS.AMP.RT.WAT.QTOT.QFLUX
 501   FCRMAT('1',36X,'HEAT TRANSFER TO NCN-NEWTCNIAN FLUID IN PLAIN
      1CIRCULAR  TUBE',/,
      220X,'*************************************************************
      3**********************',/,
      410X,'RUN NUMBER:',I5,50X,'FLUID: XD-7630.02. 1% SOLN.',/,
      510X,'SECTICN:  ',I5,//,
      65X,'SYSTEM PARAMETERS:',/,
      75X,'*****************',/,
      810X,'FLUID FLOW RATE                =',F10.3,2X,'LBM/HR',30X,'FLOW
      1INDEX=',F5.2,//,
      910X,'VOLTAGE ACROSS THE TUBE        =',F10.3,2X,'VOLTS',//,
```

```
     910X,'VOLTAGE ACROSS THE SHUNT      =',F10.3,2X,'MILLI-VOLTS',//,
     910X,'CURRENT THROUGH THE TUBE      =',F10.4,2X,'AMPS',//,
     910X,'RESISTANCE OF THE TUBE        =',E15.6,2X,'OHMS',//,
     910X,'ELECTRICAL HEAT INPUT         =',F10.3,2X,'WATTS',//,
     910X,'TOTAL HEAT INPUT              =',F10.3,2X,'BTU/HR',//,
     910X,'TOTAL INPUT HEAT FLUX         =',F10.3,2X,'BTU/(HR-SQ.FT)')
C
C      CALCULATION OF WALL TEMPERATURE
C
      READ (5,5) (TEMP(I), I=1,5)
 5    FORMAT (5F10.4)
      DO 10 I=1,3
 10   TWI(I)= TEMP(I) - DTW
C
C   SIMPSONS RULE IS USED TO CALCULATE MEAN WALL TEMPERATURE
C
      TWM=(TWI(1)+4.*TWI(2)+TWI(3))/6.
C
C      CALCULATION OF THE FLUID TEMPERATURE
C
      TEMPIN = TEMP(4)
      TEMPOU = TEMP (5)
      QOUT=FLOW*(TEMPOU-TEMPIN)
      QDIFF=100.0*(QTOT-QOUT)/QTOT
      TLTC=TL1
      IF(NS.EQ.2) TLTC=TL2
      IF(NS.EQ.3) TLTC=TL3
      IF(NS.EQ.4) TLTC=TL4
      IF (NS.EQ.5) TLTC=TL5
      IF (NS.EQ.6) TLTC=TL6
      IF (NS.EQ.7) TLTC=TL7
      IF (NS.EQ.8) TLTC=TL8
      QIN=QTOT*TLTC/TL
      TFB=(QIN/FLOW)+TEMPIN
      TFLM=(TFE+TWM)/2.0
C
      DELTAT=TWM-TFB
      HTC=QFLUX/DELTAT
C
      NUB=HTC*D1/THCNL(TFB)
C
      GZB=FLOW/(THCNL(TFB)*TLTC)
       GZW=GZB*THCNL(TFB)/THCNL(TWM)
      PLUSXB=PI/(2.0*GZB)
      PLUSXW=PI/(2.0*GZW)
      WRITE(6,504) TWI(1),TWI(2),TWI(3),TWM,TEMPIN,TEMPOU,TFB,TFLM,QIN,
     1QOUT,QDIFF
504   FORMAT('0',5X,'TUBE WALL TEMPERATURES',/,
     15X,'**************************',//,
     235X,F10.2,//,45X,F10.2,//,35X,F10.2,//,
     310X,'MEAN WALL TEMPERATURE         =',F10.2,2X,'F',//,
     410X,'INLET FLUID TEMPERATURE       =',F10.2,2X,'F',//,
     510X,'OUTLET FLUID TEMPERATURE      =',F10.2,2X,'F',//,
     710X,'FLUID BULK TEMPERATURE        =',F10.2,2X,'F',//,
     810X,'MEAN FLUID TEMPERATURE        =',F10.2,2X,'F',//,
     910X,'HEAT INPUT UPTO  LENGTH X     =',F10.3,2X,'BTU/HR',//,
     910X,'HEAT OUTPUT                   =',F10.3,2X,'BTU/HR',//,
     910X,'PERCENTAGE HEAT  BALANCE          =',F10.3,/)
      WRITE(6,510) HTC,NUB,GZB,GZW,PLUSXB,PLUSXW
510   FORMAT('0',5X,'HEAT TRANSFER RESULTS',/,
```

```
     15X,'**********************',/,
     210X,'HEAT TRANSFER COEFFICIENT     =',F10.3,2X,'BTU(HR SQ.FT-F)',/,
     310X,'NUSSELT NUMBER BULK, NUB      =',F10.3,//,
     410X,'GRATEZ NUMBER,BULK,WALL       =',F10.3,5X,F10.3,//,
     510X,'(2.X/D)/RED/PR     ,BULK,WALL =',E15.6,10X,E15.6,/ )
C
C      CALCULATION OF THE FLUID VELOCITY
C
       VB=FLOW/(3600.0*RHO(TFB)*AREA)
       VW=VB*RHO(TFB)/RHO(TWM)
C
C      CALCULATION OF VISCOSITY
C
       D=D1
       MUEB=GC*K(TFB)*((8*VB/D)**(N(TFB)-1.0))
       MUEW=GC*K(TWM)*((8*VW/D)**(N(TWM)-1.0))
       RENB=RHO(TFB)*D1*VB/MUEB
       RENW=RHO(TWM)*D1*VW/MUEW
       PRB=3600.*CP(TFB)*MUEB/THCNL(TFB)
       PRW=CP(TWM)*MUEW*3600./THCNL(TWM)
       GRW=32.2*BETA(TWM)*(TWM-TFB)*D13*(RHO(TWM)**2.0)/(MUEW**2.0)
       RAW=GRW*PRW
       WRITE(6,515) GRW,RAW
 515   FORMAT('+',
      110X,'GRASHOF  NUMBER  WALL         =',E15.6,/,
      210X,' RAYLEIGH  NUMBER WALL        =',E15.6 )
       WRITE(6,520) VB,VW,MUEB,MUEW,RENB,RENW,PRB,PRW
 520   FORMAT('1',5X,'DIMENSIONLESS NUMBERS',/,
      15X,'**************************',/,
      210X,'FLUID VELOCITY ,BULK,      WALL    =',2E15.6,2X,'FT/SEC',//,
      310X,'EFFECTIVE FLUID VISCOSITY,"  ,"  =',2F10.3,2X,'LBM/(FT-SEC)',
      4//,
      510X,'REYNOLDS NUMBER,BULK,      WALL    =',2F10.3,//,
      610X,'PRANDTL NUMBER,BULK,      WALL     =',2F10.3,//)
C
C      COMPARISON WITH THE PREVIOUS DATA
C
       DELW = 4*N(TWM)/ (3*N(TWM)+1)
       KAB=XKA(TFB)
       KAW=XKA(TWM)
       VISCAW = 32.2 * KAW * ((D1/VW) ** (1-N(TWM)))
       PRAW=3600.0*VISCAW*CP(TWM)/THCNL(TWM)
       GRAW=32.2*BETA(TWM)*(TWM-TFB)*(RHO(TWM)**2.)*D13/(VISCAW**2.0)
       VISCRR=KAB/KAW
       VISCR=VISCRR**0.14
       XAXIS = GZB + 0.0063 *(( GRAW* PRAW)** 0.75)
       NUC=VISCR*1.46*((XAXIS/DELW)**(1/3.0))
       YAXIS=(DELW**(1./3.))*NUC/VISCR
       YAXISP=(YAXIS*NUB)/NUC
       DD = TLTC / D1
       XNW=N(TWM)
        XNB=N(TFB)
       WRITE(6,540) K(TFB),K(TWM),KAB,KAW,XNB,XNW,VISCAW,PRAW,GRAW,
     1VISCR,XAXIS,YAXIS,YAXISP,NUC,DD
 540   FORMAT('0',5X,'FLUID VISCOSITY RESULTS',/,
      A5X,'************************',/,
      B10X,'K-DASH     BULK,WALL,              =',2E15.6,2X,'(LBF,SEC**N/FT
      CFT)',//,
      D10X,'K-CONSISTANCY INDEX,BULK,WALL      =',2E15.6,2X,'(LBF-SEC**N/SQ
      E,FT)',//,
```

```
      F10X,'FLOW BEHAVIOR INDEX,BULK,WALL    =',2E15.6,//,
      G10X,'APPERANT VISCOSITY AT THE WALL   =',F10.6,2X,'LBM/(FT-SEC)',/
      1/,
      H10X,'APPARENT PRANDTLE NUMBER AT THE WALL=',F10.3,//,
      I10X,'APP. GRASHOF NUMBER AT THE WALL  =',E15.6,//,
      J10X,'VISCOSITY RATIO (K(BULK)/KWALL)**0.14=',F10.6,//,
      K10X,'X-AXIS ON MAHALINGAMS PLOT       =',F10.6,//,
      L10X,'Y-AXIS MAHALINGAMS, PRESENT      =',2F10.3,//,
      M10X,'NUSSELT NUMBER  MAHALINGAMS CORR.=',F10.3,//,
      N10X,'X/D                              =',F10.3)
C
C     COMPARISON WITH PRESENT NUMERICAL RESULTS
C
      A1=0.12392
      B1=0.05420
      A2=0.010133
      B2=0.0068
      BK=BKA(TFB)
      C1N=A1-B1*XNB
      C2N=A2-B2*XNB
      CFD=-QFLUX*BK*D1/2./THCNL(TFB)
      XNUR=1.0+C1N*CFD-C2N*CFD*CFD
       XMB=0.58-0.44*XNB
       XM=0.58-0.44*XNW
      XKCRIT=XNUR**(1/XME)
      XNUL=NUB*(DELW**(1./3.))
      IF(VISCRR.LE.XKCRIT) XMNV=XNUL/(VISCRR**XM)
      IF(VISCRR.GT.XKCRIT) XMNV=XNUL/(XKCRIT**XM)
      WRITE(6,550) VISCRR,XKCRIT,XM,CFD,NUB,XNUL,XMNV
  550 FORMAT('0',5X,'COMPARISON WITH PTESENT NUMERICAL ANALYSIS',/,
     15X,'*************************************************',/,
     210X,'KAB/KAW,       XKCRIT              =',F10.4,5X,F10.4,/,
     310X,'CORR.INDEX OF VISC. AND CFD        =',F10.3,5X,F10.3,/,
     210X,'NUSSELT NO. NUB                    =',F10.3,/,
     410X,'NUC=NUB/(DELW**(1/3))              =',F10.3,/,
     510X,'NUC/(VISC. CORRECT.) = XMNV        =',F10.3)
      WRITE(7,600) NR,NS,XAXIS,YAXIS,YAXISP,NUB,XNUL,XMNV,PLUSXB,PLUSXW,
     1XNW
  600 FORMAT(I2,I3,F10.3,5F6.2,2E15.6,F5.3 )
       IF (NS.GE. 8) GO TO 20
      GO TO 1
C
C     CALCULATION OF FRICTION FACTOR
C
   20 TFBC=TEMPIN+(QTOT/FLOW)
      TBM=(TFBC+TEMPIN)/2.0
      RHOI=RHO(TEMPIN)
      RHOE=RHO(TFBO)
      RHOM=RHO(TBM)
      VM=VB*RHO(TFB)/RHOM
      VI=VB*RHO(TFB)/RHOI
      VO=VB*RHO(TFB)/RHOE
      NI=N(TEMPIN)
      NE=N(TFBC)
C
C     CALCULATION OF  VISCOSITY
C
      MUEI=GC*K(TEMPIN)*((8*VI/D)**(NI-1.0))
      MUEM=GC*K(TBM)*((8*VM/D)**(N(TBM)-1.0))
      MUEO=GC*K(TEMPOU)*((8*VO/D)**(NE-1.0))
```

```
      REM=RHOM*D1*VM/MUEM
      REI=RHOI*D1*VI/MUEI
      REO=RHOE*D1*VO/MUEO
C
      FRINI=64.0/REI
      FRINO=64.0/REO
      FRINM=64.0/REM
C
      DPI=FRINI*LI*RHOI*VI*VI/(288.0*GC*D1)
      DPO=FRINO*LO*RHOE*VO*VO/(288.0*GC*D1)
      RHOXT=RHO(RCOMT)
      RHOMT=RHOME(RCOMT)
      DPHL=H2*(RHOMT-RHOXT)/1728.00
      DPF=DPHL-DPI-DPO
      FRM=288.0*GC*D1*DPF/(RHOM*TL*VM*VM)
      FRMF=FRM/4.0
      WRITE(6,560) FRM,FRMF,REM
  560 FORMAT('0',5X,'FRICTION FACTOR  CALCUTION',/,
     15X,'**********************************',/,
     210X,'FRICTION FACTOR, DARCYS      =',E15.6,/,
     310X,'FRICTION FACTOR, FANNINGS    =',E15.6,/,
     410X,'MEAN REYNOLDS NUMBERS        =',F10.3)
C
C     CALCULATION OF RAYLEIGH NUMBER
C
      FRIRT=FRM/FRINM
      GRQ=GC*BETA(TBM)*RHOM*RHOM*D13*D1*QFLUX/(MUEM*MUEM*THCNL(TBM))
      PRBM=3600.0*MUEM*CP(TBM)/THCNL(TBM)
      RAQM=GRQ*PRBM
      WRITE(6,580) TFBC,TBM,GRQ,PRBM,RAQM,FRIRT
  580 FORMAT('0',5X,'TEMPERATURE OUTLET,MEAN             =',F10.2,'F',F10
     1.2, 2X,'F',/,
     25X,'GRASHOF NO. HEAT FLUX BASIS       =',E15.6,/,
     35X,'PRANDTL NO. BASED ON MEAN TEMP.   =',F10.3,/,
     45X,'RAYLEIGH NUMBER                   =',E15.6,/,
     55X,'FRICTION FACTOR (NON-ISO/ISOTH)   =',F10.4)
      GO TO 1
  500 STOP
      END
      FUNCTION RHO(T)
C           DENSITY AS A FUNCTION OF TEMPERATURE (F) FOR XD-0.9%SOLN.
C                 UNITS LBM/CU.FT
C
      DATA X1,X2,X3,X4/62.422,-0.21862,-0.21785,0.01077/
      ETA=(T-50.0)/50.0
      RHO=(X1+X2*ETA+X3*ETA*ETA+X4*(ETA**3.0))*1.0012
      RETURN
      END
      FUNCTION BETA (T)
C           COEFFICIENT OF THERMAL EXPANSION AS A FUNCTION OF
C           TEMPERATURE (F) FOR 0.9%SOLUTION OF XD-7630:.02
C                 UNITS 1/F
C
      DATA X1,X2,X3,X4 /-0.21862,-0.43570,0.03231,64.422/
      DATA X5,X6/-0.21785,0.01077/
      ETA=(T-50.0)/50.0
      VOL=X1+X2*ETA+X3*(ETA**2.0)
      DVOL=X4+X1*ETA+X5*ETA*ETA+X6*(ETA**3.0)
      BETA=-(VOL/(50.0*DVOL))
      RETURN
```

```
      END
      FUNCTION  THCNL(T)
C             THERMAL CONDUCTIVITY AS A FUNCTION OF TEMPERATURE (F)
C             FOR XD:0.9%--7630:0.02
C                     UNITS BTU/(HR.FT.F)
C
      DATA X1,X2,X3/0.3392,0.0275,-0.0034/
      ETA=(T-50.0)/50.0
      THCNL=X1+X2*ETA+X3*ETA*ETA
      RETURN
      END
       FUNCTION   CP(T)
C       SPECIFIC   HEAT   AS A  FUNCTION    OF  TEMPERATURE   (F)   FOR
C            XD-7630:0.02
C       UNITS     BTU/(LBM.F)
      CP=1.0
      RETURN
      END
      REAL  FUNCTION  N(T)
C          N,THE FLOW BEHAVIOUR INDEX FOR FLUID XD:7630.02
C                   N IS DIMENSIONLESS
       DATA X1,X2/45.07073E-02,48.054E-04/
      N=X1*EXP(X2*T)
       RETURN
      END
      REAL  FUNCTION K(T)
C       K-DASH AS A FUNCTION OF TEMPERATURE   FOR
C  XD:0.9%--7630:0.02
C                  UNITS    LBF.SEC**N/(FT*FT)
       DATA X1,X2,X3/70.10345E-03,-96.6042E-04,-13.95E-05/
       K=X1*EXP(X2*T+X3*T*T)
      RETURN
      END
C
C     DENSITY AS A FUNCTION OF TEMPERATURE(F), FOR MERCURY
      FUNCTION   RHOME(T)
C                  UNITS  LBM/CU.FT
      THETA=(T-68.0)/54.0
      RHOME=847.71-(4.57*THETA)
      RETURN
      END
       FUNCTION  EKA(T)
C    THIS FUNCTION INDICATES CONSTANT IN THE VISCOSITY POWER INDEX
       IF(T.LE.130.0)  EKA=.422419E-01
       IF(T.LE.110.0)  EKA=.374545E-01
       IF(T.LE.95.00)  EKA=.340334E-01
       IF(T.LE.85.00)  EKA=.306167E-01
       IF(T.LE.70.00)  EKA=.02650
      EKA=-EKA
      RETURN
      END
      FUNCTION  XKA(T)
C    THIS FUNCTION INDICATES CONSISTENCY INDEX FOR THE FLUID
      DATA X1,X2/.105855,-0.2650E-01/
      DATA X3,X4/0.141263,-0.306167E-01/
       DATA X5,X6/0.188437,-0.340334E-01/
       DATA X7,X8/0.261358,-0.374545E-01/
       DATA X9,X10/0.444107,-0.422419E-01/
C
      IF (T.GT.55.0) XKA=X1*EXP(X2*T)
```

```
IF (T.GT.70.0) XKA=X3*EXP(X4*T)
IF (T.GT.85.0) XKA=X5*EXP(X6*T)
IF (T.GT.95.00)XKA=X7*EXP(X8*T)
IF (T.GT.110.0)XKA=X9*EXP(X10*T)
 RETURN
END
```

APPENDIX M: TABULATION OF EXPERIMENTAL DATA

Experimental Results for Solution I (0.9 percent HEMC)

Table M.1. Experimental variables

Run No.	$\dot{m}$ lb_m/hr	q''_w $Btu/hrft^2$	Re[a]	Pr	f[b]
1 to 4	82.02	1104.8	8.5	1061.0	6.46
5 to 8	156.00	1709.2	20.6	837.6	2.72
9 to 12	234.00	2140.1	36.9	702.8	1.54
13 to 16	52.2	1753.0	4.3	1343.7	10.17
17 to 20	52.8	2425.4	4.5	1281.6	8.63
21 to 24	78.6	3246.9	8.0	1080.4	4.90
25 to 28	125.2	2479.7	14.8	934.4	3.36
29 to 32	130.6	4349.8	16.3	886.4	2.52
33 to 36	188.7	4241.7	28.0	743.0	1.65
37 to 40	308.8	4110.2	60.7	560.7	0.85
41 to 44	309.8	5440.9	59.5	878.4	0.83
45 to 48	78.2	4205.7	9.7	878.4	2.98
49 to 52	88.4	2233.1	11.9	806.5	3.40
53 to 56	59.4	1995.7	6.3	1025.2	5.68
57 to 60	51.6	1992.4	5.5	1029.1	5.87
61 to 64	279.4	4813.3	52.4	587.9	0.88
65 to 68	254.1	4844.8	45.4	618.2	0.97
69 to 72	35.5	1818.2	3.4	1125.5	8.05

[a]Evaluated at Station 1, where x/D = 27.

[b]Evaluated at t_{am} for Test Section I.

Table M.2. Experimental results for Solution I (0.9% HEMC)

Run	$X^+ x10^3$	t_b °F	t_w °F	$\gamma\Delta T$	m	n_w	a	b	Nu	c	d	Ref
1	6.12	63.59	74.59	1.19	0.32	0.59	1.32	1.34	9.69	9.18	8.41	1-1
2	12.90	65.03	78.64	1.36	0.32	0.60	1.43	1.39	7.82	7.43	6.69	1-2
3	24.57	67.49	83.74	1.35	0.31	0.61	1.39	1.56	6.52	6.21	5.61	1-3
4	33.66	69.40	86.85	1.35	0.31	0.62	1.63	1.39	6.06	5.78	5.22	1-4
5	3.20	59.87	74.18	1.85	0.32	0.59	1.42	1.52	11.59	10.98	9.82	2-1
6	6.74	61.04	78.86	1.85	0.32	0.60	1.57	1.52	9.29	8.82	7.73	2-2
7	12.83	63.05	84.68	1.84	0.31	0.62	1.78	1.52	7.63	7.23	6.38	2-3
8	17.58	64.60	88.31	1.84	0.30	0.63	1.93	1.52	6.94	6.63	5.83	2-4
9	2.13	59.33	75.00	2.32	0.32	0.59	1.46	1.65	13.26	12.57	11.13	3-1

a $\left(\frac{K}{K_w}\right)$

b $\left(\frac{K}{K_w}\right)_{crit}$

c $\frac{Nu}{(\Delta_w)^{1/3}}$

d $\frac{Nu}{(\Delta_w)^{1/3}(C_c)^m}$

Table M.2. (continued)

Run	$X^+ \times 10^3$	t_b °F	t_w °F	$\gamma\Delta T$	m	n_w	__a	__b	Nu	__c	__d	Ref
10	4.49	60.31	79.85	2.32	0.31	0.60	1.65	1.65	10.62	10.09	8.63	3-2
11	8.54	61.98	85.71	2.31	0.31	0.62	1.88	1.65	8.72	8.32	7.13	3-3
12	11.70	63.28	89.17	2.31	0.30	0.63	2.04	1.65	7.98	7.62	6.54	3-4
13	9.57	61.02	80.39	1.90	0.31	0.61	1.65	1.54	8.77	8.34	7.28	4-1
14	20.25	64.61	88.22	1.89	0.30	0.63	1.92	1.54	7.15	6.83	5.99	4-2
15	38.79	70.75	97.93	2.13	0.29	0.65	2.26	1.62	6.16	5.91	6.13	4-3
16	53.35	75.51	103.65	2.38	0.29	0.67	2.44	1.70	5.91	5.68	4.89	4-4
17	9.50	63.84	89.10	2.61	0.30	0.63	2.01	1.74	9.26	8.84	7.48	5-1
18	20.14	68.75	99.41	2.96	0.29	0.66	2.50	1.84	7.57	7.27	6.09	5-2
19	38.69	77.16	112.52	3.29	0.27	0.70	3.26	1.95	6.49	6.27	5.23	5-3
20	53.31	83.66	119.27	3.26	0.26	0.72	3.52	1.96	6.39	6.19	5.18	5-4
21	6.38	63.62	93.53	3.50	0.30	0.64	2.32	1.95	10.47	10.02	8.21	7-1
22	13.52	68.04	104.69	3.97	0.28	0.67	2.07	2.07	8.49	8.17	6.64	7-2
23	25.93	75.59	118.56	4.41	0.27	0.72	4.31	2.20	7.17	6.94	5.63	7-3
24	35.71	81.45	125.85	4.37	0.26	0.74	4.98	2.22	6.88	6.69	5.46	7-4

Table M.2. (continued)

Run	$X^+ \times 10^3$	t_b °F	t_w °F	$\gamma\Delta T$	m	n_w	a	b	Nu	c	d	Ref
25	3.98	58.96	79.77	2.69	0.31	0.60	1.69	1.75	11.58	11.01	9.33	8-1
26	8.40	61.08	86.96	2.68	0.31	0.62	2.00	1.75	9.28	8.85	7.46	8-2
27	16.04	64.70	95.82	2.67	0.30	0.65	2.45	1.75	7.68	7.36	6.24	8-3
28	22.00	67.51	100.98	3.03	0.29	0.66	2.73	1.85	7.11	6.83	5.71	8-4
29	3.83	61.72	95.34	4.70	0.30	0.65	2.57	2.19	12.52	11.99	9.51	9-1
30	8.10	65.28	107.05	5.33	0.28	0.68	3.59	2.31	10.02	9.65	7.63	9-2
31	15.51	71.37	121.37	5.29	0.26	0.72	5.40	2.33	8.30	8.05	6.45	9-3
32	21.34	76.08	129.18	5.90	0.25	0.75	6.71	2.44	7.77	7.56	6.04	9-4
33	2.66	62.88	92.28	4.57	0.30	0.64	2.27	2.17	13.94	13.33	10.56	10-1
34	5.61	65.29	102.01	5.20	0.29	0.67	3.00	2.29	11.11	10.68	8.42	10-2
35	10.71	69.40	113.65	5.17	0.27	0.70	4.18	2.30	9.17	8.86	7.06	10-3
36	14.70	72.58	120.30	5.15	0.26	0.72	5.00	2.32	8.47	8.21	6.58	10-4
37	1.62	62.09	87.10	4.59	0.30	0.64	1.95	2.21	15.89	15.22	12.48	11-1
38	3.42	63.51	94.98	4.58	0.29	0.67	2.43	2.21	12.60	12.11	9.64	11-2
39	6.51	65.94	104.32	4.57	0.28	0.69	3.19	2.22	10.30	9.94	7.98	11-3

Table M.2. (continued)

Run	$X^+ x10^3$	t_b °F	t_w °F	$\gamma\Delta T$	m	n_w	a	b	Nu	c	d	Ref
40	8.92	67.83	109.78	4.55	0.27	0.71	3.70	2.23	9.39	9.09	7.33	11-4
41	1.61	59.24	90.86	6.11	0.29	0.65	2.35	2.41	16.71	16.03	12.49	12-1
42	3.39	61.12	100.70	6.09	0.28	0.68	3.13	2.42	13.31	12.83	10.02	12-2
43	6.45	64.33	112.63	6.06	0.26	0.72	4.50	2.43	10.86	10.52	8.31	12-3
44	8.88	66.82	119.57	6.04	0.26	0.74	5.59	2.45	9.90	9.63	7.66	12-4
45	6.48	70.77	109.42	5.58	0.27	0.71	3.40	2.42	10.39	10.05	7.93	13-1
46	13.75	76.52	124.20	5.53	0.25	0.75	5.27	2.45	8.36	8.14	6.51	13-2
47	26.44	86.37	138.55	6.23	0.23	0.80	7.53	2.61	7.54	7.39	5.93	13-3
48	36.47	93.98	146.39	6.17	0.22	0.83	8.62	2.69	7.43	7.31	5.91	13-4
49	5.75	73.02	94.72	2.95	0.29	0.66	1.90	1.87	9.80	9.42	7.87	14-1
50	12.14	75.72	102.52	2.94	0.28	0.69	2.32	1.87	7.90	7.62	6.40	14-2
51	23.19	80.34	112.01	2.92	0.27	0.72	2.89	1.88	6.64	6.44	5.44	14-3
52	31.84	83.92	116.71	2.91	0.26	0.73	3.15	1.89	6.39	6.20	5.26	14-4
53	8.50	68.06	90.82	2.21	0.29	0.65	11.91	1.65	8.40	8.06	6.96	15-1
54	17.98	71.65	99.44	2.64	0.28	0.68	2.33	1.78	6.85	6.60	5.61	15-2

Table M.2. (continued)

Run	$X^+ \times 10^3$	t_b °F	t_w °F	$\gamma\Delta T$	m	n_w	__a	__b	Nu	__c	__d	Ref
55	34.42	77.79	110.18	2.62	0.27	0.71	2.89	1.79	5.83	5.64	4.83	15-3
56	47.32	82.55	115.23	2.61	0.26	0.72	3.09	1.80	5.74	5.57	4.78	15-4
57	9.83	71.23	94.84	2.64	0.29	0.66	2.01	1.78	8.05	7.74	6.56	16-1
58	20.80	75.36	104.03	2.63	0.28	0.69	2.47	1.78	6.59	6.36	5.42	16-2
59	39.86	82.42	115.37	2.60	0.26	0.73	3.12	1.80	5.68	5.16	4.73	16-3
60	54.85	87.89	120.11	2.95	0.25	0.74	3.18	1.92	5.77	5.61	4.76	16-4
61	1.79	61.61	92.20	5.38	0.29	0.66	2.32	2.34	15.23	14.62	11.44	17-1
62	3.78	63.45	101.66	5.37	0.28	0.68	3.07	2.34	12.15	11.72	9.24	17-2
63	7.20	66.60	112.89	5.34	0.26	0.72	4.32	2.36	9.99	9.68	7.72	17-3
64	9.88	69.04	119.44	5.32	0.26	0.74	5.28	2.37	9.14	8.88	7.13	17-4
65	1.97	60.66	92.95	5.43	0.29	0.66	2.43	2.34	14.54	13.96	10.91	18-1
66	4.15	62.69	103.02	5.41	0.28	0.69	3.28	2.35	11.61	11.20	8.84	18-2
67	7.92	66.18	114.98	5.38	0.26	0.72	4.73	2.36	9.54	9.26	7.39	18-3
68	10.86	68.88	121.96	5.36	0.25	0.75	5.89	2.37	8.74	8.50	6.84	18-4
69	14.34	74.42	98.56	2.40	0.28	0.68	2.09	1.72	7.16	6.89	5.91	19-1

Table M.2. (continued)

Run	$X^+ x10^3$	t_b °F	t_w °F	$\gamma\Delta T$	m	n_w	a	b	Nu	c	d	Ref
70	30.40	94.38	108.88	2.38	0.27	0.71	2.59	1.72	5.91	5.72	4.94	19-2
71	58.41	89.25	121.45	2.68	0.25	0.74	3.22	1.84	5.26	5.12	4.39	19-3
72	80.51	96.50	124.56	2.99	0.25	0.75	2.92	1.96	5.99	5.83	4.93	19-4

Experimental Results for Solution II (1.0 percent HEMC)

Table M.3. Experimental variables

Run No.	$\dot{m}$ lb_m/hr	q''_w $Btu/hrft^2$	Re[a]	Pr	f[b]
1 to 8	107.5	930.9	7.3	1271.4	6.89
9 to 16	105.3	1584.9	6.9	1326.6	6.55
17 to 24	91.9	1324.0	5.8	1360.8	6.83
25 to 32	49.2	886.3	2.4	1814.2	14.80
33 to 40	48.8	1135.6	2.3	1802.8	13.41
41 to 48	41.8	701.2	1.8	1986.9	18.76
49 to 56	41.3	1093.0	1.8	1980.9	15.52
57 to 64	230.9	1882.5	21.6	918.0	2.20
65 to 72	286.8	1791.0	26.5	937.1	1.77

[a]Evaluated at Station 1, where x/D = 9.6.

[b]Evaluated at t_{am} for Test Section II.

Table M.4. Experimental results for Solution II (1.0% HEMC)

Run	$X^+ x10^3$	t_b °F	t_w °F	$\gamma\Delta T$	m	n_w	__a	__b	Nu	__c	__d	Ref
1	2.06	64.48	74.05	1.50	0.30	0.64	1.31	1.45	11.83	11.30	10.46	2-1
2	5.05	65.15	77.25	1.50	0.29	0.65	1.42	1.45	9.35	8.97	8.10	2-2
3	12.55	66.84	82.20	1.50	0.29	0.67	1.58	1.45	7.35	7.07	6.35	2-3
4	20.23	68.57	85.89	1.49	0.28	0.68	1.70	1.46	6.50	6.27	5.64	2-4
5	28.00	70.30	88.75	1.72	0.28	0.69	1.79	1.53	6.09	5.88	5.23	2-5
6	35.75	72.02	91.52	1.72	0.27	0.70	1.86	1.53	5.75	5.55	4.95	2-6
7	40.08	72.98	92.93	1.71	0.27	0.70	1.90	1.53	5.61	5.43	4.84	2-7
8	44.40	73.93	94.39	1.71	0.27	0.71	1.94	1.53	5.46	5.29	4.72	2-8
9	2.10	64.24	79.48	2.56	0.29	0.66	1.56	1.77	12.66	12.16	10.70	3-1

a $\left(\frac{K}{K_w}\right)$

b $\left(\frac{K}{K_w}\right)_{crit}$

c $\frac{Nu}{(\Delta_w)^{1/3}}$

d $\frac{Nu}{(\Delta_w)^{1/3}(C_c)^m}$

Table M.4. (continued)

Run	$X^{+}x10^{3}$	t_b °F	t_w °F	$\gamma\Delta T$	m	n_w	a	b	Nu	c	d	Ref
10	5.16	65.42	84.84	2.55	0.28	0.68	1.78	1.77	9.92	9.55	8.14	3-2
11	12.85	68.36	92.96	2.54	0.27	0.71	2.17	1.77	7.79	7.54	6.46	3-3
12	20.74	71.35	99.06	2.92	0.26	0.73	2.49	1.90	6.89	6.69	5.66	3-4
13	28.75	74.37	103.88	2.91	0.25	0.74	2.71	1.90	6.44	6.27	5.32	3-5
14	36.78	77.36	108.21	2.90	0.25	0.76	2.91	1.91	6.14	5.98	5.10	3-6
15	41.26	79.02	110.95	2.89	0.24	0.77	3.07	1.92	5.92	5.78	4.94	3-7
16	45.75	80.68	113.00	2.89	0.24	0.78	3.18	1.93	5.84	5.70	4.88	3-8
17	2.41	65.81	79.27	2.13	0.29	0.66	1.48	1.65	11.94	11.47	10.23	4-1
18	5.92	66.93	84.20	2.13	0.28	0.68	1.68	1.65	9.30	8.95	7.77	4-2
19	14.75	69.75	91.54	2.12	0.27	0.70	2.00	1.65	7.34	7.09	6.19	4-3
20	23.80	72.61	97.12	2.44	0.26	0.72	2.22	1.76	6.50	6.30	5.43	4-4
21	32.99	75.50	101.55	2.43	0.26	0.73	2.40	1.76	6.09	5.92	5.11	4-5
22	42.19	78.36	105.51	2.42	0.25	0.75	2.55	1.77	5.82	5.66	4.91	4-6
23	47.32	79.95	107.90	2.41	0.25	0.76	2.66	1.77	5.64	5.50	4.77	4-7
24	52.46	81.54	109.92	2.41	0.24	0.76	2.73	1.78	5.54	5.41	4.70	4-8

Table M.4. (continued)

Run	$X^+ \times 10^3$	t_b °F	t_w °F	$\gamma\Delta T$	m	n_w	__a	__b	Nu	__c	__d	Ref
25	4.51	65.52	79.96	1.43	0.29	0.65	1.39	1.43	9.41	9.03	8.19	5-1
26	11.06	66.93	81.28	1.42	0.29	0.67	1.53	1.43	7.49	7.20	6.49	5-2
27	27.58	88.07	70.45	1.64	0.28	0.69	1.74	1.50	6.07	5.85	5.23	5-3
28	44.56	74.03	93.30	1.63	0.27	0.71	1.86	1.51	5.52	5.34	4.78	5-4
29	61.82	77.64	97.60	1.62	0.26	0.72	1.94	1.51	5.30	5.14	4.61	5-5
30	79.11	81.22	101.33	1.61	0.26	0.73	2.00	1.52	5.24	5.09	4.57	5-6
31	88.79	83.21	103.85	1.61	0.25	0.74	2.07	1.52	5.09	4.95	4.46	5-7
32	98.48	85.20	105.69	1.78	0.25	0.75	2.08	1.58	5.11	4.98	4.44	5-8
33	4.55	65.59	79.82	1.83	0.29	0.66	1.52	1.55	9.70	9.32	8.26	6-1
34	11.16	67.41	85.32	1.82	0.28	0.68	1.72	1.56	7.68	7.40	6.54	6-2
35	27.87	71.96	93.91	2.09	0.27	0.71	2.02	1.65	6.23	6.03	5.27	6-3
36	45.10	76.59	100.43	2.08	0.26	0.73	2.23	1.66	5.70	5.53	4.86	6-4
37	62.65	81.25	105.86	2.07	0.25	0.75	2.37	1.67	5.49	5.34	4.70	6-5
38	80.27	85.89	110.13	2.28	0.24	0.77	2.39	1.75	5.54	5.40	4.71	6-6
39	90.15	88.46	113.50	2.28	0.24	0.78	2.53	1.76	5.34	5.22	4.56	6-7

Table M.4. (continued)

Run	$X^+ x10^3$	t_b °F	t_w °F	$\gamma\Delta T$	m	n_w	__a	__b	Nu	__c	__d	Ref
40	100.05	91.02	115.43	2.27	0.23	0.79	2.51	1.76	5.46	5.34	4.68	6-8
41	5.31	65.48	75.72	1.13	0.30	0.65	1.33	1.34	8.66	8.30	4.64	7-1
42	13.02	66.79	78.98	1.13	0.29	0.66	1.43	1.34	6.98	6.70	6.15	7-2
43	32.47	70.08	84.68	1.30	0.28	0.68	1.56	1.40	5.80	5.58	5.08	7-3
44	52.45	73.42	89.54	1.29	0.28	0.69	1.67	1.40	5.22	5.05	4.60	7-4
45	72.74	76.78	93.38	1.28	0.27	0.71	1.72	1.40	5.05	4.89	4.46	7-5
46	93.07	80.12	96.81	1.28	0.26	0.72	1.75	1.41	5.00	4.85	4.43	7-6
47	104.44	81.97	99.02	1.28	0.26	0.73	1.79	1.41	4.89	4.74	4.34	7-7
48	115.82	83.82	100.80	1.27	0.26	0.73	1.81	1.41	4.89	4.75	4.35	7-8
49	5.37	65.86	80.39	1.76	0.29	0.66	1.53	1.53	9.13	8.78	7.76	8-1
50	13.20	67.92	86.12	1.75	0.28	0.68	1.74	1.54	7.28	7.01	6.22	8-2
51	32.99	73.10	94.59	2.01	0.27	0.71	2.00	1.63	6.11	5.92	5.20	8-3
52	53.42	78.37	101.99	2.00	0.26	0.74	2.24	1.63	5.52	5.37	4.73	8-4
53	74.26	83.67	107.69	1.98	0.25	0.76	2.35	1.64	5.39	5.26	4.65	8-5
54	95.22	88.94	111.89	2.19	0.24	0.77	2.32	1.73	5.61	5.47	4.80	8-6

Table M.4. (continued)

Run	$X^+ x10^3$	t_b °F	t_w °F	$\gamma\Delta T$	m	n_w	__a	__b	Nu	__c	__d	Ref
55	106.97	91.86	115.60	2.18	0.23	0.79	2.46	1.74	5.40	5.28	4.64	8-7
56	118.76	94.78	117.51	2.17	0.23	0.79	2.41	1.75	5.62	5.50	4.84	8-8
57	0.96	65.96	79.68	3.03	0.29	0.66	1.50	1.91	16.65	16.00	14.24	9-1
58	2.36	66.60	84.73	3.03	0.28	0.68	1.72	1.91	12.59	12.13	10.41	9-2
59	5.86	68.19	91.51	3.02	0.27	0.70	2.08	1.91	9.77	9.45	7.92	9-3
60	9.44	69.81	96.77	3.01	0.26	0.72	2.39	1.92	8.43	8.17	6.88	9-4
61	13.06	71.44	100.63	3.47	0.26	0.73	2.63	2.05	7.77	7.55	6.27	9-5
62	16.67	73.07	104.39	3.46	0.25	0.74	2.88	2.05	7.22	7.03	5.86	9-6
63	18.69	73.97	106.23	3.46	0.25	0.75	3.00	2.06	7.00	6.82	5.70	9-7
64	20.70	91.56	108.26	3.46	0.25	0.76	3.15	2.06	6.76	6.59	5.51	9-8
65	0.78	66.49	78.98	2.88	0.29	0.66	1.45	1.87	17.40	16.71	15.02	10-1
66	1.90	66.97	83.24	2.88	0.28	0.67	1.63	1.87	13.35	12.85	11.19	10-2
67	4.72	68.19	89.10	2.87	0.28	0.69	1.91	1.87	10.37	10.01	8.43	10-3
68	7.59	69.44	93.49	2.87	0.27	0.71	2.15	1.87	9.00	8.70	7.35	10-4
69	10.50	70.69	96.70	3.31	0.26	0.72	2.32	2.00	8.31	8.05	6.70	10-5

Table M.4. (continued)

Run	$X^+ x10^3$	t_b °F	t_w °F	$\gamma\Delta T$	m	n_w	__a	__b	Nu	__c	__d	Ref
70	13.40	71.93	99.88	3.30	0.26	0.73	2.52	2.00	7.71	7.49	6.25	10-6
71	15.02	72.62	101.34	3.30	0.26	0.73	2.60	2.01	7.50	7.29	6.09	10-7
72	16.63	73.31	103.08	3.30	0.25	0.74	2.72	2.01	7.23	7.03	5.88	10-8